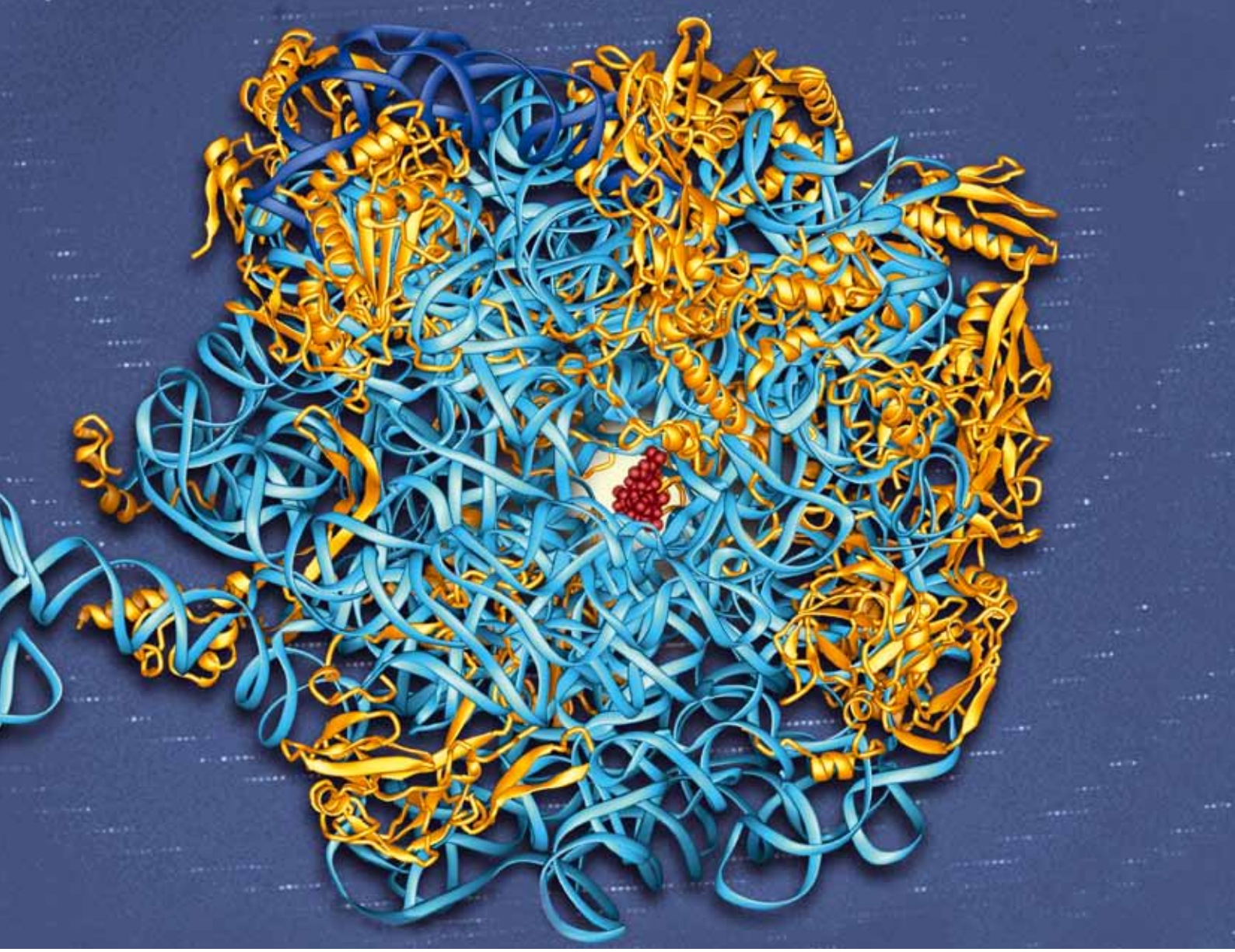

PHOTON SCIENCE 2009.

Highlights and HASYLAB Annual Report

Accelerators | Photon Science | Particle Physics

Deutsches Elektronen-Synchrotron
A Research Centre of the Helmholtz Association

Cover

Structure of a ribosomal particle (ribosomal RNA (blue) and ribosomal proteins (orange)) with a bound macrolide antibiotic (red). The background shows an X-ray diffraction pattern of a ribosome single crystal.
For the finding of the structure and function of the ribosome the Nobel prize for chemistry 2009 was given in equal parts to Venkatraman Ramakrishnan, Thomas A. Steitz and Ada E. Yonath. The israeli Ada Yonath was head of the Max-Planck Group for ribosome structure at DESY in 1986-2004 when significant measurements for the decoding of the ribosome structure were performed at the DORIS storage ring.
More information about the research that led to the Nobel Prize can be found in the contribution by the Max-Planck Group on pages 68-69 of this report.

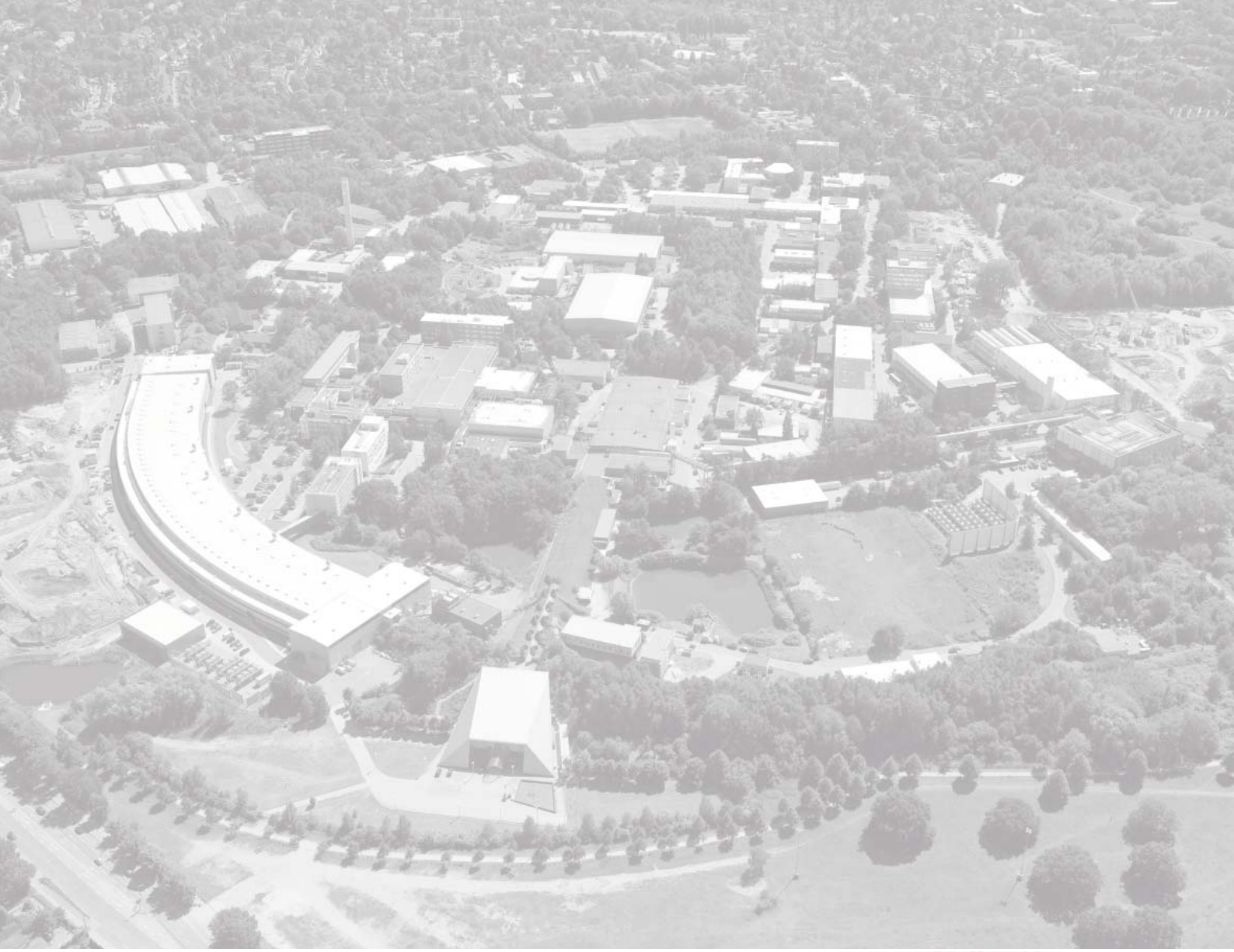

PHOTON SCIENCE 2009.

Highlights and HASYLAB Annual Report

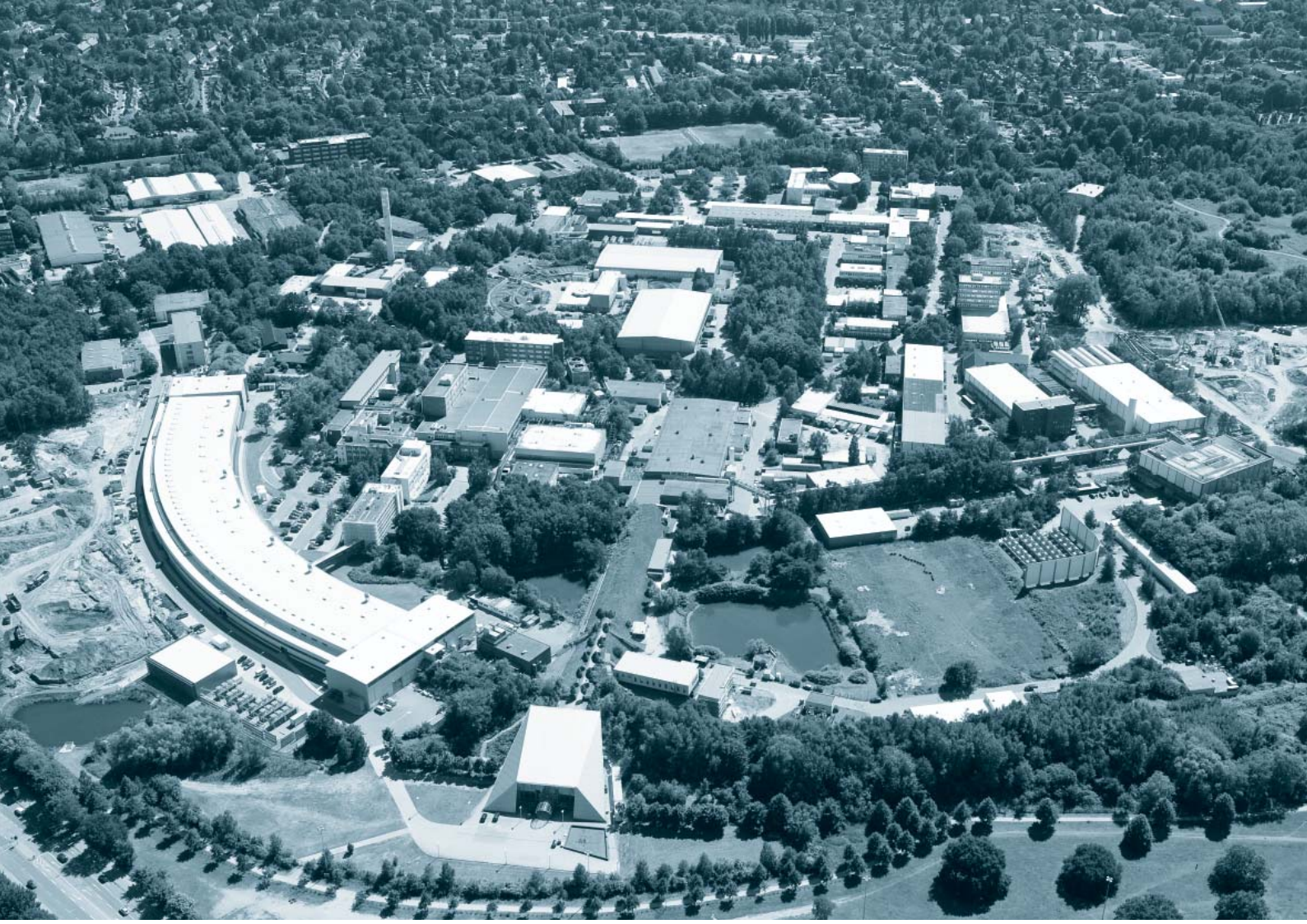

Contents.

The year 2009 at DESY.

Chairman's foreword

2009 is a special year for DESY. We are celebrating the 50th anniversary of DESY and the Nobel Prize of Chemistry 2009 which has been awarded to Ada Yonath for her pioneering work in deciphering the structure and function of the ribosome, the molecular machine which assembles the proteins according to the genetic alphabet encoded in the DNA. Ada has been working here at DESY for more than 20 years, when she has carried out her celebrated X-ray Laue experiments at the DORIS III facility. Ada called me one day after the announcement from Stockholm and thanked DESY for the perfect research conditions she experienced during her work at DORIS III.

Ada Yonath's Nobel Prize demonstrates convincingly which ingredients are necessary for scientific breakthroughs: Excellent large scale facilities – top instrumentation – brilliant scientists with novel ideas and the strong will to achieve the goals. Thus, developing, building and operating the best facilities in the world as well as attracting brilliant young people must be the overarching strategy of DESY to secure its future and to assure that our motto "Wir machen Erkenntnis möglich" turns into reality.

PETRA III is the best synchrotron radiation facility ever built. In the years to come, this brilliant high-energy light source will offer excellent and unique experimental opportunities and allow scientists from all disciplines revolutionary high-resolution insights into the molecular structure of advanced materials and biological samples. Already before the official start of user operation the attraction of this new facility is enormous. All major players in structural biology have joined forces to set up at DESY a novel centre for structural systems biology (CSSB) with a focus on infection biology and on the use of the new X-ray nanobeams of PETRA III. The beginning of a new success story. I am convinced that the decision making bodies will soon give green light to this initiative.

The final act of the PETRA III inauguration - a perspective on future science.

Inauguration ceremony of the PETRA III synchrotron radiation facility (November 2009).

It is the tradition of DESY to address the grand challenges of today and tomorrow but also to tackle the challenges of the day after tomorrow. Our Free-Electron Lasers FLASH and the European XFEL are aiming for nothing less than science fiction: to monitor molecular processes, i.e. the formation and breaking of chemical bonds, in real time. In other words, to make life reports from the nano world. FLASH, the world´s first Free-Electron Laser, has developed into a user facility which produces scientific highlights every week. The user demand has increased so much that we must upgrade and expand the facility as soon as possible: FLASH II also will become a milestone in the FEL roadmap: the first seeded SASE laser and the first FEL with multiplexed user service. FLASH II and the European XFEL are clearly the priority projects of DESY in the coming years (remark: in my notation, PETRA III is no longer a project but an operating facility).

FLASH, FLASH II and the European XFEL do and will further exert an unprecedented world-wide attraction for scientists. The best example is CFEL, the Center for Free-Electron Laser Science. After luring Andrea Cavalleri and Henry Chapman to DESY, the University of Hamburg, the Max-Planck Society and DESY could convince in a remarkable joint effort Professor Dwayne Miller from Toronto to join CFEL. A great success for Hamburg. I have no doubt that each of the remaining two appointments will become a similar highlight.

It is gratifying to see how successfully DESY has managed the transition from a particle physics lab to a photon science lab. The fact that we have been able to decide by ourselves to phase out DORIS III (a painful thought for all of us) gives us further strength for the future which will be brilliant. Let’s work together for this goal. ●

Helmut Dosch
Chairman of the DESY board of directors

Photon Science at DESY.

Introduction

At the end of the year 2009 we are looking back on a important year for Photon Science at DESY. During the year of the 50th anniversary of DESY's foundation we are very proud that Ada Yonath (Weizmann Institute, Israel), leading for 18 years the Max-Planck group "Ribosomenstruktur" on the DESY campus was awarded the Nobel Prize for Chemistry for her work on the structure of ribosomes together with two colleagues from the United States (see MPG-contribution on pages 68-69). We also celebrated the inauguration of our new third generation synchrotron radiation source PETRA III in the presence of the Federal Minister for Education and Research, Annette Schavan, and the Hamburg Senator for Science and Research, Herlind Gundelach, together with a large number of guests of honour from all around the world. The year 2009 was also a year of major construction, upgrade, and commissioning of our new facilities for Photon Science.

After a nine month shutdown in 2008, DORIS III was fully operational in 2009 providing 5409 hours of user operation for about 2200 users (and roughly 200 FLASH users). As in all the years before, users at DORIS III continue to produce very good science results leading to 500–600 peer reviewed publications per year. The final shutdown of DORIS III has tentatively been scheduled for end of 2012 or beginning of 2013. In order to continue those experimental techniques at DORIS III that are not yet available at PETRA III, the latter one will be extended by two additional experimental halls with a total of 5 insertion devices and 5 bending magnet beamlines serving about 13-14 experimental stations. A first successful workshop with more than 150 participants was organized in November to discuss the experimental techniques and the instrumentation of these new beamlines. Further workshops will follow during the year of 2010 to discuss and finalize the design of these new beamlines and stations.

Progress at PETRA III was almost as expected. On Easter Monday the first particle beam could be stored in the new storage ring. Not too long later the first undulator was closed and first light could be observed in the front-end. The next major milestone was the installation of the first monochromator providing the monochromatic beam in June. The design emittance of 1 nmrad, a new world record for synchrotron light sources, has been achieved in September and the maximum achieved positron current is already now within 90 % of the design value. In the second half of 2009 the beamline vacuum system, experimental equipment, and safety systems for the first three beamlines were completed. Meanwhile, the first users have installed their instruments and are carrying out test experiments. The remaining beamlines are currently being constructed and it is expected that all 14 beamlines will be at least in their commissioning phase by end of 2010. A number of these PETRA III beamlines will be in regular user operation by that time and everyone will be very curious to see the first exciting experimental results.

After an extended final run with a number of amazing results at FLASH, some of them described in the Highlights section of this report, a major shutdown started in September 2009. Significant upgrade work will take place in the accelerator section and at the photon beamlines. The accelerator will be upgraded to a final particle energy of 1.2 GeV by the installation of an additional accelerating module thus enabling lasing at photon wavelengths below 5 nm. More importantly, there will be the installation of a third harmonic cavity providing means for a better control of the electron bunch in phase space. Together with the variable bunch charge provided by the electron gun, this will enable tailoring the photon bunch length in a range from below 10 fs to more then 100 fs. The third change in the accelerator tunnel concerns the installation of a seed experiment called sFLASH which is carried out in collaboration with groups from the University of Hamburg. The aim of this experiment is, for the first time, to seed an FEL in the VUV wavelength range by an external High Harmonic Generation (HHG) laser system. sFLASH will deliver transform limited FEL photon bunches

Offices and laboratories in the PETRA III experiment hall.

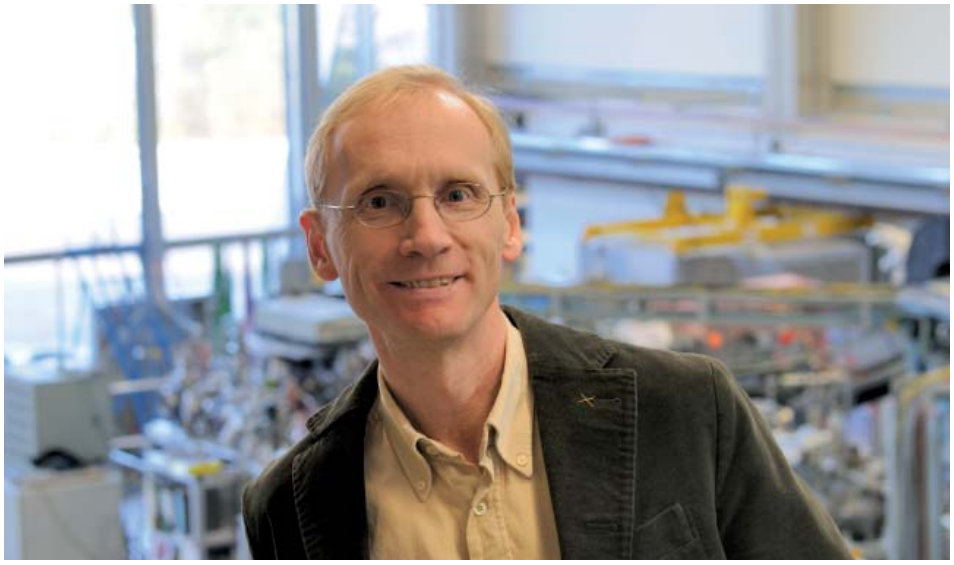

of defined timing with respect to the external seed laser thus providing ideal conditions for pump – probe experiments with very high temporal resolution. In the experimental hall the main improvement concerns the beamline optics (e.g. installation of a fast switching mirror) and an upgrade of the pump laser towards higher repetition rate at high power and shorter photon pulses. FLASH, in its new configuration, is expected to resume user operation in mid 2010. The plans for the proposed extension of FLASH called FLASH II (in collaboration with the Helmholtz Zentrum Berlin (HZB)) consisting of an additional tunnel housing a seeded FEL undulator and a second experimental hall doubling the capacity or user experiments at FLASH have further been refined. The project has a very high priority at DESY, however, funding is not yet secured. In order not to further delay this project DESY will launch a preparatory project phase at the beginning of 2010.

Meanwhile, the European XFEL project is proceeding well. The construction work for the underground buildings started in early 2009 and is well on track. Detailed design work has continued and calls for tender for a number of major components have been issued. The bare brickwork of the hall for the accelerator module test facility is almost finished. Most important and long awaited, the European XFEL GmbH company has finally been founded through the signing of the convention by a majority of the European partner countries on November 30th, 2009. After this major milestone, the European XFEL can get up to full steam and hopefully provide the first beams by the end of 2014.

The Center for Free-Electron Laser science (CFEL), a joint activity of the Max-Planck Society, University of Hamburg, and DESY, is taking up shape. The heads of three out of the five core groups have been appointed meanwhile. The CFEL groups are continuously growing and have already become major players in FEL science together with the CFEL advanced study groups. The construction work for the new CFEL building has started this year and the topping out ceremony is expected for mid 2010.

In 2008 the Helmholtz Associated issued a call for the establishment of so called Helmholtz Institutes in those federal states where no Helmholtz center exists so far. GSI Darmstadt, Friedrich-Schiller University of Jena, and DESY proposed successfully to establish the Helmholtz Institute Jena on development of and research with high power short pulse laser systems, which play an increasingly important role especially for the photo cathode gun, seeding and pump probe experiments at free-electron lasers as well as for new concepts for particle acceleration.

The plans for the Centre for Structural System Biology (CSSB) have significantly matured. About 14 partner institutions working in the field of structural biology in Northern Germany have expressed their interest to join this research platform. Consultations on the political level have been very promising. A possible start of the construction project for a new building in 2010 is very likely. The first junior group in structural biology in the frame of CSSB has already started on site mid 2009.

Also in 2009 was the second 5-year evaluation of the Helmholtz Association program PNI (Research with large scale facilities using Photons, Neutrons, and Ions) within the research area “Structure of Matter” to which the DESY photon sources belong. The scientific and strategic aims of the entire PNI program were very well received. Most import for the user operation of our large scale facility is, that measures have been identified in order to ensure a sufficient operation budget also in case of, e.g., increasing energy costs.

All these achievements were only possible due to the high motivation of the DESY staff and our dedicated user community. Also, the generous support by the national funding agencies and the EU is gratefully acknowledged. I would like to thank everyone who contributed to make Hamburg such an exciting place for multi-disciplinary research and I’m sure we are facing fascinating times for research with photons at DESY. ●

Edgar Weckert
Director Photon Science

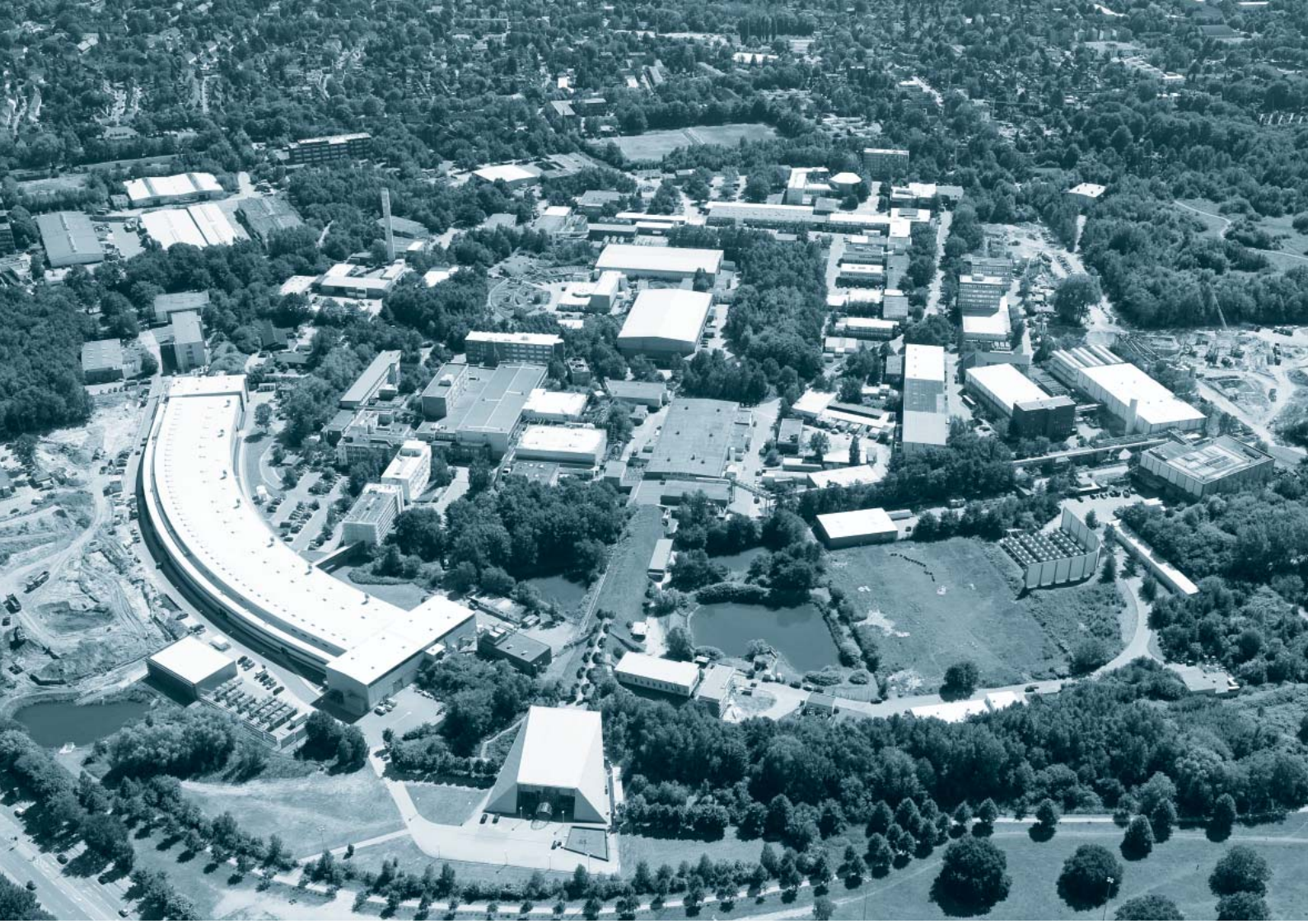

News and Events.

News and Events.

A busy year 2009

January

January 28:
DESY and India will collaborate in advanced materials research

On January 28, 2009, a delegation of scientists and government representatives from India and the DESY Directorate signed a Letter of Intent to establish a scientific collaboration in nano science, nano technology, and advanced materials research. Professor Chintamani Nagesa Ramachandra Rao, chairman of the Scientific Advisory Council to the prime minister of India, led the delegation. The formal agreement will be signed at government level.

C.N.R. Rao and Albrecht Wagner shake hands after signing the Indian-DESY Letter of Intent for scientific collaboration.

January 28–29:
Third users' meeting of the European XFEL

The third users' meeting of the European XFEL took place on January 28-29 and was attended by 256 registered participants; the attendance was quite international, as about one half of the participants came from countries other than Germany, with particularly large delegations from Russia (15), Sweden (13) and the UK (12). Thanks to the support of the EU grant "Pre-XFEL" for the preparation phase of the European XFEL project, it was possible to support travel costs for young scientists from the participating countries (see some of them in the picture, together with four not-so-young project team members in the upper right side).
In addition to a short welcome session and to an extensive report on the status of the project, the program of the first day included a report from the LCLS, presented by J.B. Hastings; reports on the four users' workshops held in 2008, and a presentation of the forthcoming "High Energy Density Workshop" (March 2009) by J. Wark. A session on "Time-dependent Phenomena" and a lively poster session concluded the first day. On January 29, the full morning was devoted to an extensive discussion of "Soft X-ray Spectroscopies", and the meeting adjourned by lunchtime.

XFEL project team members with some of the young scientists attending the XFEL users' meeting.

The audience seemed to appreciate the fact that all sessions left ample time for discussions and questions. The active participation of the attendees in the discussions, in the lecture hall as well as outside, during the poster session and the breaks, was very stimulating.

January 29:
Status and perspectives of small angle X-ray scattering at HASYLAB – a satellite meeting of the annual HASYLAB users' meeting

Since 2002 every year a satellite meeting on the status and perspectives of small angle X-ray scattering at HASYLAB has been organized one day before the annual HASYLAB users' meeting. Thus, this year's meeting on January 29 was the eighth in a row, attended by 72 participants. The introduction given by R. Gehrke was dominated by the planned shutdown of DORIS III and the opportunities offered to the SAXS community by a bending magnet beamline in the frame of a foreseen PETRA III extension. After this outlook the responsible scientists for the SAXS beamlines A2, B1, and BW4 reported on the status and recent developments at the corresponding instruments followed by presentations of the status of the new MINAXS beamline at PETRA III for microfocus small angle X-ray scattering and of the planned nanofocus endstation for MINAXS which is under construction in collaboration with the University of Kiel.

The remaining talks presented the work of eleven user groups involved in experiments at the DORIS III small angle scattering instruments. Each talk was followed by a lively discussion which gave many indications for future trends in the investigations and for the required technical and experimental developments to achieve this. The final discussion came back to the main topic of the introduction and the participants clearly expressed the need to have also SAXS facilities available at PETRA III which do not aim for extremely small beam size but make use of the original strength of SAXS, namely to provide information averaged over sufficiently large sample volumes or areas. The possibility of complementary use of micro- and nanofocus instruments like MINAXS and of instruments like the existing SAXS facilities at DORIS III has to be maintained after the final DORIS shutdown.

January 29:
Satellite meeting of the users of X-ray absorption spectroscopy and microfluorescence

Another satellite meeting was held on January 29, one day before the HASYLAB users' meeting for the user community of X-ray absorption spectroscopy together with the users interested in the activities at the DORIS III microfluorescence beamline L. Although due to the long shutdown period of DORIS in 2008 no user talks were scheduled, over 40 participants from both communities attended the meeting.

The first talk was given by W. Drube, who reported on the future perspectives for additional spectroscopy beamlines for EXAFS and hard X-ray microprobe at PETRA III. Those beamlines are going to replace beamline L and the three existing EXAFS beamlines after the final shutdown of the DORIS III storage ring in 2012. After this talk K. Rickers-Appel reported on the status and experimental developments at beamline L and E. Welter on the EXAFS beamlines, especially on the status of beamline A1, which was completely reconstructed during the extended shutdown of DORIS in 2008. W. Caliebe gave a short presentation about newly available bent crystals and detectors for the Johann spectrometer at the wiggler beamline W1. The successful implementation of a cryostream environment at beamline L to measure hydrated biological samples was then presented by G. Wellenreuther.

The second part of the meeting was devoted to the new hard X-ray micro/nano-probe beamline P06 at PETRA III. G. Falkenberg gave an introduction to the beamline concept featuring separate hutches for the microprobe and nanoprobe experiments.

For the microprobe experiments achromatic X-ray optics are employed for (sub) micro-spectroscopy with high flux and ample space for sample environments. The nanoprobe experiments are aiming for utilizing the smallest possible beam for tomographic nano-XRF and coherent diffraction imaging. Details of the nanoprobe setup were presented by J. Feldkamp from TU Dresden. G. Wellenreuther reported on vibration measurements on the concrete slab at the P06 site. The meeting ended with a guided tour of participants through the new PETRA III experimental hall, including a visit of the location of beamline P06, which is expected to see first beam in summer 2010.

January 30:
Annual HASYLAB users' meeting

The 350 participants of the HASYLAB users' meeting received a warm welcome by the DESY chairman of the board of directors, Albrecht Wagner, and his designated successor Helmut Dosch. Following an overview on recent photon science activities on the DESY campus given by Edgar Weckert, three presentations focused on FLASH and the science done with it.
Josef Feldhaus (DESY) reported on recent developments at the facility and Henry Chapman (DESY/CFEL) presented results of ultrafast coherent diffractive imaging. New frontiers in atomic, molecular, and optical physics with free-electron lasers were outlined by Joachim Ullrich (MPI Heidelberg/CFEL).

In the afternoon session, Thomas Schneider (EMBL Hamburg outstation) talked about "EMBL@PETRA3", the planned integrated facility for structural biology at PETRA III. The last scientific presentation was given by Peter Siffalovic (Academy of Sciences, Bratislava) on self-assembled nanoparticle templates for future spintronic devices.
In addition, general user affairs were discussed by Peter Müller-Buschbaum (TU Munich) who is chairing the HASYLAB Users

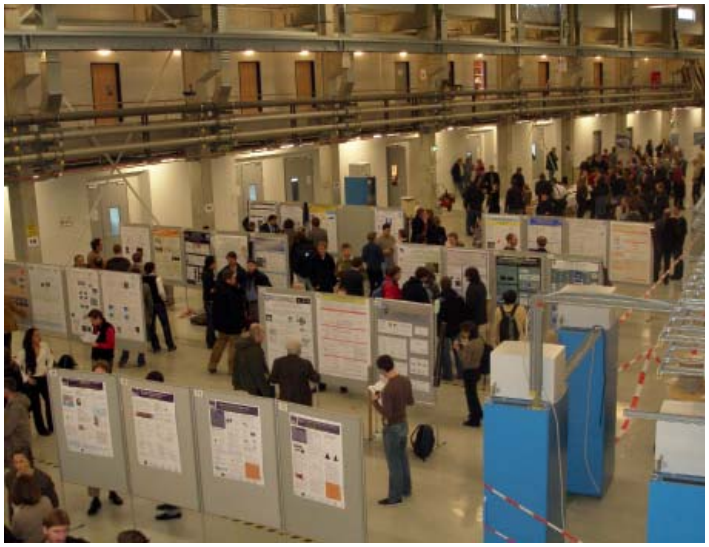

The poster session of the Annual HASYLAB Users' Meeting in the new PETRA III experimental hall.

Committee, and special topics of interest for the German synchrotron radiation community were addressed by the KFS chairman Ullrich Pietsch (University of Siegen). The meeting was concluded with a poster session in the PETRA III experimental hall giving ample space for the display of the 161 poster presentations.

February

February 18–20:
8th Research course on new X-ray science

On February 18-20 DESY hosted the "Research Course on New X-ray Science". The research course is intended to provide basic knowledge about new directions of X-ray research and addresses diploma (master) students, PhD students, and young research fellows at their early career. The 8th course was dedicated to the investigation of structural and dynamical properties of magnetic materials using the properties of highly brilliant X-ray sources.

The event was attended by 82 students from all over Europe. 14 renowned international experts in the field of magnetic scattering gave 60 minutes lectures covering the topics of X-ray scattering from magnetic materials, X-ray magnetic circular dichroism, magnetic materials in data storage technology, time resolved magnetic scattering, scattering from magnetic interfaces, and coherent magnetic scattering. A poster session offered the opportunity to the participants to present and discuss their own scientific results.

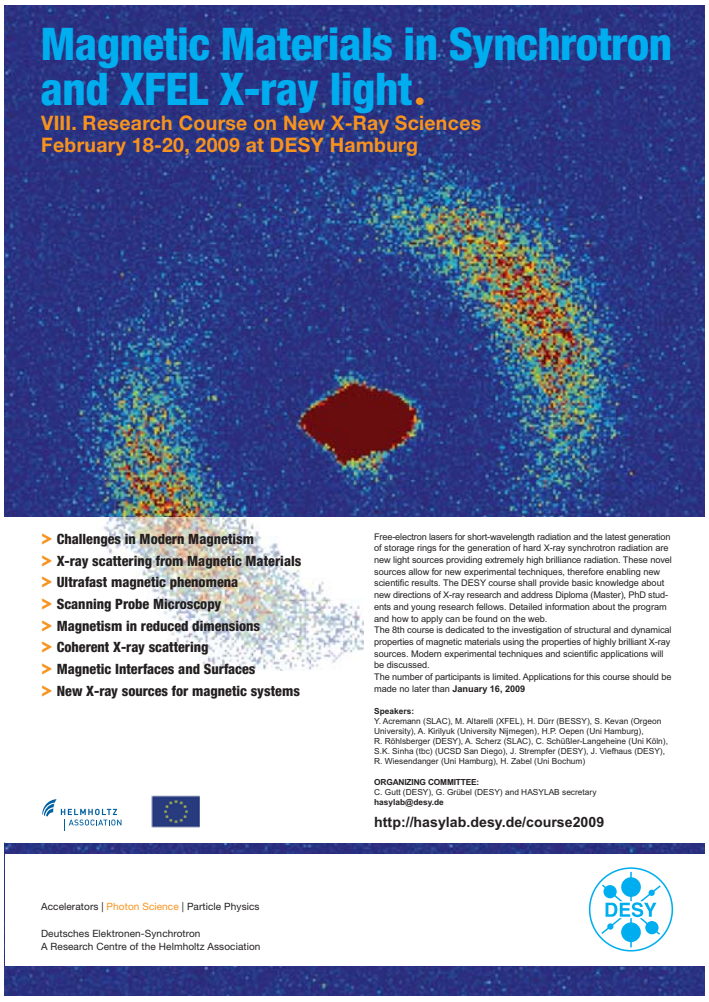

March

March 5–6:
User workshop on the PETRA III coherence beamline

A workshop on the coherence beamline P10 at PETRA III was held from March 5-6 on the DESY site. The main goals of this event were to present the current status and development plans related to the coherence beamline before the operation start of PETRA III, to inform the scientific community about the new and unique research possibilities at this new instrument, and to gather input about possible future scientific directions and experimental setup needs from the user community.

The workshop was attended by 40 participants from DESY and other synchrotron radiation sources and from institutes working with applications using coherent synchrotron radiation. Following the presentation of the PETRA III project and various technical and scientific aspects of beamline P10, there were 12 invited lectures on X-ray photon correlation spectroscopy (XPCS) and coherent diffraction imaging (CDI). The conclusions of the lively and fruitful discussions clearly showed a general tendency to investigate smaller objects i.e. structures manifesting itself at larger Q-values. This implies e.g. the necessity of finding multiple reflections from the same nanocrystal using nanobeams on micron sized spheres of confusion or the need to use faster and better detectors for XPCS. Versatile nanopositioning systems and extreme vibration and temperature stability of all beamline components are essential prerequisites for the work. Both, CDI and XPCS, have strong needs to use focusing techniques. However, the required beam size varies from about 100 nm for CDI to 1 – 5 µm for XPCS applications.

Generally, XPCS studies tend to focus on systems showing much more complex dynamic behaviour, which can only be described by more sophisticated correlation in time and space, and requires a corresponding software development. CDI and XPCS need to provide standard analysis software packages to make these techniques available to larger user communities.

May

May 4:
Gerhard Grübel received the 2009 Compton Award

The ninth Arthur H. Compton Award was presented by the Department of Energy's Advanced Photon Source (APS) and the APS Users Organization jointly to Gerhard Grübel from DESY, Simon Mochrie (Yale University, New Haven, U.S.), and Mark Sutton (McGill University in Montreal, Canada), for their pioneering efforts in X-ray photon correlation spectroscopy (XPCS), which exploits the coherent properties of synchrotron X-rays to study the slow dynamics of condensed matter at short length scales.
Gerhard Grübel brought the XPCS technique to Europe, leading the development at the European Synchrotron Radiation Facility (ESRF) in Grenoble, France, and pioneered many innovative applications of XPCS. He now is a leading senior scientist at DESY.

The 2009 Arthur H. Compton Award was presented jointly to (from right) Gerhard Grübel, Simon Mochrie, and Mark Sutton for their pioneering efforts in X-ray photon correlation spectroscopy (XPCS).

May 7–8:
Workshop on inelastic X-ray scattering at PETRA III

A short workshop dedicated to the inelastic X-ray scattering (IXS) end station at the PETRA III beamline P01 was organized in the beginning of May. The purpose of this workshop was to identify research fields which can profit from a dedicated IXS instrument and to inform potential users about possibilities for IXS at PETRA III. Therefore, scientists from different fields like geology, condensed matter physics, material sciences, and chemistry were invited to discuss possible applications and existing experience with IXS in their fields.

The main advantage of IXS is its ability access soft X-ray absorption edges with hard X-rays. The high penetration depth of hard X-rays is of extreme importance for all fields, where bulk properties of samples in non-UHV compatible environments or even under extreme conditions like high pressure and high temperatures, are studied. Also the different angular dependence of transitions – optical like transitions at low scattering angles and mono- and multi-pole transitions at higher scattering angles – is an attractive tool for several scientific applications since additional information can be gained.

All participants were enthusiastic about the new instrument and its envisaged beam properties. The instrument will make use of recent new developments in analyzer technology at other synchrotron radiation sources, and close communication with scientists at IXS-instruments at other synchrotron radiation facilities is ongoing.

This workshop was jointly organized by DESY, IfW Dresden, Technical University Dortmund and DELTA, and GFZ Potsdam.

May 18–19:
First workshop on the extreme conditions beamline at PETRA III

This workshop was convened to provide a forum for 60 scientists from 9 countries to discuss and sharpen the scientific focus of the extreme conditions beamline P02.2 based on the anticipated needs of the German, European and International community and to find a consensus regarding the best possible design. The workshop gathered experts from comparable extreme conditions beamlines at the ESRF and APS as well as specialists from all areas of extreme conditions research.

Presentations in five sessions started with plenary talks covering new developments and directions in extreme conditions research followed by an overview of existing beamlines and the proposal for the new extreme conditions beamline at PETRA III. The second day of the workshop focused on talks by expert users on a variety of subjects to gain an overview of their future needs related to a new beamline in this field. The workshop concluded with a discussion of the proposed layout of the new beamline. During the course of the discussion it became apparent that the pink beam option will be a key feature of the new beamline and thus should be available as soon as possible. Pink beam diffraction is a prerequisite to conduct single crystal Laue diffraction in a laser heated diamond anvil cell as well as for time resolved single crystal experiments. There was a strong plea to advance this capability since it will add a unique feature to the extreme conditions beamline at PETRA III in comparison to other competing beamlines and it will position DESY at the forefront of extreme conditions research.

Participants of the extreme conditions beamline workshop.

May 20:
PhD Thesis Prize for Sebastien Couet and Michael Röhrs

This year's PhD Thesis Prize of the Association of the Friends and Sponsors of DESY is shared by Dr. Sebastien Couet and Dr. Michael Röhrs, both from the University of Hamburg.

Sebastien Couet received the prize for his excellent thesis on "The Structural and Magnetic Properties of Fe/Native Oxide Systems Resolved by X-ray Scattering and Spectroscopy Methods". Couet produced sandwich-layered systems consisting of alternating layers of iron and its natural oxide, and observed their growth using synchrotron radiation. Remarkably, the magnetic alignment of the individual iron layers is not parallel, but rather perpendicular to each other. This is due to the particular structure of the oxide that forms between the iron layers. The results of Couet's thesis point out a new way of stabilizing novel magnetic structures in the nano world.

From left: Dr. Sebastien Couet, DESY Director Professor Helmut Dosch, and Dr. Michael Röhrs.

Michael Röhrs received the prize for his thesis on the "Investigation of the Phase Space Distribution of Electron Bunches at the FLASH Linac Using a Transverse Deflecting Structure".

His work was dedicated to characterize the longitudinal electron bunch compression necessary to reach the peak currents of several thousand Amperes required for the FEL. Röhrs analysed the compressed electron bunches with a time resolution enhanced by a factor of thousand compared to conventional methods. He used methods of computed tomography to determine the spatial and temporal structure of the electron bunches with unprecedented precision.

The annual PhD thesis prize from the Association of the Friends and Sponsors of DESY acknowledges the best doctoral thesis on physics at DESY every year.

June

June 24–25:
Brainstorming meeting "Perspectives for Time-Resolved Studies and Imaging with Laser based and FEL Photon Sources"

On June 24 and 25 researchers from all over the world took part in a "Brainstorming Meeting" at DESY on "Perspectives for Time-Resolved Studies and Imaging with Laser based and FEL Photon Sources". The goal was to bring together experts in conventional laser and FEL research, with a few but top-class speakers and plenty of time for discussions. It was a successful and stimulating meeting with 101 participants and many productive discussions.

FLASH has been the successful test bed for XUV-FEL physics and science for many years. Josef Feldhaus (DESY) described recent progress and gave examples of outstanding science done at FLASH. Zhirong Huang (SLAC) reported on the exciting results obtained in the start-up phase of LCLS. The LCLS first lased in April this year, outperforming the design expectations and successfully proving that FELs also work in the X-ray region. This is a crucial step on the road to the European XFEL under construction in Hamburg. Even before experiments have begun, dreams were discussed for even shorter and more powerful pulses at high repetition rates. These were stimulated by the work carried out with laser-generated attosecond pulses, which reach the fastest timescales ever accessed in exploring the dynamics of atomic, molecular, and solid systems.

Ferenc Krausz (MPQ Munich) demonstrated that these laser based sources provide well-characterized and controlled few-cycle attosecond pulses with reasonable power up to photon energies of several 100 eV. In pilot studies monitoring and steering of the motion of electrons in atoms, molecules, and solids have already been achieved. Andrea Cavalleri (CFEL) showcased the possibilities which these sources offer for investigating the dynamics of complex systems.

Dame Louise Johnson (Diamond Light Source / Oxford) outlined the wealth of information that images of the components of cells, the fundamental units of living system, could provide if taken with the right resolution in space and time. Henry Chapman gave an overview on the progress of time resolved imaging made at FLASH. Intense, ultra short photon pulses are a very attractive means to create well characterised ultra short electron pulses for time resolved electron diffraction. Paul Corkum (Ottawa) discussed how the elegant method of light induced electron diffraction can yield images of molecular wave functions.

June 25:
In cooperation with DESY: Foundation of the "Helmholtz-Institut Jena"

On June 25, all partners (BMBF, TKM, HGF, and GSI, FSU, DESY) signed the memorandum on the foundation of the "Helmholtz-Institut Jena" (HIJ). This new Helmholtz-Institute with focus on lasers and accelerators investigating extreme states of matter will resume operation as outstation of the GSI in July 2009.

The Federal Ministry of Education and Research (BMBF) will cover 90 % of the funding, as it is the case with all Helmholtz institutes. After a start-up phase this funding will amount to five million Euros per year. The remaining ten percent will be granted by the Free State of Thuringia ("Thüringer Kultusministerium" (TKM)).

"The newly founded institute combines the high competence in high power laser physics of the Friedrich Schiller University of Jena with the expertise in accelerator, laser and X-ray technologies of the Helmholtz centres DESY and GSI ", says Professor Dr. Jürgen Mlynek, president of the Helmholtz Association (HGF).

"Also, the expertise of the Friedrich Schiller University in optical lasers in combination with the accelerator-driven X-ray sources at DESY offers unique possibilities for the investigation of e.g. the dynamics of excited states of matter or molecular interaction", added Professor Dr. Edgar Weckert, DESY director of photon science.

This ensures an intensive collaboration among the GSI Helmholtzzentrum für Schwerionenforschung GmbH (GSI), the Friedrich Schiller University of Jena (FSU), and DESY. In future, further partners are expected to join. Founding director of the new "Helmholtz-Institut Jena" with a staff of around 20 - 30 will be Professor Dr. Thomas Stöhlker of GSI.

July

July 3:
DESY participating in six projects of the Hamburg State Excellence Initiative

The winners of the Hamburg State Excellence Initiative were named on July 3. From a total of 21 competing applications, eight clusters of excellence and five graduate schools – institutions for the structured education of junior scientists – were selected to be funded in the coming one and a half years with 16.5 million Euros. DESY is participating in six of the 13 projects and is involved in research collaborations covering topics ranging from nanotechnology and nano spintronics to the development of resistant and light materials and the combination of particle physics and cosmology. Through the Center for Free-Electron Laser Science (CFEL) DESY is also taking part in a post-graduate programme for infectional and structural biology.

The grants amount to about 200 000 Euros per year for a graduate school and up to 1.3 million Euros per year for a cluster of excellence. The cluster of excellence "Frontiers in Quantum Photon Science" bundles the Hamburg expertise of laser physics, quantum optics, X-ray and accelerator physics. It is supported with funds from the Joachim Herz Foundation, a partner of the Hamburg State Excellence Initiative. The clusters "Nanospintronics" and "Nanotechnology in Medicine" are devoted to reveal the nanoscopic mechanisms that lie at the heart of new functionalities in low-dimensional magnetic or biological systems, respectively. All the mentioned clusters involve strong collaboration of the University of Hamburg with DESY scientists to exploit the opportunities offered by the photon sources on the DESY campus. Together with the Technical University Hamburg-Harburg DESY participates in the cluster "Integrated Materials Systems" that is devoted to the development and characterisation of new materials with embedded functionalities.

July 20:
First X-ray beam at the PETRA III light source

During the weekend before July 20 an important milestone of the transformation of PETRA into a dedicated source for synchrotron radiation was reached. The first X-ray light was generated at the new reconstructed storage ring PETRA III. This means that the most brilliant storage ring based X-ray source in the world is now available for experiment operation and on its way to meet the high demand of science for highly brilliant synchrotron radiation. The 2.3-kilometre electron storage ring went through a two-year 225-million Euro upgrade which converted it into a brilliant X-ray light source. Following the upcoming test runs of the individual experiment facilities, PETRA III will start regular user operation in 2010.

As the most powerful light source of its kind, PETRA III will offer excellent research possibilities, in particular to researchers who investigate ever smaller samples with ever finer details, or to those who require tightly focused and very short-wavelength X-rays for their experiments. After the first storing of particles at PETRA III in April this year, the undulators – special magnets producing synchrotron radiation – were positioned close to the particle beam, forcing the accelerated particles onto a zigzag course to make them emit synchrotron radiation.
The PETRA accelerator was originally built for particle physics. More recently, PETRA was used as a pre-accelerator for DESY's successful particle accelerator HERA. In less than two years PETRA was completely refurbished and modernised. The remodelling into the most modern storage ring X-ray source in the world was largely funded by the Federal Ministry of Education and Research (BMBF), the City of Hamburg, and the Helmholtz Association. A 300-metre-long experimental hall was built over the PETRA storage ring, housing 14 synchrotron beamlines and up to 30 experimental stations.

Eye witnesses of the first synchrotron radiation beam in the PETRA III hall.

July 21:
Federal Government, Hamburg, and Schleswig-Holstein sign European XFEL participation agreement and lay the cornerstone for an XFEL test hall

On July 21, Federal Research Minister Professor Annette Schavan, Hamburg's Science Senator Dr. Herlind Gundelach, and Schleswig-Holstein's Research Minister Dr. Jörn Biel met at DESY to sign an agreement for the participation in the European XFEL X-ray facility. With 90 million Euros, the federal states Hamburg and Schleswig-Holstein will cover nearly 16 percent of Germany's contribution to the European XFEL. In order to symbolically cement this considerable investment in research the three politicians also laid the cornerstone for a test hall which from 2011 on will be used to perform functional tests of the more than 800 superconducting accelerator cavities and the 101 accelerator modules under real operation conditions at liquid helium temperature. After these tests the twelve-metre long modules, each weighing 10 tons, will be transferred to the main tunnel of the X-ray facility to be assembled into a 1.7-kilometre-long electron accelerator.

Schleswig-Holstein's Research Minister Dr. Jörn Biel (left), Federal Research Minister Professor Annette Schavan and Hamburg's Science Senator Dr. Herlind Gundelach laid the cornerstone for a test hall (AMTF) at DESY.

The total length of the European X-ray laser facility will be 3.4 kilometres and it will extend from the DESY site to the town of Schenefeld in Schleswig-Holstein. It will generate ultra short pulses of X-ray light – 30 000 times per second and with a light intensity a billion times higher than the best conventional X-ray radiation sources. For this purpose, bunches of electrons are first accelerated to high energies and then directed through long arrays of magnets in which they emit X-ray laser flashes. With its superconducting accelerator, the facility has unique characteristics that will open up completely new research opportunities for scientists and industrial users. In Schenefeld also the research campus will be located which from the year 2015 will be home of about 300 people.

DESY is the leader of the international consortium for the construction of the accelerator, the "heart" of the research facility. The components of the accelerator modules – the cavities – are industrially produced in several countries and assembled into the twelve-metre modules in France. The accelerator units must be produced to highest standards. Particles are accelerated in the cavities with very strong electromagnetic fields. Any bumps or impurities on the surface of the superconducting cavities made of the metal niobium would cause a breakdown of the accelerating field, meaning that the X-ray laser facility would not be able to function properly.

The construction costs of the European XFEL facility amount to 1.08 billion Euros. It will be carried out as an international project. Alongside Germany, twelve European countries and China are participating in the facility. The total German contribution to the construction costs amount to 580 million Euros, the rest is funded by the participating countries.

July 21:
Start of the HASYLAB summer student program

The HASYLAB summer student program started on July 21 as part of the general DESY summer student program and offered 30 selected undergraduate students from 9 countries (Armenia, Germany, Estonia, Italy, Poland, Russia, Slovakia, Spain, and Thailand) the opportunity to stay for eight weeks at DESY and to take part in the daily work of synchrotron radiation related working groups of HASYLAB, EMBL, and CFEL where they worked on their own small projects. The students (17 male, 13 female) were mainly studying physics but came also from other fields of study like chemistry, medical physics, biophysics, materials science, and chemical engineering. Due to the increasing requests especially from the groups working at PETRA III and CFEL the number of accepted students could be increased by a factor of 1.5 compared to the previous years.

Besides the work in their groups the students attended a series of lectures about DESY activities in general and research with synchrotron radiation. The latter covered the technical basics of synchrotron radiation from generation and properties to optics and detectors and the whole range of scientific applications like diffraction, small angle scattering, VUV-spectroscopy, microfluorescence, X-ray absorption spectroscopy, inelastic scattering, powder- and surface diffraction, X-ray tomography, research with high energy photons, and coherence. One day was especially devoted to life science applications with synchrotron radiation. In total the students got an overview of research with synchrotron radiation as it will hardly be offered by university courses. A special event of the HASYLAB summer student program is the so called exercise week with practical exercises at selected DORIS beamlines. This year the instruments at A2 (small angle scattering), B1 (anomalous small angle scattering), BW4 (small angle scattering under grazing incidence), F3 (powder diffraction), G3 (diffraction imaging), A1 (absorption spectroscopy), and E2 (diffraction) were available for this week. In small groups the students practiced the work at a synchrotron radiation instrument from alignment over data acquisition to data evaluation. The exercise week which again was very much appreciated by the students ended with a small seminar, where each group presented their work in short lectures to the other students.

This year's program ended on September 10 with a final session of all 75 summer students at DESY. By then each student had to deliver a report on the work done in his/her group and selected students gave short presentations of this work in the final session. In the concluding discussion the students appreciated the stimulating atmosphere at DESY, the international spirit, and especially pointed out the engagement of all the DESY staff members involved in the program. They all stated that the stay in Hamburg was a great experience and many of the students consider returning to DESY as PhD student or postdoc.

September

September 20–23:
GISAS2009 – A satellite conference to the international conference on small angle scattering (SAS2009)

Encouraged by the great success of two international GISAXS workshops at DESY in 2005 and 2007 and by the strong development of both neutron and X-ray based grazing incidence small angle scattering (GISAS) in the recent years, a conference dedicated to GISAS was held at DESY as a satellite event to the 8th International Conference on Small Angle Scattering (SAS2009) in Oxford. It took place from September 20 to September 23. More than 120 participants attended the conference which started with a welcome evening on Sunday, September 20, followed by three days with an intense program including three keynote lectures, eleven invited lectures, eighteen contributed talks, and two poster sessions with more than 40 contributions. The presentations were grouped in eleven sessions which covered the fields of BioGISAS, polymers and soft matter, GISAS with neutrons, two-dimensional nanocomposites, new methods and instrumentation, magnetic thin films, application of coherence in GISAS, kinetics in two-dimensional systems, and modelling, simulation and data analysis. The PETRA III facilities received special interest in guided tours offered to the participants of the conference.
The keynote lectures where given by M. Ree (U Pohang, Korea) who gave a broad insight into the detailed GISAXS analysis of nanostructures in thin films of block copolymers using synchrotron radiation sources, H. Zabel (U Bochum, Germany) who addressed GISANS and GISAXS for the analysis of magnetic nanostructures, especially showing the perspectives in this field, and T. Russell (U Massachusetts, Amherst, USA) who showed, how macroscopic arrays from block copolymers with high lateral order can be used in ultra-high density magnetic storage materials.

Although the conference was densely packed with presentations it was accompanied by many lively discussions after the presentations, during the poster sessions and coffee breaks, and last but not least at the social evening which took place on a boat on the Elbe river. All participants agreed that the GISAS 2009 was a big success and that it has nicely demonstrated the interdisciplinary importance and power of surface sensitive SAS-techniques.

Group photo of the GISAS2009 participants.

September 24–25:
First international symposium on structural systems biology

The first “International Symposium on Structural Systems Biology” was organised by a consortium led by Hamburg University (Institute of Biochemistry and Molecular Biology, Laboratory for Structural Biology of Infection and Inflammation), including EMBL, DESY, and the Helmholtz Centre for Infection Research. It took place in the main building of the Hamburg University. About 240 participants attended the symposium which was represented by international top-class experts. It addressed current topics in the rapidly growing field of structural systems biology focusing on problems related to the central molecular processes and networks that are of importance for live on a molecular level. Leading scientists from the fields of X-ray structure analysis, electron microscopy, cell- and molecular biology reported on actual results and future trends in the area of structural systems biology. Other talks presented the most recent technological achievements in this field.

The symposium was the first one in a foreseen row and at the same time the starting signal for the planned Centre for Structural Systems Biology (CSSB) which is going to be built on the DESY campus. At this centre, scientists from northern German universities, institutes of the Helmholtz- and Leibniz-Societies, MPG, and EMBL will work interdisciplinary on the analysis of the molecular architecture and dynamics in biological systems by making use of the new light sources at DESY. The close collaboration of physics and biology at DESY will further strengthen the role of Hamburg as an important location for top-class science.

September 29:
Laying of the foundation stone for the CFEL building

A first milestone in the construction of the Center for Free-Electron Laser Science (CFEL) building was achieved with the laying of the foundation stone on September 29. The building is funded by the town of Hamburg at a cost of almost 50 million Euros. It will have over 8000 square meters of office and laboratory space and is going to host up to 300 scientists from all over the world. The completion of the construction is scheduled for late summer 2011.
Despite of the rainy weather approximately 150 people attended the laying of the foundation stone. Dr. Herlind Gundelach, Hamburg’s Senator for Science and Research opened the ceremony with a short greeting. Prof. Dr.-Ing. Hans Siegfried Stiehl, Vice President of the University of Hamburg and the DESY Director of Administration Christian Scherf gave short addresses underlining the importance of CFEL for their organisations. Both speakers acknowledged the town of Hamburg for supporting this new building that enables this interdisciplinary institution to attract the best scientists from all over the world. Prof. Dr. Joachim H. Ullrich, Director of the Max Planck Institute for Nuclear Physics in Heidelberg addressed the audience on behalf of the Max Planck Society, agreeing with the

previous speakers about the importance of CFEL for the three organisations and the town of Hamburg. As current head of the CFEL Management Board, he pointed out the successful start of CFEL and the excellent scientific standing that CFEL has gained in the short time since it was established.

Finally, the four speakers placed the traditional items into the copper time capsule: a local newspaper of the day, current coins, one set of the architects' drawings of the CFEL building, several scientific papers by the CFEL group leaders, and two special items related to the CFEL research - the prototype of a pnCCD detector chip for fast X-ray detection and the CFEL logo drilled in a silicon wafer by a focused ion beam. The copper capsule was then sealed and buried in the central ground plate of the building. At the end of the ceremony, the audience celebrated the event with a small reception in the adjoining PETRA III hall.

Laying of the foundation stone for the CFEL building (From left: H. Gundelach (Hamburg's Senator for Science and Research), C. Scherf (DESY), J. Ullrich (MPG Heidelberg), and H. S. Stiehl (University of Hamburg).

October

October 7:
Nobel Prize in chemistry awarded to Ada Yonath

Prof. Ada E. Yonath receives the Noble Prize in Chemistry 2009 together with Venkatraman Ramakrishnan und Thomas A. Steitz for her research work on structure and function of the ribosome, the complex molecule which builds the protein molecules needed for life on the basis of the information encoded in the DNA. Ada Yonath, born 1939 in Jerusalem, was head of the Max Planck Ribosome Structure Working Group at DESY from 1986 to 2004. With this group she used the synchrotron radiation from the storage ring DORIS to perform groundbreaking X-ray crystallographic work on the way to unveil the detailed molecular structure of the ribosome. By now this structure and its fundamental molecular functionality related to the creation of proteins are known in great detail. This knowledge allows new ways in medicine to design new drugs like antibiotics.

Ada E. Yonath, surrounded by her colleagues and students, at the Nobel Prize press conference at Weizmann Institute in Rehovot, Israel (Photo: Weizmann Institute).

With her idea to reveal the structure of the ribosome Ada Yonath was always searching for the best X-ray sources in the world. Her strength of purpose in this field will be of great benefit for mankind and DESY is proud of having been able to significantly support her outstanding research work.
The Noble Prize to Ada Yonath is especially savoured in the MPG report on pages 68-69.

October 8:
The European XFEL GmbH has been founded

"Now its official and we are legally authorized to operate" Massimo Altarelli and Karl Witte rejoiced on taking up their new functions as Managing Directors of the European XFEL GmbH. Here, the word "we" stands for the "European X-ray Free-Electron Laser Facility GmbH", as the company was officially named upon its registration into the Commercial Register of the Hamburg District Court on October 8. The new company with limited liability under German law is listed as number HRB 111165. Now the project can assume full speed at business level which is of utmost importance to conclude employment contracts, place orders, subcontract machine components, plan the future research operation, etc.
Work for the European XFEL has been in full swing for several years now both at DESY and in the international partner countries of the company. The co-operation between the European XFEL GmbH and DESY will continue to play an important role in the future. On this subject, chapter I, article 2 of the Articles of Association states: "The company and DESY in Hamburg will collaborate on construction, commissioning, and operation of the XFEL on the basis of a long-term agreement."
The foundation of the European XFEL GmbH became possible after representatives from the currently 13 partner states initialled the six different language versions of the international state convention on September 23 in Berlin (China plans to join the project at a later date). To avoid losing time, it was decided to establish the limited liability company with DESY as the first and initially only shareholder. Other shareholders from the partner countries will then join in after signing of the convention.

November

November 2:
MetLife Foundation Award for Medical Research 2010 awarded to Eckhard und Eva-Maria Mandelkow

For their outstanding research on the causes for Alzheimer's disease, the Max Planck scientists Eckhard and Eva-Maria Mandelkow were awarded the renowned "MetLife Foundation Award for Medical Research" 2010. Both scientists and their team work on the DESY campus using synchrotron radiation from the storage ring DORIS III to investigate the molecular causes of Alzheimer's disease.
The award from the US Metropolitan Life Insurance Group that includes 250 000 US dollars prize money will be presented to the two scientists on February 25 next year during an official ceremony in Washington. The prize money will go into further Alzheimer research by the Max Planck working group.

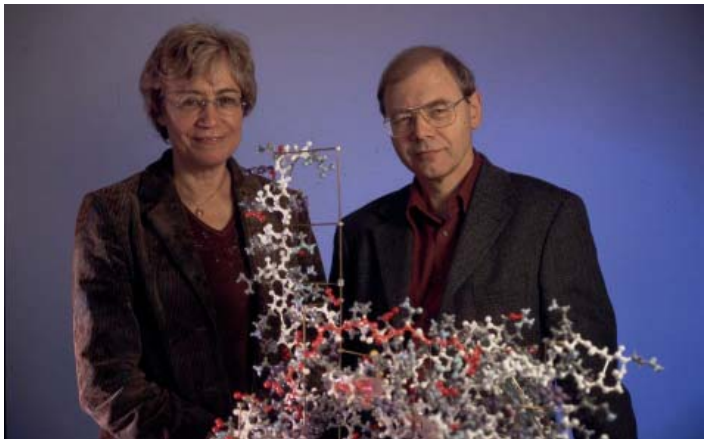

Eva-Maria and Eckhard Mandelkow with a structure model of the motor protein kinosin.

More than one million people in Germany suffer from Alzheimer's, the disease that destroys memory in the human brain. Scientists hope that by knowing the molecular causes of this so far incurable disease it will be possible to find new therapy approaches. For this purpose, they examine the characteristic plaques and tangles – deposits from deficient and function-free proteins that are formed in the brains of patients suffering from Alzheimer's. The intense research of the Max Planck scientists focuses on the protein "Tau". The Tau proteins regulate the composition and decomposition of microtubules, hollow cylindrical structures of the cytoskeleton. In the nerve cells, the microtubules work as "rails" for motor proteins which are responsible for transport in nerve fibres. The Tau proteins are the "sleepers" of these "rails", i.e. they stabilise the microtubules. When they lose their function, the microtubules fall apart, which means transport in the nerve cells collapses. This is exactly what happens in Alzheimer's disease: the molecular structure of the Tau protein is altered, a lot of function-free "protein debris" is deposited in the nerve cells. As a consequence, the cells die.
The Mandelkow working group is studying these molecular proceedings. A number of proteins that take part in this pathological state have been structurally investigated with the help of DESY´s synchrotron radiation. In collaboration with the Hamburg university hospital UKE, the scientists have developed cell and mouse models which mimic Alzheimer's disease, with the purpose of developing more effective therapies.

November 5–6:
Combined workshop on the instruments of sector 6 at PETRA III – 4th workshop on high resolution diffraction and 2nd workshop on the resonant scattering and diffraction beamline

Sector 6 at DESY's new synchrotron radiation facility PETRA III became operational in October 2009. At this sector two independent beamlines are installed: The high resolution diffraction beamline P08 and the resonant scattering and diffraction beamline P09.
Since both beamlines started first operation at the same time and put the main emphasis on scattering and diffraction techniques the workshops were combined to give the user groups a comprehensive overview over the two beamlines and the available infrastructure. Opportunities for co-operation and complementary use of both beamlines were discussed. In particular the talks and posters presented by the future users served as a basis to discuss many scientific and experimental questions related to the instruments. Involved DESY staff members presented talks on the status and the first results of the beamlines and encouraged the users to apply as "robust users" for a first scheduled beamtime in spring 2010.

Attendees of the combined workshop on the PETRA III beamlines of sector 6.

The high resolution diffraction beamline is optimized for experiments with high resolution in reciprocal space using photons in the energy range from 5.4 to 29.4 keV. It features four modes of operation, a "collimating mode" with extremely high resolution but reduced photon flux, a "raw mode" with reduced resolution but highest photon flux, a "focusing mode" using a 200 µm x 20 µm beam spot at the sample with resolution comparable to the "raw mode", and finally a "µ-mode" with 20 µm x 2 µm beam size. The experimental hutch is equipped with a high precision multi circle diffractometer for solid samples and a diffractometer for liquids (LISA, University of Kiel) which allows scanning of angles or photon energy without moving the sample. The resonant scattering and diffraction beamline is a general diffraction instrument with specific options to investigate materials using

resonant X-ray scattering. It operates at photon energies ranging from 2.4 to 50 keV and features focusing up to 24 keV leading to a beam size down to 7 µm x 4 µm. The beamline provides variable linearly and circularly polarized X-rays using an in vacuum phase plate setup. Experiments at low temperatures, high magnetic fields using a 14 Tesla magnet, and high pressure will be possible.

November 7:
A great day for everyone – DESY Open Day 2009

On Saturday, November 7 the DESY campus was open to the public for 12 hours. More than 13 000 visitors came to satisfy their curiosity, to broaden their scientific knowledge, or just for fun. They took the chance to witness live research and to get vivid explanations on research at DESY and the partner institutes. DESY's photon science activities were presented mainly in the experimental halls of FLASH and PETRA III where far more than 100 colleagues from DESY, GKSS, MPG, EMBL, and many partners from Universities were well prepared to show and explain the experimental stations and the scientific work. Many demonstration objects and hands-on experiments were attractions for our visitor of all ages and even our youngest guests enjoyed to see experiments like friction stir welding of chocolate, chocolate marshmallows in the vacuum, and gummy bears on the stretching bank, or to build their own monochromator. All this showed that science can be fun and despite of the bad weather one could clearly feel from the reactions that within the warm and friendly atmosphere of this open day our enthusiasm was transferred to our visitors.
In the afternoon a small ceremony was held in which the new synchrotron radiation source PETRA III was nominated "Selected Landmark" by the "Germany – Land of Ideas" initiative and the Deutsche Bank. When the doors closed at midnight one could state: The Open Day 2009 was a great day for everyone.

The Open Day 2009 was a great day for everyone.

November 10–11:
Workshop on the planned PETRA III extension

The planned shutdown of DORIS III by the end of 2012 will discontinue a number of very successful instruments and techniques not currently implemented at PETRA III. To enable a continuation of these activities in the future, DESY plans to build additional beamlines at PETRA III. This extension project was at the focus of a two-days workshop held on November 10-11 where options for instrumentation at the new endstations were discussed. The extension project has attracted large interest among the HASYLAB user community evidenced by more than 150 registered workshop participants.

The workshop on the PETRA III extension was well received by more than 150 attendees.

The current status of the PETRA III facility was presented by Edgar Weckert who also outlined other ongoing and future projects on the DESY campus linked to research with photons at the different sources on site. Wolfgang Drube described details of the planned PETRA III extension and pointed out the boundary conditions concerning machine parameters and beamline topology in the two arcs of the storage ring where additional experimental halls are planned. He also discussed some ideas for instruments and techniques at the new beamlines.

Preceding this workshop, German user groups were asked to submit letters of intent for new instruments that could be subject of a funding proposal to the federal ministry (BMBF). These LOIs were evaluated by the DESY Photon Science Committee (PSC) and their recommendations were presented by Edgar Weckert at the workshop. The major part of the workshop was devoted to discussions of these LOIs and other specific instrumentation options within 5 working groups addressing different techniques. Summaries of the results were presented on the next day by Bart Vekemans (X-ray micro fluorescence), Ulrich Bismayer (chemical crystallography), Norbert Stribeck (small-angle X-ray scattering), Ronald Frahm (X-ray absorption spectroscopy), and Martin von Zimmermann (high energy X-ray scattering & materials science).

November 16:
Inauguration of PETRA III – Official starting shot for the world's most modern synchrotron radiation source

On November 16 DESY celebrated the inauguration of the world's most modern storage-ring based synchrotron radiation source in a big event with many international guests. PETRA III has already established a record before its final commissioning: the facility produced the world's finest X-ray beam which led Professor Helmut Dosch, Chair of the DESY Board of Directors to the statement: "With PETRA III we inaugurate the world's best synchrotron radiation source of its kind. Its hair-thin high-energy X-ray beams will give researchers from many disciplines the opportunity to obtain an accurate view of nano- and bio-materials, a vital prerequisite for tomorrow's medications and high-performance materials."

From left to right: Jürgen Mlynek, President of the Helmholtz Association, Herlind Gundelach, Hamburg´s Science Senator, Annette Schavan, Federal Minister for Education and Research and DESY Director Helmut Dosch push the start button for PETRA III.

"This facility offers unique perspectives," said Federal Research Minister Annette Schavan in her speech on the occasion of this event. Acknowledging the achievements of the project team around DESY Photon Science Director Professor Edgar Weckert, she said "PETRA III is now inaugurated after a refurbishment of barely two and a half years, within the projected cost and time schedule. This is exemplary. I look forward to the discoveries that will be made with the PETRA III X-ray light." With PETRA III, scientists expect to get fundamental new insights in the structure of matter. "I welcome the plans to build a Centre for Structural Systems Biology (CSSB) in the immediate vicinity of PETRA III", Minister Schavan said. "The collaboration between physicists, biologists, and infection researchers offers great opportunities for important medical applications."

Also the Hamburg Senator for Science and Research Dr. Herlind Gundelach emphasised in her speech that "interdisciplinary projects based on the co-operation of universities with non-university research facilities are a trademark of the Hamburg science region. New large-scale facilities bring about the creation of focal points, for example in the field of structural biology, for which scientific concepts are currently being designed, or for the field of materials science." In this context Senator Gundelach expressed her pleasure about the participation of DESY in four successful clusters of the Federal Excellence Initiative which are all related to the use of PETRA III.

The modernisation of PETRA and the construction of the new experimental hall were jointly funded with 233 million Euros by the German Government (90 %) and the City of Hamburg (10 %). Within the framework of collective research, the Federal Ministry of Education and Research provided additional 12.2 million Euros for experiments in the current funding period, which gives scientists from German universities the opportunity to optimally exploit PETRA III for their research projects.

November 23–25:
The "Science Corridor" - Scientific symposium

The opportunities for scientific co-operation between Northern Germany and the Scandinavian countries were discussed during a symposium that attracted more than 80 participants to meet at DESY from November 23 – 25. This meeting was the third in a series of conferences aiming at the implementation of a dedicated organisational structure to identify, stimulate, and support common research and teaching activities within a "Science Corridor" reaching from Northern Germany northwards towards the Scandinavian countries.
The backbone of this research area is formed by four new world leading research facilities that will be established in Hamburg (European XFEL and PETRA III) and Lund/Copenhagen (ESS and MAX IV). These new facilities together with their associated research communities, other existing facilities, and several universities within the Science Corridor have the potential to form one of the largest science communities worldwide.
The first two days the symposium featured presentations by representatives from universities and research facilities who introduced their scientific portfolio with particular emphasis on materials and life sciences. During the morning of the third day the participants met in three working groups to discuss potential concepts for co-operation not only in these scientific fields but also with respect to organisational and financial aspects. Finally, the chairman of the DESY Directorate, Helmut Dosch,

and the president of the University of Lund, Allan Larsson, signed a “Letter of Intent” as an agreement for future co-operation. A working group consisting of representatives from DESY, MaxLab, the Hamburg universities, and delegates from the participating states and regions within the Science Corridor shall work out detailed plans for co-operation until July 2010.

The participants of the symposium to identify fields of co-operation in the “Science Corridor” between Northern Germany and Scandinavia.

November 26:
First workshop on the high resolution powder diffraction beamline at PETRA III

Beamline experts and users from eight different countries met for this workshop to discuss latest research results and technical developments related to synchrotron X-ray powder diffraction. The first half of the workshop focused on the state of the art in high resolution powder diffraction research and advances in instrumentation at other facilities dedicated to this field. In this context the scientific focus and the design of the new high energy powder diffraction beamline P02.1 at PETRA III was presented to the community. The workshop concluded with presentations from different user groups on a variety of topics that could be implemented at P02.1. The final discussion on the proposed layout indicated overall agreement on the proposed scope of the beamline.

The participants of the high resolution powder diffraction beamline workshop.

November 30:
European XFEL established under international law

With their signatures in the large banquet room of Hamburg’s town hall, representatives from ten nations laid the foundations for the European XFEL under international law. They signed the “Convention concerning the Construction and Operation of a European X-ray Free-Electron Laser Facility” and the “Final Act”. The two documents lay the foundations of the European XFEL project, define the financial contributions of the currently 14 partner countries, and confer the responsibility for the construction and operation of the X-ray free-electron laser facility on the non-profit company European XFEL GmbH.

Ministers, state secretaries and other government representatives from ten partner countries met in the Hamburg City Hall to sign the international European XFEL agreement.

From left to right: Mauro Dell’Ambrogio (State Secretary, State Secretariat for Education and Research, Switzerland), Peter Honeth (State Secretary, Ministry of Education and Research, Sweden), Andrey Fursenko (Minister of Education and Science of the Russian Federation), Prof. Jerzy Szwed (Undersecretary of State, Ministry of Science and Higher Education, Poland), Ole von Beust (First Mayor of Hamburg), Giuseppe Pizza (State Secretary, Ministry for Education, Universities and Research, Italy), Prof. Dr. Frieder Meyer-Krahmer (State Secretary, Federal Ministry for Education and Research, Germany), Dr. Peter Ammon (State Secretary, Federal Foreign Office, Germany), Prof. Mikuláš Šupín (Director General, Division of Science and Technology, Ministry of Education of the Slovak Republic), Dr. Christos Vasilakos (Representative of the ‘General Secretariat for Research and Technology’ in the Permanent Delegation of Greece at the European Union), István Varga (Minister for National Development and Economy, Hungary), Hans Müller Pedersen (Deputy Director General of the Danish Agency for Science, Technology and Innovation), Peter Harry Carstensen (Prime Minister of Schleswig-Holstein)

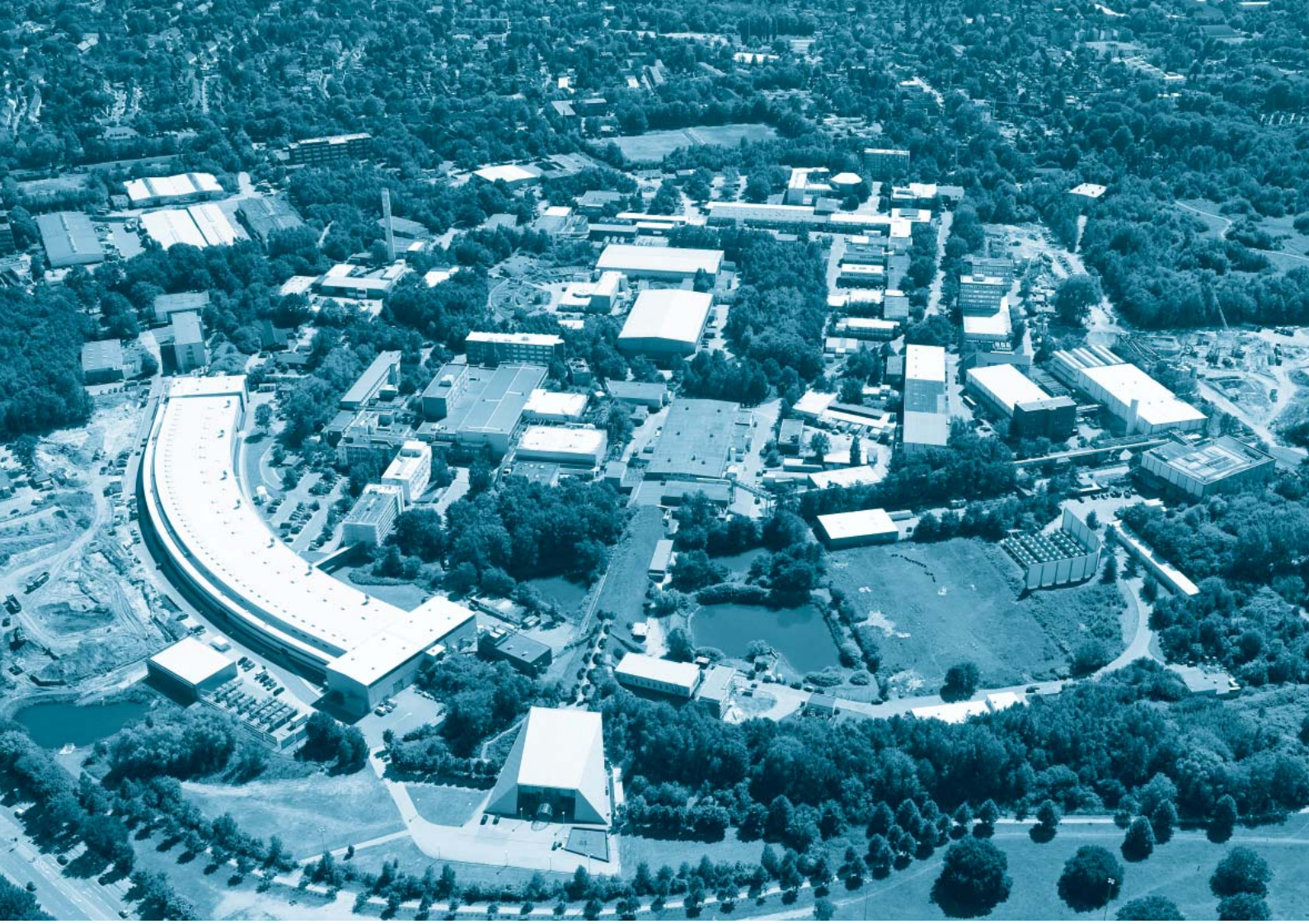

Research Highlights.

Single-shot THz field driven X-ray streak camera.

Measurement of the temporal sub-structure in FLASH's pulses

A few-femtosecond X-ray streak camera for the temporal characterisation of ultrashort pulses produced by a free-electron laser has been realised at FLASH. In this experiment the electric field of an intense terahertz (THz) pulse is used to accelerate photoelectrons which have been ionised by XUV pulses from FLASH.
Borrowing its concept from attosecond metrology, the femtosecond X-ray streak camera fills the gap between conventional streak cameras with typical resolutions of hundreds of femtoseconds and streaking techniques operating in the sub-fs regime. Its single-shot capability permits to determine the duration and time structure of individual X-ray pulses which – at SASE FELs – is known to fluctuate from shot to shot.

Due to the currently employed self-amplified spontaneous emission (SASE) mode of FELs operating in the X-ray range, the pulse duration as well as their detailed temporal profile is subject to erratic fluctuations [1]. For a single-shot measurement of the temporal profile, a new few-femtosecond THz-field driven streak-camera has been realized at FLASH. In this new device the FLASH soft X-ray pulses are collinearly overlapped with synchronized pulses from the FLASH THz undulator [2,3] in a krypton gas target. The gas atoms are ionized by the soft X-ray radiation and the resulting photoelectrons are immediately accelerated by the electromagnetic THz field. The final kinetic energies of the photoelectrons are measured with time-of-flight-spectrometers. The momentum transferred to the electrons due to the acceleration in the THz field depends on the phase of the field at the time of ionization, thus the temporal profile of the ionizing soft X-ray pulse is mapped onto changes of photoelectron energies. This technique is intensively used in attosecond metrology utilizing a near infrared streaking field [4,5,6]. In order to adapt it for the analysis of pulse durations of a few tens of femtoseconds rather than attoseconds, the oscillation period of the streaking field had to be shifted by two orders of magnitude into the THz range.

For any reconstruction of the temporal profile of the soft X-ray pulse duration out of measured streaked photoelectron spectra a precise knowledge of the time dependent streaking THz field is essential. It can be sampled by measuring the field-induced energy shift of the photoelectrons upon scanning the time delay between the THz and the soft X-ray pulses. This energy shift directly represents the vector potential A_{THz} of the THz pulse [7]. Fig. 1a) shows a series of kinetic energy spectra of krypton 4p electrons detached by 13.5 nm FLASH pulses in the presence of 92 µm THz pulses.

To determine the duration and the linear chirp of the FLASH soft X-ray pulses the delay between the soft X-ray and THz pulses was set to a zero-transition of the THz vector potential. Streaked and non-streaked single-shot photoelectron spectra were measured simultaneously in two spectrometres. By comparing the streaked spectra taken at two consecutive zero transitions of A_{THz} an average linear chirp of c = (5 ± 7) meV/fs was determined. For a rapid determination of the pulse dura-

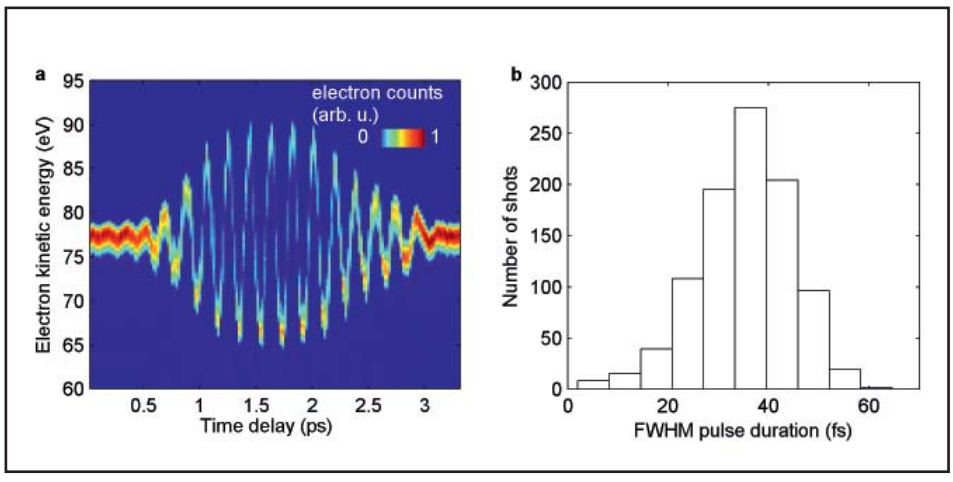

Figure 1

a) Series of kinetic energy spectra of 4p photoelectrons detached from krypton atoms by a 13.5 nm FLASH pulse in the presence of an intense pulsed THz field. The energy shift of the electrons versus the X-ray/THz delay directly maps the vector potential of the THz pulse. Each spectrum represents an average over 25 shots. A band pass filter was used to narrow and smoothen the THz spectrum.

b) Reconstructed FWHM pulse durations of 1000 individual 13.5 nm pulses from FLASH. The average pulse duration was 35 fs with a standard deviation of 9 fs.

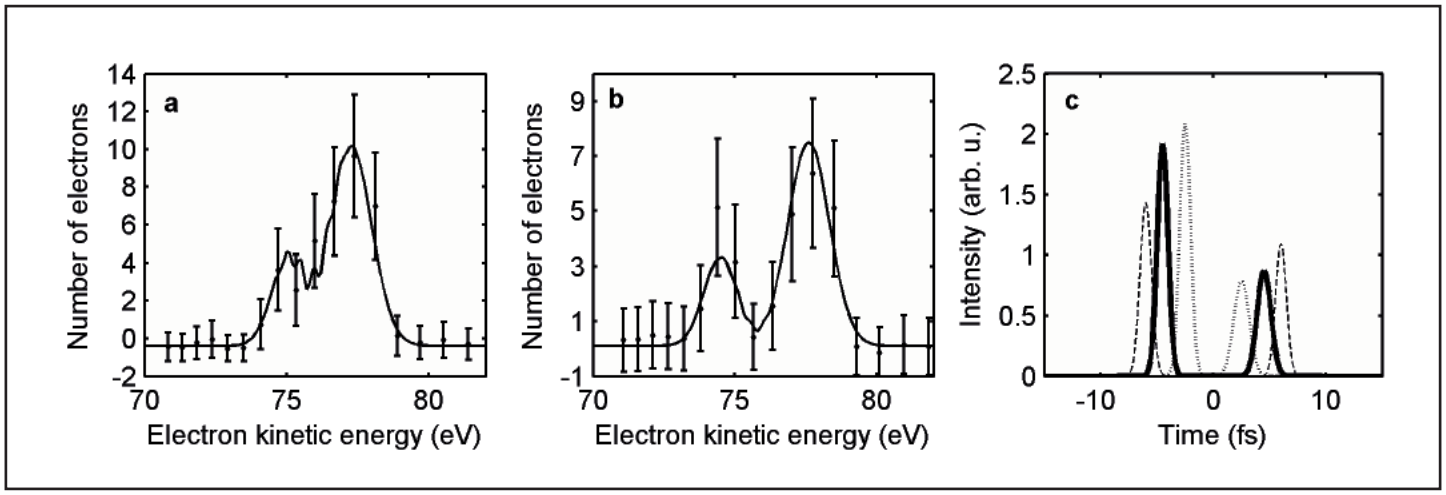

Figure 2

Non-streaked (a) and streaked (b) photoelectron spectra of a single FLASH soft X-ray pulse. Plotted as lines are simulated spectra that best fit the measured ones. The bold line in (c) is the reconstructed temporal structure that best fits the measured spectra. The dashed and dotted lines correspond to the upper and lower limit of the 90 % confidence region for the delay.

tion of many shots a Gaussian pulse shape and a constant linear chirp was assumed. Within this model, the pulse durations of the individual X-ray pulses were reconstructed (Fig. 1b). The average pulse duration was 35 fs FWHM with a standard deviation of 9 fs. A small percentage of the pulses have a pulse duration of less than 7 fs FWHM.

In addition, for some pulses it is possible not only to provide a pulse duration but also to reconstruct a temporal sub-structure consisting of separated spikes. Fig. 2 shows an example of a streaked spectrum with two clearly resolved peaks (b) and the corresponding non-streaked photoelectron spectrum (a). In order to reconstruct the temporal structure of the soft X-ray pulse, two Gaussian sub-pulses were assumed and the corresponding streaked and non-streaked spectra were calculated and optimized to fit the measured spectra. The corresponding temporal structure is plotted as a bold line in fig. 2c. The dashed and dotted curves show temporal structures corresponding to the upper and lower limits of the 90 % confidence region of the fit.

It is demonstrated in this work, that a single-shot characterization of the temporal pulse profile of the intense soft X-rays from FLASH is feasible with a resolution of less than ten fs. Besides that, it was for the first time possible to measure the linear spectral chirp of the FLASH pulses. Since the employed gas target does not dissipate the X-ray beam, it will become possible to measure the X-ray pulse profile simultaneously to other time-resolved experiments. Sorting the measured data according to the X-ray pulse duration should therefore significantly increase the temporal resolution of X-ray -pump/X-ray -probe experiments. It should finally be underlined, that the applicability of the THz-streak camera is not restricted to soft X-rays as delivered from FLASH. Since the principle does not rely on any resonant states and higher electron energies will enhance the streaking, it will also become a valuable tool for the upcoming generation of hard X-ray FELs.

Contact: Markus Drescher, markus.drescher@desy.de

Authors

Ulrike Frühling[1], Marek Wieland[2], Michael Gensch[1,3], Thomas Gebert[2], Bernd Schütte[2], Maria Krikunova[2], Roland Kalms[2], Filip Budzyn[2], Oliver Grimm[2,4], Jörg Rossbach[2], Elke Plönjes[1] and Markus Drescher[2]

1. Deutsches Elektronen-Synchrotron DESY, Notkestr. 85, 22603 Hamburg, Germany
2. Universität Hamburg, Institut für Experimentalphysik, Luruper Chaussee 149, 22761 Hamburg, Germany
3. Helmholtz-Zentrum Berlin, Albert-Einstein-Str. 15, 12489 Berlin, Germany
4. ETH Zürich, Institut für Teilchenphysik, Schafmattstr. 20, CH - 8093 Zürich, Switzerland

Original publication

"Single-shot terahertz field-driven X-ray streak-camera", Nature Photonics 3, 523–528 (2009).

References

1. **W. Ackermann et al., "Operation of a free-electron laser from the extreme ultraviolet to the water window", Nature Photon. 1, 336-342 (2007).**
2. **B. Faatz et al., "Development of a pump-probe facility combining a far-infrared source with laser-like characteristics and a VUV free electron laser", NIM A 475, 363-367 (2001).**
3. **M. Gensch et al., "New infrared undulator beamline at FLASH", Infrared Phys. Techn. 51, 423-425 (2008).**
4. **M. Drescher et al., "X-ray pulses approaching the attosecond frontier"; Science 291, 1923-1927 (2001)**
5. **R. Kienberger et al., "Atomic transient recorder", Nature 427, 817-821 (2004)**
6. **J. Itatani et al., "Attosecond streak camera"; Phys. Rev. Lett. 88, 173903 (2002).**
7. **E. Goulielmakis et al., "Direct measurement of light waves"; Science 305, 1267-1269 (2004)**

Creating transparent aluminium with FLASH.

Saturable absorption by ultra-intense and ultra-short soft X-ray photoionization

When focussed to sub-micrometre spot sizes, the free-electron laser FLASH reaches record intensities over 10^{16} W/cm² in the soft X-ray wavelength regime. With these extreme intensities it was possible to saturate the absorption of an L-shell transition in aluminium at 13.5 nm (92 eV photon energy): The samples become transparent for soft X-rays. This has never been observed before and is an ideal method to create homogenous warm dense matter, which is highly relevant to planetary science, astrophysics and inertial confinement fusion.

A well-known phenomenon in the visible and near-visible region of the electromagnetic spectrum is saturable absorption, where the absorption of light decreases with increasing intensity [1]. With the FEL light source FLASH, due to the short pulse duration (~15 fs) [2] and the high intensities (up to 10^{16} W/cm²) with ~1 µm focussing, it was possible to saturate an L-shell transition in aluminium. The aluminium sample predominantly absorbs the 92 eV photons via L-shell photoionization and becomes transparent during the duration of the FLASH photon pulse. Because of the high intensities the photoionization rate surpasses the recombination rate, leading to a severe depletion of the inner-shell absorbers. This process leads to the storage of ~100 eV per atom which in turn evolves to a warm dense matter (WDM) state reaching temperatures of about 25 eV (~290 000 K) by subsequent Auger decays. This manner of creation leads to highly uniform warm dense matter conditions, which are of great interest in high-pressure science [3], the geophysics of large planets [4], astrophysics [5], plasma production and inertial confinement fusion [6]. In the experiment the collimated FEL beam was focused onto 53 nm thick solid aluminium samples using a Mo/Si multilayer-coated off-axis parabola with a focal length of 269 mm [7]. The best focus was determined by using Nomarski optical microscopy and atomic force microscopy (AFM) to look offline at damage craters induced by irradiating polymethyl methyacrylate (PMMA) at low FEL fluences [8]. With this method the focal spot size in best focus has been determined to 1.5 µm. By changing the FEL pulse energy and varying the sample position, three orders of magnitude of FEL fluence were scanned. The transmission of 53-nm-thick aluminium was measured as a function of FEL fluence using a silicon photodiode. The measurements were done on a single shot basis irradiating always a fresh, non-irradiated aluminium sample. The resulting transmission curve is shown in Fig. 1. At low fluences (~1 J/cm²) our experimental transmission data matches very well the values which one would expect for transmission through 53 nm thick cold aluminium taking into account 10 nm thick aluminium oxide layers on either side

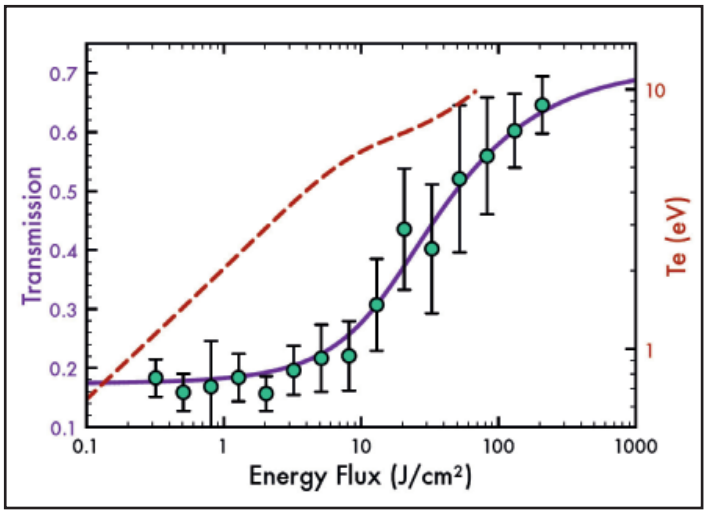

Figure 1

Transmission of aluminium target as a function of fluence. The circles represent the experimental data points; the solid line is the theoretical prediction (for more details please refer to the published paper). The dashed curve is the predicted electron temperature in electronvolts (right Y-axis) in the valence band after the FEL pulse has passed, but before the L-shell holes are filled and the Auger recombination heats the band further.

of the sample. At higher fluences (3-200 J/cm², with a pulse duration of ~15 fs this corresponds to a maximal irradiance of $1.5 \cdot 10^{16}$ W/cm²) the material becomes more and more transmissive (up to 65 %). At these intensities, the fraction of aluminium atoms with an L-shell hole is very high (almost 100%). Since the missing L-shell electron does not screen the atomic core any longer, the L-edge of the atom increases to 93 eV. Therefore the FEL is not further able to eject a second L-shell electron, which leads to a quenching of the bound-free absorption. The absorption coefficient is reduced to the value of the free-free absorption coefficient which is about two orders of magnitude lower. The lifetime of the L-shell hole is estimated to be around 40 fs, significantly longer than the FEL pulse duration, but short compared to the electron-phonon coupling times

(~1 ps), or hydrodynamic motion, when the ions are heated. The hole will be refilled by means of either radiative decay, or the dominant Auger decay. This Auger decay leads finally to the heating of the electrons (up to 25 eV at highest fluences) which were, after the FEL pulse has passed the sample, relatively cold (up to 9 eV at highest fluences, see Fig. 1). Information about the electron distribution in the valence band can be inferred from soft X-ray emission spectra. In a separate experiment such spectra have been measured at relatively low fluences and are shown in Fig. 2. The spectra show the radiative recombination of the valence band electrons into the L_{III} and L_{II} levels. The emission ranges from ~62 eV (energy difference between the L levels and the bottom of the valence band) to a thermally broadened region at an energy corresponding to the difference between the Fermi energy and the L-shell (an energy of around the L-edge at 73 eV). The thermal broadening at higher fluences is clearly visible and from the shape of the spectrum the electron temperature at emission time can be inferred.

In summary, we have created a very transient exotic state of highly ionized crystalline matter, where electrons are heated to several eV directly after the FEL pulse has passed, while at this time the ions are still at the origin positions at room temperature. This allows us to create very homogenous warm dense matter conditions: for example at a fluence of 100 J/cm² (50 % of the FEL pulse is absorbed) the temperature difference between the front and the back of the aluminium is calculated to be only 5 %. What needs to be further explored, is how this transient state finally evolve into equilibrated WDM. However, physical properties of this exotic state are largely unknown. Therefore accurate measurements of electron-phonon coupling times and ion-ion interactions at these WDM conditions are still needed.

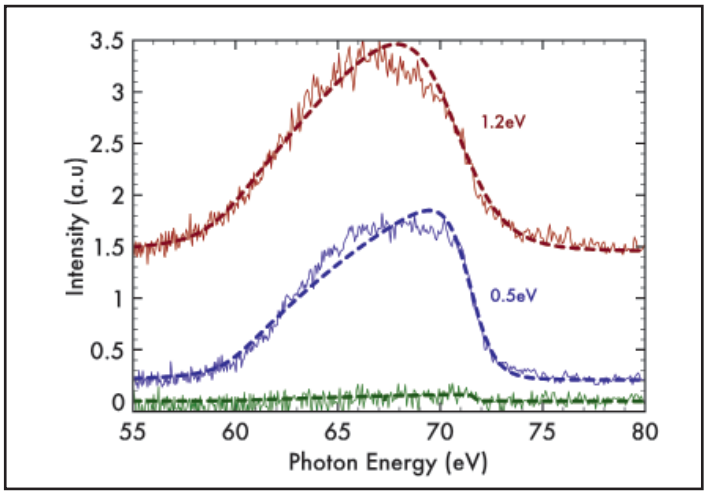

Figure 2

Recorded X-ray emission spectra from aluminium at three different fluences (0.6 J/cm², 0.3 J/cm², 0.04 J/cm², corresponding to the red, blue, and green spectrum). Shown is the radiative recombination of the valance band to the LIII and LII levels. The spectra have been fitted giving different electron temperatures (1.2 eV, 0.5 eV, and 0.1 eV). The spectra are offset for clarity

Contact: Bob Nagler, bnagler@slac.stanford.edu
Sven Toleikis, sven.toleikis@desy.de

Authors

Bob Nagler[1], Ulf Zastrau[2], Roland R. Fäustlin[3], Sam M. Vinko[1], Thomas Whitcher[1], A. J. Nelson[4], Ryszard Sobierajski[5,6], Jacek Krzywinski[7], Jaromir Chalupsky[8], Elsa Abreu[9], Saša Bajt[3], Thomas Bornath[10], Tomas Burian[8], Henry Chapman[11,12], Jaroslav Cihelka[8], Tilo Döppner[4], Stefan Düsterer[3], Thomas Dzelzainis[13], Marta Fajardo[9], Eckhart Förster[2], Carsten Fortmann[10], Eric Galtier[14], Siegfried H. Glenzer[4], Sebastian Göde[10], Gianluca Gregori[1], Vera Hajkova[8], Phil Heimann[15], Libor Juha[8], Marek Jurek[5], Fida Y. Khattak[16], Ali Reza Khorsand[6], Dorota Klinger[5], Michaela Kozlova[9], Tim Laarmann[3], Hae Ja Lee[17], Richard W. Lee[4], Karl-Heinz Meiwes-Broer[10], Pascal Mercere[18], William J. Murphy[1], Andreas Przystawik[10], Ronald Redmer[10], Heidi Reinholz[10], David Riley[13], Gerd Röpke[10], Frank Rosmej[14], Karel Saksl[19], Romain Schott[14], Robert Thiele[10], Josef Tiggesbäumker[10], Sven Toleikis[3], Thomas Tschentscher[20], Ingo Uschmann[2], Hubert J. Vollmer[4] and Justin S.Wark[1]

1. Department of Physics, Clarendon Laboratory, University of Oxford, Parks Road, Oxford, OX1 3PU, UK
2. Institut für Optik und Quantenelektronik, Friedrich-Schiller-Universität, Max-Wien-Platz 1, 07743 Jena, Germany
3. Deutsches Elektronen-Synchrotron DESY, Notkestrasse 85, 22607 Hamburg, Germany
4. Lawrence Livermore National Laboratory, 7000 East Avenue, Livermore, California 94550, USA
5. Institute of Physics, Polish Academy of Sciences, Al. Lotnikow 32/46, 02-668 Warsaw, Poland
6. FOM-Institute for Plasma Physics Rijnhuizen, NL-3430 BE Nieuwegein, The Netherlands
7. SLAC National Accelerator Laboratory, 2575 Sand Hill Road, Menlo Park, California 94025, USA
8. Institute of Physics, Academy of Sciences of the Czech Republic, Na Slovance 2, 182 21 Prague 8, Czech Republic
9. GoLP/IPFN, Instituto Superior Tecnico, 1049-001 Lisboa, Portugal
10. Institut für Physik, Universität Rostock, 18051 Rostock, Germany
11. Centre for Free-Electron Laser Science, DESY, 85 Notkestrasse, 22607 Hamburg, Germany
12. Universität Hamburg, Luruper Chaussee 149, 22761 Hamburg, Germany
13. Queen's University Belfast, University Road, Belfast, BT7 1NN, Northern Ireland, UK
14. UPMC, 4 place Jussieu 75005 Paris, France
15. Lawrence Berkeley National Laboratory, 1 Cyclotron Road, California 94720, USA
16. Department of Physics, Kohat University of Science and Technology, Kohat-26000, NWFP, Pakistan
17. Department of Physics, 366 LeConte Hall, University of California, Berkeley, California 94720, USA
18. SOLEIL, L'Orme des Merisiers Saint-Aubin, BP 48 91192 GIF-sur-YVETTE, France
19. Institute of Materials Research, Slovak Academy of Sciences, Watsonova 47, 040 01 Kosice, Slovak Republic
20. European XFEL GmbH, Albert-Einstein-Ring 19, 22761 Hamburg, Germany

Original publication

"Turning solid aluminium transparent by intense soft X-ray photoionization", Nature Physics 5, 693 (2009).

References

1. **G.N. Lewis, D. Lipkin, and T.T. Magel, "Reversible photochemical processes in rigid media. A study of the phosphorescent state", J. Am. Chem. Soc. 63, 3005-3018 (1941).**
2. **W. Ackermann et al., "Operation of a free-electron laser from the extreme ultraviolet to the water window", Nature Photonics 1, 336–342 (2007).**
3. **R. Davidson, "Frontiers in High Energy Density Physics: The X-Games of Contemporary Science", National Academies Press (2003).**
4. **T. Guillot, "Interiors of giant planets inside and outside the solar system", Science 286, 72-77 (1999).**
5. **M. Turner, "Connecting Quarks with the Cosmos: Eleven Science Questions for the New Century", National Academies Press (2003).**
6. **J.D. Lindl et al., "The physics basis for ignition using indirect-drive targets on the National Ignition Facility", Phys. Plasmas 11, 339-491 (2004).**
7. **A.J. Nelson et al., "Soft X-ray free-electron laser microfocus for exploring matter under extreme conditions", Opt. Exp. 17, 18271 (2009).**
8. **J. Chalupský et al., "Characteristics of focused soft X-ray free-electron laser beam determined by ablation of organic molecular solids", Opt. Express 15, 6036-6043 (2007).**

FLASH light on magnetic materials.

First resonant magnetic scattering experiments at FLASH.

The quest for smaller and faster magnetic storage devices is a formidable challenge in modern magnetism research. Ideally, one would like to probe elementary magnetization dynamics such as spin-flip processes and their coupling to the electronic system on their intrinsic time scales in the femtosecond (fs) regime. At the same time nanometer spatial resolution and element-specific information is required in order to account for the complex composition of technologically relevant magnetic media and devices. Simultaneous fulfilment of these requirements mandates ultrafast magnetic scattering experiments using flashes of resonantly tuned soft X-rays, in particular for the technologically relevant transition metals Cr, Mn, Fe, Co, and Ni. We report here on the first resonant magnetic scattering experiment using soft X-ray pulses generated from the free-electron laser FLASH at DESY.

FLASH provides uniquely intense coherent short pulses in the extreme ultraviolet (EUV) energy range with the shortest fundamental wavelength of 6.5 nm. Evidence for lasing at higher harmonics of the fundamental mode has been reported recently [1]. Using the fundamental wavelength of FLASH at 7.97 nm we were able to detect the 5th harmonic at a wavelength of 1.59 nm with an average energy of 4 nJ per pulse and a relative spectral bandwidth of 0.7- 0.9 %. We demonstrated the feasibility of resonant magnetic scattering at an FEL source by using a Co/Pd multilayer as prototype sample that was illuminated with 20 femtosecond-long soft X-ray pulses tuned to the Co L_3 absorption edge at 778.1 eV (1.59 nm).

FLASH was operated at the fundamental with an average energy per pulse of 15 µJ and 10 fs pulse duration. Self amplified spontaneous emission (SASE) soft X-ray radiation at the fifth harmonic (778.1 eV photon energy) was thus in resonance with the magnetically dichroic transitions of Co $2p_{3/2}$ electrons and providing magnetic scattering contrast for the experiment. The experiment has been performed at the FLASH beamline PG2 [2] (Fig. 1). A plane grating monochromator separates the fifth harmonic from the other wavelengths contained in the FEL beam. The carbon coated optical elements (optimized for FLASH fundamental wavelengths) lead to a low beamline transmission coefficient of 2.3×10^{-4} at 1.59 nm. Due to this fact, only

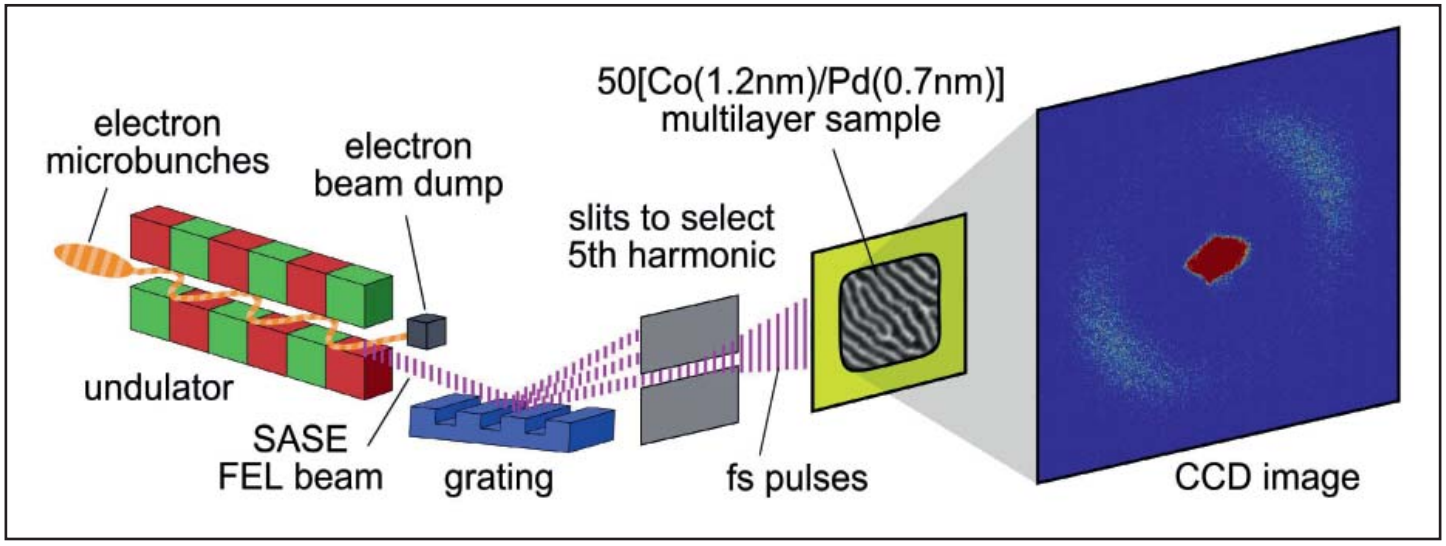

Figure 1

Scheme of the experimental setup. Flashes of soft X-ray laser light are produced by self-amplified stimulated emission (SASE) in a planar undulator with a photon wavelength of λ=7.97 nm in the fundamental mode. A plane grating monochromator is used to select the fifth harmonic with λ=1.59 nm, matching the energy of the Cobalt L_3 edge. A resonant magnetic scattering signal from a Co/Pd multilayer sample exhibiting a magnetic domain structure is recorded on a CCD detector.

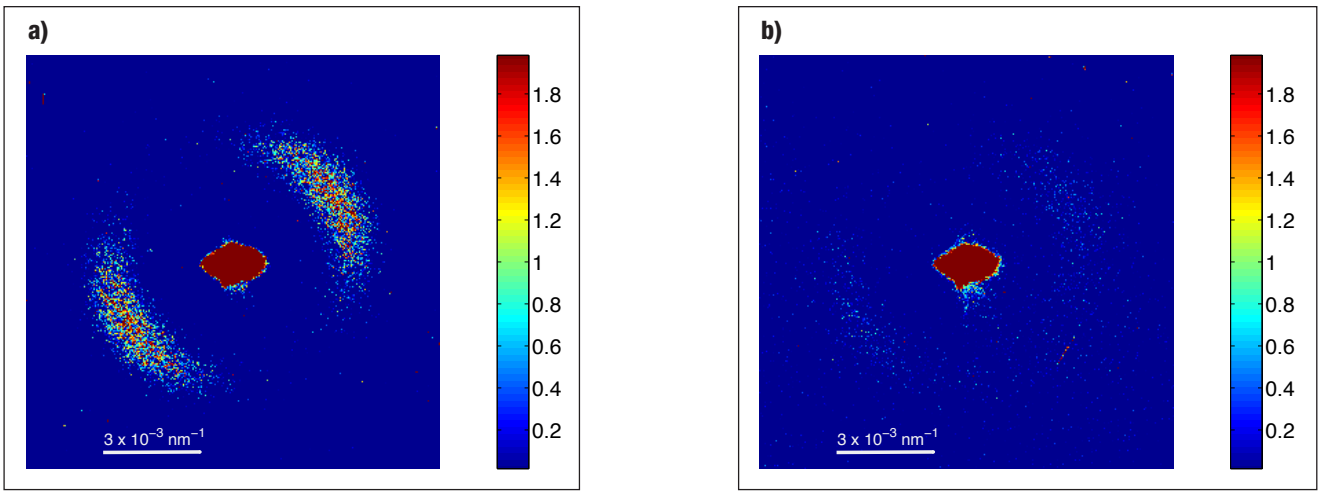

Figure 2

(a) CCD image of the magnetic diffraction pattern recorded with soft X-ray SASE laser light at a wavelength of 1.59 nm (Co L_3 edge, photon energy 778.1 eV). The pattern originates from the magnetic domain structure of a Co/Pd multilayer. The intensity maximum reflects the average periodicity of an up-down domain pair of 190 nm. The asymmetry is due to a preferred orientation of the domains – a so-called aligned state. The colour bar indicates the number of photons recorded per pixel.

(b) CCD image of the magnetic diffraction pattern recorded with a photon energy of 783.5 eV, slightly off-resonance.

7×10^3 photons per pulse were available for the experiment here. Using the soft X-ray SASE photons we demonstrated resonant magnetic diffraction with a $[Co(1.2nm)/Pd(0.7nm)]_{50}$ multilayer sample in transmission geometry. In multilayer samples of this composition magnetic domains with alternating up and down magnetization form with a typical spatial correlation length of the order of 200-300 nanometers. Fig. 2a shows the measured magnetic scattering pattern with a pronounced small-angle signal. The observed intensity maximum at a wavevector transfer of $q_{max} = 0.033$ nm^{-1} reflects the mean distance of 190 nm between two domains with the same orientation of the magnetic moment which implies a domain size of about 95 nm. The diffraction pattern has been recorded within 1000 seconds and contains 6.7×10^4 scattered photons.

Detuning the photon energy away from the resonance reduces the magnetic scattering contrast. Figure 2b shows the CCD image measured with a photon energy of 783.5 eV, which is slightly off resonance. The scattered intensity has decreased considerably leading to a very weak small angle scattering ring. Taking the relatively large bandwidth into account we estimate, with the help of the energy dependent magnetic scattering factors, a signal reduction of a factor 4-6, which is in good agreement with the observation. However, we would like to point out that this bandwidth is sufficient to generate contrast for resonant magnetic scattering. This implies that there is no narrow bandwidth monochromator required. As a result, the beamline transmission losses could be easily reduced by two to three orders of magnitude with suitably designed optical elements.

In conclusion, we have demonstrated that the higher harmonics of FLASH reach well into the soft X-ray regime, and provide access to the absorption edges of the 3d transition metals. In particular, we have demonstrated the feasibility of resonant magnetic scattering using soft X-ray laser pulses via the 5th harmonic. This opens the way for measuring element-specific magnetization dynamics on femto- and picosecond timescales and on nanometer spatial length scales.

Optimized setups for soft X-ray wavelengths will lead to intensity gains of 2-3 orders of magnitude which will make optical pump and X-ray diffraction probe measurements possible at FLASH by using a single FEL pulse. The high intensities delivered on ultrafast timescales in combination with the high degree of spatial coherence of the FEL radiation will allow in the future the measurement of element specific spatial correlation functions in magnetic systems.

Contact: Christian Gutt, christian.gutt@desy.de

Authors

C. Gutt[1], L.-M. Stadler[1], S. Streit-Nierobisch[1], A. Mancuso[1], A. Schropp[1], B. Pfau[2], C.M. Günther[2], R. Könnecke[2], J. Gulden[1], B. Reime[1], J. Feldhaus[1], E. Weckert[1], I.A. Vartanyants[1], O. Hellwig[3], F. Staier[4], R. Barth[4], M. Grunze[4], A. Rosenhahn[4], D. Stickler[5], H. Stillrich[5], R. Frömter[5], H.P. Oepen[5], M. Martins[6], T. Nisius[7],T. Wilhein[7], B. Faatz[1], N. Guerassimova[1], K. Honkavaara[1], V. Kocharyan[1], R. Treusch[1], E. Saldin[1], S. Schreiber[1], E.A. Schneidmiller[1], M.V. Yurkov[1], S. Eisebitt[2,8], and G. Grübel[1]

1. Deutsches Elektronen-Synchrotron DESY, Notkestraße 85, D-22607 Hamburg, Germany
2. Helmholtz-Zentrum Berlin für Materialien und Energie GmbH, Glienicker Str. 100, D-12409 Berlin, Germany
3. Hitachi Global Storage Technology, 650 Harry Road, San Jose, CA 95120, USA
4. Institut für Physikalische Chemie, Universität Heidelberg, Im Neuenheimer Feld 229, D-69120 Heidelberg, Germany
5. Institut für Angewandte Physik, Universität Hamburg, Jungiusstraße 11, D-20355 Hamburg, Germany
6. Institut für Experimentalphysik, Universität Hamburg, Luruper Chaussee 149, D-22761 Hamburg, Germany
7. Institute for X-ray-Optics, RheinAhr-Campus Remagen, FH Koblenz, Südallee 2, D-53424 Remagen, Germany
8. TU Berlin, Institut für Optik und Atomare Physik, Hardenbergstr. 36, D-10623 Berlin

Original publication

"Resonant magnetic scattering with soft X-ray pulses from a free-electron laser operating at 1.59 nm", Phys Rev B 79, 212406 (2009)

References

1. **W. Ackermann et al. Nature Photonics 1, 336-342 (2007)**
2. **M. Martins, M. Wellhöfer, J.T. Hoeft, W. Wurth, J. Feldhaus and R. Follath, Rev. Sci. Instrum. 77, 115108, 1-6 (2006)**

FLASH excites giant atomic resonance.

Gas and light, unite!

FLASH produces the highest irradiance of extreme ultraviolet (EUV) and soft X-ray pulses in the world. When these pulses are focused even further by a spherical multi-layer mirror developed for EUV lithography, the levels of irradiance can reach 10^{16} W cm^{-2} [1]. The mechanism of light-matter interaction is not very well understood at these wavelengths and extremely high irradiance levels and needs to be investigated to further our understanding about the structure of atomic matter and the photoelectric effect. Our measurements show that the nature of the interaction between the EUV light and matter is heavily dependent on the atomic structure of the target and the excitation of strong resonances.

Different rare gases were investigated under equivalent conditions in the microfocus region of the mirror. The mirror could be moved along the FEL beam to shift the position of the focus in and out of the interaction region of the gases, therefore allowing us to control the levels of photon intensity and the beam diameter. As a result, the beam irradiance varied between 10^{12} and 2 x 10^{16} W cm^{-2}, while the beam diameter varied between 4 and 200 µm. The gases filled the chamber homogeneously to a pressure of about 10^{-4} Pa.

The results of our experiments at FLASH showed that xenon became significantly more ionized than the other gases. The highest charge state seen for xenon in the range between 1.5 and 1.7 x 10^{15} W cm^{-2} was Xe^{14+}, whereas the other gases, neon, argon, and krypton, were only excited up to 7+, as shown in Figures 1 and 2. If the difference in the charge states between xenon and the other gases was based on the molecular weight or number of valence shell electrons of the gases, the numbers would be expected to be non-uniform. However, the much higher achieved charge state of xenon offers the tantalizing possibility that the 4d resonance around 13.7 nm may be responsible. Standard non-perturbative theories that are used to model the excitation of gases (like the Keldysh theory) are not dependent on the type of gas used, but rather the properties of the photon beam [2-4].

Furthermore, the 4d giant resonance in xenon and the subsequent elements in the periodic table represent prime examples for strong electron correlation within an atomic system [6,7].

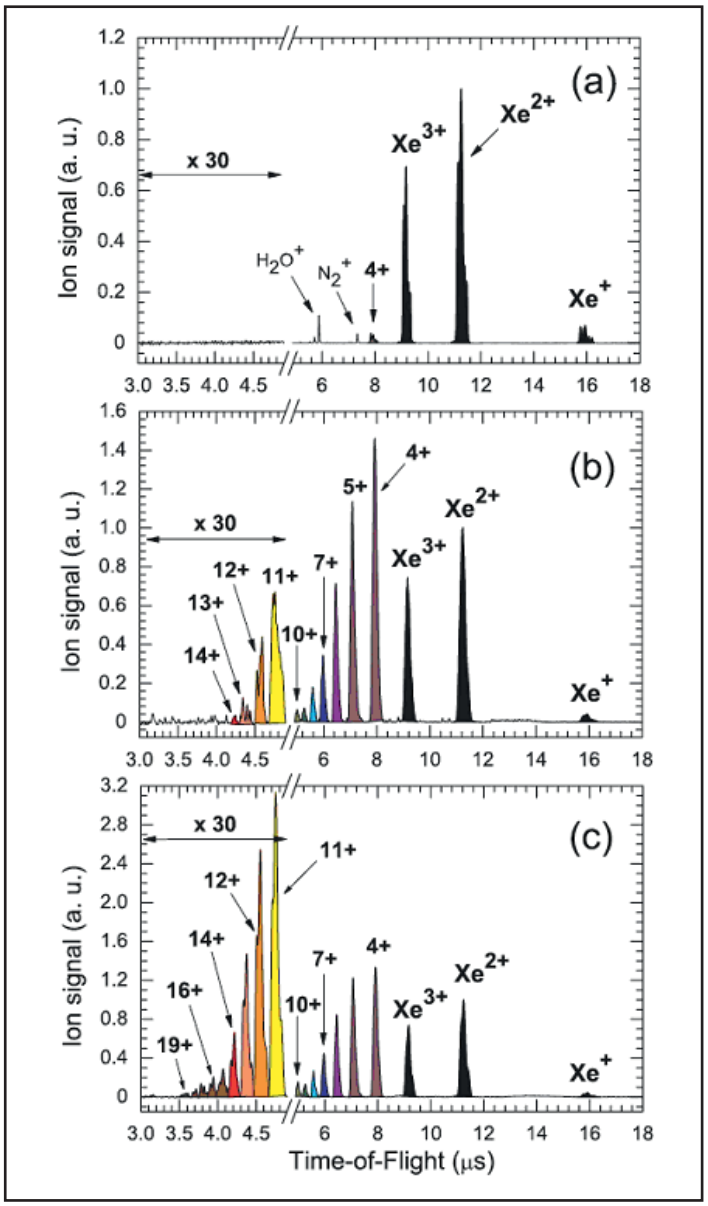

Figure 1

Ion time-of-flight (TOF) mass-to-charge spectra of xenon (Xe) taken at 90.5 eV photon energy and irradiance levels of (a) 2.5 x 10^{12} W cm^{-2}, (b) 1.7 x 10^{15} W cm^{-2}, and (c) 2.0 x 10^{15} W cm^{-2}. Signals from residual gas are also indicated.

The correlations may be described by a collective motion of a full ensemble of quantum particles, where the ten electrons of the xenon 4d shell, driven by the oscillating electromagnetic field of the FEL, emit one of their members. The mechanism is in analogy to nuclear giant resonances of protons and neutrons, or plasmon excitation in solids and has been applied, for many years, to describe atomic giant resonances at low irradiances [5-6]. The application of this idea to high irradiance can explain our xenon results: due to the higher amplitudes, the collective oscillations within the 4d shell may lead to the emission of more than one 4d electron, up to all ten, simultaneously and coherently. Subsequent Auger decay cascades result in the higher charge states.

A direct multiple ionization of xenon in the inner 4d shell represents, however, a higher order effect and is expected to principally occur at the higher irradiance levels. Each additional 4d electron simultaneously emitted should affect the corresponding ion spectrum because it is related to additional energy transferred to the atom. The sudden rise of the higher charge states from Xe^{15+} to Xe^{19+} when we increased the irradiance from 1.7 to 2 x 10^{15} W cm^{-2}, demonstrated in Fig. 1(b) and 1(c), might indicate such a step in the direct multiple 4d ionization.

In conclusion, our comparative rare-gas study at FLASH and the particular behaviour of xenon show that the interaction of high-power lasers with matter cannot be described the same way in the optical and ultraviolet regime. Nonperturbative theories based on ponderomotive motion of quasifree electrons are not applicable. On the other hand, the inner shell electrons structure, electron correlation, and resonances play a significant role in explaining strong-field phenomena on photoionization in the short-wavelength regime of Einstein's photoelectric effect. First theoretical approaches to explain our xenon results have recently been published [7-8], starting a lively debate about the nature of this effect. We hope to stimulate further theoretical investigation, particularly of the role of giant resonances and collective effects on photoionization in the high-intensity short-wavelength regime.

Contact: Pavle Juranić, pavle.juranic@desy.de

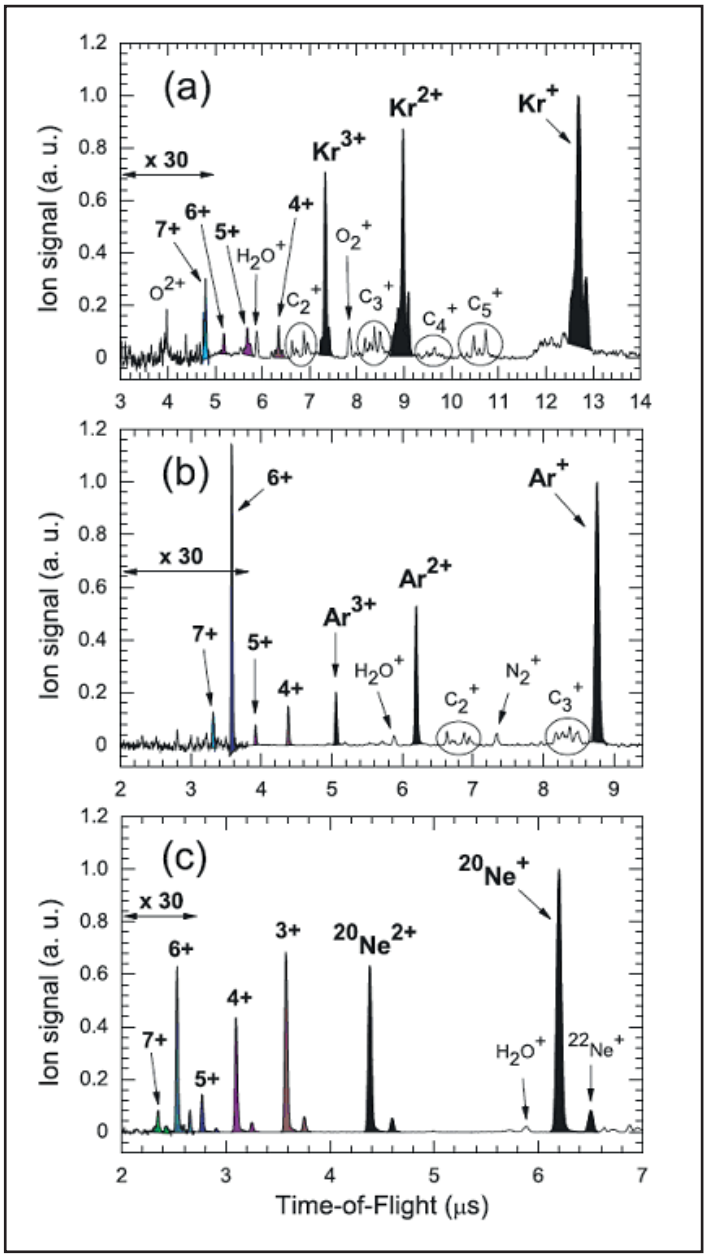

Figure 2

Ion time-of-flight (TOF) mass-to-charge spectra of (a) krypton (Kr), (b) argon (Ar), and (c) neon (Ne), taken at 90.5 eV photon energy and irradiance levels between 1.5 and 1.8 x 10^{15} W cm^{-2}.

Authors

P. N. Juranić[4], M. Richter[1], M.Ya. Amusia[2], S.V. Bobashev[2], T. Feigl[3], M. Martins[5], A. A. Sorokin[1,2], and K. Tiedtke[4]

1. Physikalisch-Technische Bundesanstalt, Abbestraße 2-12, 10587 Berlin, Germany
2. Ioffe Physico-Technical Institute, Polytekhnicheskaya 26, 194021 St. Petersburg, Russia
3. Fraunhofer-Institut für Angewandte Optik und Feinmechanik, Albert-Einstein-Straße, 07745 Jena, Germany
4. Deutsches Elektronen-Synchrotron, Notkestraße 85, 22603 Hamburg, Germany
5. Universität Hamburg, Institut für Experimentalphysik, Luruper Chaussee 149, 22761 Hamburg, Germany

Original publication

"Extreme Ultraviolet Laser Excites Atomic Giant Resonance", Phys. Rev. Lett. 102, 163002 (2009).

References

1. **A. A. Sorokin, S.V. Bobashev, T. Feigl, K. Tiedtke, H. Wabnitz, and M. Richter, Phys. Rev. Lett. 99, 213002 (2007).**
2. **L.V. Keldysh, Sov. Phys. JETP 20, 1307 (1965).**
3. **M. Protopapas, C. H. Keitel, and P. L. Knight, Rep. Prog. Phys. 60, 389, and references therein (1997).**
4. **N. Delone and V. Krainov, Multiphoton Processes in Atoms (Springer, New York, 2000), and references therein.**
5. **J. P. Connerade, J. M. Esteva, and R. C. Karnatak, "Giant Resonances in Atoms, Molecules, and Solids" and references therein, Plenum Press, New York (1987).**
6. **M.Ya. Amusia and J.-P. Connerade, Rep. Prog. Phys. 63, 41 (2000).**
7. **S.V. Popruzhenko, V. D. Mur, V. S. Popov, and D. Bauer, Phys. Rev. Lett. 101, 193003 (2008).**
8. **M. G. Makris, P. Lambropoulos, and A. Mihelic, Phys. Rev. Lett. 102, 033002 (2009).**

Coherent-pulse 2D crystallography at free-electron lasers.

Towards higher resolution at the world's brightest light sources

Crystallization and radiation damage are presently bottlenecks in protein structure determination. We propose to use two-dimensional (2D) finite crystals and ultrashort free-electron laser (FEL) pulses to reveal the structure of macromolecules. This can be especially important for membrane proteins that in general do not form 3D crystals, but easily form 2D crystalline structures. We have demonstrated single pulse train coherent diffractive imaging for a finite 2D crystalline sample, and conclude that this alternative approach to single molecule imaging is a significant step towards revealing the structure of proteins with sub-nanometer resolution at the newly built X-ray free-electron laser (XFEL) sources.

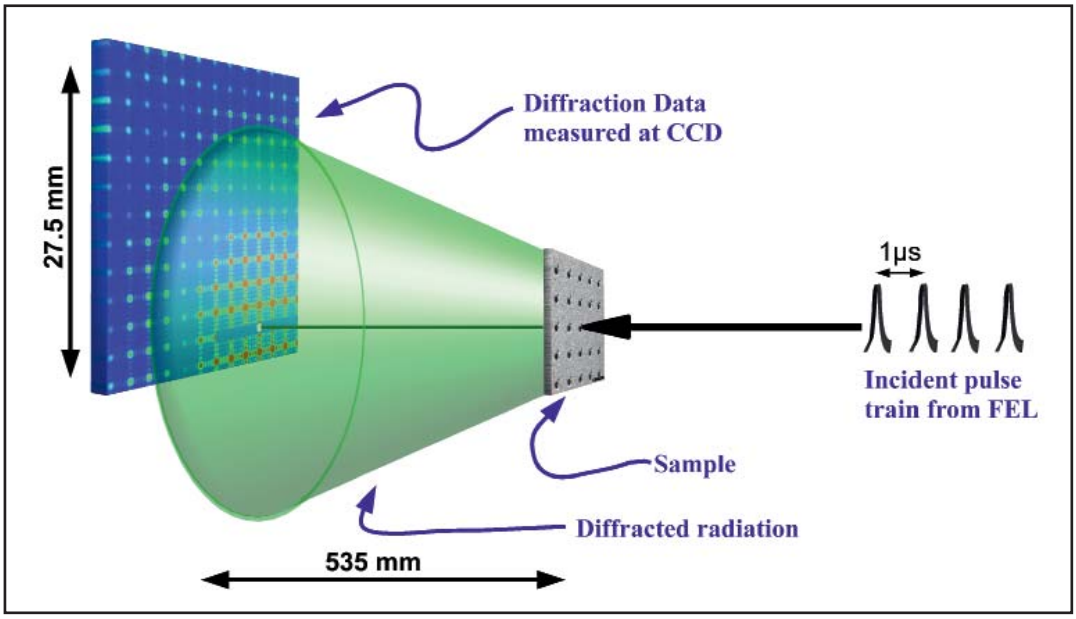

Figure 1
A sketch of the experiment. The beam from the beamline first interacts with the sample, and then the diffracted radiation propagates to a CCD detector. To enhance the measured resolution of the data the direct beam was incident near the corner of the detector.

Revealing the structure of protein molecules is mandatory for understanding the structure of larger biological complexes. The major progress in uncovering the structure of proteins in past decades was due to the development of phasing methods [1] allowing the determination of the structure of complex molecules that crystallize. One new approach to overcome these difficulties is based on the use of ultrashort pulses of X-ray free-electron lasers [2]. This elegant idea is based on measuring a sufficiently sampled diffraction pattern from a single molecule illuminated by an FEL pulse [3]. However, in spite of the extreme intensity of the FEL pulses, a diffraction pattern from only one molecule will not be sufficient to obtain a high resolution diffraction pattern. Many reproducible copies will need to be measured to get a sufficient signal to noise ratio for each projection necessary for three-dimensional (3D) imaging at sub-nanometer spatial resolution.

FELs are especially well suited for coherent 2D crystallography, providing femtosecond, coherent pulses [4] with extremely high power. Only the combination of these unique properties will allow the realization of 2D crystallographic X-ray imaging of biological systems. Brilliant, ultrashort pulses could overcome the radiation damage problem [3] which is a severe limitation of conventional crystallography [5]. Higher luminosity and hence improved statistics for such experiments can be obtained through the use of pulse trains provided by FLASH [6].

We demonstrate finite crystallography using a micro-structured array that was prepared on a silicon nitride membrane substrate coated with 600 nm of gold, and 200 nm of palladium. The sample was manufactured by milling holes in the film in a regular array pattern using a Focused Ion Beam (FIB). The 'unit cell' of our crystal consists of a large hole of 500 nm diameter (representing a 'heavy atom') and a smaller hole of 200 nm diameter (a 'light atom'). The whole structure is composed of five unit cells in each direction, making the total structure size about 10 x 10 μm^2. The diffraction data were measured at FLASH on the PG2 monochromator beamline [7] with a fundamental wavelength of 7.97 nm.

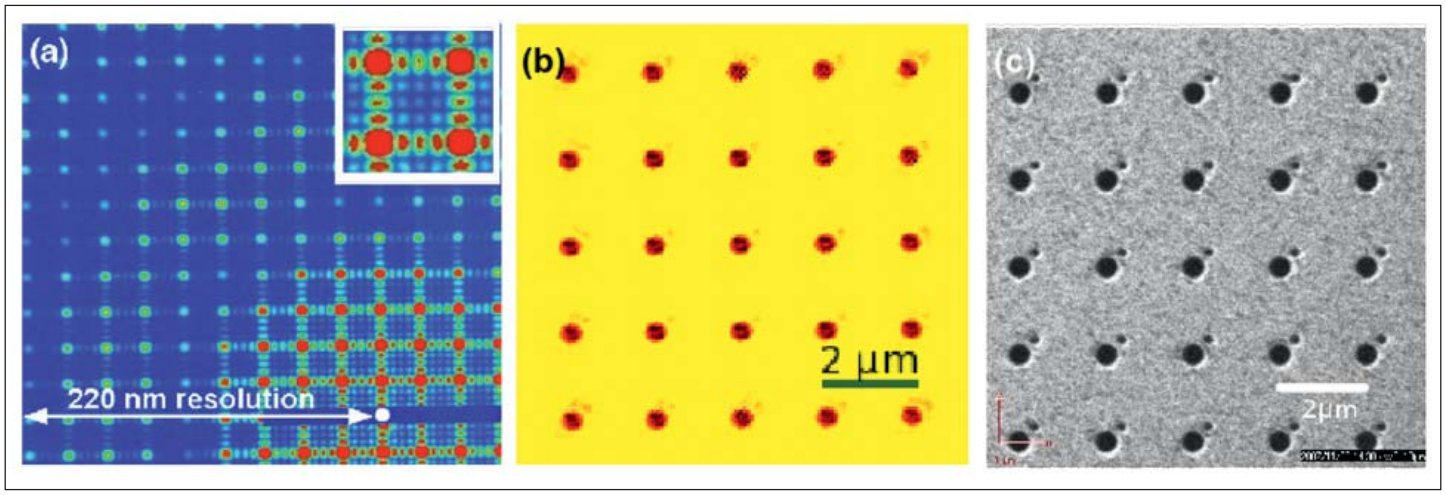

Figure 2

(a) Far-field diffraction data measured from a single train of 21 femtosecond pulses from the FEL. The white dot corresponds to the centre of the incoming beam. (Inset) Enlarged region of diffraction pattern. (b) The final reconstructed image of the sample using the original data binned 5x5 and exhibiting a resolution as measured in the experiment. (c) Scanning Ion Micrograph (SIM) image of the finite, periodic structure.

A scheme of the experiment is shown in Fig. 1. We used a 0.2 s exposure time to collect single train data from our sample with a coherent flux on the sample area of 1.5×10^{10} photons per train. This is an order of magnitude higher than that expected for the same sample area and exposure time at a 3rd generation synchrotron (~3×10^{9} photons). A typical data set is shown in Fig. 2(a). The diffraction pattern contains signal up to the edge of the detector, corresponding to a minimum feature size of 220 nm. We note that all expected features of a finite, crystalline structure are observed. The Bragg peaks are clearly seen, as are the oscillations between the Bragg peaks due to the finite extent and coherent illumination of our sample. Also seen is the form factor of the large holes, which can be observed as a radial intensity modulation across the pattern produced.
Due to the limited signal to noise ratio of the initial data set and the symmetry of the unit cell the initial reconstructions stagnated with two equivalent solutions superimposed. To solve this we have binned the data 5x5 and used a more constrained support of 25 rectangular boxes each centred on the positions of the unit cell. By increasing the signal-to-noise ratio and reducing the symmetry in real space we were able to improve the reconstruction to resolve the smallest features in our sample (Fig. 2(b)). The resolution in real space was better than 238 nm. This compares favourably with our measured maximum momentum transfer corresponding to a 220 nm resolution.
In summary, we have demonstrated single pulse train coherent diffractive imaging for a finite crystalline sample with the reconstructed image exhibiting resolution commensurate with the measured diffraction data. We have shown that the non-crystalline framework of coherent diffractive imaging is applicable to 2D finite crystals. In this experiment the 2D crystalline structure has been essential in providing the necessary signal to determine the structure of the unit cells. If only a single unit cell were used, simulations suggest that a successful reconstruction to the resolution shown here would be impossible. We conclude that this alternative approach to single molecule imaging is a significant step towards revealing the structure of proteins with sub-nanometer resolution at the newly built XFEL sources.

Contact: Ivan Vartaniants, ivan.vartaniants@desy.de

Authors

A.P. Mancuso[1], A. Schropp[1], B. Reime[1], L.-M. Stadler[1], A. Singer[1], J. Gulden[1], S. Streit-Nierobisch[1], C. Gutt[1], G. Grübel[1], J. Feldhaus[1], F. Staier[2], R. Barth[2], A. Rosenhahn[2], M. Grunze[2], T. Nisius[3], T. Wilhein[3], D. Stickler[4], H. Stillrich[4], R. Frömter[4], H.P. Oepen[4], M. Martins[5], B. Pfau[6], C.M. Günther[6], R. Könnecke[6], S. Eisebitt[6], B. Faatz[1], N. Guerassimova[1], K. Honkavaara[1], V. Kocharyan[1], R. Treusch[1], E. Saldin[1], S. Schreiber[1], E.A. Schneidmiller[1], M.V. Yurkov[1], E. Weckert[1], and I.A. Vartanyants[1]

1. HASYLAB at DESY, 22607 Hamburg, Germany
2. Angewandte Physikalische Chemie, Universität Heidelberg, Im Neuenheimer Feld 253, D-69120 Heidelberg, Germany
3. Institute for X-ray-Optics, RheinAhr-Campus Remagen, FH Koblenz, Südallee 2, D-53424 Remagen, Germany
4. Institut für Angewandte Physik, Universität Hamburg, Jungiusstraße 11, D-20355 Hamburg, Germany
5. Institut für Experimentalphysik, Universität Hamburg, Luruper Chaussee 149, D-22761 Hamburg, Germany
6. Berliner Elektronenspeicherring-Gesellschaft für Synchrotronstrahlung m.b.H. (BESSY), Albert-Einstein-Straße 15, D-12489 Berlin, Germany

Original publication

"Coherent-Pulse 2D Crystallography Using a Free-Electron Laser X-ray Source", Phys. Rev. Lett. 102, 035502 (2009).

References

1. **M. Woolfson and F. Hai-fu, "Physical and non-physical methods of solving crystal structures", (Cambridge University Press, Cambridge, 1995).**
2. **P. Emma, et al., www-ssrl.slac.stanford.edu/lcls/commissioning/documents/th3pbi01; T. Tanaka and T. Shintake, www-xfel.spring8.or.jp/SCSSCDR.pdf; M. Altarelli, et al., http://xfel.desy.de/tdr/index_eng.html.**
3. **R. Neutze, R. Wouts, D. van der Spoel, E. Weckert and J. Hajdu, Nature 406, 752-757 (2000).**
4. **A. Singer, et al., Phys. Rev. Lett., 101, 254801 (2008).**
5. **M. R. Howells, et al., J. Elect. Spectrosc. and Relat. Phenom., 170, 4–12 (2009).**
6. **W. Ackermann et al., Nature Photonics 1, 336-342 (2007).**
7. **M. Wellhöfer, et al., J. Opt. A: Pure Appl. Opt. 9, 749-756 (2007).**

X-ray absorption spectroscopy at FLASH.

Everything changes, everything stays

A new method to perform X-ray absorption spectroscopy experiments at a free-electron laser has been developed. Instead of selecting a narrow bandwidth of the incident beam with a grating-monochromator, a dispersive set-up is used. The incident pink radiation from the SASE-FEL is dispersed by the grating and collected by an area detector. A special sample-preparation method has been used in order to measure the intensity and energy distribution of the incident and absorbed beam simultaneously. This method can be improved in the future to perform pump-probe experiments with XAS as the probe with fs-temporal resolution at an FEL.

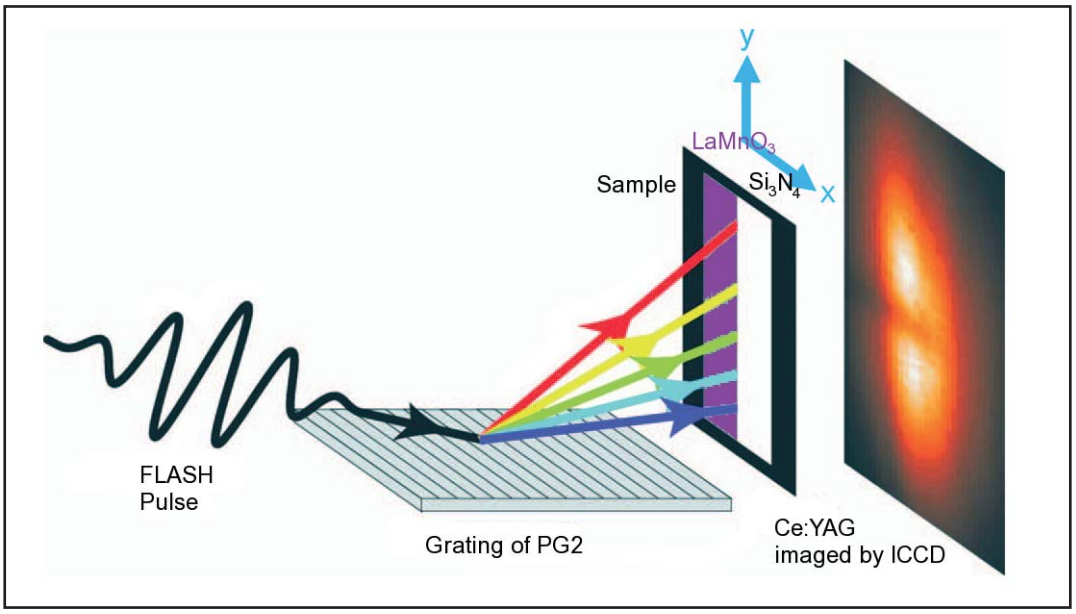

Figure 1
Experimental set-up at FLASH: The pulses of FLASH are dispersed by a grating-monochromator. The sample intercepts the beam. One half of the beam is transmitted through the Si_3N_4-membrane, while the half on the side of the $LaMnO_3$-film is partly absorbed.

Near edge X-ray absorption spectroscopy (NEXAFS or XANES) is uniquely powerful [1-3] to learn about the electronic structure properties of matter, which determines materials properties like magnetism. With femtosecond X-ray pulses, transient states and ultra-fast dynamics in matter are accessible and have been explored so far at femtosecond slicing facilities at synchrotron radiation facilities. Turning to the brilliant femtosecond X-ray pulses from Free-Electron Laser Sources we now want to expand femtosecond time resolved electronic structure studies further and explore how brilliant X-ray pulses modify electronic properties in matter.

To this end, we adapted the way NEXAFS is measured to the requirements imposed by the nature of SASE-FEL radiation. The main point is that we do not scan the monochromator, but use it in dispersive geometry, where the spectrum is then measured by an area detector, where the position on the detector corresponds to one specific energy. For our experiment we chose a thin film of $LaMnO_3$ (75 nm) deposited by pulsed laser deposition on a thin Si_3N_4 membrane (100nm) in such a way that the $LaMnO_3$ film covered just one half of the membrane [4]. The other half was left intentionally blank in order to determine the spectral distribution of the incident beam as a

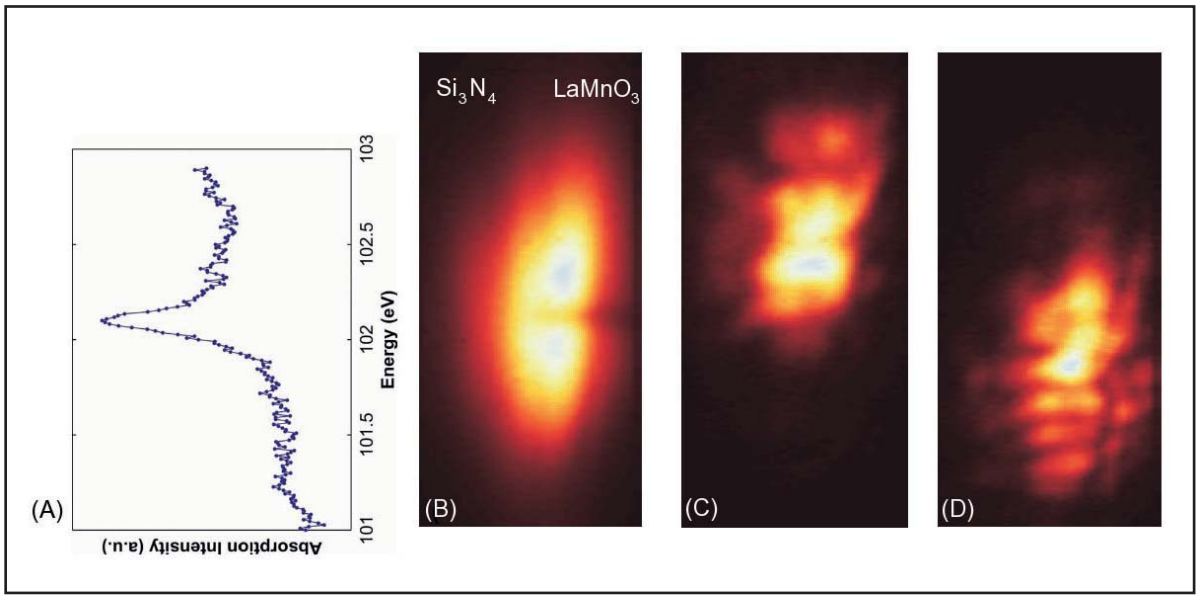

Figure 2

(B) Accumulated spectra on the position sensitive detector. The left half shows the beam which is transmitted through the membrane. The intensity distribution is rather uniform. The right side shows the transmission through the $LaMnO_3$-film, which reflects the absorption by the sample. The white line with strong absorption is clearly visible in the right half. The other two spectra (C and D) show the intensity and energy fluctuations of the incident beam. These pictures are examples of two of the many spectra, which were measured without a sample, in order to determine the detector calibration function. (A) The normalised weighted sum of the spectra. This spectrum is obtained by using the spectra in figure (B).

reference. The beauty of this system is, that the $N_{4,5}$ edge of the La^{3+} ions in $LaMnO_3$ exhibits an atomically sharp $^3D_1$ absorption resonance at a photon energy of 102.17 eV, where the Si_3N_4 membrane is highly transparent. The radiation-fan from the grating at the PG2 beamline at FLASH [5] is passing through the sample, where one-half of the fan is absorbed by the $LaMnO_3$ film and the membrane and the other passed through the uncovered membrane. The half that is transmitted through the membrane is used for determining the intensity and spectral distribution of the incident flashes, the other half absorbs the radiation based on its energy. Since energy and intensity are measured simultaneously, it is possible to normalise each individual spectrum, which reflects only a small part of the total absorption spectrum.

These measurements have brought us a good step towards femtosecond time resolved NEXAFS for materials science and high field induced studies in solids. Future improvements will aim to bring the interaction region just between the X-ray source and the monochromator grating in order to ensure the shortest possible and eventually the most brilliant X-ray pulses to interact with the sample.

Contact: Alexander Föhlisch,
alexander.foehlisch@helmholtz-berlin.de

Authors

D.P. Bernstein[1], Y. Acremann[1], A. Scherz[1], M. Burkhardt[1], J. Stöhr[1], M. Beye[2], W.F. Schlotter[2], T. Beeck[2], F. Sorgenfrei[2], A. Pietzsch[2], W. Wurth[2], A. Föhlisch[2]

1. SLAC National Accelerator Laboratory, 2575 Sand Hill Road, Menlo Park, California 94025, USA
2. Institut für Experimentalphysik and Centre for Free-Electron Laser Science, Universität Hamburg, Luruper Chaussee 149, 22761 Hamburg, Germany

Original publication

"Near edge X-ray absorption fine structure spectroscopy with X-ray free-electron lasers", Appl. Phys. Lett. 95, 134102 (2009).

References

1. **J. Stöhr, "NEXAFS Spectroscopy", Springer, Berlin (1992).**
2. **P. Zeppenfeld, in Physics of Covered Solid Surfaces. I. Adsorbed Layers on Surfaces, edited by H. P. Bonzel and W. Martinssen, Springer, Berlin, Vol. 42 (2005).**
3. **P. Wernet, D. Nordlund, U. Bergmann, M. Cavalleri, M. Odelius, H. Ogasawara, L. A. Näslund, T. K. Hirsch, L. Ojamäe, P. Glatzel, L. G. M. Pettersson, and A. Nilsson, "The structure of the first coordination shell in liquid water Science", 304, 995 (2004).**
4. **S. Fourmaux, L. Lecherbourg, M. Harmand, M. Servol, and J. C. Kieffer, "High repetition rate laser produced soft X-ray source for ultrafast X-ray absorption near edge structure measurements", Rev. Sci. Instrum. 78, 113104 (2007).**
5. **M. Martins, M. Wellhofer, J. T. Hoeft, W. Wurth, J. Feldhaus, and R. Follath, "Monochromator beamline for FLASH", Rev. Sci. Instrum. 77, 115108 (2006).**

Voltage induced Ti valence switching in $SrTiO_3$.

Perovskite-like crystal in an electric field

Strontiumtitanate $SrTiO_3$ (STO) is a prototypical perovskite, a class of substances, which find wide applications based on their interesting ferroic properties. STO itself is not ferroic, but it is used as a substrate for many perovskite thin films due to its well matching lattice constant and its chemical inertness. However, STO also has an interesting property: Upon the application of an electric field, structural changes and a degradation of the surface are observed. This can be explained by mobile oxygen vacancies. Therefore, X-ray absorption near edge structure measurements of STO in an electric field were performed in grazing incidence geometry. Density functional theory calculations were used to explain the data.

During the last decade, extensive scientific research has focused on materials exhibiting ferroic properties – ferroelectrics, ferromagnetics and ferroelastics. The ferroic properties arise from a spontaneous long-range ordering of electric dipoles, magnetic moments or deformation moments. Important characteristics of these materials are, among others, piezoelectricity, which is used for e.g. conventional lighters, pyroelectricity, which is used for e.g. temperature sensors, or giant magnetoresistance, an effect, which is used in every day data storage devices. If these characteristics are coupled, a large diversity of upcoming applications, e.g. micro electro-mechanical systems, magnetoelectric transducers, ferroelectric field effect transistors as well as data storage and random access memory devices is possible. Among (multi-) ferroic materials, oxides with the perovskite-type of structure have gained great importance due to their comparably straightforward synthesis and controllable diverse properties.

Pristine STO is characterized by a perovskite-type cubic structure (Fig. 1) at room temperature (RT) and exhibits no ferro- or piezoelectric behaviour down to helium temperatures. The growth as well as processing of oxide single crystals, such as STO, introduces a specific density of Schottky point defects. Although several defect-reducing approaches are utilized, in particular near-surface regions still exhibit a distorted structure [1]. Essentially, statistically distributed or periodically arranged oxygen vacancies show a strong impact on structural and electronic properties, e.g., phase transitions, ionic conductivity and resistance switching [2].

Application of a static (DC) electric field to a STO crystal results in a redistribution of oxygen vacancies and subsequently in structural changes [2,3]. It has been suggested that either oxygen vacancies or SrO complexes gain an enhanced diffusion coefficient when transported along dislocation lines or planar defects. Recently, for (001) STO wafers we have found a reversible change of the X-ray reflection profiles using Wide-Angle X-ray Diffraction under application of a DC electric field at RT [4]. This phenomenon has been attributed to structural variations observed beneath the anode and promises application in the field of adaptive X-ray optics [5].

In order to identify the atomic species, which are responsible for the observed structural changes, we focused on the characterization of STO under the influence of an electric field *in situ* at RT. We performed dedicated XANES investigations at the Sr-K and Ti-K absorption edges using a (001) STO single-crystal plate with electrodes (Fig. 1). An electric field of $E = \pm 10^6$ V/m parallel to the [001] direction was applied. This experiment allows investigating changes of the valence states of the Sr and Ti atoms based on the binding energy of the

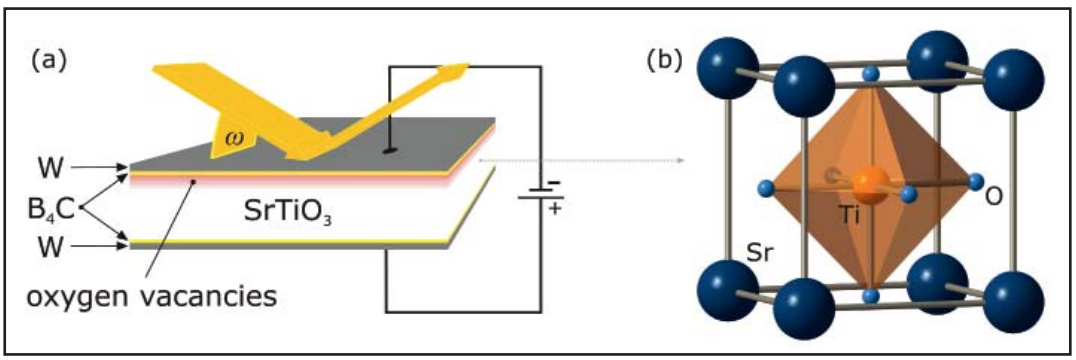

Figure 1
Schematic representation of the experimental set-up and the sample. The STO-crystal is coated on both sides with B_4C and W-films in order to connect the electrodes. To be most sensitive to the surface, the experiment was performed in grazing incidence geometry (a). Perovskite-type crystal structure of STO at room temperature (b).

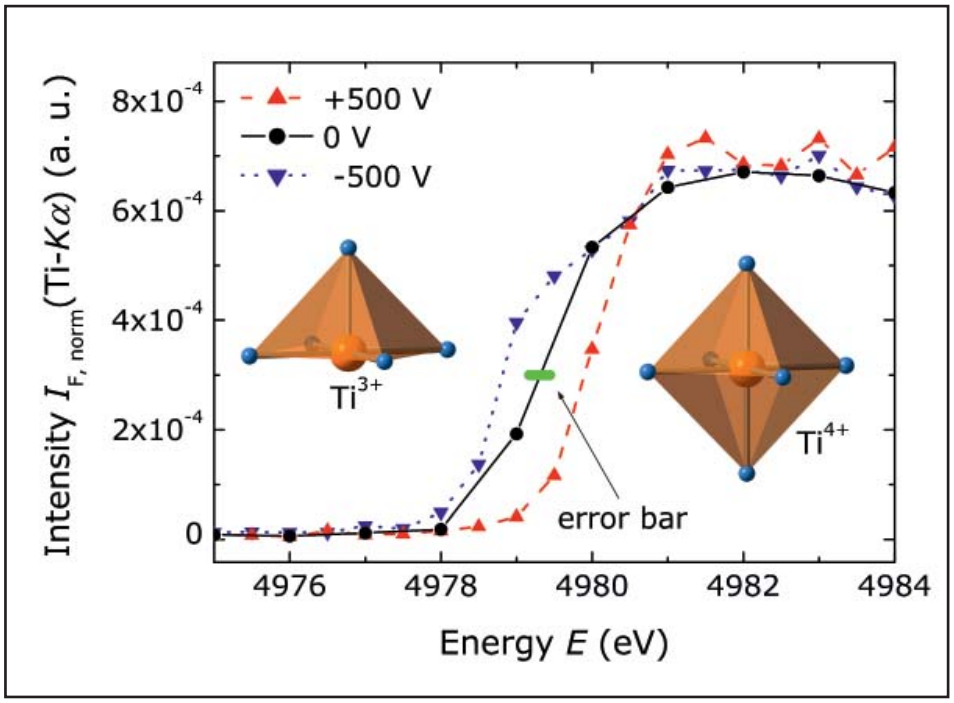

Figure 2

XANES spectra for photon energies at the Ti-K absorption edges under application of a DC electric field. Oxygen (small blue spheres) coordination polyhedra of Ti (large orange spheres) cations are illustrated.

resonantly excited 1s K-shell electrons.

The in situ XANES spectra indicated an unchanged oxidation state of the Sr atoms under the influence of the electric field. In case of the Ti atoms, a significant shift of the Ti-K absorption edge energy of (1.29 ± 0.05) eV due to the electric field of varying polarity was observed (Fig.2).

A qualitative interpretation of the results was drawn in terms of ionic conductivity. By applying a voltage of positive polarity to the sample surface, oxygen is forced to migrate from the bulk to the anode so that it compensates the intrinsic oxygen vacancies in the near-surface region. Thereby, the coordination of Ti atoms changes (Fig. 2) and the formal Ti valence state shifts from $Ti^{(4-\delta)+}$ next to a vacancy back to Ti^{4+}. Hence, the ideal $SrTiO_3$ structure is recovered in the near-surface volume. Inversion of the polarity reverses the oxygen anion transport, implying a change of the formal oxidation state from Ti^{4+} to $Ti^{(4-\delta)+}$.

Density functional theory provides a quantitative basis for the observations made. The influence of neutral oxygen vacancies on the Ti 1*s* core level was calculated for a vacancy-containing supercell. We obtained a reduction of binding energy of 1.1 eV for the Ti atom near the vacancy, which reflects very well the experimentally observed shift of the Ti-*K* absorption edge energy.

In conclusion, XANES measurements proved a shift of the Ti-K absorption edge energy of STO under applied DC electric fields. A controlled switching of the Ti valance may give rise to a large variety of interesting applications and physical phenomena, e.g., dedicated valence states for controlled catalytic behaviour on STO surfaces or tuning of superconductivity, insulator-to-metal transition or magnetic behaviour connected to the Ti atoms [6].

Contact: Dirk C. Meyer, dirk-carl.meyer@physik.tu-freiberg.de

Authors

T. Leisegang[1], H. Stöcker[1], A. A. Levin[1], T. Weißbach[1], M. Zschornak[1], E. Gutmann[1], K. Rickers[2], S. Gemming[3], and D. C. Meyer[1]

1. Institut für Strukturphysik, Technische Universität Dresden, 01062 Dresden, Germany
2. Deutsches Elektronen-Synchrotron DESY, Notkestr. 85, 22603 Hamburg, Germany
3. Institut für Ionenstrahlphysik und Materialforschung, Forschungszentrum Dresden-Rossendorf, 01314 Dresden, Germany

Original publication

"Switching Ti Valence in $SrTiO_3$ by a dc Electric Field", Phys. Rev. Lett. 102, 087601 (2009)

References

1. **K. Rabe, Ch.H. Ahn, and J.-M. Triscone (Eds.), "Physics of Ferroelectrics: A Modern Perspective" (Topics in Applied Physics), Springer, Berlin, No. 105 (2007).**
2. **K. Szot, W. Speier, G. Bihlmayer, and R. Waser, "Switching the electrical resistance of individual dislocations in single-crystalline SrTiO3", Nat. Mater. 5, 312 (2006).**
3. **E. Hegenbarth, "Die Feldstärkeabhängigkeit der Dielektrizitätskonstanten von SrTiO3-Einkristallen im Temperaturbereich von 15 bis 80 °K", phys. status solidi 6, 333 (1964).**
4. **D.C. Meyer, A.A. Levin, S. Bayer, A. Gorbunov, W. Pompe, P. Paufler, "An electrical field-induced structural effect in strontium titanate at room temperature", Appl. Phys. A 80, 515 (2005).**
5. **D.C. Meyer, A.A. Levin, T. Leisegang, E. Gutmann, P. Paufler, M. Reibold, W. Pompe, "Reversible tuning of a series of intergrowth phases of the Ruddlesden–Popper type SrO(SrTiO3)n in an (001) SrTiO3 single-crystalline plate by an external electric field and its potential use for adaptive X-ray optics", Appl. Phys. A 84, 31 (2006).**
6. **K. Potzger, A.A. Levin, A. Shalimov, J. Osten, D.C. Meyer, J. Phys. D (2009) submitted.**

Red wine and diabetes mellitus.

Lipid membranes trigger fibril formation of diabetes proteins – red wine compound inhibits fibrillation

The islet amyloid polypeptide (IAPP) or amylin plays a major role in the pathogenesis of type-II diabetes mellitus (T2DM). Using X-ray reflectivity, atomic force microscopy and infrared spectroscopy in concert, we obtained a molecular picture of how lipid interfaces trigger the fibrillation process and how fibrillation can be inhibited by small-molecule inhibitors such as the red wine compound resveratrol.

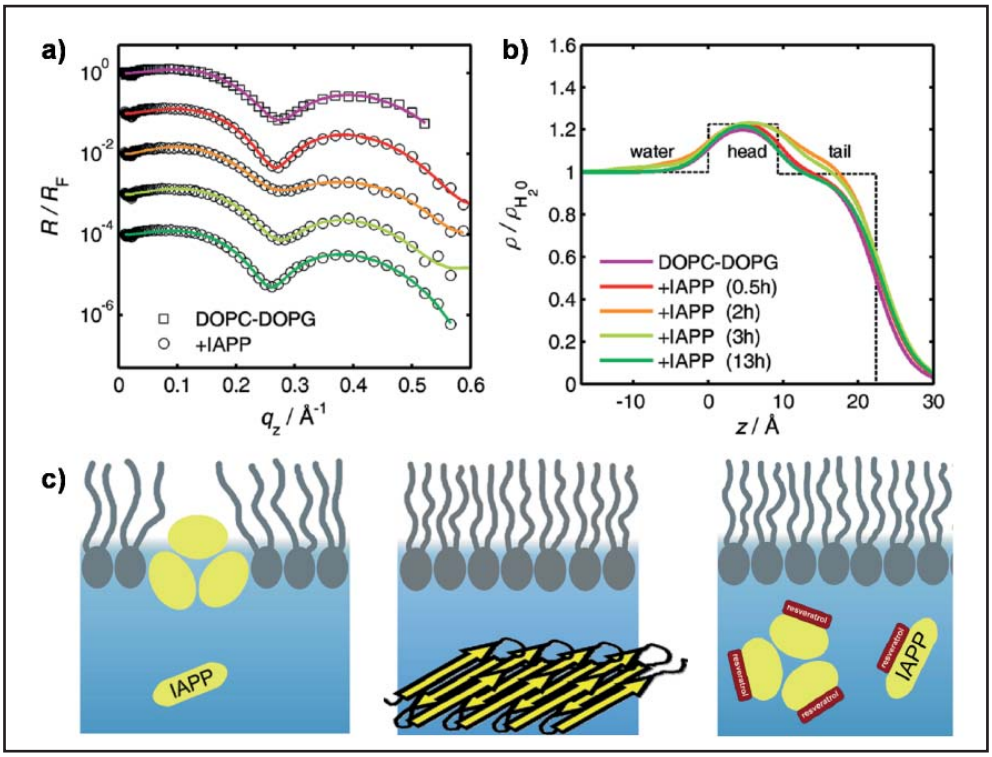

Figure 1

Interaction of IAPP with an anionic DOPC/DOPG lipid film spread at the air-water interface. (a) X-ray reflectivity data normalized to the Fresnel reflectivity at different times. (b) Corresponding electron density profiles indicate marked IAPP-induced changes in the intermediate time range. (c) Schematic illustration of lipid-induced aggregation of IAPP and its inhibition by resveratrol. IAPP adsorbs and oligomerizes at the anionic lipid interfaces and, eventually, larger aggregate structures detach from the lipid interface. In the presence of resveratrol at stoichiometric concentrations, the interaction of IAPP with anionic lipid films is blocked.

Inside a biological cell, protein folding into the biochemically functional form results from highly regulated processes. Given certain conditions, ordered assemblies of (partially) unfolded monomers or protein fragments may be formed, such as cross ß-sheet rich structures called amyloid fibrils [1,2]. Protein aggregation and subsequent amyloid formation of proteins, such as Aβ, islet amyloid polypeptide (IAPP), prion protein and α-synuclein, is linked to the pathogenesis of many incurable human diseases, including Alzheimer's and Parkinson's disease, transmissible spongiform encephalopathies and type-II diabetes mellitus (T2DM).

IAPP or amylin is a 37 amino acid residue peptide hormone that is synthesized by ß-cells of the pancreatic islets of Langerhans. Naturally, it is involved in controlling the level of glucose in the blood. However, IAPP has also been found to be the main component of the extracellular amyloid plaques involved in T2DM.

The mechanism ruling fibril formation of IAPP that triggers its conversion from a functional monomer into insoluble amyloid fibrils is still not well understood. Recent studies [3] have shown that the interaction of IAPP with lipid membranes may induce fibril formation. Despite the efforts toward a biophysical characterization of the different states of aggregation [3,4], the lack of structural information still impedes a detailed molecular understanding of IAPP fibrillogenesis.

In this study, synchrotron X-ray reflectivity, atomic force microscopy and ATR-FTIR spectroscopy were applied in order to explore the mechanism of how lipid interfaces influence IAPP fibrillogenesis and how this may be inhibited.

X-ray reflectivity measurements were performed using the liquid surface scattering set-up of beamline BW1 at HASYLAB. In order to mimic the conditions present in a biological cell, we spread a mixture of neutral, zwitterionic DOPC and anionic

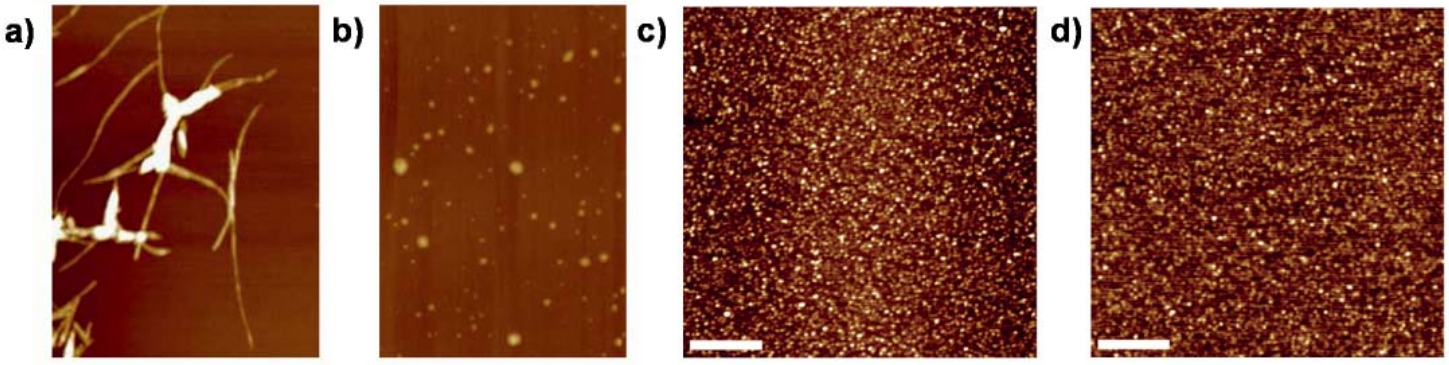

Figure 2

Inhibitory effect of resveratrol in bulk solution (a,b) and in the presence of lipid interfaces (c,d) as observed by atomic force microscopy. (a) IAPP without resveratrol and (b) 10 µM IAPP in the presence of 10 µM resveratrol (height scale: 0-5 nm). (c) No IAPP aggregation is observed in the presence of a neutral, zwitterionic DOPC monolayer. (d) A similar IAPP morphology is encountered in the presence of aggregation-fostering anionic DOPC/DOPG monolayer when stoichiometric concentrations of resveratrol were added (height scale: 0-1 nm; scale bar: 300 nm).

DOPG on a Langmuir trough and compressed the lipid film to a physiological surface pressure of 30 mN/m. Figure 1 shows the X-ray reflectivity data of the DOPC/DOPG lipid film in the presence of IAPP. Distinct IAPP-induced changes are observed in the intermediate time range indicating insertion of IAPP into the lipid's upper chain region. IAPP oligomers with a maximum size of 20 Å are formed in the lipid monolayer leading to an increase in electron density.

Together with the AFM and ATR-FTIR data, the following scenario of IAPP fibril formation in the presence of anionic lipid interfaces could be deduced: Lipid-induced fibrillation of IAPP is initiated by lipid-induced nucleation, oligomerization, followed by detachment of larger IAPP aggregate structures from the lipid membrane, and terminated by the formation of mature fibrils in the bulk solution (Fig. 1c).

Inhibiting amyloid fibril formation is regarded as a potentially key therapeutic approach toward amyloid-related diseases [1,2,5,6]. Here, we used the phenolic red wine compound resveratrol which is known for its inhibitory effect on Aß fibrillogenesis (the Alzheimer peptide) as a potential inhibitor for IAPP fibrillogenesis. The potential of resveratrol to inhibit IAPP fibril formation in bulk solution is revealed from the AFM data shown in Figure 2. Furthermore, resveratrol is able to block IAPP-lipid membrane interactions and thus to inhibit IAPP aggregation also in the presence of aggregation-fostering negatively charged lipid interfaces. Inhibition takes place during the very early stages of the fibrillogenesis and is efficient already at stoichiometric concentrations of resveratrol and IAPP. Only very small IAPP particles, probably consisting of non-reactive resveratrol/ IAPP complexes, are found in the bulk phase. In the presence of resveratrol, the N-terminus of IAPP is masked hindering IAPP-lipid interactions.

In conclusion, first X-ray reflectivity studies on IAPP at lipid interfaces have been carried out. Together with atomic force microscopy and infrared spectroscopy, these measurements provide a molecular picture of the time-dependent scenario occurring upon aggregation of IAPP at anionic lipid interfaces. Moreover, the inhibitory potential of the polyphenolic red wine compound resveratrol on IAPP aggregation also in the presence of aggregation-fostering negatively charged lipid interfaces is demonstrated. Meanwhile it has been shown by cellular studies that this polyphenolic compound is also able to arrest IAPP fibril formation at an early stage in vivo [7].

Contact: Roland Winter, roland.winter@tu-dortmund.de

Authors

Florian Evers[2], Christoph Jeworrek[1], Sebastian Tiemeyer[2], Katrin Weise[1], Daniel Sellin[1], Michael Paulus[2], Bernd Struth[3], Metin Tolan[2], Roland Winter[1]

1. Faculty of Chemistry, TU Dortmund, 44221 Dortmund, Germany
2. Faculty of Physics / DELTA, TU Dortmund, 44221 Dortmund, Germany
3. DESY, Notkestr. 85, 22607 Hamburg, Germany

Original publication

"Elucidating the Mechanism of Lipid Membrane-Induced IAPP Fibrillogenesis and Its Inhibition by the Red Wine Compound Resveratrol: A Synchrotron X-ray Reflectivity Study", J. Am. Chem. Soc. 131, 9516-9521 (2009).

References

1. **F. Chiti, C. M. Dobson, "Protein misfolding, functional amyloid, and human disease", Annu. Rev. Biochem. 75, 333-366 (2006).**
2. **F. E. Cohen, J. W. Kelly, "Therapeutic approaches to protein-misfolding diseases", Nature 426, 905-909 (2003).**
3. **D. H. J. Lopes, A. Meister, A. Gohlke, A. Hauser, A. Blume, R. Winter, "Mechanism of islet amyloid polypeptide fibrillation at lipid interfaces studied by infrared reflection absorption spectroscopy", Biophys. J. 93, 3132-3141 (2007).**
4. **C. Jeworrek, O. Hollmann, R. Steitz, R. Winter, C. Czeslik, "Interaction of IAPP and Insulin with Model Interfaces Studied Using Neutron Reflectometry", Biophys. J. 96, 1115-1123 (2009).**
5. **R. Mishra, B. Bulic, D. Sellin, S. Jha, H. Waldmann, R. Winter, "Small-molecule inhibitors of islet amyloid polypeptide fibril formation", Angew. Chem. Int. Ed. 47, 4679-4682 (2008).**
6. **R. Mishra, D. Sellin, D. Radovan, A. Gohlke, R. Winter, "Inhibiting Islet Amyloid Polypeptide Fibril Formation by the Red Wine Compound Resveratrol", ChemBioChem 10, 445-449 (2009).**
7. **D. Radovan, N. Opitz, R. Winter, "Fluorescence microscopy studies on islet amyloid polypeptide fibrillation at heterogeneous and cellular membrane interfaces and its inhibition by resveratrol", FEBS Letters 583, 1439-1445 (2009).**

From islands to a layer.

How a gold contact on a conducting polymer film is formed

Almost all applications using conducting polymers require a metal contact. In a typical device, the interface between the polymer and the metal layer is of importance. Here we observe how a gold contact is formed on the conducting polymer polyvinylcarbazole (PVK) during sputter deposition. This growth process was observed in-situ via grazing incidence small-angle X-ray scattering (GISAXS). The GISAXS data were simulated with a cluster model, from which cluster morphology and arrangement were extracted. According to this model the growth proceeds in four steps where each stage is dominated by a characteristic kinetic process: Nucleation is followed by lateral cluster growth, then coarsening occurs and finally a continuous layer grows in thickness. In addition to the contact formation, gold is incorporated inside the PVK film near the interface to the metal layer.

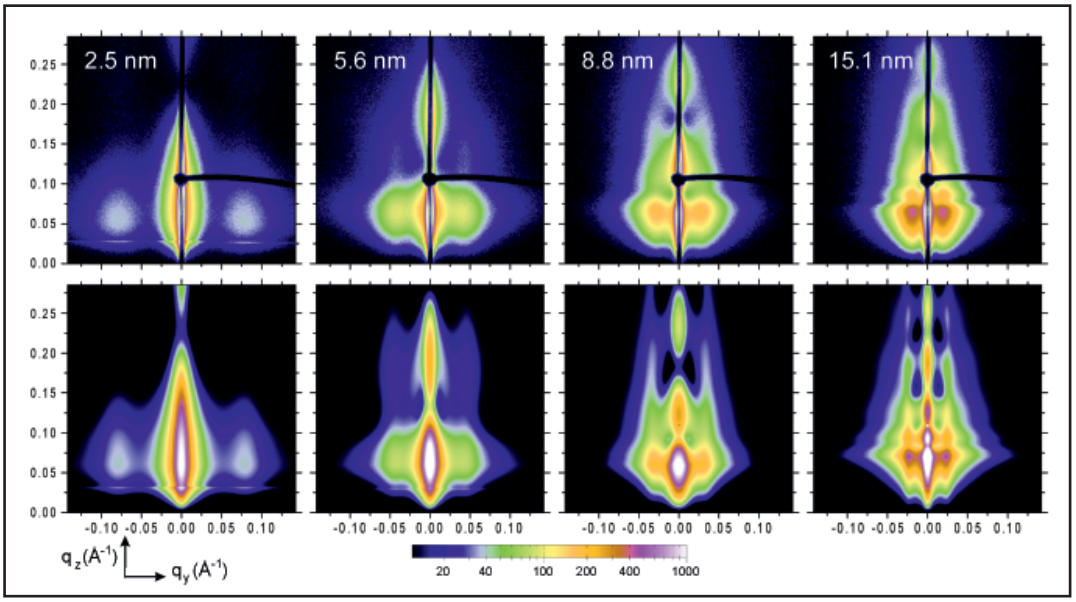

Figure 1

Composite image of four selected scattering images taken after deposition of a gold film with a thickness of 2.5, 5.6, 8.8 and 15.1 nm (upper row) and the corresponding simulations (lower row). The evolving maxima in vertical direction originate from the growth in height, the lateral maximum is related to the centre-to-centre distance of the clusters.

The field of organic electronics is emerging very rapidly, and newly-discovered materials and interfacial processes result in fascinating new applications. In these applications typically a thin metal film is used to apply an electrical contact to the active layer of an electronic device, e.g. an organic light emitting diode (OLED), an organic field effect transistor (OFET) or an organic solar cell (OSC). In a typical preparation procedure the metal film is deposited directly on top of the active layer, which corresponds to the introduction of an interface with the organic material in the device layout. Of rapidly growing interest is the class of conductive polymers, because they are easily processable by wet-chemical methods like spin coating. Moreover, conducting polymers can be tuned chemically and physically to meet the desired properties [1]. Independent from the polymer and metal used, an important concern in an organic electronic device are the interactions occurring at the polymer-metal interface, because characteristics like film adhesion and electric contact properties are strongly influenced by the interface structure and the incorporation of metal inside the polymer film. This in turn is determined by the growth of the metal film on the polymer surface, which makes a detailed understanding of the principles governing the growth process necessary.

Of particular interest for applications in organic electronic devices are polymers based on carbazole, because these polymers are characterized by high thermal and chemical stability and a low HOMO energy level [2]. For our investigation we prepared a 10 nm thick film of polyvinylcarbazole (PVK) and deposited a gold film on top of it by DC magnetron sputtering [3]. The film growth was monitored in-situ via grazing incidence small angle X-ray scattering (GISAXS) [4]. To achieve time resolution the experiment was performed in a stop-sputtering mode. In other words, cycles of gold deposition for 1 minute and subsequent recording of the GISAXS image were carried out. In total, 49 deposition cycles were done while a 15.1 nm

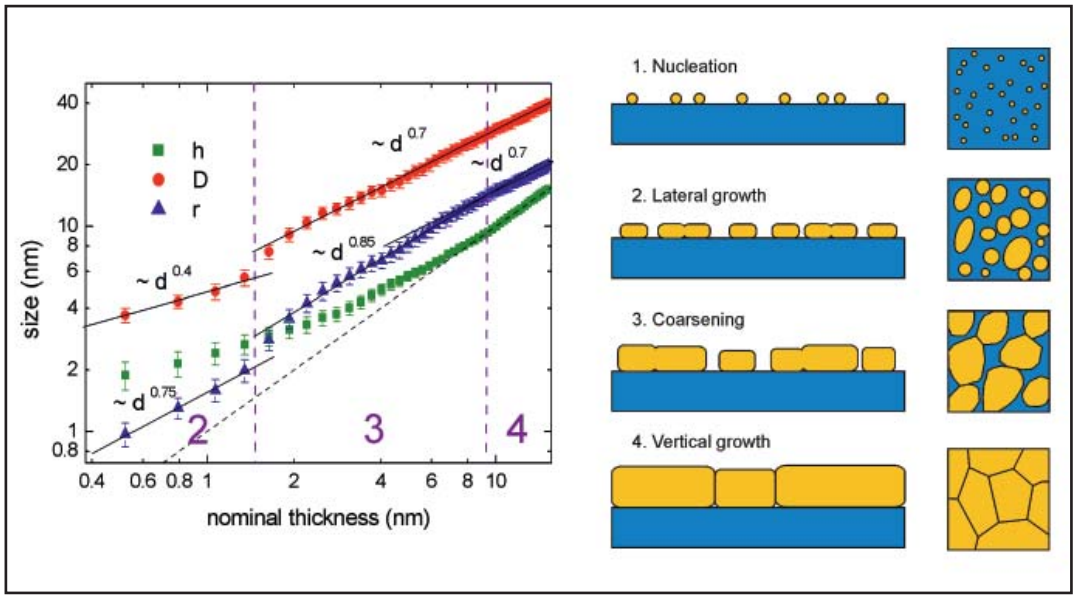

Figure 2

Left: Evolution of cluster height (squares), radius (triangles) and centre-to-centre distance (circles) within the four growth stages. The stage of nucleation is completed at a deposition of less than 0.2 nm and therefore completely within the first deposition cycle. The dashed line marks the nominal film thickness. Right: Schematic drawing of the cluster growth process. After nucleation small clusters grow laterally, then coarsening occurs and finally a continuous layer grows in thickness.

thick gold layer was deposited. Afterwards the scattering images were simulated with a cluster model. Figure 1 shows a comparison of four selected scattering images and the corresponding simulations.

These simulations delivered the key parameters cluster radius r, height h and distance D to describe the evolution of the cluster morphology with the deposited film thickness (Figure 2). For the cluster height, a nonlinear progress with the deposited gold amount is obvious: Up to a value of 9 nm the cluster height exceeds the film thickness, which indicates a growth of the gold film in the form of three-dimensional, spherical clusters in the early stage of deposition. Over the whole deposition the cluster radius as well as the centre-to-centre distance of the clusters increase constantly with the deposited gold amount, indicating a cluster growth with permanent coalescence. Three distinct growth regimes with different scaling laws are observed.

When complete surface coverage is reached at a nominal film thickness of d = 9nm the scaling law for the radius r shows a second transition to an identical scaling as the cluster distance. This progress of the cluster morphology suggests a cluster growth proceeding in four stages, with a characteristic kinetic process dominating each stage. The growth process begins with a stage of nucleation, where impinging gold atoms diffuse across the polymer surface and form nuclei when two of them meet [5]. In the second stage, these nuclei grow laterally by capturing further diffusing atoms. As a result, small spherical gold clusters form. At a point where two clusters come in close contact to each other coalescence occurs and a larger cluster is formed. At a layer thickness of 1.3 nm enhanced coalescence sets in, cluster radius as well cluster distance increase very fast and the clusters start to assume an irregular shape (coarsening stage). In the final stage, the clusters form a continuous layer, which grows vertically in thickness as long as deposition goes on. Simultaneously coarsening continues and a grain structure, as it is well-known for vapour-deposited thin films, develops.

In addition to the formation of the metal layer on the conducting polymer, metal atoms diffuse into the PVK. An amount of 6.5 wt% gold is incorporated up to a depth of 1.2 nm in the PVK film.

Eventually, the gold contact has evolved from isolated islands to a closed layer, and the observation gave us more insight how a metal film forms on a polymer surface and which processes determine the final film structure.

Contact: Peter Müller-Buschbaum, muellerb@ph.tum.de

Authors

Gunar Kaune[1], Matthias A. Ruderer[1], Ezzeldin Metwalli[1], Weinan Wang[1], Sebastien Couet[2], Kai Schlage[2], Ralf Röhlsberger[2], Stephan V. Roth[2], Peter Müller-Buschbaum[1]

1. Physik-Department E13, Technische Universität München, James-Franck-Straße 1, D-85747 Garching, Germany
2. HASYLAB at DESY, Notkestraße 85, D-22607 Hamburg, Germany

Original publication

"In situ GISAXS study of gold film growth on conducting polymer films", ACS Applied Materials and Interfaces 1, 353–362 (2009).

References

1. **C.J. Brabec, N.S. Sariciftci, J.C. Hummelen, "Plastic solar cells", Adv. Funct. Mater. 11, 15-26 (2001).**
2. **N. Blouin, M. Leclerc, "Poly(2,7-carbazole)s: structure-property relationships", Acc. Chem. Res. 41, 1110-1119 (2008).**
3. **S. Couet, Th. Diederich, K.Schlage, R. Röhlsberger, "A compact UHV sputtering system for in situ study of ultrathin films via hard X-ray scattering and spectroscopy", Rev. Sci. Instrum. 79, 093908 (2008).**
4. **S.V. Roth, R. Döhrmann, M. Dommach, M. Kuhlmann, I. Kröger, R. Gehrke, H. Walter C. Schroer, B. Lengeler, P. Müller-Buschbaum, „Small-angle options of the upgraded ultrasmall-angle X-ray scattering beamline BW4 at HASYLAB", Rev. Sci. Instrum. 77, 085106 (2006)**

Insight into the human inner ear.

From morphological to functional analysis of the cochlear system

Microtomography using monochromatic synchrotron radiation (SRμCT) allows for the non-destructive, three-dimensional visualization with micrometer resolution and high contrast. The routine application of microtomography on different length scales at low and high photon energies allows one to characterize the complex anatomical structures of the human inner ear. The combination of SRμCT at DORIS III and conventional light microscopy after sectioning (histology) was used to uncover the morphology of the temporal bone in cochlea with neural tube defects and Pelizaeus Merzbacher disease. Parts of cochlea were carefully prepared using osmium tetroxide staining to visualize nerve fibre bundles and membranes in the two-and-a-half turn of the cochlea. Performing microtomography at PETRA III will give more detailed access to the interior structures of the human sensors down to subcellular level.

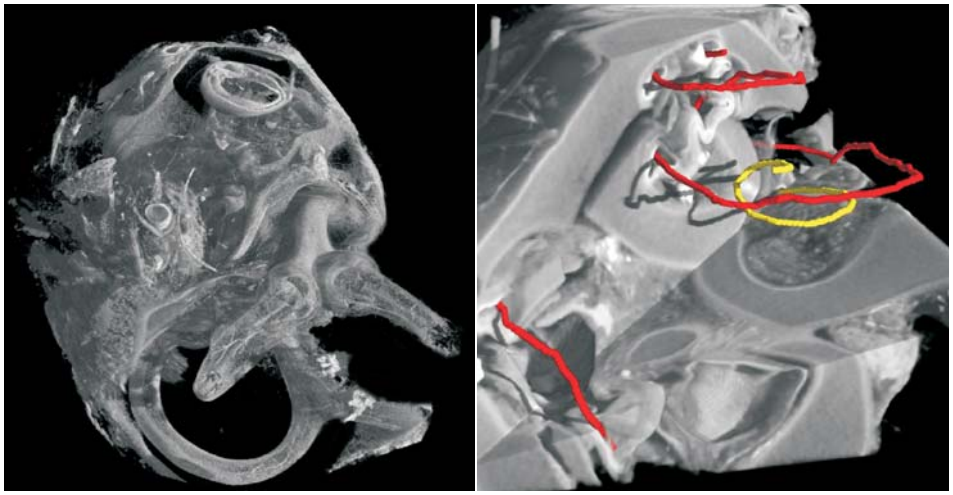

Figure 1

SRμCT was used to uncover the morphology of the temporal bone in cochlea with neural tube defects (left). The cochlea displayed the vestibular organ (foreground) and the fully developed 2.5 cochlear turns with an intact cochlear duct (background). The cochlear nerve with spiral ganglion neurons and nerve fibres showed a distinct contrast in SRμCT that allows for following neuronal tissue in the 3D dataset. The morphological analysis of the vestibulo-cochlear system in Pelizaeus Merzbacher disease is shown on the right. Based on the 3D dataset the centre lines (trajectories) of the cochlear duct (red) and of the Rosenthal canal (yellow) are represented together with the virtual cut lateral through the cochlea.

The hearing organ belongs to the most complex anatomical structures in the human body combining different types of delicate hard and soft tissues. Since already minor morphological deviations may result in crucial hearing deficiencies, the detailed knowledge of the human inner ear morphology is essential to achieve a better understanding of the inner ear pathologies (malformations), to improve the design and the insertion procedures of adapted cochlear implants as well as the treatment of hearing diseases. Imaging techniques allowing to simultaneously access the morphology of not only the complex bony structure, but also the soft tissue parts of the inner ear like membranes, nerve fibre bundles, ganglion cells are under ongoing developments. By now, neither clinical imaging techniques nor any kind of magnetic resonance imaging succeed within the required quality [1,2]. Currently, detailed morphological studies of the delicate microstructures such as sensory membranes, ganglion cells and nerve fibre bundles as parts of the inner ear exclusively rely on histological sectioning. By the sectioning, however, the soft tissues are mechanically deformed near the blade that often leads to damages of the thin membranes but at least to their relaxation to straight linear objects. This means that the complex anatomical structures of the inner ear can notably change their morphology, so that tissue shape and thickness can only be estimated [3]. Only microtomography using monochromatic synchrotron radiation on carefully prepared samples results in high detailed 3D datasets allowing to access the morphological structures within the cochlea. At the beamlines W2 (HARWI-II) and BW2 of the storage ring DORIS III SRμCT is routinely applied to small and large samples showing not only a high spatial resolution but also high density resolution in the tomograms [4]. Several bony structures and the implant bone interfaces within the human hearing organ for different types of implants were recently investigated using high-energy synchrotron radiation [5].

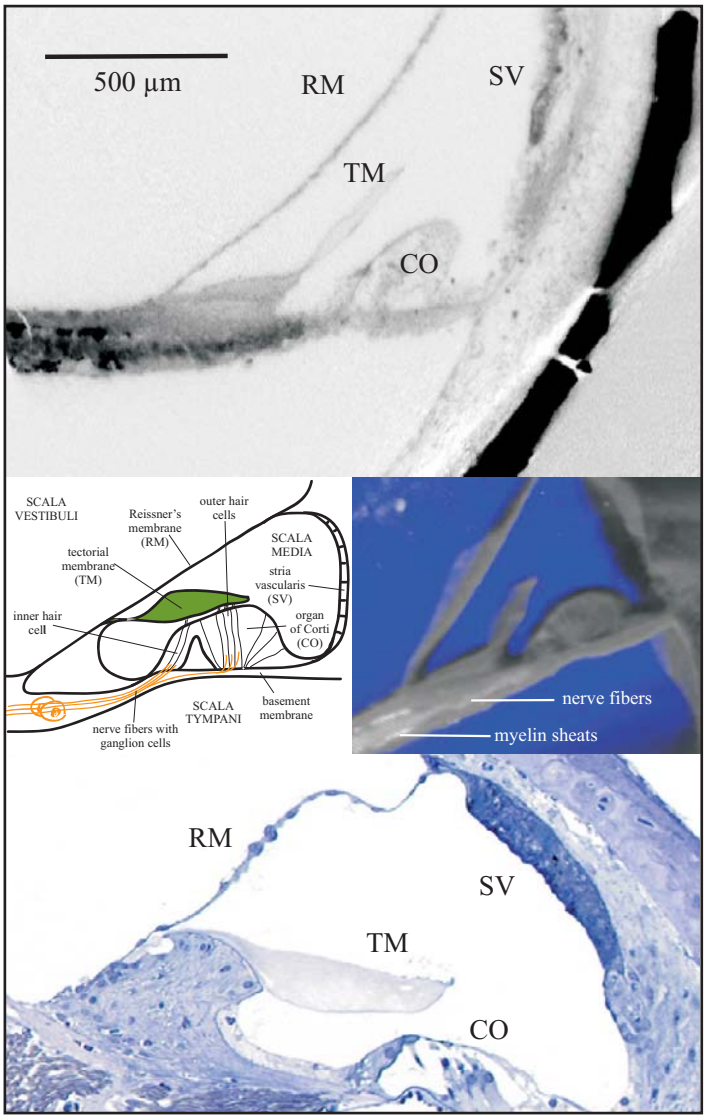

Figure 2

The selected tomographic slice (top) of the apical turn of the inner ear reveals the morphology of the Reissner's membrane (RM), the tectorial membrane (TM), the organ of Corti (CO) and the stria vascularis (SV). The scheme (middle left) helps identifying the features of the representative slice and of the 3D volume rendering (middle right) of the human cochlea. For comparison a representative histological slice of the apical turn (3 weeks old C57 black 6N mice) is presented at the bottom.

Within the current studies we used the combination of light microscopy and SRµCT to uncover the development and morphology of the vestibulo-cochlear system in temporal bone in Pelizaeus Merzbacher disease (PMD) and in cochlea with neural tube defects (NTD) (Fig. 1). PMD is a consequence of X-Linked mutation of the main central nervous system myelin protein resulting in a complex neurological syndrome. NTD are a frequent and heterogeneous group of malformations, ranging from the survivable spina bifida to fatal anencephaly. To increase the X-ray absorption of the soft tissues within the surrounding petrous bone, which is the hardest human tissue, osmium tetroxide staining was applied. This staining method, routinely applied to prepare tissues for electron microscopy, reacts with the unsaturated fatty acids and therefore essentially increases the X-ray absorption of cell membranes. Most of the petrous bone was removed to advance the spatial resolution of the tomographic data. For accessing the morphology of nerve fibre bundles and membranes low-energy SRµCT was applied to part of the cochlea (Fig. 2). The different delicate microstructures in the three-dimensional (3D) space was uncovered with isotropic sub-cellular resolution non-destructively and serve as complementary method to the classical histology of the inner ear.

By the availability of the new stations for micro- and nanotomography at PETRA III the tomographical method will be boosted to access the interior structures of the human hearing organ down to cellular or even sub-cellular level. This will give new insights in the understanding of hearing diseases.

Contact: Felix Beckmann, felix.beckmann@gkss.de

Authors

Felix Beckmann[1], Joachim Schmutzhard[2], Anita Lareida[3,4], Rudolf Glückert[2], Ilona Schwentner[2], Irene Abraham[2], Mario Bitsche[2], Christina Falkeis[5], Wolfgang Freysinger[2], Consolato Sergi[5], Annelies Schrott-Fischer[2], Herbert Riechelmann[2], and Bert Müller[3,4]

1. Institute for Materials Research, GKSS Research Centre, Max-Planck-Strasse 1, 21502 Geesthacht, Germany
2. Department of Otorhinolaryngology, Innsbruck Medical University, Anichstrasse 35, A6020 Innsbruck, Austria
3. Biomaterials Science Center, University of Basel, c/o University Hospital, 4031 Basel, Switzerland
4. Computer Vision Laboratory, ETH Zürich, Sternwartstrasse 7, 8092 Zürich, Switzerland
5. Institute of Pathology, Innsbruck Medical University, Austria

Original publication

"The cochlea in fetuses with neural tube defects", Int. J. Devl. Neuroscience 27, 669-676 (2009).

"Pelizaeus Merzbacher disease: morphological analysis of the vestibulo-cochlear system", Acta Oto-Laryngologica, 99999:1, (2009).

"High-resolution X-ray tomography of the human inner ear: synchrotron radiation-based study of nerve fibre bundles, membranes and ganglion cells", Journal of Microscopy, Vol. 234, Pt 1, 95-102 (2009).

References

1. **U. Vogel, "New approach for 3D imaging and geometry modelling of the human inner ear", J. Otorhinolaryngol. Relat. Spec. 61, 259-267 (1999).**
2. **F. Plouraboué, P. Cloetens, C. Fonta, A. Steyer, F. Lauwers, J.-P. Marc-Vergnes, "X-ray high-resolution vascular network imaging", J. Microsc. 215, 139-148 (2004).**
3. **S.F. Li, T.Y. Zhang, Z.M. Wang, "An approach for precise three-dimensional modeling of the human inner ear", J. Otorhinolaryngol. Relat. Spec. 68, 302-310 (2006).**
4. **F. Beckmann, J. Herzen, A. Haibel, B. Müller, A. Schreyer, "High density resolution in synchrotron-radiation-based attenuation-contrast microtomography", Proc. SPIE 7078, 70781D (2008).**
5. **B. Müller, R. Bernhardt, T. Weitkamp, F. Beckmann, R. Bräuer, U. Schurigt, A. Schrott-Fischer, R. Glückert, M. Ney, T. Beleites, C. Jolly, D. Scharnweber, "Morphology of bony tissues and implants uncovered by high-resolution tomographic imaging", International Journal of Materials Research 98, 613-621 (2007).**

The fate of ecotoxic hexavalent chromium in the environment.

Combined X-ray absorption, UV-Vis spectroscopy, and DPS voltammetry analysis.

Chromium occurs naturally in the Earth's crust in various oxidation states ranging from 0 to 6+. After entering the soil, hexavalent chromium Cr^{6+}, being a strong oxidant, can be readily reduced to trivalent chromium Cr^{3+} in the presence of various electron donors, including soil organic matter. Cr^{3+} readily precipitates or becomes immobilised after sorption onto soil colloids. However, it is known that Cr^{6+} may persist, especially in organic soils, for prolonged periods of time, even years. Our work focused on the elucidation of the possible interaction of Cr^{6+} with humic acids (HAs) by complementary analytical techniques: X-ray absorption spectroscopy (XANES, EXAFS), UV-Vis spectroscopy, and DPS voltammetry. The results show that HAs does not induce reduction of Cr^{6+} to its trivalent chemical form. The interaction between Cr^{6+} and HAs rather leads to the formation of Cr^{6+}–HAs chemical adducts via supramolecular chemical processes, which can explain the relatively high persistence of ecotoxic hexavalent chromium in soils.

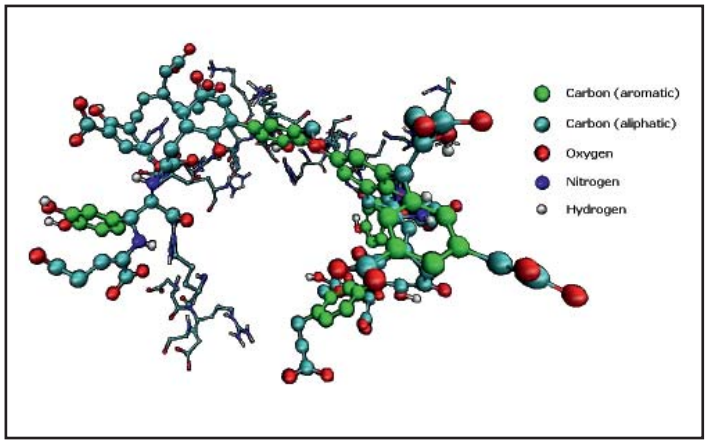

Figure 1

Schematic structure of humic acids (HAs) - natural carbon-rich biopolymers, ubiquitous in terrestrial and aquatic environments.

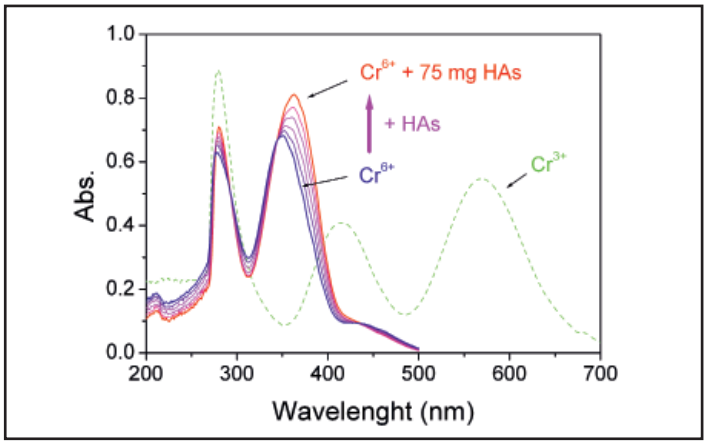

Figure 2

UV-Vis curves of spectrophotometric titration of K_2CrO_4 solution before and after addition of HAs. The dashed line represents the spectrum of trivalent chromium

The presence and fate of chromium in the soil system is of concern mainly due to the high toxicity and carcinogenicity of the hexavalent form (Cr^{6+}). Even though naturally elevated levels of Cr^{6+} can be found in some soils (e.g. Arizona, Chile) distressing amounts of Cr^{6+} in soil are largely restricted to sites contaminated by human activities.

After entering the soil, Cr^{6+} remains thermodynamically metastable in the pore solution and is generally much more mobile in soil than Cr^{3+}. Hexavalent chromium, a strong oxidant, can be readily reduced to Cr^{3+} in the presence of electron donors. However, even when dealing with propitious soil composition and favourable physical conditions, Cr^{6+} may persist, especially in organic soils, for prolonged periods of time, even years [1].

Humic acids (HAs) are carbon-rich polydisperse polyanionic biopolymers (Fig. 1). Their basic binding block consists of a hydrophobic framework of aromatic rings with various functional groups, all interlinked together by more flexible carbon chains. Chemically, HAs behave as supramolecules which are able to polymerise and aggregate, to form micelles and also to form supramolecular ensembles with other compounds. HAs represent a strongly pH-dependent reservoir of electron donors/acceptors, which can hypothetically contribute to reduction of several inorganic and organic contaminants. HAs can therefore affect the uptake, bioavailability, transport, fixation and toxicity of xenobiotics in the environment [2].

In this research, we focused on the elucidation of interactions of Cr^{6+} with standard HAs under sub-neutral conditions using complementary analytical methods: UV-Visible (UV-Vis) spectroscopy, X-ray Absorption Near Edge Structure (XANES), Extended X-ray Absorption Fine Structure (EXAFS), and Differential Pulse Stripping (DPS) voltammetry.

The UV-Vis spectra of K_2CrO_4 water solution at pH 6.5 without and with added increasing concentrations of HAs were recorded in the region between 200 and 600 nm, where the main chro-

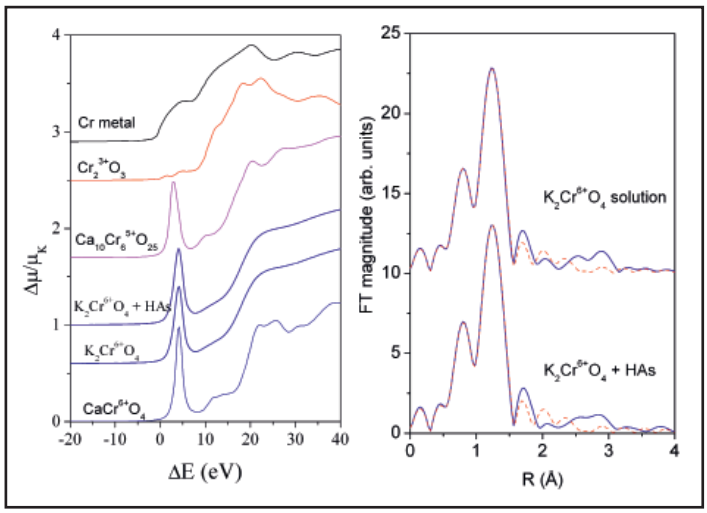

Figure 3

a) Normalized Cr K-edge profiles displaced vertically, K_2CrO_4 solution before and after addition of HAs and reference samples with Cr valence state 0, 3+, 5+ and 6+. The energy scale is set relative to the Cr K-edge in metal (5989.0 eV). (b) Fourier transforms of Cr EXAFS spectra (experiment: solid line; best-fit EXAFS model with FEFF6: dashed line).

mate absorption bands occur (Fig. 2). The spectra revealed two intense absorption bands at 277 nm and 351 nm, characteristic for O–Cr^{6+} electronic charge transfer of chromate species in a tetrahedral conformational structure [3]. Both peaks increased in intensity with increasing levels of HAs, and they shifted to higher wavelengths by 4nm and 13nm, respectively. We did not observe any absorption bands at 425 nm and 583 nm, characteristic for the Cr^{3+} oxygen octahedron. These responses indicated that HAs promoted the probability of intramolecular O–Cr^{6+} electronic charge transfer together with an energetic benefit, without inducing reduction of Cr^{6+} to Cr^{3+}.

In addition, the results of DPS voltammetry, obtained during a stepwise addition of HAs to K_2CrO_4 solution showed a strong interaction of CrO_4^{2-}-complex with HAs, which indicated the formation of Cr^{6+}–HAs micelles (data not shown).

X-ray absorption spectroscopy was used to directly probe the O– Cr^{6+} charge transfer and eventual structural distortion of tetrahedral chromates because of interaction with HAs. X-ray absorption spectra of K_2CrO_4 solution at pH 6.5 with or without HAs were measured in the energy region of the Cr K-edge in transmission mode at beamline E4 at DORIS III(Fig. 3a). The characteristic pre-edge line-shape clearly indicated that Cr in solution remained tetrahedrally coordinated. From the energy position of the pre-edge peak and from the Cr K-edge profile we could deduce that the valence state of chromium in the samples was Cr^{6+} [4,5]. The spectra of chromate with and without HAs were identical within the noise level, which clearly demonstrated that local symmetry and valence state of hexavalent Cr in the aqueous solution did not change due to interaction of CrO_4^{2-} with HAs.

In order to verify whether the interaction between HAs and CrO_4^{2-} involved any structural modifications, we analysed Cr K-edge EXAFS spectra using the IFEFFIT [6] and FEFF6 [7] program packages. The comparison of the EXAFS spectra of K_2CrO_4 solution before and after addition of HAs did not show any structural changes in the local Cr neighbourhood: Both spectra were identical within the noise level. Fourier transform of EXAFS spectra (Fig. 3b) exhibited a single peak. The Cr K-edge EXAFS results therefore clearly showed that interaction with HAs did not induce any structural modifications of the CrO_4^{2-}-complex. From these results, we can conclude that presence of HAs did not favour reduction of Cr^{6+} to Cr^{3+}. In fact, the zwitterionic character of HAs could putatively allow formation of chemical adducts [HAs – Cr^{6+}] which hinder the reduction of Cr^{6+} to Cr^{3+}. The reported observations could contribute to the explanation of the relative persistence of Cr^{6+} in soils.

Contact: Iztok Arčon, iztok.arcon@ung.si

Authors

Liviana Leita[1], Alja Margon[1], Arnold Pastrello[1], Iztok Arčon[2,3], Marco Contin[4], Davide Mosetti[1], Alojz Kodre[3,5]

1. A.R.C. Agricultural Research Council-Research Group on Soil–Plant Systems, Via Trieste 23, 34170 Gorizia, Italy
2. University of Nova Gorica, Vipavska 13, SI-5000 Nova Gorica, Slovenia
3. Jožef Stefan Institute, Jamova 39, SI-1000 Ljubljana, Slovenia
4. Dipartimento di Scienze Agrarie e Ambientali, University of Udine, Via delle Scienze 208, 33100 Udine, Italy
5. Faculty of Mathematics and Physics, University of Ljubljana, Jadranska 19, SI-1000 Ljubljana, Slovenia

Original publication

"Soil humic acids may favour the persistence of hexavalent chromium in soil," Environmental Pollution 157, 1862 (2009).

References

1. **C.D. Palmer, P.R. Wittbrodt, "Processes affecting the remediation of chromium-contaminated sites", Environ. Health Perspect., 92, 25 (1991).**
2. **P.A. Campitelli, M.I. Velasco, S.B. Ceppi, "Chemical and physicochemical characteristics of humic acids extracted from compost, soil and amended soil", Talanta, 69, 1234 (2006).**
3. **K. Takehira, Y. Ohishi, T. Shishido, T. Kawabata, K. Takaki, O. Zhang, Y. Wang, "Behavior of active sites on Cr-MCM-41 catalysts during the dehydrogenation of propane with CO_2", J. Catal., 224, 404 (2004).**
4. **A. Pantelouris, H. Modrow, M. Pantelouris, J. Hormes, D. Reinen, "The influence of coordination geometry and valency on the K-edge absorption near edge spectra of selected chromium compounds", Chem. Phys., 300, 13 (2004).**
5. **I. Arčon, B. Mirtič, A. Kodre, "Determination of Valence States of Chromium in Calcium Chromates by Using X-ray Absorption Near-Edge Structure (XANES) Spectroscopy", J. Am. Ceram. Soc., 81, 222 (1998).**
6. **B. Ravel, M. Newville, "ATHENA, ARTEMIS, HEPHAESTUS: data analysis for X-ray absorption spectroscopy using IFEFFIT", J. Synchrotron Rad., 12, 537 (2005).**
7. **J.J. Rehr, R.C. Albers, S.I. Zabinsky, "High-order multiple-scattering calculations of X-ray-absorption fine structure", Phys. Rev. Lett., 69, 3397 (1992).**

A picosecond hard X-ray delay line.

A tool for studying ultrafast dynamics

Although X-ray free-electron lasers provide extremely intense and coherent pulses, their time structure can compromise the applicability of experimental techniques such as X-ray pump/X-ray probe or X-ray photon correlation spectroscopy (XPCS). To fully exploit the potential of XFEL light with the aforementioned techniques we have developed a hard X-ray delay line, i.e. a device capable of splitting a single X-ray pulse into two, delaying one of the pulses and recombining both pulses on a common path. The initial tests of the device were carried out with 8.39 keV radiation. Delay times between the two split pulses of up to 2.63 ns have been achieved with a 16.7 ps time resolution.

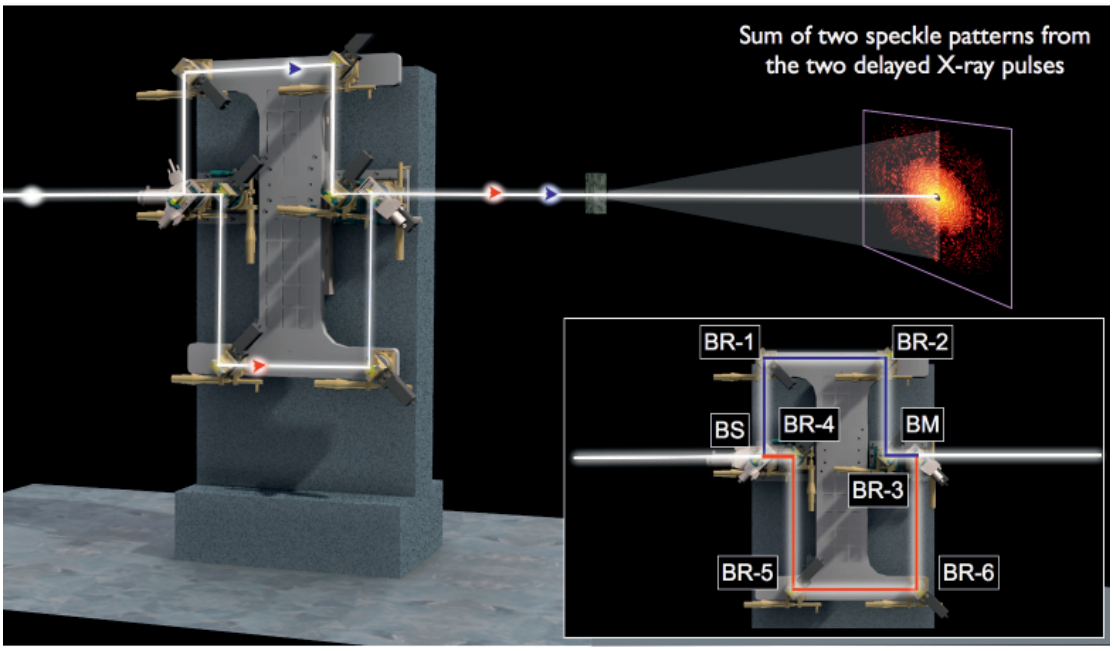

Figure 1
Illustration of the split-and-delay XPCS technique. A single X-ray pulse is split into two equal intensity pulses using the hard X-ray delay line. The pulses propagate collinearly in the sample direction. Inset: Concept of the hard X-ray delay line. BR-1 to BR-6, Bragg reflectors; BS: beam splitter, BM: beam mixer. The paths of the upper and lower branch of the delay line are denoted by blue and red lines, respectively.

X-ray free-electron laser sources will produce ultrashort, coherent and very intense pulses creating excellent conditions for investigation of ultrafast phenomena [1,2].
The accessible time windows are however influenced by the intrinsic time structure of the machine. The European XFEL facility in Hamburg, Germany will provide 100 fs short single pulses separated by 200 ns arranged into bunch trains of 3000 pulses arriving with a repetition rate of 10 Hz [1]. Studying dynamics with XPCS [3] or via the X-ray pump/X-ray probe technique on time scales shorter than 200 ns will thus not be feasible at the European XFEL. One way to overcome this limitation is the split-and-delay approach [4]. Fig. 1 illustrates this approach with the XPCS method. The technique is based on splitting each X-ray pulse into two equal pulses, separating them in time and bringing them back on the primary beam path. The speckle pattern obtained from the sample, which is illuminated by both pulses, is summed on the area detector. Dynamics of the sample are studied by analyzing the contrast in the summed speckle patterns as a function of the applied delay times (i.e. time intervals between the two pulses) [5].
The concept of an X-ray delay line is shown in the inset of Fig. 1. The device consists of eight single crystals arranged in 90° vertical-scattering geometry. An incoming X-ray pulse is split by a first crystal (BS) into two pulses that propagate along two unequal rectangular paths. One part of the pulse is guided by Bragg crystal reflectors BR-1, BR-2, and BR-3 (blue line). The path of the second pulse is defined by the crystals BR-4, BR-5, and BR-6 (red line). Both beams are recombined with the help of the beam mixer (BM). The beam is reflected inside the delay line by using perfect Si(511) crystals oriented in symmetric Bragg geometry (called Bragg crystals) [6]. Beam splitting and mixing is accomplished by wedge-shaped Si(511) perfect

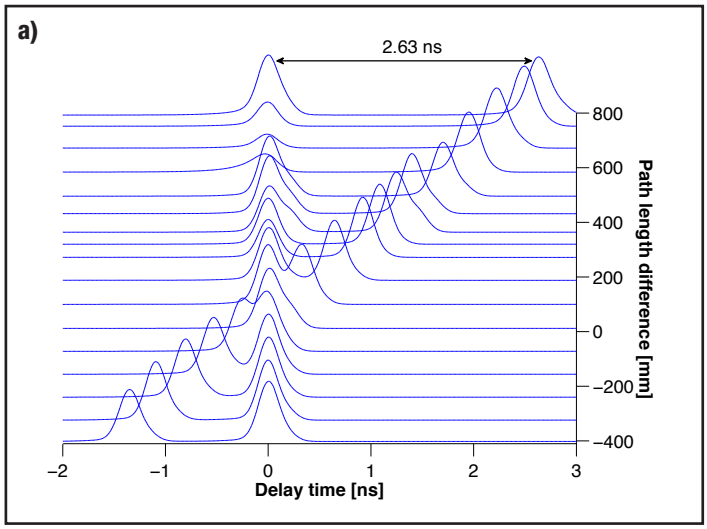

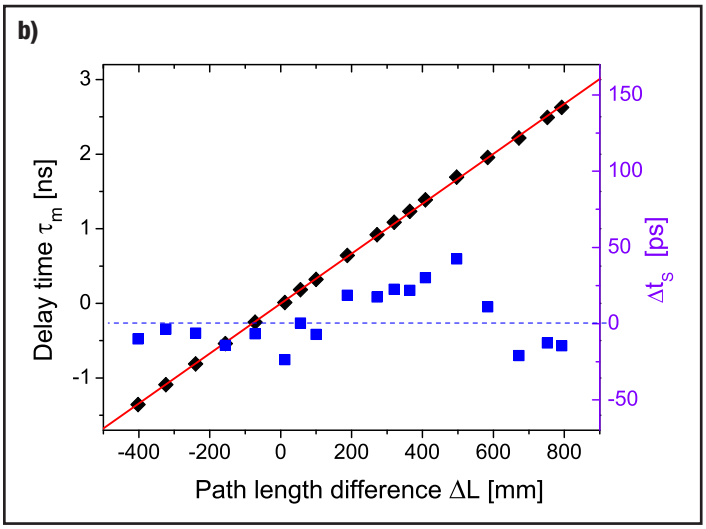

Figure 2

a) Time patterns corresponding to delayed X-ray pulses measured as a function of the path length difference ΔL.

b) Left axis: Measured delay time vs. path length difference ΔL. The red solid line denotes a linear fit to the data. Right axis: The difference between expected and measured delay time is quantified by the blue squares.

crystals oriented in Laue geometry (called Laue crystals). The time interval τ_c between the two split pulses is defined by ΔL/c, where c and ΔL are the speed of light and the path length difference between the upper and lower branch of the delay line, respectively. A change of the delay time τ_c is achieved by simultaneous vertical movements of the crystals BR-1, BR-2, BR-5, BR-6 in the direction perpendicular to the incident beam. The setup works in a fixed 90° scattering geometry to optimize the delay time adjustment. In this case a single translation is sufficient to change ΔL. The present design limits the operation of the delay line to a single energy. A 3D model of the delay line is shown in Fig. 1.

Preliminary performance tests of the delay line were carried out at the beamlines C and W1 of the DORIS III storage ring at HASYLAB. The results, which we present here, were obtained at beamline ID10C at ESRF. The performance of the delay line optics has been verified with 8.39 keV X-rays. The throughput of the delay line obtained with a Si(333) pre-monochromator and a photon beam divergence of 17 µrad was measured by comparing incident and exit intensities, yielding a value of 0.6 %.

Fig. 2(a) shows a graph of pulse patterns recorded during four-bunch mode operation of the ESRF storage ring. The time interval between detected photons and the synchrotron bunch clock signal was measured in a stroboscopic manner [7] with different path length differences ΔL of the delay line. A maximum delay time of 2.626 ± 0.003 ns was achieved in the experiment. Fig. 2(b) shows a plot of the measured delay time τ_m as a function of the path length difference ΔL. The solid line is a least-squares fit to the data, which yields a slope of 3.35 ± 0.01 x 10^{-3} ns/mm. In addition the delay time error $\Delta t_s = \tau_m - \Delta L/c$ was extracted for every data point. The results are also shown in Fig. 2(b). The mean error is 16.7 ps. Since the uncertainty of setting ΔL is only 0.5 µm (i.e. 7 fs), the main contribution to the obtained error is due to the limited time resolution of the detection system.

The results have shown that the X-ray delay line is operational for first experiments with XFEL radiation. Upgrades are under further development to achieve higher throughput and broader energy tunability.

Contact: Wojciech Roseker, wojciech.roseker@desy.de

Authors

Wojciech Roseker[1], Hermann Franz[1], Anita Ehnes[1], Horst Schulte-Schrepping[1], Olaf Leupold[1], Federico Zontone[2], Aymeric Robert[3], Gerhard Grübel[1]

1. Hamburger Synchrotronstrahlungslabor am Deutschen Elektronen Synchrotron (DESY), Notkestrasse 85, D-22603 Hamburg, Germany
2. ESRF, European Synchrotron Radiation Facility, BP 220, 38043 Grenoble CEDEX, France
3. SLAC National Accelerator Laboratory, 2575 Sand Hill Road, Menlo Park, CA 94025, USA

Original publication

"Performance of a picosecond X-ray delay line unit at 8.39 keV", Optics Letters 34, 1768–1770 (2009).

References

1. **M. Altarelli, et al., "XFEL: The European X-ray Free-Electron Laser", Technical Design Report (2006).**
2. **J. Arthur, et al., "LCLS Ultrafast Science Instruments: Conceptual Design Report" (2007).**
3. **G. Grübel and F. Zontone, "Correlation spectroscopy with coherent X-rays", J. Alloys Compd., 362, 3-11 (2004).**
4. **G. Grübel et al. "XPCS at the European X-ray free-electron laser facility, Nucl. Instrum. and Methods B", 262, 357-367 (2007).**
5. **C. Gutt, et al., "Measuring temporal speckle correlations at ultrafast X-ray sources", Opt. Express 17, 55-61 (2009).**
6. **B. W. Batterman and H. Cole, "Dynamical diffraction of x rays by perfect crystals", Rev. Mod. Phys. 36, 681-717 (1964).**
7. **S. Kishimoto, "High time resolution X-ray measurements with an avalanche photodiode detector", Rev. Sci. Instrum. 63, 824-827 (1992).**

Revealing the molecular rules of muscle protein assembly.

High resolution structures of protein complexes to understand the molecular architecture of human muscle cells

The contraction/relaxation cycle of muscle cells translates into large molecular movements of several filament systems in sarcomeres, requiring special molecular mechanisms to maintain their structural integrity. Recent structural and functional data from filaments with extensive arrays of immunoglobulin-like domains have for the first time unravelled a common function of their terminal domains: assembly and anchoring of the respective filaments. The available data have also revealed a number of common principles governing terminal filament assembly. In all these cases, protein-protein interactions are mediated by antiparallel dimerisation modules, via intermolecular β-sheets. These observations provide an attractive model for several other filament proteins, which have not yet been structurally characterized.

Skeletal and cardiac muscle cells are organized in sarcomeric units that form the basic compartment of the contractile apparatus [1]. The architecture of the sarcomeric units is established by a number of major filaments, seen as characteristically shaded regions in electron microscopy images. Many of these filaments are connected and anchored either at the most peripheral area, referred to as the Z-disk, or within the central region, the so-called M-band, which divides each sarcomeric unit into two mirrored halves. We have recently outlined some of the emerging molecular principles that define how sarcomeric filaments are assembled, connected and anchored [2]. In this summary we focus on some of the recent key achievements from our laboratory on the self-assembly of two sarcomeric filament proteins, titin and myomesin.

N-terminal titin assembly and connecting bridges

Perhaps the most remarkable and unexpected filament assembly complex has been found at the N-terminus of titin [3]. Complex formation of titin with the scaffold protein telethonin was initially considered to be binary, and a telethonin function as a “cap” or “bolt” was proposed [4]. The structure of the titin/telethonin complex, however, revealed an assembly with 2:1 stoichiometry, in which one telethonin molecule mediates an antiparallel arrangement of two titin filaments (Figure 1, left). In the presence of titin, telethonin forms a central β-sheet that is flanked by two wing-like b-hairpins with related sequences and structures. These telethonin “wings” generate a total of four binding sites, thus exhibiting a unique palindromic arrangement of titin with internal two-fold symmetry [3]. Comparison of the structures of the titin N-terminus in the absence and presence of telethonin [3,5] reveals that telethonin rigidifies the titin N-terminus, in addition to its function as an assembly mediator.

C-terminal myomesin assembly

All three known members of the myomesin filament family are localized in the central M-band of the sarcomere and display a closely related domain organization [6]. Immuno-electron microscopy data indicated that the orientation of the C-terminal region of myomesin is parallel to the principal filament orientation in sarcomeric units [7]. Biochemical data revealed that myomesin assembles into a dimer via its C-terminus [8]. A recent crystal structure of the two myomesin C-terminal Ig domains 12 and 13 showed that the assembly has a direct and antiparallel arrangement, forming an end-to-end filament structure across the central M-line of sarcomeres [9] (Figure 1, right). The assembly involves two surface patches from Ig domain 13, one of which leads to the formation of an intermolecular β–sheet and the other which is formed from a number of specific side-chain interactions. The linker next to IG domain 13 is of substantial length (~20 residues) and folds into an a-helix, which is not involved in further dimer assembly interactions, thus demonstrating that terminal assembly in myomesin is restricted to Ig domain 13.

Future perspectives for structures of muscle filament assemblies

Sarcomeric filament proteins belong to the largest gene products of the human genome. Because of their large size and flexibility, it is not possible to apply conventional structural biology methods for determination of their structures. Within the projects presented, we have mostly made use of methods that are provided by EMBL-Hamburg; X-ray crystallography and Small Angle X-ray Scattering (SAXS). We anticipate that their use will become even more powerful once our new beamlines at PETRA III have started operation. In present unpublished projects, we have

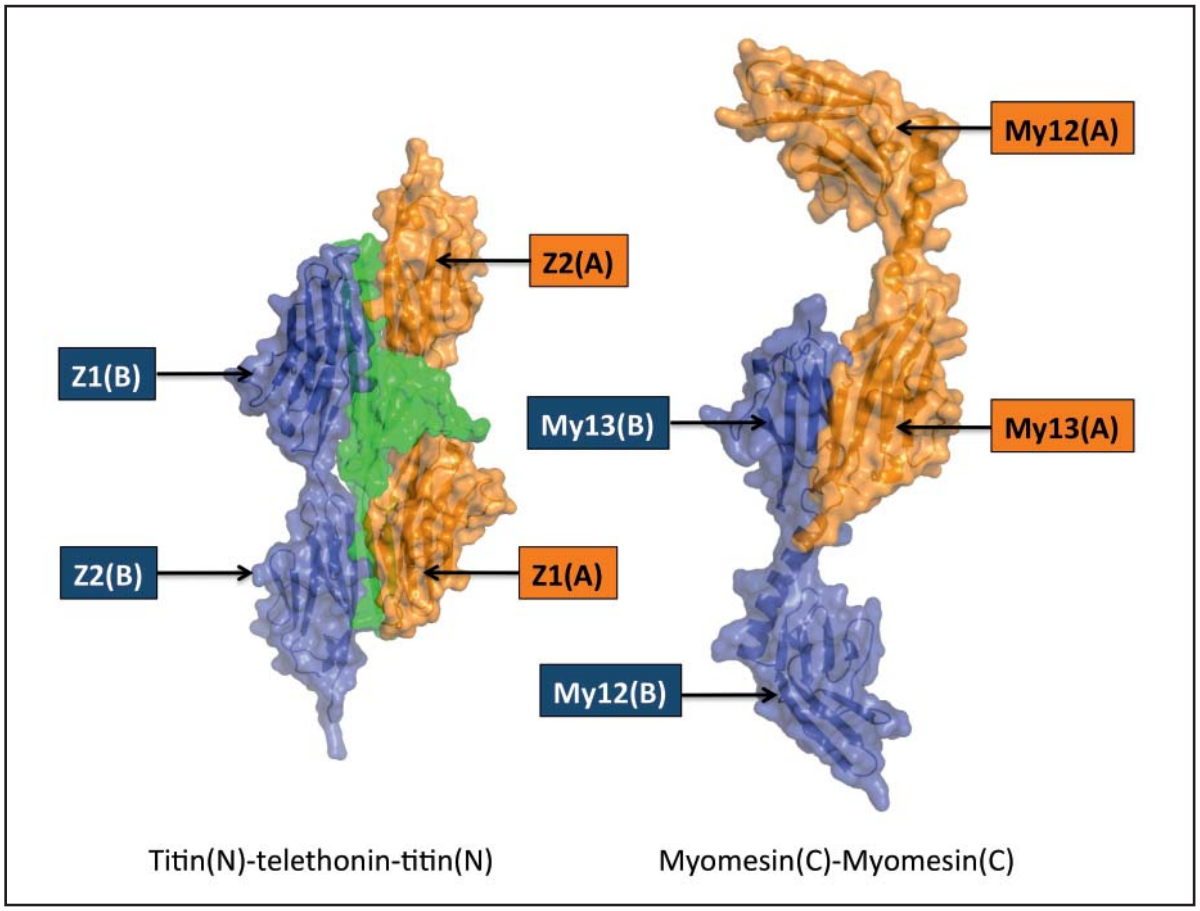

Figure 1

Structures of the N-terminal titin assembly (left) and C-terminal myomesin assembly. The two assembly molecules are coloured in blue and orange. Telethonin, which mediates N-terminal titin assembly, is shown in green. The immunoglobulin-like (Ig) domains are labelled, using the nomenclature used in the original research papers

also included electron microscopy. As shown by recent data on the titin/telethonin complex, steered atomic force microscopy presents a powerful tool to test the elastic properties of the assemblies investigated [10]. In addition, there will be increasing need to test new structural data obtained with purified protein components by *in vivo* functional assays and imaging methods. We hope that the future Centre for Structural Systems Biology (CSSB) will allow us to fill this gap seen at present research infrastructures.

Contact: Matthias Wilmanns, wilmanns@embl-hamburg.de

Authors

Nikos Pinotsis[1,2], Matthias Wilmanns[1]

1. EMBL Hamburg, Notkestrasse 85, D-22603 Hamburg, Germany.
2. Section of Structural Biology, Institute of Cancer Research, Chester Beatty Laboratories, 237 Fulham Road, London SW3 6JB, UK.

Original publication

Terminal assembly of sarcomeric filaments by intermolecular beta-sheet formation. Trends Biochem Sci. 34, 33-39 (2009). PubMed PMID: 18996015.

References

1. **J.M. Squire, H.A. Al-Khayat, C. Knupp and P.K. Luther, "Molecular architecture in muscle contractile assemblies", Adv. Protein Chem. 71, 17-87 (2005).**
2. **N. Pinotsis, P. Abrusci, K. Djinovic-Carugo and M. Wilmanns, "Terminal assembly of sarcomeric filaments by intermolecular beta-sheet formation", Trends Biochem Sci. 34, 33-9 (2009).**
3. **P. Zou et al., "Palindromic assembly of the giant muscle protein titin in the sarcomeric Z-disk", Nature 439, 229-33 (2006).**
4. **C.C. Gregorio, H. Granzier, H. Sorimachi and S. Labeit, "Muscle assembly: a titanic achievement?", Curr Opin Cell Biol 11, 18-25 (1999).**
5. **M. Marino et al., "The Ig doublet Z1Z2: a model system for the hybrid analysis of conformational dynamics in Ig tandems from titin", Structure 14, 1437-47 (2006).**
6. **R. Schoenauer, S. Lange, A. Hirschy, E. Ehler, J.C. Perriard and I. Agarkova, "Myomesin 3, a novel structural component of the M-band in striated muscle", J Mol Biol 376, 338-51 (2008).**
7. **W.M. Obermann, M. Gautel, F. Steiner, P.F. van der Ven, K. Weber and D.O. Furst, "The structure of the sarcomeric M band: localization of defined domains of myomesin, M-protein, and the 250-kD carboxy-terminal region of titin by immunoelectron microscopy", J Cell Biol 134, 1441-53 (1996).**
8. **S. Lange, M. Himmel, D. Auerbach, I. Agarkova, K. Hayess, D.O. Furst, J.C. Perriard and E. Ehler, "Dimerisation of myomesin: implications for the structure of the sarcomeric M-band", J Mol Biol 345, 289-98 (2005).**
9. **N. Pinotsis, S. Lange, J.C. Perriard, D.I. Svergun and M. Wilmanns, "Molecular basis of the C-terminal tail-to-tail assembly of the sarcomeric filament protein myomesin", Embo J 27, 253-64 (2008).**
10. **M. Bertz, M. Wilmanns and M. Rief, "The titin-telethonin complex is a directed, superstable molecular bond in the muscle Z-disk", Proc. Natl. Acad. Sci U S A 106, 13307-133310 (2009).**

Recycling the ribosome.

Structural characterization of a complex that mediates termination of protein synthesis

Developments in Small-Angle X-ray Scattering (SAXS) at the EMBL, Hamburg Outstation made this method a high-throughput, low resolution tool providing information about overall structure and conformational changes of biological macromolecules in solution. SAXS is often employed along with protein crystallography to elucidate structure of functional complexes, such as that of proteins eRF1 and eRF3, which assure fast release of peptides from the ribosome during termination of protein synthesis. It was found that the M domain of eRF3 stimulates a GTPase activity of eRF1. The latter protein recognizes the stop codon of the messenger RNA, and in concert with eRF3 mediates dissociation of ribosome, which plays a critical role in the recycling of the ribosome before the next translation event.

Synchrotron Small-Angle X-ray Scattering (SAXS) is a rapid technique to study the overall structure of native biological macromolecules in solution. Using modern analysis methods, low resolution shapes of individual macromolecules or complexes may be determined *ab initio* [1]. For multidomain proteins or complexes, where high resolution structures of domains or subunits are available, rigid body modelling may be employed to determine the quaternary structure [2]. SAXS studies in solution are particularly useful in analyzing changes induced by ligand binding or change of temperature, ionic strength, pH etc. These structural responses may be difficult to assess in a crystal, where the biological macromolecules are constrained by interaction with the crystal lattice. Moreover, the macromolecular complexes may be flexible and/or transient, which makes it difficult to apply high resolution methods like protein crystallography or nuclear magnetic resonance.

The EMBL X33 beamline at DORIS III is optimized for SAXS on biomacromolecular solutions and has recently been upgraded [3] to significantly improve its performance and user friendliness. In particular, the beamline is equipped with a PILATUS photon-counting detector (DECTRIS, Switzerland), and a liquid handling robot for high throughput experiments [4]. An automated data analysis pipeline provides the users with the fully processed data and *ab initio* three-dimensional structural models within a few minutes following the data collection. The EMBL-developed program package ATSAS [5] allows for further comprehensive structural modelling of the experimental data in terms of biologically sensible models. The X33 beamline is employed in a rapidly growing number of collaborative biological projects by user groups worldwide.

An example of the use of SAXS to validate and complement structural models provided by protein crystallography is given by a recent study of a functional complex involved in termination of protein synthesis in eukaryotes. Termination of protein synthesis occurs when the stop codon of the messenger RNA enters the ribosomal A site, and is conducted in eukaryotes by a

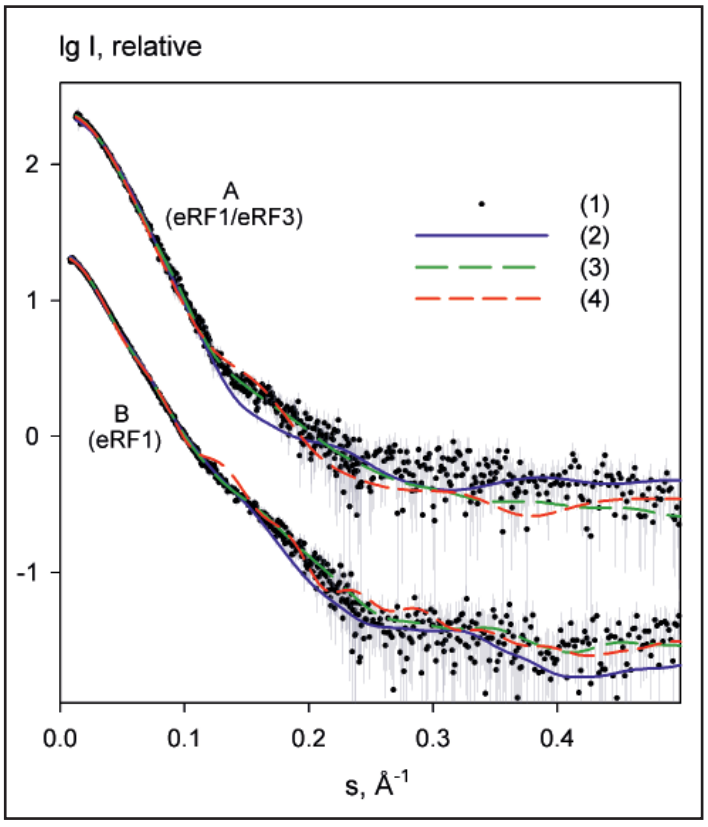

Figure 1

Experimental and computed SAXS scattering data. A, the eRF1/eRF3/GTP complex, B, free eRF1. The logarithm of the scattering intensity is plotted against the momentum transfer $s = 4\pi \sin\theta/\lambda$, where 2θ is the scattering angle and $\lambda = 1.5$ Å is the X-ray wavelength. The plots are displaced along the ordinate for better visualization. (1), experimental scattering; (2) computed scattering from the molecular model of eRF1-eRF3 (in A) and from the crystallographic dimer of eRF1 (in B); (3) computed scattering from these two models after rigid body refinement; (4) computed scattering from the rigid body model of eRF1-eRF3 using extended eRF1 (A) and from the rigid body model of eRF1 dimer using a compact eRF1 monomer (B).

complex consisting of release factors 1 (eRF1) and 3 (eRF3). The crystal structure of human eRF1 release factor has been solved [6], and high resolution structures of both yeast eRF1 and eRF3 are also available.

In the work presented here we report on the formation and structure of the full human eRF1*eRF3 complex by crystallography, SAXS, and mutagenesis studies. Crystal structures of full-length eRF1 (human and *S. pombe*) in complex with a truncated eRF3 (lacking the so-called GTPase domain) were solved. They reveal details of the interface between domain 3 of eRF3 and the domain C of eRF1, and suggest a marked conformational change in eRF1 upon eRF3 binding. SAXS experiments were performed on both components of the complex separately, and on a full complex, see data on Figure 1. These data confirm that compaction of eRF1 occurs only upon binding with eRF3.

An *ab initio* low resolution shape of the complex was computed using DAMMIF [7] (Figure 2a) and revealed structural mimicry to a complex of tRNA with an elongation factor EF-Tu.

The rigid body modeling of the SAXS data from the full-length eRF1*eRF3 complex constrained by the inter-residue contacts between the two proteins in the crystal was done using SASREF [2] to yield a quasi-atomic model in Figure 2a. Here, the C-terminal domains of eRF1 and eRF3 bind together, but also the M domain of eRF1 binds with this eRF3 domain proximal to the hydrolyzation site of guanosine triphosphate, which is known as activator of the peptide release reaction. Biochemical study confirmed the hypothesis, based on SAXS and crystallographic models, that residue Arg192 is stimulating the eRF3 activity in hydrolysing the guanosine triphosphate.

The synergistic study using crystallography, SAXS and mutational analysis provides new structural insights into the stop codon recognition by eRF1 and the process of translation termination in protein synthesis. This underlines the possibilities of SAXS and multidisciplinary approaches for structural characterisation of biomacromolecular complexes.

Contact: Dmitri I. Svergun, svergun@embl-hamburg.de

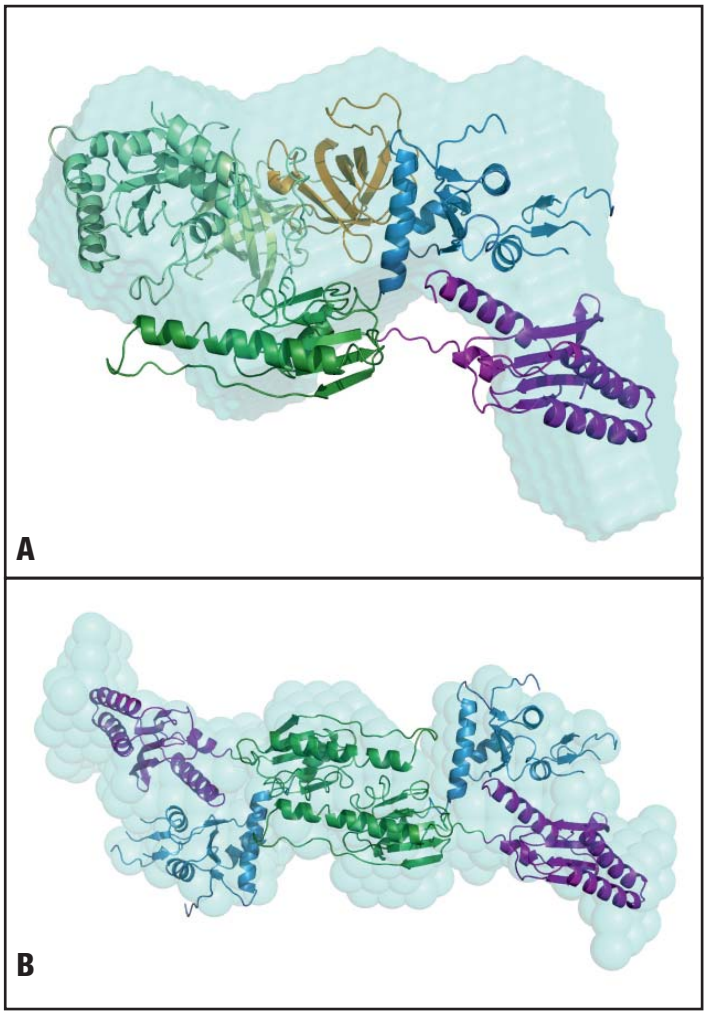

Figure 2

SAXS-derived models of eRF1*eRF3 complex (panel A) and dimeric eRF1 (panel B). The rigid body models provided by SASREF are displayed in cartoons. For eRF1, the N-terminal domain is drawn in purple, the middle domain in blue and the C-terminal domain in dark green, respectively. For eRF3, the N-terminal domain is in light green, the middle domain in lime, and the C-terminal domain in orange, respectively. In both panels, the models are superposed onto the *ab initio* shapes reconstructed with DAMMIF (light blue spheres).

Authors

Zhihong Cheng[1], Kazuki Saito[2], Andrey V. Pisarev[3], Miki Wada[2], Vera P. Pisareva[3], Tatyana V. Pestova[3], Michal Gajda[4], Adam Round[4], Chunguang Kong[1], Mengkiat Lim[1], Yoshikazu Nakamura[2], Dmitri I. Svergun[4,5], Koichi Ito[2,6], and Haiwei Song[1]

1. Cancer and Developmental Cell Biology Division, Institute of Molecular and Cell Biology, A*STAR (Agency for Science, Technology and Research), 61 Biopolis Drive, Singapore 138673, Singapore
2. Department of Basic Medical Sciences, Institute of Medical Science, University of Tokyo, 4-6-1 Shirokanedai, Minato-ku, Tokyo 108-8639, Japan.
3. Department of Microbiology and Immunology, SUNY Downstate Medical Center, Brooklyn, NY 11203, USA
4. European Molecular Biology Laboratory, Hamburg Outstation, Notkestrasse 85, 22603 Hamburg, Germany
5. Institute of Crystallography, Russian Academy of Sciences, Leninsky pr. 59, 117333 Moscow, Russia
6. Precursory Research for Embryonic Science and Technology (PRESTO), Japan Science and Technology Agency (JST),

Original publication

"Structural insights into eRF3 and stop codon recognition by eRF1", Genes and Development Vol. 23 No. 9, 1106-1118, (2009).

References

1. **M.V. Petoukhov and D. I. Svergun, "Analysis of X-ray and neutron scattering from biomacromolecular solutions", Curr. Opin. Struct. Biol. 17, 562-571 (2007).**
2. **M.V. Petoukhov and D.I. Svergun, "Global rigid body modeling of macromolecular complexes against small-angle scattering data", Biophys J. 89, 1237-1250 (2005).**
3. **M.W. Roessle, R. Klaering, U. Ristau, B. Robrahn, D. Jahn, T. Gehrmann, P. Konarev, A. Round, S. Fiedler, C. Hermes and D. Svergun, "Upgrade of the small-angle X-ray scattering beamline X33 at the European Molecular Biology Laboratory", Hamburg. J. Appl. Cryst. 40, S190-S194 (2007).**
4. **A. R. Round, D. Franke, S. Moritz, R. Huchler, M. Fritsche, D. Malthan, R. Klaering, D. Svergun and M. Roessle, "Automated sample-changing robot for solution scattering experiments at the EMBL Hamburg SAXS station X33", J. Appl. Cryst. 41, 913-917 (2008).**
5. **P. V. Konarev, M.V. Petoukhov, V. V. Volkov and D. I. Svergun, "ATSAS 2.1, a program package for small-angle scattering data analysis", J. Appl. Crystallogr. 39, 277–286 (2006).**
6. **H. Song, P. Mugnier, A.K. Das, H.M. Webb, D.R. Evans, M.F. Tuite, B.A. Hemmings and D. Barford, "The crystal structure of human eukaryotic release factor eRF1 – mechanism of stop codon recognition and peptidyl-tRNA hydrolysis", Cell 100, 311-321 (2000).**
7. **D. Franke and D. I. Svergun, "DAMMIF, a program for rapid ab-initio shape determination in small-angle scattering". J. Appl. Cryst. 42 342-346 (2009).**

Magnetic stability at the nanoscale.

When ferromagnetism supports antiferromagnetism

Ferromagnetic order in thin films is strongly affected when their thickness is reduced to the nanometer regime. The main reason for this are thermal excitations that lead to fluctuations of the magnetic moments. It is well known that thick antiferromagnetic buffer layers with a high magnetic anisotropy can be used to stabilize magnetic order in ultrathin ferromagnetic films. This effect is of high importance for modern data storage technology. On the way to further miniaturization one consequently asks what happens to antiferromagnetic layers in the ultra thin limit and how their magnetic properties are influenced by surrounding magnetic material. These questions are subject of an investigation involving ultrathin layers of Fe and its native oxide.

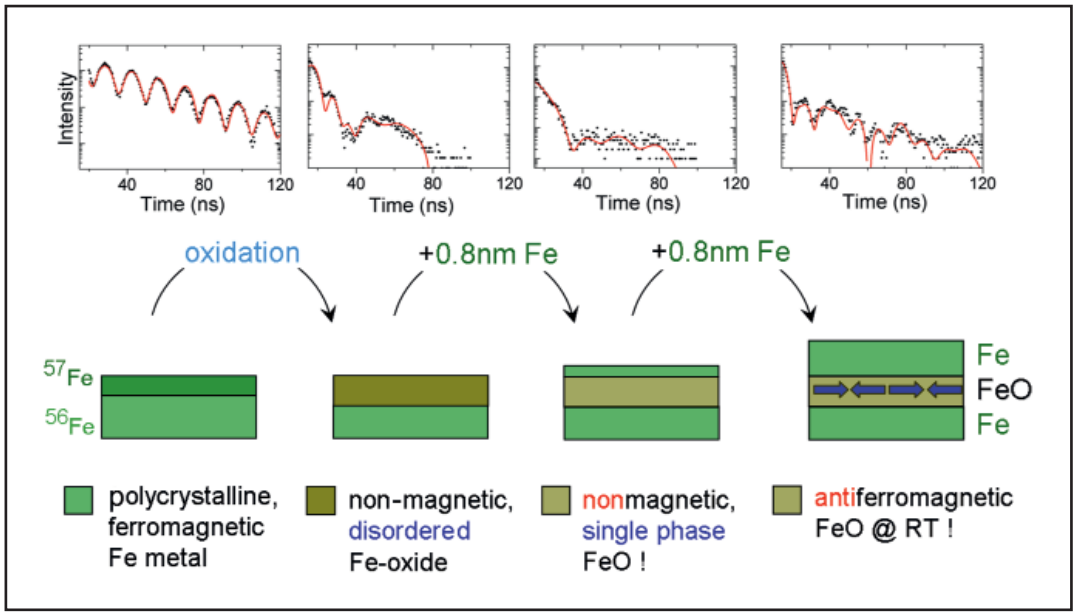

Figure 1

Evolution of the magnetic state of a thin FeO layer during growth, investigated via nuclear resonant scattering. The disappearance of temporal beats after oxidation indicates that a predominantly non-magnetic oxide is formed. Deposition of Fe leads to the formation of a chemically pure FeO layer. Further deposition leads to ferromagnetic ordering in the top Fe layer and hence, to the increase of the magnetic ordering temperature of the FeO, which becomes antiferromagnetic at room temperature.

Following the pioneering work of Beach et al. who revealed intriguing magnetic properties of ultrathin native iron oxide layers [1], we studied the growth of nanometer thin FeO layers via nuclear resonant scattering (NRS). Surprisingly, we found that once a FeO layer is sandwiched between ferromagnetic layers, a drastic increase of its Néel temperature (the temperature below which antiferromagnetic order appears) is observed. The high sensitivity of the experimental method to magnetization dynamics (close to the GHz regime) allowed to reveal that at very low temperatures interfacial spin freezing occurs that leads to exchange bias.

The NRS experiment was performed in-situ at the ID18 beamline of ESRF. The isotope sensitivity of NRS, in combination with a probe layer approach, was used to select only the signal originating from the oxide layer (see Fig. 1). In this way one discriminates against the strong magnetic signal of the neighbouring Fe metal, which normally prevents the detection of the oxide's magnetic state using conventional techniques. This approach was used to monitor the chemical and magnetic state of the oxide layer during its growth. The basic results are summarized in Fig. 1. We start with a 2 nm ^{56}Fe layer on top of which a 0.6 nm ^{57}Fe layer (the NRS active isotope) is deposited. This layer is subsequently oxidized by controlled admission of oxygen into the vacuum chamber. A sudden change from pure magnetic Fe to a chemically disordered, predominantly non-magnetic oxide is observed. Remarkably, the deposition of one atomic layer of Fe on top of this non-stoichiometric oxide leads to the formation of a chemically pure FeO layer [2], which appears to be non-magnetic. With further deposition of Fe, a sharp magnetic transition is observed in the oxide, which in-

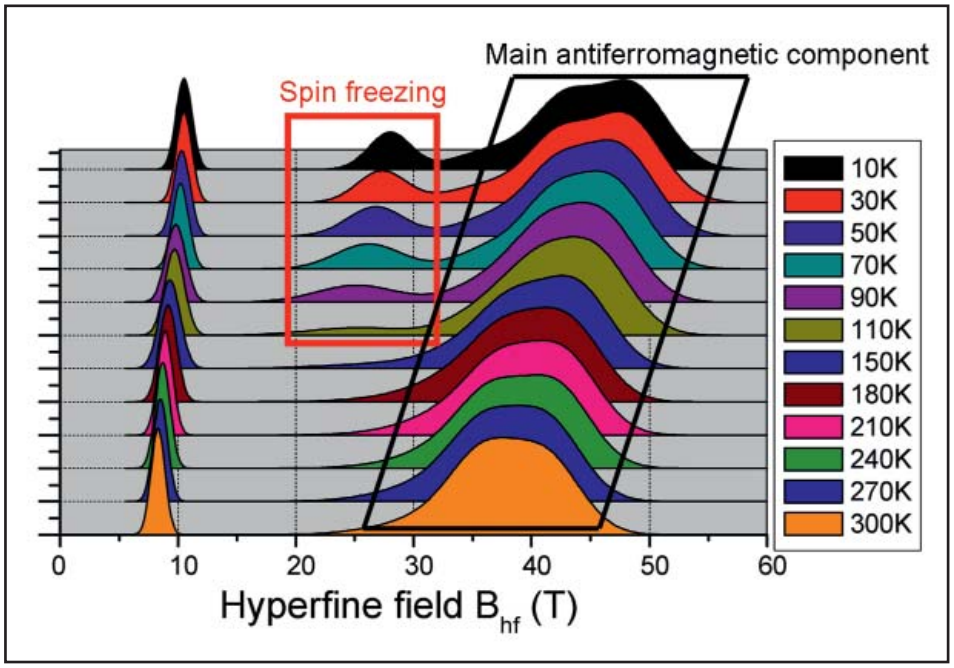

Figure 2

Temperature dependence of the magnetic hyperfine field distribution of a buried FeO layer, as extracted from evaluation of the nuclear timespectra. Below 90 K an additional component appears around a hyperfine field of 25 T that is attributed to interfacial spin freezing.

dicates that its Néel temperature T_N has effectively climbed above room temperature. We expect that this magnetic transition coincides with the appearance of long range ferromagnetism in the top Fe layer, which is only possible once a critical thickness is reached. Ex-situ temperature dependent measurements allowed us to estimate the T_N to be as high as 800 K, very close to the Curie temperature T_C of the neighbouring Fe layer. This similarity is not a coincidence, as the proximity of very thin ferromagnetic layers often leads to a convergence of T_N towards the T_C of the ferromagnetic material.

For antiferromagnetic FeO in contact with a ferromagnet one expects a horizontal shift of the hysteresis loop, the so-called exchange bias phenomenon. Here, however, this shift is observed only at temperatures below 30 K. The analysis of the NRS data revealed that at the same temperature where the exchange bias transition takes place an extra magnetic component in the hyperfine field distribution appears, shown in Fig. 2. This component could be attributed to spins which progressively freeze in with decreasing temperature and remain in a fixed orientation below 30 K. From that we can deduce that exchange bias in this system is linked with interfacial spin freezing.

In conclusion, this study unravels in a remarkably clear fashion how the magnetic state of an ultrathin antiferromagnetic layer can be stabilized by adjacent ferromagnets. As a result its effective Néel temperature raises by several hundreds of Kelvin. In the case of FeO, this leads to antiferromagnetic order at room temperature, an effect which mediates strong interlayer coupling in Fe/FeO multilayers [3]. In contrast, the temperature below which exchange bias is observed decreases with decreasing thickness of the oxide layer, pointing to a stabilization mechanism that is related to interfacial spin freezing.

Contact: Ralf Röhlsberger, ralf.roehlsberger@desy.de

Authors

S. Couet[1,2], K. Schlage[1], R. Rüffer[3], S. Stankov[3], Th. Diederich[1], B. Laenens[2], R. Röhlsberger[1]

1. Deutsches Elektronen Synchrotron (DESY), Notkestrasse 85, 22603 Hamburg, Germany
2. K.U.Leuven, Instituut voor Kern- en Stralingsfysica & INPAC, Celestijnlaan 200D, B-3001 Leuven, Belgium
3. European Synchrotron Radiation Facility (ESRF), BP 220, 38043 Grenoble cedex, France

Original publication

"Stabilization of Antiferromagnetic Order in FeO Nanolayers", Physical Review Letters 103, 097201 (2009).

References

1. **G.S.D. Beach, F.T. Parker, D.J. Smith, P.A. Crozier, A.E. Berkowitz, "New Magnetic Order in Buried Native Iron Oxide Layers", Phys. Rev. Lett. 91, 267201 (2003).**
2. **S. Couet, K. Schlage, K. Saksl, R. Röhlsberger, "How Metallic Fe Controls the Composition of its Native Oxide", Phys. Rev. Lett. 101, 056101 (2008).**
3. **S. Couet, K. Schlage, Th. Diederich, R. Rüffer, K. Theis-Bröhl, B.P. Toperverg, K. Zhernenkov, H. Zabel, R. Röhlsberger, "The magnetic structure of coupled Fe/FeO multilayers revealed by nuclear resonant and neutron scattering methods", New J. Phys. 11, 013038 (2009).**

Hidden local symmetries in disordered matter.

Order in disorder uncovered by X-ray speckle cross correlation

The different local symmetries in colloidal glasses were investigated by coherent X-ray scattering beyond the standard pair correlation analysis. By analyzing the resulting speckle patterns with a newly developed X-ray cross correlation analysis (XCCA) concept, it is possible to access and classify the otherwise hidden local order within disorder. Four-, six-, ten- and, most prevailing, five-fold symmetries are observed coupled to distinct momentum transfer (Q) values, which do not coincide with the maxima of the amorphous structure factor. The observation of dynamical evolution of these symmetries forms a connection to dynamical heterogeneities in glasses. The XCCA concept opens up a fascinating view into the world of disorder and will definitely allow, with the advent of free-electron X-ray lasers, an accurate and systematic experimental characterization of the structure of the liquid and glass states.

Disordered matter, such as glasses and liquids, does not exhibit translational symmetry and in turn is able to accommodate different local symmetries in the same system, among them the icosahedral local order, which belongs to the forbidden motifs in periodic structures. This mysterious and so far experimentally inaccessible localized order within disorder has been fascinating scientists for many decades [1-3], as it is held responsible for the undercooling of liquids and the existence of the glass state. Yet, it has been frustratingly difficult to characterize it quantitatively, since commonly used tools such as X-ray and neutron scattering, which are capable of probing structure at atomic dimensions in bulk materials, yield only orientationally averaged information embodied in the so-called “radial pair distribution function” which simply tells you the average number of particles at a certain distance from a given particle. Without a periodic crystal lattice, the elegant methods of conventional crystallography cannot be applied. This limitation can be overcome if coherent light is scattered, like in a snapshot, from the instantaneous positions of all the atoms in the disordered sample. In this case a speckle pattern is generated in the far field due to the interference of radiation coming from the entire scattering volume and the (not completely) random phase shifts by the particles [4]. A speckle pattern represents a unique fingerprint via Fourier transform of the individual sample, rather than the usual ensemble average accessed by scattering with standard incoherent radiation [5].

An example of a speckle pattern is shown in Fig. 1 together with a sketch of the experiment. In this study, highly concentrated glassy suspensions of sterically stabilised PMMA particles were investigated by coherent X-ray scattering at beamline ID10A of the ESRF with a similar experimental setup as for XPCS [6]. The envelope of the fluctuating speckle intensities is in fact the ensemble-averaged S(Q) scattering function that is normally measured from a glass or liquid as shown in Fig. 2a. S(Q) depends only on pair-correlations and for amorphous samples does not depend on bond angles. To extract information on the local ordering hidden in the speckle pattern, the instantaneous scattered intensity was analysed for angular correlations by calculating a 4-point correlation function

$$C_Q(\Delta) = \frac{\langle I(Q,\varphi)I(Q,\varphi+\Delta)\rangle - \langle I(Q,\varphi)\rangle^2}{\langle I(Q,\varphi)\rangle^2}$$

where Δ is the azimuthal angle difference between two points in the speckle pattern (see Fig. 1b). The averaging indicated by the brackets is taken over the entire ring $\varphi \in [0;2\pi]$ with $|\mathbf{Q}|=Q$. Most fascinating is that $C_Q(\Delta)$ in Fig. 2b clearly reveals a very

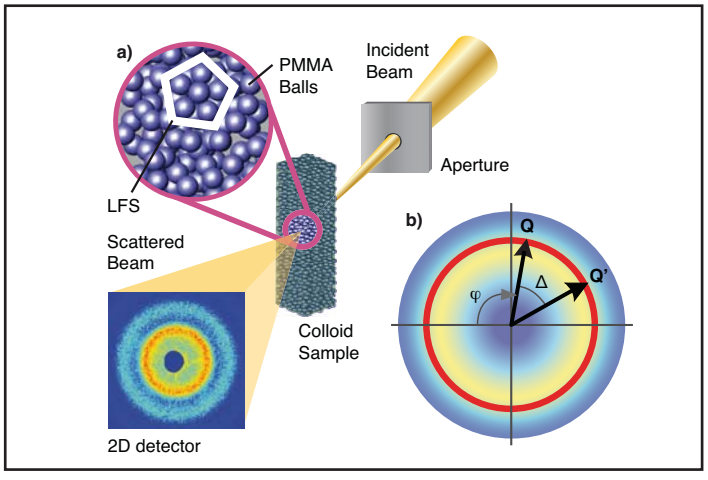

Figure 1

Sketch of the experimental setup where a speckle diffraction pattern is generated in the far field when coherent X-rays illuminate a disordered sample. a) illustrates the local icosahedral symmetry of the arrangement of PMMA balls in the colloidal sample and b) outlines the XCCA analysis method.

pronounced anisotropy with 5-fold symmetry specifically for the intensity ring associated with Q=0.04 nm^{-1}, which points to a so far hidden local symmetry in the colloidal system. The different Q-dependent symmetries are a signature of the specific local order. The colloidal glasses investigated here are slowly evolving; hence the analysis could be performed over time intervals much shorter than the typical speckle decay time (~200s) to yield the temporal evolution of the local ordering. It is found that the bond-orientational order symmetries slowly relax as a function of time and switch e.g. from 5-fold to 6-fold at a given Q value. This is qualitatively related to the structural rearrangement of local entities or clusters that could be the cages in the so-called alpha relaxation [7]. The emerging picture is that clusters of icosahedral order reorganize themselves and are formed either in nano-crystalline environments or out of complete disorder, all of which involves the breaking and formation of bonds. This bears similarities to the behaviour observed in simulations of supercooled molecular liquid glass-formers and underlines the importance of local rearrangements in the understanding of the dynamical properties of this important class of non-periodic materials [8]. Clearly, there is a wealth of new information about the kinetics and the origin of the glass transition to be mined from such experiments, by e.g. applying correlators testing for medium range order. The application of these techniques to metallic glasses and liquids require scattering experiments at much shorter length scales and thus higher Q values, where even at the current high-brilliance synchrotron X-ray sources, one is fighting battles against both intensity and the degree of coherence of the X-ray beam, particularly for liquids where one would have to take fast snap-shot pictures of the speckle patterns. The availability of short-pulse XFEL radiation in the 0.1-nm regime and with sub 100-fs pulse length will open up the fascinating option to analyze the local structure of liquids (in particular also water) by applying the new concept of X-ray cross correlation analysis (XCCA) to single laser shot speckle diffraction pattern. This single shot technique is also suited to study nano-powders and transient complex molecular structures in solutions via a pump-probe scheme.

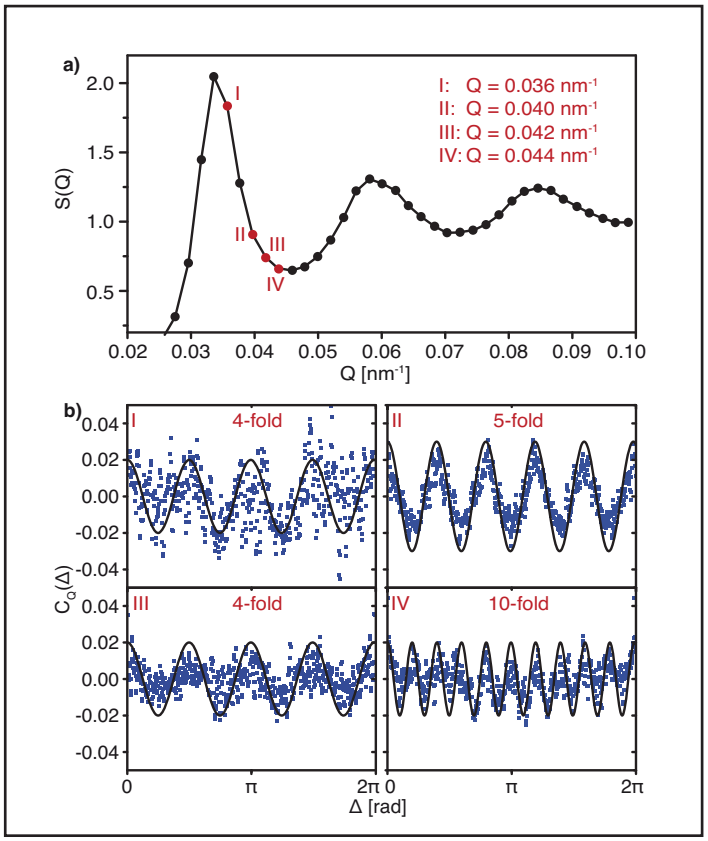

Figure 2

a) Angular averaged structure factor, which is the standard radial intensity distribution. **b)** Experimental result after applying the cross-correlator $C_Q(\Delta)$ to the data at different Q values indicated in (a). Solid lines are a guide to the eye.

Contact: Peter Wochner, wochner@mf.mpg.de

Authors

Peter Wochner[1], Christian Gutt[2], Tina Autenrieth[2], Thomas Demmer[1], Volodymyr Bugaev[1], Alejandro Díaz Ortiz[1], Agnès Duri[2], Federico Zontone[3], Gerhard Grübel[2], Helmut Dosch[1,2]

1. Max-Planck-Institut für Metallforschung, Heisenbergstrasse 3, D-70569 Stuttgart, Germany.
2. DESY, Notkestrasse 85, D-22607 Hamburg, Germany.
3. European Synchrotron Radiation Facility, 6 rue Jules Horowitz BP 220, 38043 Grenoble Cedex 09, France.

Original publication

"X-ray cross correlation analysis uncovers hidden symmetries in disordered matter", Proceedings of the National Academy of Sciences 106, 11511-11514 (2009).

References

1. **F.C. Frank, "Supercooling of liquids", Proc. Roy. Soc. Lond A 215, 43-46 (1952).**
2. **J.D. Bernal, "Geometry of the structure of monatomic liquids", Nature 185, 68-70 (1960).**
3. **P.J. Steinhardt, D.R. Nelson, M. Ronchetti, "Bond-orientational order in liquids and glasses", Phys. Rev. B 28, 784-805 (1983).**
4. **B. Lengeler, "Coherence in X-ray physics", Naturwissenschaften 88, 249-260 (2001).**
5. **M. Sutton, et al., "Observation of speckle by diffraction with coherent X-rays", Nature 352, 608-610 (1991).**
6. **G. Grübel, F. Zontone, "Correlation spectroscopy with coherent X-rays", J. Alloys Comp. 362, 3–11 (2004).**
7. **W. Götze, L. Sjögren, "Relaxation processes in supercooled liquids", Rep. Prog. Phys. 55, 241-376 (1992).**
8. **H. Shintani, H. Tanaka, "Frustration on the way to crystallization in glass", Nat. Phys. 2, 200-206 (2006).**

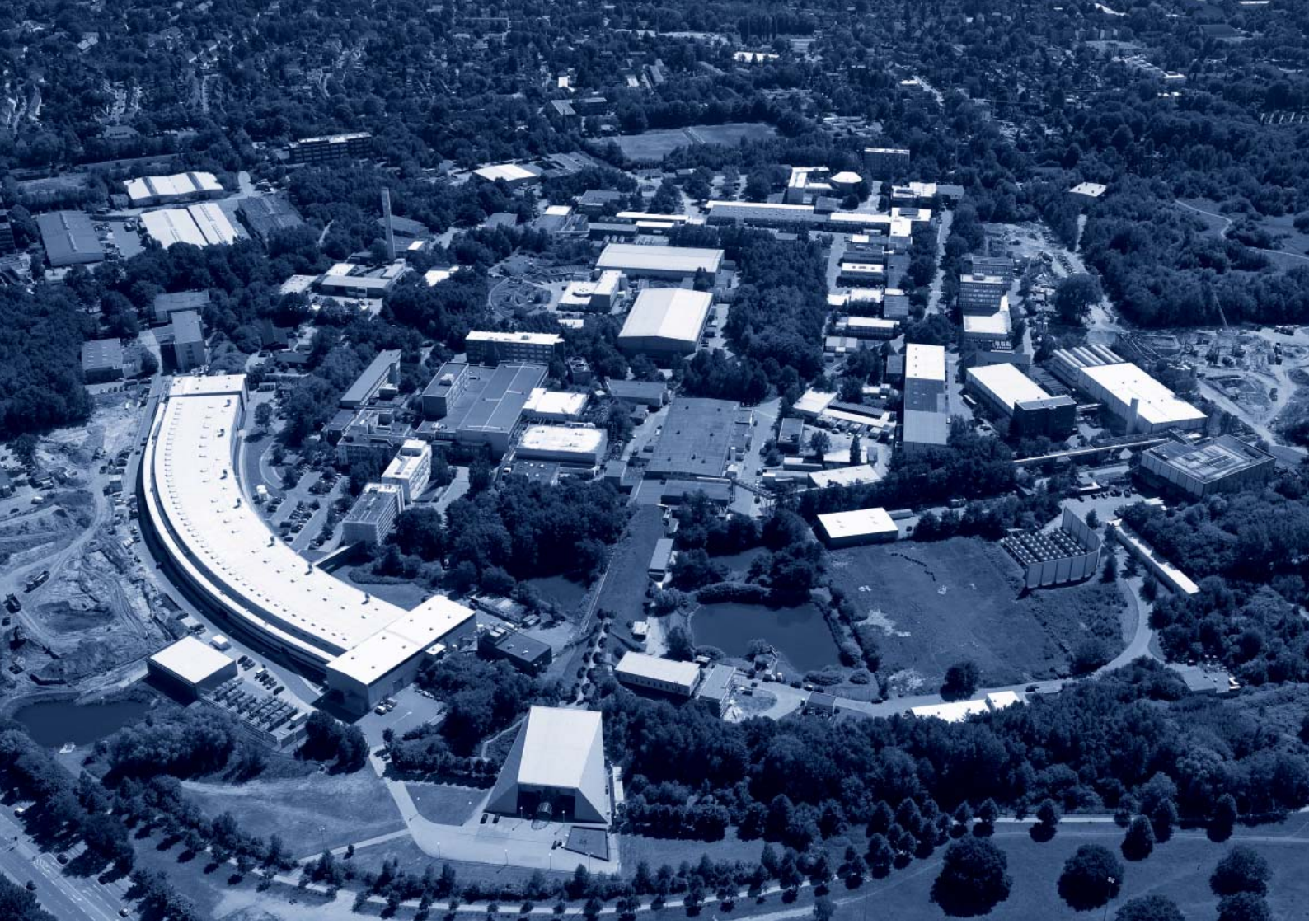

Research Platforms and Outstations.

Center for Free-Electron Laser Science CFEL.

The cooperation in ultra-fast photon science continues to grow

VUV and X-ray free-electron lasers are now a reality and are producing ultrafast X-ray pulses of unprecedented peak power and fluence. The Center for Free-Electron Laser Science (CFEL) was established to pursue research that is opened up by these and other next generation sources such as high-harmonic attosecond lasers or femtosecond pulsed electron beams, capitalizing on Hamburg's world leading environment of X-ray science that includes the European XFEL and DESY's FLASH and PETRA III facilities. CFEL aims to study and control the structure and dynamics of matter at atomic length and time scales. In addition to pursuing fundamental science experiments we also aim to develop instrumentation and methods to extend the capabilities and applications of next generation sources.

The CFEL is a common effort between DESY, the Max Planck Society, and the University of Hamburg. The structure of the Center has been specifically developed to enhance collaboration of all groups to make use of the wealth of expertise that is found within the individual organizations. The CFEL will consist of five core groups, consisting of two experimental groups from DESY, two from the University of Hamburg (in the Max Planck Research Group for Structural Dynamics, MPSD), and a theory group at DESY. With the arrival of R. J. Dwayne Miller from the University of Toronto, who will lead the Department for Atomically Resolved Dynamics within the MPSD, the current number of core groups is now three. Prof. Miller joins the DESY Research Group for Coherent X-ray Imaging, led by Henry Chapman,

Figure 2

CFEL construction site end of November 2009.

and the Department for Condensed Matter Dynamics in MPSD, led by Andrea Cavalleri. Those two groups also continue to grow, and are at 17 and 16 people, respectively. Their teams are significantly enhanced by the recent additions of Anton Barty, who will conduct ultrafast time-resolved coherent scattering in the CFEL Imaging group, and Adrian Cavalieri who will run a Max Planck junior research group in attosecond science within MPSD. In addition to the core groups, the CFEL includes large and significant efforts of Advanced Study Groups (ASGs) from the Max Planck Society, headed by Joachim Ullrich, and the University of Hamburg, led by Wilfried Wurth. The growth of the CFEL is planned to continue with the searches for the heads of the DESY theory and next experimental groups ongoing.

Figure 1

Laying of the foundations stone of the CFEL Building on September, 29th 2009 (from left to right: DESY director of administration Christian Scherf, Hamburgs' Senator for Science and Research Dr. Herlind Gundelach, Chairman of the CFEL managing board MPI Director Prof. Dr. Joachim H. Ullrich, and Vice President of the University of Hamburg Prof. Dr.-Ing. Hans Siegfried Stiehl).

The construction of the new CFEL laboratory and office building began in June 2009, just to the north of the PETRA III hall. The CFEL building is funded by the State of Hamburg and the Federal Government and will consist of 3800 m^2 of office space and 3600 m^2 of laboratory space. The first milestone in the construction was the laying of the foundation stone on September 29th, 2009 (Figure 1). A short greeting by Hamburg's Senator for Science and Research, Dr. Herlind Gundelach, opened the ceremony. She was followed by addresses from the Vice President of the University of Hamburg Prof. Dr.-Ing. Hans Siegfried Stiehl, the DESY director of administration, Christian Scherf, and the head of the CFEL managing board, MPI Director Prof. Dr. Joachim H. Ullrich at the same time representing the Max Planck Society. Afterwards the four speakers placed contemporary items into a time capsule, including the newspaper of the day, current coins, the architects' drawings, several scientific papers of the CFEL group leaders, and some special items related to their research: the prototype of a pnCCD detector chip and the CFEL logo, microfabricated in a silicon wafer with a focused ion beam at 10 nm resolution. The copper capsule was sealed and buried in the ground plate of the building. The topping out ceremony is scheduled for July 2010 and the final completion of the building is planned for early fall 2011. The scientists from all CFEL groups should be able to start moving into the new complex before Christmas 2011.

In the meantime, the ongoing and rapid growth of the CFEL has required a similar expansion of current infrastructure and

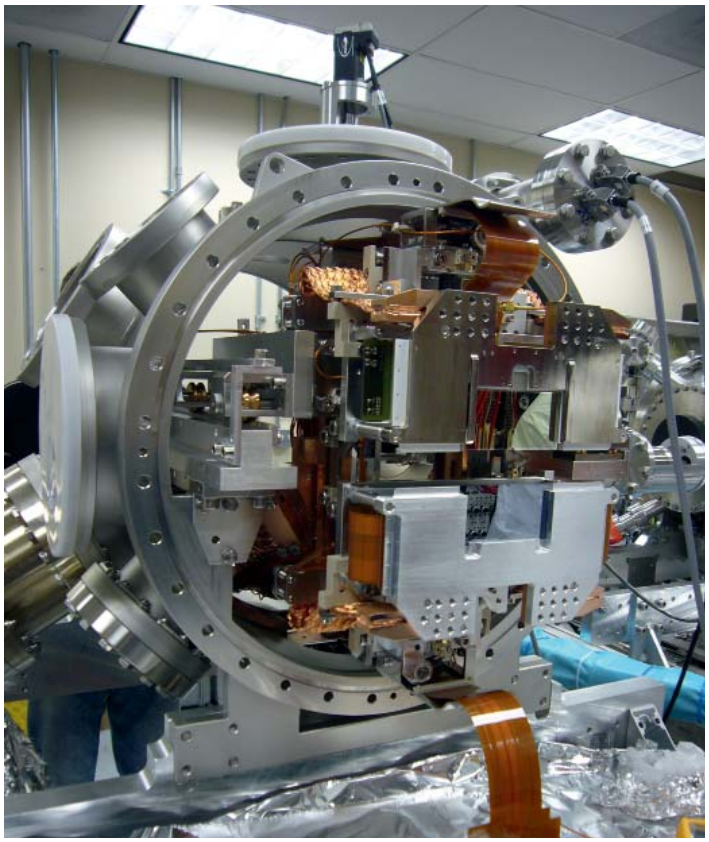

Figure 3a

View into the heart of the CAMP Instrument during installation at the LCLS in November 2009.

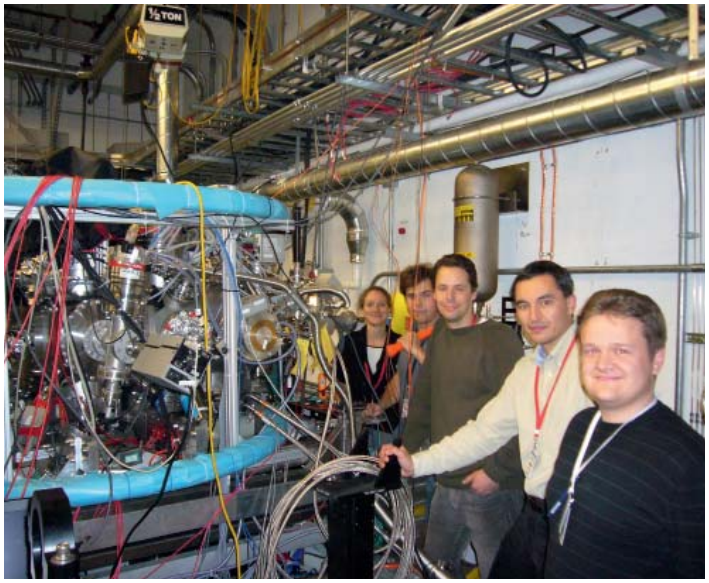

Figure 3b

CFEL has carried out several experiments at the Linac Coherent Light Source (LCLS) at SLAC, utilizing the **C**FEL MP-**A**SG **M**ulti-**P**urpose (CAMP) Instrument. Pictured here next to CAMP in the LCLS hutch are (left to right) Tais Gorkhover, Sebastien Schorb (TU Berlin), Christoph Bostedt (SLAC), Artem Rudenko, and Benjamin Erk (CFEL MP-ASG).

facilities. Ralf Koehn (ralf.koehn@desy.de) has joined as the research coordinator of CFEL, providing a point of contact for all the affiliated organizations of the Center. Office containers will be rented for the MP-ASG, providing 18 spaces, and a 150 m^2 laser laboratory, now fully equipped with a femtosecond laser and a plasma X-ray source, has been provided in the former cyclotron building by the University. Building 49, housing the Chapman and Cavalleri groups, was extended with an annex (Building 49a), funded by the State of Hamburg, with space for another 40 desks. Building 49 accommodates research laboratories of the Chapman and Cavalleri groups. In Henry Chapman's group these labs include an imaging laboratory, metrology and microscopy, X-ray instrumentation, and a particle delivery methods laboratory. The microscopy lab houses a FEI Helios 600 Nanolab system, which is a dual-column scanning electron microscope and focused ion beam microscope. This system is in full use fabricating nanostructures for FEL and synchrotron-based experiments in coherent diffractive imaging, as well as being used in the development of novel X-ray optics. In addition, new large-format CCD detectors are being developed for pursuing coherent imaging at FLASH at resolutions below 10 nm. In the last days of user time in 2009 at FLASH, the group and collaborators demonstrated high-resolution coherent diffraction patterns captured from icosahedral virus particles captured as they flew across the FEL beam. The diffraction patterns from these mimivirus particles, cultured and injected by collaborators from Uppsala University, are being assembled into the 3D transform of an average oriented virus particle.

The Department for Condensed Matter Dynamics in MPSD, headed by Andrea Cavalleri, has built up a new ultrafast optical laser laboratory, where much of the work is performed to prepare a new generation of experiments in the area of structural dynamics. High filed terahertz sources are being developed with a variety of frontier experimental techniques, which will be used to control the crystallography and the various excitations of condensed matter coherently. These pulses will be synchronized to FEL X-ray pulses, UV radiation from FLASH or from tabletop sources, or even electron pulses developed in the Miller group, and will allow for dynamic monitoring of coherently controlled properties of complex matter. This facility will cover pulse durations from 10 fs down to the attosecond timescale. The development includes new ultrafast X-ray diagnostics, which will be applied to X-ray FELs like FLASH and LCLS, as well as various synchrotrons around the world. The group is also doing experiments with Infrared FEL, FELBE, in Dresden. The Max Planck ASG has moved into Building 67, the former University of Hamburg cyclotron building. The group of Dwayne Miller will construct laboratories there too.

The CFEL as a whole is extremely busy preparing for upcoming experiments at the Linac Coherent Light Source (LCLS), at SLAC in California, USA. This X-ray FEL began user operations in September 2009. In the first round of experiments at LCLS, out of 11 approved experiments, four include substantial effort from the CFEL and depend upon a multipurpose instrument built for X-ray scattering and photoemission experiments by the

Figure 4

Inside Visualization of the CFEL Building (architect's rendition, courtesy: hammeskrause architekten).

CFEL Max Planck ASG. The so-called CAMP (**C**FEL MP-**A**SG **M**ulti-**P**urpose) Instrument is a novel combination of the world's largest and fastest X-ray pixel detectors (pnCCDs), with coincident momentum and energy mapping of ions as well as electrons with sample environments for X-ray FEL experiments (Figure 2). Three CFEL-led experiments at LCLS will utilize the CAMP Instrument, which include coherent imaging, imaging of atoms within aligned molecules, and non-linear X-ray absorption and emission. These initial successful steps have led to 19 proposals from CFEL and international groups in collaboration with the Max Planck ASG being proposed for the second round of LCLS proposals. This strong involvement at LCLS is a clear proof of the quality of science and instrument development being pursued at CFEL.

Beyond designing, manufacturing and operating the CAMP Instrument, the MP-ASG with groups from eight Max Planck Institutes actively involved pursued a lively and widespread science program. It includes investigations of non-linear effects in atoms, molecules and clusters (theory), the first successful VUV-VUV pump-probe experiment on molecules tracing 20 fs wave packet dynamics, the study of photon interactions with ultra-cold ensembles, highly-charged and molecular ions as well as pioneering two-colour time-dependent measurements on larger molecules. In collaboration with the group of Henry Chapman, biological probes are designed and prepared for coherent imaging experiments.

The University of Hamburg ASG has been carrying out a lively experimental program, with new developments in X-ray optics and interferometry at FLASH, non-linear X-ray optics, and ultrafast techniques in correlating X-ray, optical, or THz pulsed fields. The University ASG has also been instrumental in developing and constructing a new beamline at the LCLS, for soft X-ray science which will deliver monochromatized or pink-beam pulses from LCLS to users' roll-out experiments. This beamline was only made possible with substantial funding from German sources including the Federal Ministry for Education and Research and DESY, together with US colleagues at SLAC, LBNL and Stanford University. The beamline is under construction by SLAC engineers and will be commissioned in March 2010. It will be used in widespread fields such as catalysis, magnetism, correlated materials, clusters and biological structure.

Groups from CFEL worked closely with research groups from the Physics Department of the University of Hamburg and DESY Photon Science to form an Excellence Cluster in the framework of the Excellence Initiative of the Free and Hanseatic City of Hamburg. Funded by the Joachim Herz foundation, and headed by Prof. Klaus Sengstock of the University of Hamburg, the Frontiers in Quantum Photon Science Cluster focuses on new physics enabled by coherent radiation sources. CFEL is also a member of the newly formed Hamburg School for Structure and Dynamics in Infection, headed by Profs. Betzel and Aepfelbacher of the University of Hamburg. With these initiatives bringing in new students and researchers to the University, DESY, and CFEL, Hamburg is quickly growing into a world capital of X-ray science.

Contact: Henry N. Chapman, henry.chapman@desy.de

EMBL Hamburg Unit.

Structural Biology with Synchrotron Radiation

EMBL-Hamburg's activities in 2009 have been dominated by our institute's contribution to the construction of new integrated research facilities in structural biology, particularly those at "EMBL@PETRA III". The team for PETRA III beamline construction, which is coordinated by Thomas Schneider and Stefan Fiedler (deputy), is fully operational and comprises about 15 members. A new group leader for the future sample preparation characterization facility at EMBL@PETRA III, Rob Meijers, started at EMBL-Hamburg in September 2009 (Figure 1). Rob was a PhD student with Victor Lamzin (1997-2001), before going for an extended postdoctoral period at the Dana Farber Cancer Institute, Boston, USA (2001-2006) and taking a staff scientist position at Soleil, Saint Aubin, France (2006-2009). Scientifically, Rob is planning to work on projects related to immune responses during pregnancy and early embryogenesis. Manfred Weiss (team leader, now working at the Helmholtz Centre Berlin) and Arie Geerlof (staff scientist, now working at the Helmholtz Centre Munich) left EMBL in 2009. Paul Tucker, who has been a group leader at EMBL-Hamburg since 1998, will retire at the end of 2009 (Figure 1). In particular, Paul has led many training activities at EMBL and made key contributions to further develop concepts in protein crystallography.

Figure 1
Newcomers and leavers. Rob Meijers (top), Manfred Weiss and Paul Tucker at their leaving party (right).

The EMBL@PETRA III project has started to shape up in concrete terms throughout 2009. Most of the design work for the three EMBL beamlines for structural biology applications at PETRA III has been finalized and the majority of the beamline components have been ordered. In particular, a decision was made to equip all three beamlines with adaptive X-ray mirrors to make optimum and flexible use of the X-rays produced by PETRA III. Recently, the first instruments - an MD2 micro-diffractometer and a RAYONIX 225HE CCD detector for the two

Figure 2
The prototype model of the PX sample changer MARVIN (courtesy Stefan Fiedler, EMBL-Hamburg).

crystallography beamlines - have arrived. They have been initially installed on the DORIS wiggler-beamline BW7A for testing. In preparation for the future facilities at PETRA III, this beamline is now fully controlled by the TINE control system with an mxCube (ESRF) based graphical user interface. Many test data sets have been successfully collected using this prototype setup. An in-house development for a new sample changer

Figure 3

Topping out ceremony for the EMBL/DESY PETRA III Annex Building. Matthias Wilmanns (EMBL) and Helmuth Dosch (DESY); lifting of the traditional wreath and speech by the carpenter in charge; Bernd-Uwe Jahn (EMBL).

for applications in X-ray crystallography, called MARVIN, has been tested and is commissioned at the PETRA III test beamline BW7B (Figure 2). In parallel, the BioSAXS sample changer has also arrived (see below). GKSS and EMBL have signed a partnership agreement providing GKSS with privileged access to the BioSAXS beamline. As part of this agreement, GKSS will contribute a versatile flight tube and detector table that extends the scope of the BioSAXS beamline beyond its use for X-ray scattering on solutions. Progress and the status of the project was reported to, and discussed with the Scientific Advisory Board (chairs: Prof. Dino Moras, IGBMC Illkirch, France, and Dr. Liz Duke, Diamond, Didcott, UK) at a meeting in May 2009. In late 2008, DESY and EMBL agreed to add an Annex Building to the existing PETRA III beamline hall. The annex will host laboratories for sample preparation and characterization on the ground floor, additional office space on the first floor and a seminar room on the second floor. Construction of the building began in early 2009, and the shell of the building was completed in July (Figure 3). The traditional topping out ceremony, in the presence of the DESY directorate and the Administrative Director of EMBL, Dr. Bernd-Uwe Jahn, took place on July 08, 2009. We expect to start moving equipment and staff into the new building in early 2010.

At the DORIS III storage ring, EMBL has kept four beamlines operational and accessible to the external user community in 2009: X11, X12 and X13 for applications in protein crystallography and X33 for small angle X-ray scattering experiments of biological samples. Particularly at X33, great progress has been made towards experiment automation. An important milestone has been the placement of a state-of-the-art SAXS sampler changer, which was built in a trilateral collaboration by EMBL-Hamburg, EMBL-Grenoble and the ESRF, as a follow-up development on a previous prototype from Hamburg (Figure 4). Remote data collection at X33 was formally started on May 26, 2009, from Singapore, where most of the EMBL SAXS team was busy with a course on biological SAXS applications (Figure 5). The installation of a new XFLASH fluorescence detector on beamline X12 and of a microspectrophotometer on beamline X13 have further increased the versatility of the available protein crystallography beamlines operated by EMBL. The Priorities Committee for all DORIS III activities (chair: Prof. Dino Moras, IGBMC Illkirch, France) met in February 2009.

EMBL-Hamburg hosts two long-term projects on the development of state-of-the-art software for automatic interpretation of X-ray diffraction data and small angle X-ray scattering data, ARP/wARP and ATSAS, allowing rapid structure determination (X-ray crystallography) and shape analysis (SAXS). ARP/wARP and several other external software packages have been integrated into an automated pipeline, which was named “Auto-Rickshaw” by the project leader Santosh Panjikar. The Auto-Rickshaw platform is installed on a 68-CPU core cluster at EMBL-Hamburg and is remotely accessible to academic users via a web-server. To date, more than 500 registered researchers worldwide have used this platform. Overall, we expect that the provision of state-of-the-art software packages will increasingly become a key research service tool by EMBL-Hamburg, in the context of increasing experiment automation and remote experiment control (Figure 6).

A major concern by both our institute and many members of the structural biology user community is to ensure an appropriate level of support for users to access available facilities.

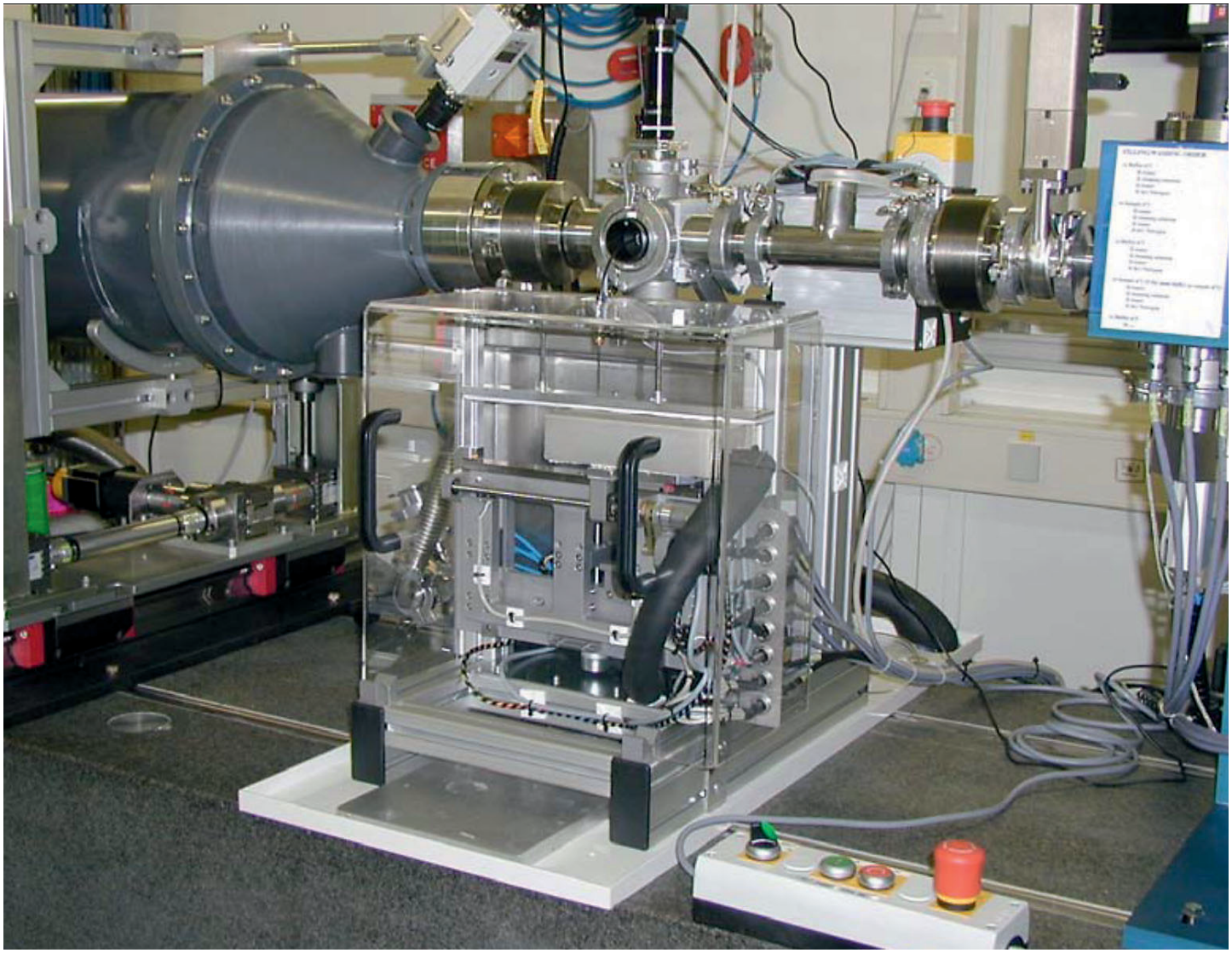

Figure 4

BioSAXS sample changer, commissioned on the SAXS beamline X33 of DORIS III.

A new EC-supported project “ELISA” (www.elettra.eu/ELISA/) to support access to laser and synchrotron infrastructures has started recently. EMBL is a partner in this project, but the overall volume of support for access of EMBL supported beamlines activities has dropped to a small fraction of previous support levels. However, for the first time, there is a coordinated support scheme for facilities dedicated to biological sample preparation and characterization. “PCUBE” (www.p-cube.eu/) complements our activities to provide research services at synchrotron radiation beamlines. Access to the high-throughput crystallization platform at EMBL-Hamburg is also supported by this project. Finally, structural biology is supported as one of the few areas of biomedical sciences by a European pilot project “INSTRUCT” (www.instruct-fp7.eu/), aiming to work out a concept for coordinated structural biology infrastructures in Europe. EMBL, with its structural biology oriented activities in Hamburg, Heidelberg and Grenoble, is one of the core centers of the project. Our aim is to improve and to extend our facilities to the benefit of the European user community in structural biology.

Training within the techniques and approaches offered by EMBL-Hamburg has remained a key activity of our institute (www.embl-hamburg.de/training). In 2009, two courses took place, one on the characterization of protein complexes and a second one on methods in macromolecular crystallography. In addition, EMBL-Hamburg offers basic training courses in biophysical and biochemical approaches and structural biology methods throughout the year.

The research portfolio of EMBL-Hamburg presents three basic directions: development and installation of new hardware and instruments for the experimental beamline stations, development and implementation of new software tools in structural biology, and activities in some of the most challenging research

Figure 6

Software services in structural biology, provided by EMBL-Hamburg (for detailed information, see:www.embl-hamburg.de/)

Figure 5
Dmitri Svergun starts remote operation of the SAXS beamline X33 from Singapore.

fields in structural biology. Two highlights of EMBL's recent research activities, one in the field of eukaryotic translation termination (Svergun) and the second covering molecular complexes from human muscle sarcomeres (Wilmanns), are presented elsewhere. In parallel, EMBL participates in an initiative to establish a new research center, "Center for Structural Systems Biology" (CSSB), on the DESY campus. A first international symposium by the future members of this center was organized in September 2009 in Hamburg. This center will allow a level of excellence driven research activities in life sciences to be established, making full use of the unique synchrotron and laser infrastructures on the DESY campus.
The city of Hamburg has recently started a new initiative ("Landesexzellensinitiative", www.hamburg.de/landesexzellenzinitiative), to promote excellent science for future initiatives. EMBL-Hamburg has become a member in two initiatives, one with the University of Hamburg for a "Hamburg Graduate School for Dynamics and Infection" and the second one with the Technical University of Hamburg-Harburg on "Fundamentals for Synthetic Biological Systems".
At the European level, EMBL has become a core partner in a new EC-funded integrated project "SystemTB", which will focus on system biology-oriented research on the pathogen Mycobacterium tuberculosis.

Contact: M. Wilmanns, wilmanns@embl-hamburg.de

	Software	Down-load	Remote access	Unique users	Unique domains	Struc-tures	Citations
	ARP/wARP	✔	✔	3,700	1,300	2,700	4,200
	BEST	✔		150	110		70
	XREC	✔		36	26		8
	Auto-Rickshaw		✔	630	250	1,100	60
	HKL2MAP	✔		390	280		110
	Rapido		✔	460	240		5
	ATSAS	✔	✔	2,800	1,000		1,520

Max-Planck Unit for Structural Molecular Biology.

Biological structure and function in order and disorder

The Max-Planck Unit for Structural Molecular Biology at DESY was established in 1986 in order to utilize the synchrotron light at DORIS III for structural studies of biological macromolecules. The unit comprised the divisions “Ribosome Structure“ (headed by A. Yonath, focussing on the elucidation of the structure and mechanism of the multi-subunit complexes of ribosomes, the machinery for synthesizing new proteins in cells), “Protein Dynamics“ (H. D. Bartunik, focussing on time-resolved protein crystallography and protein structures related to tuberculosis) and „Cytoskeleton“ (E. Mandelkow, focussing on fibrous proteins in neurons related to Alzheimer disease).
In 2009, Ada Yonath was awarded the Nobel Prize in Chemistry for her pioneering work on the structure of ribosomal subunits and their complexes with antibiotics (jointly with T. Steitz and V. Ramakrishnan). For this special occasion, the present annual report (written by Frank Schlünzen, a long-time collaborator of A. Yonath at DESY) will summarize the steps and technical breakthroughs that lead to the solution of the complex ribosomal structure and its applications to the development of antibiotics.

The early years

The first attempts to crystallize ribosomes or ribosomal particles date back to the early 1980’s. The idea of trying to crystallize ribosomal particles was triggered by the observation that some organisms tend to form quasi-crystalline sheets of ribosomes under certain conditions. Ribosomes consume roughly 80 % of the energy of cells, so that the most efficient way to save energy is shutting down the protein-production of the ribosomes. Assembling ribosomes in crystalline sheets is one mechanism whereby hibernating animals escape the energy-crisis at low temperatures. The first crystals (Fig. 1b, c) reported by A. Yonath and H. G. Wittmann (MPI for Molecular Genetics, Berlin) in 1980 were of the large (50S) ribosomal subunits from Bacillus stearothermophilus, a thermostable bacterium [1].

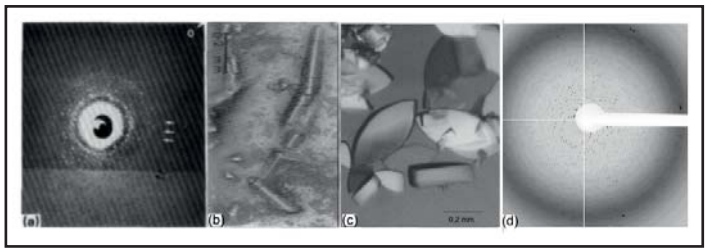

Figure 1

(a) One of the first diffraction patterns obtained from crystals of the 50S subunit from Bacillus stearothermophilus. Diffraction was taken at DORIS III at room temperature on X-ray films. The maximum resolution was around 13 Å. (b) Fragmented crystals leading to the diffraction in (a) [1,2]. (c) Crystals of the 50S subunit from Deinococcus radiodurans. (d) Diffraction obtained from crystals in (c) at a temperature of 90 K. Diffraction up to 3.1 Å resolution was taken at ESRF on a MAR CCD detector [3].

In the next decade several more ribosomal particles from a small number of species were crystallized, but only in the early 1990’s did the crystals become sufficiently well ordered for considering a full structure determination (Fig. 1c). The development of crystal data quality relied entirely on the development of synchrotron radiation facilities, combined with novel electronic detectors, novel cryo-preservation methods, and novel computational approaches. The progress is illustrated by comparing an X-ray diffraction pattern of the early period (Fig. 1a) with a later state-of-the-art pattern (Fig. 1d).

Figure 2

Ada Yonath adjusting a ribosome crystal in a diffractometer (around 1985).

As an example, cryo-methods were hardly established in protein crystallography in the early 1980’s. The first diffraction images of ribosomal crystals were hence taken at room temperature, and none of the crystals survived more than a single exposure, due to the severe and immediate radiation damage. To enhance the lifetime of the crystals, cryo-cooling of the crystals and data collection at liquid nitrogen temperature was developed and further refined at DORIS III [4]. At a temperature of 90-100 K, the crystals became sufficiently stable to survive X-rays for several days, which allowed collecting complete data-

sets from a single or just a few crystals. To get to this stage, the experimental methods needed to be constantly improved, which required to test the cryo-conditions and literally thousands of crystals in the X-ray beam. These experiments were largely performed at the DORIS III beamlines, particularly at the MPG beamline BW6.

The race for the structure of the ribosome

It took another 10 years before the first crystals from the 50S subunit from Haloarcula marismortui diffracted to a sufficiently good resolution [5]. H. marismortui is a bacterium from the Dead Sea which is able to survive extremely high salt concentrations. The choice of very stable organisms in the search for stable and compact ribosomes turned out to be one of the major keys to success – later also adopted by the other two 2009 Nobel prize awardees in Chemistry, V. Ramakrishnan and T. Steitz. Their groups started to work on the same type of ribosomal particles in the 1990's and thus opened up a strong competitive race. In 1998, T. Steitz reported the first 9 Å structure of the "large" (50S) ribosomal subunit from H. marismortui, which was extended to 5 Å a year later. At the same time, A. Yonath and independently V. Ramakrishnan published the first low resolution structures of the "small" (30S) ribosomal subunit from Thermus thermophilus. (Note: Both large and small subunits together form an intact functional ribosome.) In August 2000, N. Ban, T. Steitz and colleagues published the first high resolution structure of a ribosomal particle, the 50S subunit from H. marismortui at 2.4 Å.

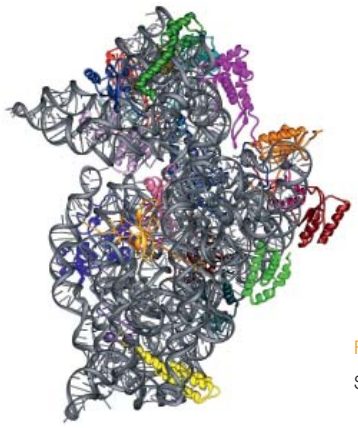

Figure 3

Structure of the 30S ribosomal subunit [7].

A month later, A. Yonath and colleagues published the first high resolution (3.3 Å) structure of the 30S ribosomal subunit from Th. thermophilus. The structure determination of the 30S ribosomal subunit became only possible by introducing large tungsten clusters into the crystals, which provided the marker to obtain the phase information by multiple isomorphous replacement – and magically improved the diffraction quality of the crystals.

The first round of crystal structures of ribosomes was completed by V. Ramakrishnan's more refined 3.1 Å structure of the 30S subunit from Th. thermophilus just three weeks later (see [6] for a recent historical review).

Antibiotics and ribosome

Since ribosomes are a major target for several clinically important antibiotics, investigation of the interaction of the antibiotics with the ribosome was the natural next step. However, H. marismortui is a so-called archaeal bacterium, which is much more similar to eukaryotic organisms than to bacteria, and the high salt-crystallization was thought to prevent inhibition by many of the relevant antibiotics. Results obtained for this organism were therefore assumed to have little pharmaceutical relevance, which later on turned out to be wrong. Yonath's group consequently continued to work on structures of the 30S ribosomal subunit from Th. thermophilus and the 50S subunit from Deinococcus radiodurans. This bacterium is again a very stable organism, able to withstand extremely high radiation doses and harsh starvation conditions. More importantly, it is a prototypical organism very similar to many common pathogens. This turned out to be one of the first essential steps to begin structure aided drug design for novel antibiotics.

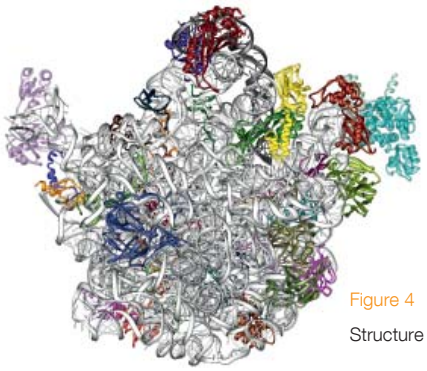

Figure 4

Structure of the 50S ribosomal subunit [3].

In summary, the pioneering work in ribosome crystallization, cryo-crystallography, phase determination by means of large heavy-metal clusters, all carried out using the synchrotron facilities at DESY and other synchrotrons, finally lead to the structure solution of protein complexes of unprecedented complexity. These methods are now adopted world-wide and form the basis for even more ambitious protein structure projects which will become possible in the future with new synchrotron radiation sources such as PETRA III and the European XFEL.

Contact: E. Mandelkow, mandelkow@mpasmb.desy.de

References

1. Yonath A., Mussig J., Tesche B., Lorenz S., Erdmann V.A., Wittmann H.G., "Crystallization of the large ribosomal subunits from Bacillus stearothermophilus", Biochem Internat 1, 428-435 (1980).
2. Yonath A., Bartunik H.D., Bartels K.S., Wittmann H.G., "Some X-ray diffraction patterns from single crystals of the large ribosomal subunit from Bacillus stearothermophilus", J Mol Biol. 177, 201-6 (1984).
3. Harms J., Schlünzen F., Zarivach R., Bashan A., Gat S., Agmon I., Bartels H., Franceschi F., Yonath A., "High resolution structure of the large ribosomal subunit from a mesophilic eubacterium", Cell 107, 679-688 (2001).
4. Hope H., Frolow F., von Bohlen K., Makowski I., Kratky C., Halfon Y., Danz H., Webster P., Bartels KS., Wittmann HG., Yonath A., "Cryocrystallography of ribosomal particles", Acta Crystallogr. B45, 190-199 (1989).
5. von Böhlen K., Makowski I., Hansen H.A., Bartels H., Berkovitch-Yellin Z., Zaytzev-Bashan A., Meyer S., Paulke C., Franceschi F., Yonath A, "Characterization and preliminary attempts for derivatization of crystals of large.
6. Moore P.B., "The ribosome returned", Journal of Biology 8, (2009).
7. Schlünzen F., Tocilj A., Zarivach R., Harms J., Gluehmann M., Janell D., Bashan A., Bartels H., Agmon I., Franceschi F., Yonath A., "Structure of functionally activated small ribosomal subunit at 3.3 Å resolution", Cell 102, 615-623 (2000).
   Schlünzen F., Zarivach R., Harms J., Bashan A., Tocilj A., Albrecht R., Yonath A., Franceschi F, "Structural basis for the interaction of antibiotics with the peptidyl transferase centre in eubacteria", Nature, 413, 814-21 (2001).

GKSS Research Centre Geesthacht Outstation at DESY.

GEMS-P – More photons for engineering materials research

The outstation of the GKSS Research Centre Geesthacht at DESY provides instrumentation for investigating engineering materials and biomaterials with imaging and diffraction techniques. From 2010 on, it will be operated as the **German Engineering Materials Science Centre for Research with Photons** (**GEMS-P**), complementing **GEMS-N** for **Research with Neutrons** (in Geesthacht until mid-2010 and at FRM II in Garching). **GEMS** will be a major point of access for users in engineering materials research with photons and neutrons.
The integrated approach of GKSS is reflected in the plan to construct an Engineering Materials Science Centre (EMSC) on the DESY site, providing support to users for sample preparation, **ex situ** experiments and data analysis. Most of the EMSC instrumentation has already been acquired in 2009 and will be made available to users in 2010, e. g. laboratory X-ray tomography and small-angle scattering instruments as well as various sample preparation equipment.
The present suite of instruments at GEMS-P, operated at DORIS III and at the new and most brilliant synchrotron radiation source PETRA III, is presented in the following.
The GKSS beamline **HARWI II** at DORIS III has been in routine user operation for three years now. Materials science experiments in the hard X-ray regime (20-250 keV) profit from the spacious experimental hutch and a broad beam of up to 70 mm in width. HARWI II continues to be highly overbooked, and a wide range of experiments in the fields of diffraction, residual stress analysis, small-angle scattering and micro-tomography were carried out in 2009. Our efforts have been continued to make unique sample environments for **in situ** experiments available, presently comprising e.g. a heavy-duty stress rig, furnaces and a friction-stir welding machine. The most prominent example in 2009 was the commissioning of a dilatometer with quenching, deformation and DSC options (Fig. 1). First experiments on a TiAl sample show that temperature-dependent phase transformations can be followed with high accuracy and on short time scales. The dilatometer's fast heating and quenching rate of up to 4000 K/s in the temperature range from 20 to 1500° C will allow for new science, such as **in situ** forging.
Another important instrumental development at HARWI II in 2009 was the implementation of a differential phase contrast (DPC) imaging experiment. Phase-contrast imaging in general is successfully used to visualise soft tissue with increased contrast in many medical and biological applications. The DPC technique makes use of a hard X-ray grating interferometer and yields, additionally to the phase contrast, dark-field information of the sample, which is sensitive for example to porous microstructures. In cooperation with PSI, where DPC imaging was initially de-

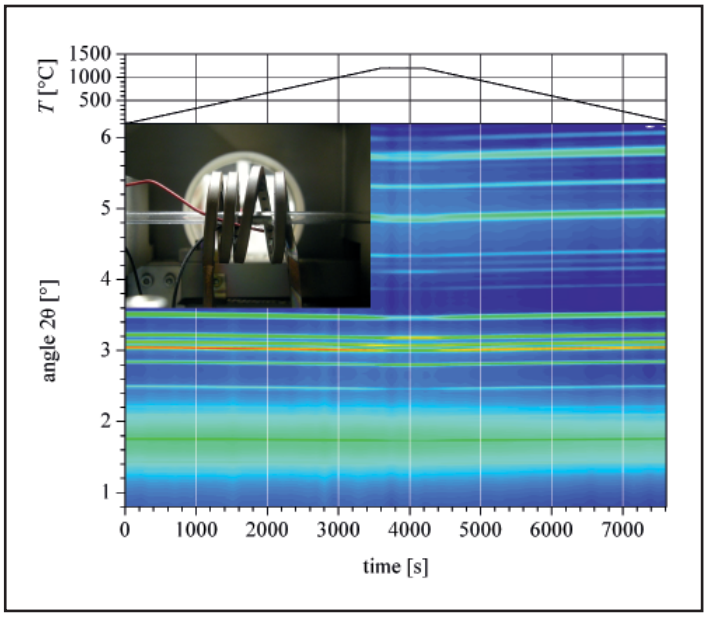

Figure 1

First results of an experiment on a TiAl alloy with the new dilatometer at HARWI II. The Bragg reflection intensity variations with temperature are caused by phase transformations in the multi-phase material. The inset shows the sample (between two quartz tubes) inside the dilatometer heating coil (view direction: against the X-ray beam).

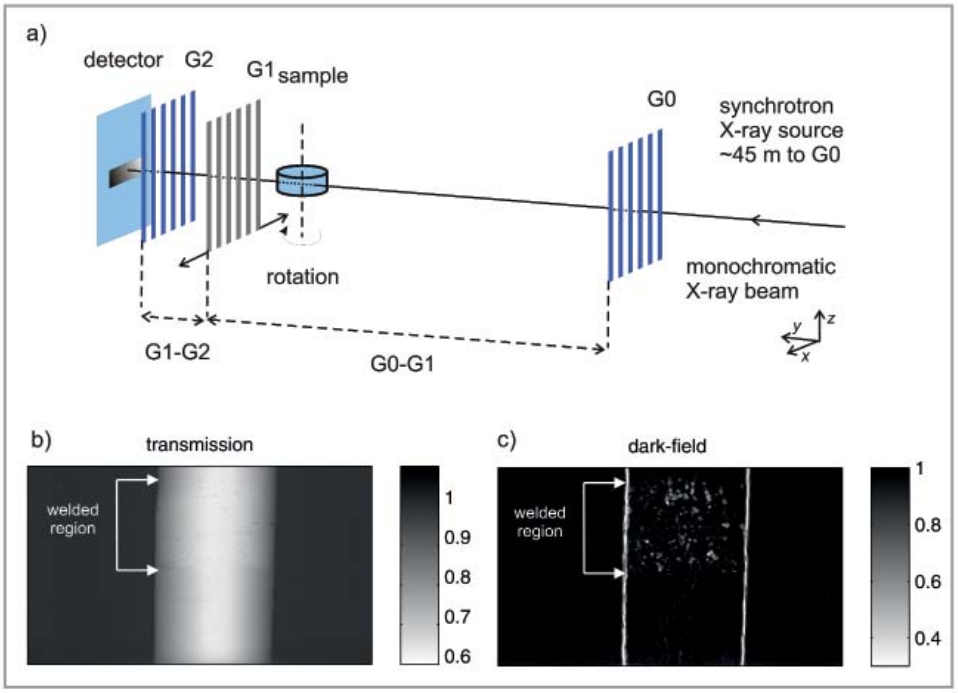

Figure 2

(a) The differential phase contrast imaging set-up at HARWI II consists of three gratings and can be used with photon energies from 22 to 30 keV. (b,c) Projection of a magnesium alloy laser weld (29.0 keV, field of view: 4 x 2 mm²); transmission (b) and dark-field (c) contrast of the same region of the sample. The contrast in the dark-field signal is strongly increased in the welded region with respect to the transmission signal.

veloped, and the TU München a grating interferometer set-up was adopted to the non-coherent beam at HARWI II (Fig. 2a). The use of DPC imaging at this beamline non-destructively provides information on the inner structure of new lightweight materials like laser-welded magnesium or aluminium alloys (Fig. 2b & c), combining the high monochromatic flux at a synchrotron radiation source with a centimetre-sized field of view.
Further activities of the GKSS Outstation **tomography** team in 2009 included the operation of a camera at BW2 (1/3 of the beamtime available), extending the photon energy range to 7-24 keV for lower absorbing samples.
The projects of GKSS beamlines at PETRA III have again made great progress in 2009. The **High Energy Materials Science (HEMS)** beamline for research with high resolution, monochromatic, high-energy X-rays (50-250 keV) targets the materials science and engineering community allowing measurements of large structural components up to 1 t, 3D-XRD investigations down to the single grain level, micro-tomography (see below) and texture determination with beam sizes from a few mm^2 down to the sub-μm^2 range. The HEMS infrastructure has essentially been completed. The optics hutch is equipped with a single-bounce monochromator for an independent side station and a double crystal Laue monochromator for the main branch. Major instrumentation has already been installed in the experimental hutches: a 1 t heavy load hexapod, heavy load tables and a surface/interfaces diffractometer. The grain mapper is in the final design phase. The HEMS commissioning phase has started in November 2009.
The construction of the optical and instrumental hutches as well as of the control cabin of the GKSS Imaging Beamline **(IBL)** has been finished. IBL will be dedicated to micro- and nano-tomography with highest spatial and density resolution. The undulator has been integrated into the reconstructed PETRA III ring and will generate highly coherent hard X-rays in the energy range between 5 and 50 keV. To generate monochromatic X-rays, IBL will offer the choice between a silicon double crystal and a multilayer monochromator. The field of view in the micro-tomography hutch at the largest distance from the source is large enough to investigate samples from materials science, geology, biology and medicine of some millimetres in diameter with (sub-)micrometre resolution. Most of the instrumentation has already been delivered. An almost identical tomographic set-up located at HEMS will extend the energy range to higher energies from 50-250 keV for the investigation of highly absorbing materials. A nano-tomography set-up for the second experimental station at IBL is in the design phase. Here, new focussing possibilities will extend the spatial resolution down to 50 nm for µm-sized samples for nano-tomography and imaging experiments. First experiments at IBL will start midyear 2010.
The collaboration agreement between GKSS and EMBL for the construction and operation of the small-angle scattering beamline **BioSAXS** at PETRA III has been signed. GKSS will contribute 15 % of the construction and operation costs. GKSS (as a Collaborating Research Group, CRG) will receive 15 % of the annual available PETRA III beamtime within the CRG scheme. Contributions of GKSS, i.e., the detector tube and the detector platform, are in the construction phase. Expected date of the installation of the detector tube and platform in the PETRA III hall is spring 2010. Adapted sample environment units for the soft matter and life science applications are currently being designed.
The GKSS Outstation at DESY covers a large range of synchrotron radiation applications in materials science by using X-ray beams of various sizes from wiggler and undulator sources. A scenario for transferring the capabilities of HARWI II to PETRA III after the DORIS III shutdown is currently being developed, giving GEMS-P a bright perspective for the years to come.

Contact: Martin Müller, martin.mueller@gkss.de
Andreas Schreyer, andreas.schreyer@gkss.de

GFZ Helmholtz Centre Potsdam Outstation at DESY.

MAX200x: Energy dispersive XRD under extreme conditions

For geoscientists, material scientists, physicists and chemists it is very important to study the samples under extreme conditions. It is necessary to use in-situ X-ray diffraction experiments at synchrotron beamlines because of the high intensity and the broad energy range to figure out the stability of minerals under high pressure and temperature, the determination of bulk moduli, the thermal expansion, phase diagrams, and the behaviour of kinetic measurements.

Today new materials and the use of high brilliant synchrotron sources allow constructing double-stage multi-anvil systems for X-ray diffraction to reach much higher pressures. The newly designed high-flux hard wiggler (HARWI II) beamline is an ideal X-ray source for this kind of experiments at the MAX200x.
The MAX200x is operated in the double-stage compression mode, in which the first stage is the DIA-type apparatus with six anvils (Figure 1) and the second stage consists of eight anvils.

Either tungsten carbide or cubic boron nitride is used for the second stage anvils. This system has a capability of generating pressures up to 25 GPa and temperatures of 2000° C by a resistance furnace.
This successful experiment is operated by Helmholtz-Centre Potsdam, GFZ, German Centre for Geosciences and is used by more than ten groups from different countries every year.

An important issue, not only for geoscientists, is to obtain the thermoelastic properties of materials, that means the bulk modulus and the thermal expansion. These values can be derived from the changes of the unit-cell-parameters of the sample as function of pressure and temperature.

Contact: Jörn Lauterjung, lau@gfz-potsdam.de
Frank Schilling, frank.schilling@gfz-potsdam.de
Christian Lathe, lathe@gfz-potsdam.de

Figure 1
MAX200x - High pressure cell

University of Hamburg on the DESY site.

Together with DESY: Excellence in research and teaching

Photon Science is one of the major research areas of the University of Hamburg. The collaboration with HASYLAB and the research with synchrotron radiation have a long tradition. From the early days of synchrotron radiation research at DESY members of the Institute of Experimental Physics have been actively involved in these activities. Today many groups from the Faculty of Mathematics, Informatics and Natural Sciences are active users of the DESY photon science facilities. Even more importantly, groups of the University have been and still are developing and running beamlines and instruments at HASYLAB.

At DORIS III, traditionally spectroscopy in the VUV and XUV spectral range has been one of the focal points of research. The SUPERLUMI beamline for VUV luminescence spectroscopy was built and operated by the institute for many years (Georg Zimmerer); further instruments developed and still operated by University groups are the angle-resolved photoemission endstation at FLIPPER 2 (Robert Johnson) and the Kappa diffractometer for single-crystal X-ray diffraction at beamline F1 (Ulrich Bismayer, Department of Geosciences). Today groups from the University are actively involved in building endstations at PETRA III in the framework of the BMBF Verbundforschung: a low temperature cryostat with integrated high-field magnet for X-ray absorption spectroscopy will be operational next year at the variable polarization XUV beamline P04 (Wilfried Wurth), Michael Martins is leading an effort to build an ion-storage ring for spectroscopy (PIPE) and Robert Johnson is involved in the hard X-ray photoemission project. Research in structural biology which has started at DORIS III and is now moving to PETRA III (Christian Betzel, Institute for Biochemistry and Molecular Biology) will be considerably expanded in the future with the foundation of the Centre for Structural Systems Biology where the University of Hamburg is one of the partners. Even before that the University of Hamburg and the University of Lübeck (Rolf Hilgenfeld) have started a joint Laboratory for Structural Biology of Infection and Inflammation on the DESY site in 2007.

University groups are heavily involved in research at FLASH. They are major partners in the BMBF Research Centre (Forschungsschwerpunkt) “FLASH: Matter in the light of ultra short and extremely intense X-ray pulses” coordinated by Wilfried Wurth. This priority program which is the first BMBF priority program in condensed matter research was initiated to develop and perform pioneering experiments at FLASH. Projects from the University of Hamburg are among others the instrumental efforts at the plane-grating monochromator beamline (Wilfried Wurth) including a soft X-ray split and delay unit and the new VUV Raman spectrometer (Michael Rübhausen). During the shutdown period at the end of this year the seeding experiment “sFLASH” (Markus Drescher and Jörg Roßbach) will be implemented and first tests will be performed next year. Markus Drescher and his group have also performed first experiments at the THz-beamline demonstrating perfect synchronization and phase stability between THz- and XUV-pulses. The Center for Free-Electron Laser Science (CFEL) which was founded by the University of Hamburg together with DESY and the Max-Planck Society to foster interdisciplinary science with free-electron laser sources is growing and the construction of the new building has started, as outlined in detail in the CFEL chapter.

Most recently, the research groups from the University involved in the newly founded Centre for Optical Quantum Technologies (ZOQ) and CFEL have been successful within the framework of the excellence initiative of the federal state of Hamburg. As a result the Excellence Cluster “Frontiers in Quantum Photon Science” which combines the expertise from laser-physics, quantum optics, short-time- and X-ray-physics as well as condensed matter physics has been started this year as new and highly profiled research activity. As a special honour, the Joachim Herz Stiftung has taken over the full funding of this Cluster.

At the same time, academic education is pursued in collaboration between HASYLAB and the Department of Physics of the University. Examples are a joint master course in X-ray physics and the multidisciplinary approach in the university graduate training program (Graduiertenkolleg) GRK 1355 “Physics with new advanced coherent radiation sources”, dedicated to the development, characterization and application of modern sources for light and matter waves. The latter combines the expertise of scientists from the fields of laser physics, quantum optics, X-ray physics, ultra-short pulse physics and accelerator physics in order to study the joint and complementary aspects of systems like fibre-lasers, crystalline waveguide lasers, fs-lasers, XUV free-electron lasers, and synchrotron radiation as well as atom lasers.

Contact: Wilfried Wurth (University of Hamburg), wilfried.wurth@desy.de

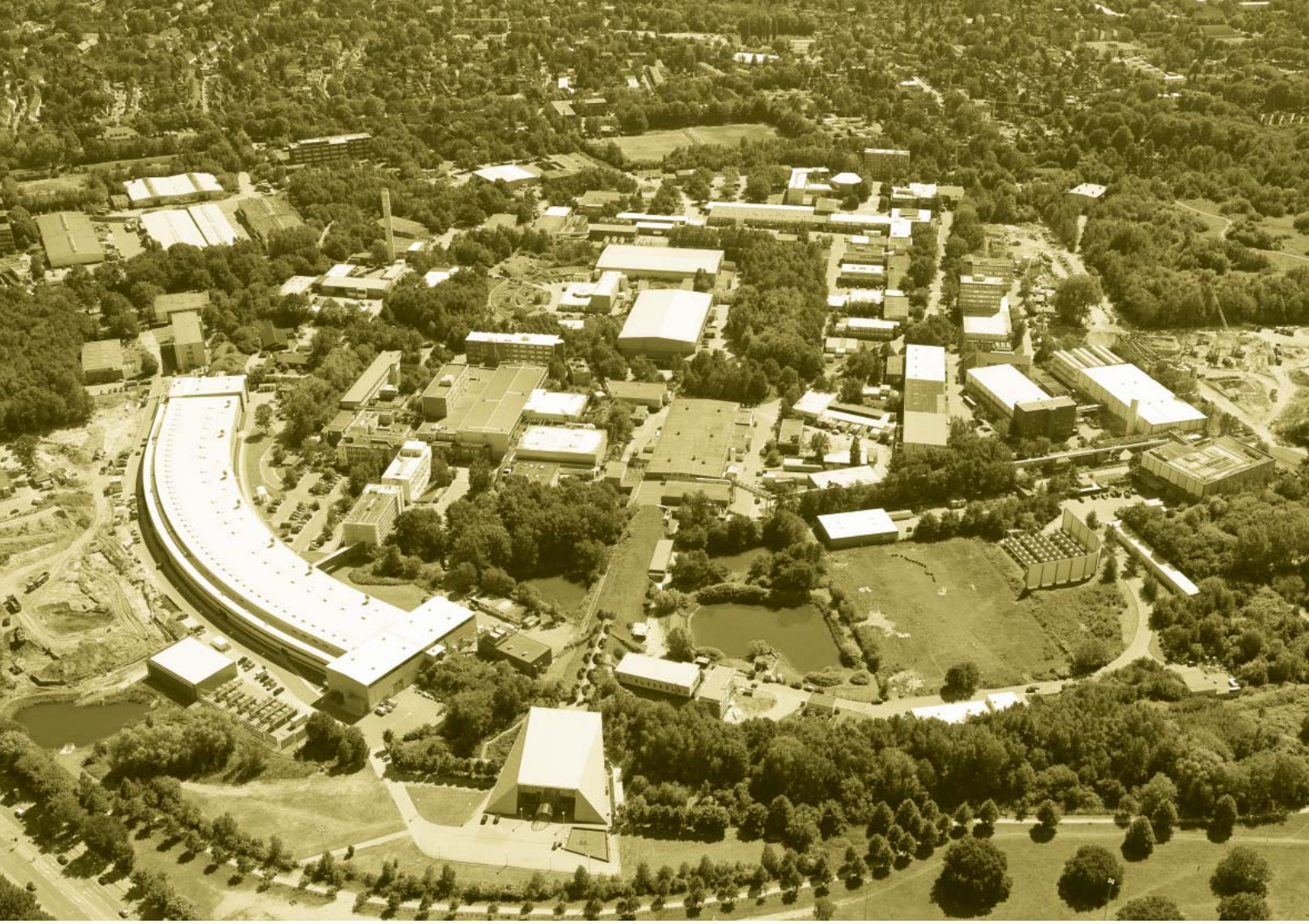

Lightsources.

DORIS III.

Productive routine operation

The new year started with reliable conditions and very good beam lifetimes between 25h to 35h for the user operation. In total, seven user beamtime periods were scheduled yielding 5409 h for experiments (Fig. 1). A few technical problems occurred, however, which affected user experiments to some degree. In March, three days of beamtime were lost because part of the vacuum system had to be vented in order to replace a leaky beam current monitor. After the scheduled summer shutdown, the beam refills took somewhat longer than usual due to a faulty magnet coil in the pre-accelerator transport path. Fortunately, it could be replaced without breaking the vacuum thus maintaining good beam lifetimes.

In October, the machine suffered spurious beam losses which became increasingly frequent. This problem turned out to be caused by a shorted coil in a dipole magnet. In order to ensure a reliable operation until the end of the year, it was decided to replace the magnet coils during the November service week which required another venting of a major part of the machine vacuum system. Following this repair, the operation was back to stable conditions but it took some time for the lifetimes to recover and to reach the usual values.

In 2009, a record number of research proposals for experiments at DORIS III were submitted. In total, 257 new proposals were accepted by HASYLAB, 200 in category I (1 year term) and 57 in category II (2 years term). As in previous years, the number of proposals submitted by international research groups is high (50.6 %), where the share of proposals from EU countries amounts to 46.7 %. Following a slight decrease in 2008 this number is back to the level well-known from previous years (~47 %). The numbers above do not include proposals for structural biology research at the EMBL and MPG beamlines. The distribution of the new projects among the research fields of the different review panels is shown in Fig. 2.

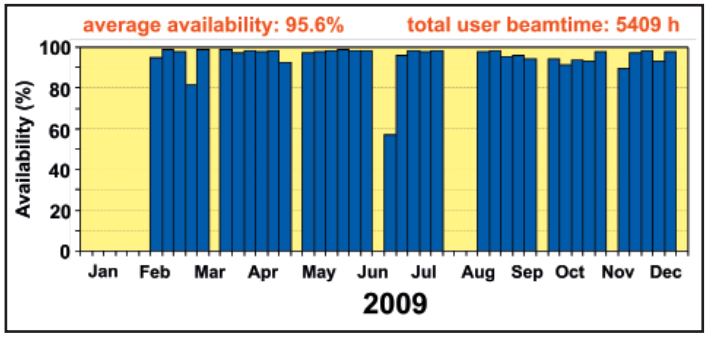

Figure 1

DORIS III beamtime statistics for 2009.

The upgrade of beamline A1 for X-ray absorption spectroscopy (XAS) was completed in Spring 2009 and the commissioning of all new optical components went very smoothly. The beamline is optimized for low energy XAS experiments reaching down to the S K-edge (2.47 keV) and going up to 8 keV (Fig. 3). In this energy range effective harmonics rejection is an issue and therefore a pair of new mirrors were installed in the monochromatic beam which also provide a focused beam at the instrument. The precision mirror chambers for A1 were designed as prototypes for PETRA III beamlines (Fig. 4). Regular user operation at A1 resumed after the summer shutdown. Since the refurbished beamline is performing very nicely, XAS beamline E4 was shut down as planned in the middle of September. Also, beamline G1, the former instrument for reflectometry studies in the XUV regime, was closed.

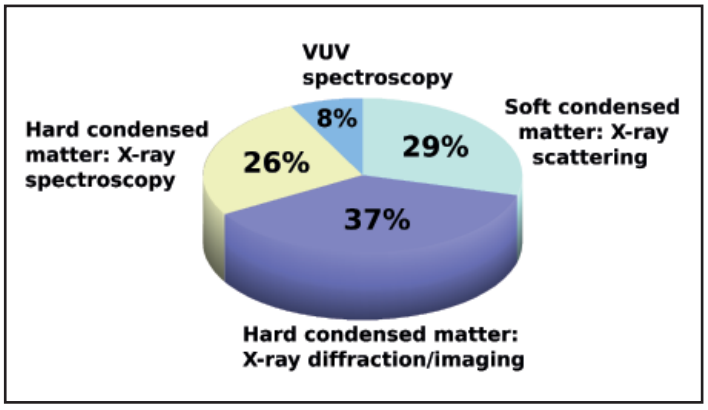

Figure 2

Distribution of DORIS III proposals accepted by HASYLAB in 2009 (not including structural biology research).

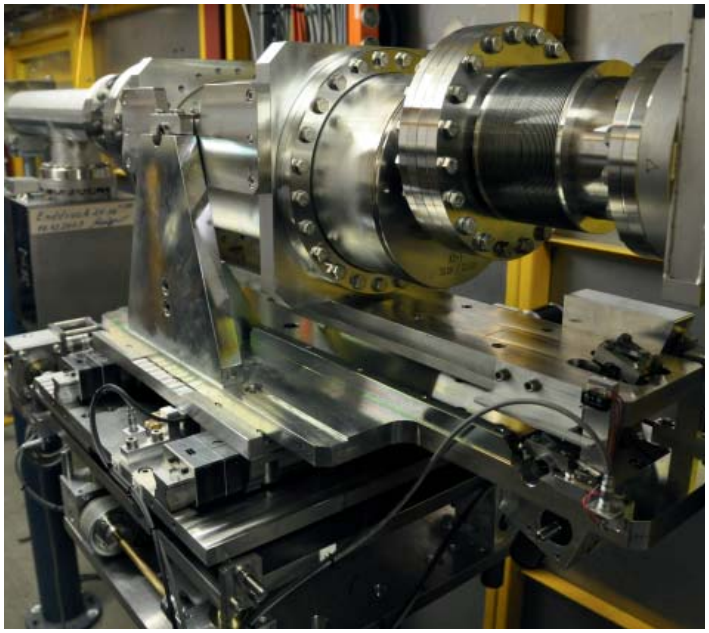

Figure 4
New X-ray mirror in DORIS III X-ray absorption beamline A1. The chamber is a prototype developed for PETRA III beamlines.

Beamline D3 for chemical crystallography was available again for regular user experiments in March 2009. Also this instrument was partly refurbished during the summer shutdown: new monochromator crystals in combination with the replacement of mechanical stages resulted in considerably increased intensity at the sample. In addition, new data acquisition electronics for energy dispersive detectors were obtained to allow continuous angle scanning. New detectors are now also available such as an avalanche photo diode, a $LaCl_3$ scintillation counter and a vortex detector. A new motorized (x,y,z)-stage specifically designed for closed cycle displex cryostats now facilitates a precise re-alignment of the sample position after cooling.

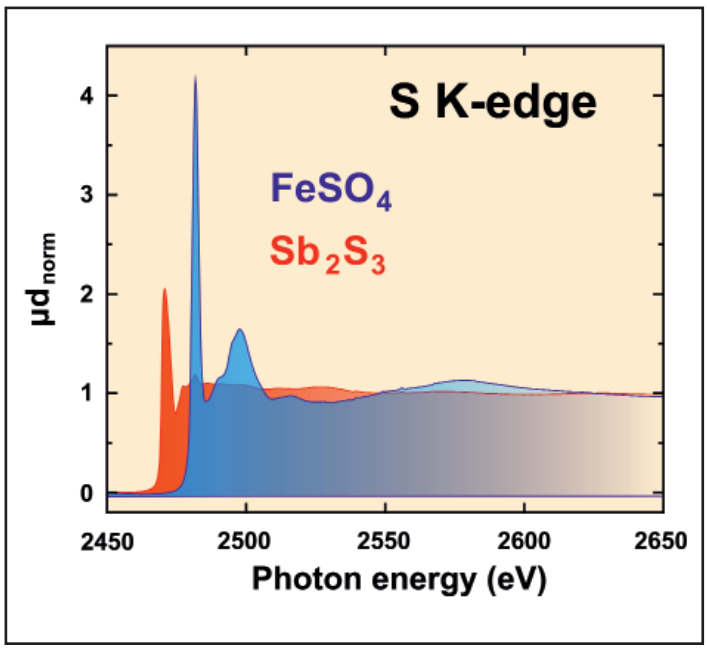

Figure 3
Typical sulphur K-edge X-ray absorption spectra measured at the refurbished X-ray absorption beamline A1.

At the EMBL bioSAXS beamline X33 (D1) completely automated operation with a liquid handling robot and a data processing and analysis pipeline including remote operation capability is now being offered for users. The world's first remotely controlled SAXS experiment was performed in May 2009. New instrumentation was also made available at the EMBL protein crystallography beamlines. For further details see page 64.
At the materials science beamline HARWI II, which is operated by the GKSS research centre in collaboration with DESY and GFZ, a dilatometer with quenching, deformation and DSC options was commissioned adding to the suite of unique sample environments available for in situ experiments. Also, a new imaging experiment utilizing differential phase contrast was implemented which is most effective for the study of low-Z materials. More details can be found on page 70.

The operation of DORIS III will continue in its present configuration until it will be shut down by the end of 2012. In order to continue many of its successful techniques and to provide competitive instrumentation for X-ray applications not available at PETRA III in the present phase, it is planned to extend the new facility by building two experimental halls which will accommodate additional insertion device and bending magnet beamlines. This extension project has been discussed during a workshop held in November. A detailed discussion on beamline layouts will begin in Spring 2010.

Contact:
Wolfgang Drube (DESY-HASYLAB), wolfgang.drube@desy.de
Frank Brinker (DESY-MDO), frank.brinker@desy.de

FLASH.

New upgrade after a long, successful period of operation

Figure 1

The FLASH experimental hall during the open day on 7th November.

A long period of continuous operation that started after the FLASH upgrade in 2007 and was only interrupted for maintenance, ended on 21st September 2009. On this day the FLASH facility was shut down for five months in order to carry out another major upgrade. In 2009, until September 2955 hours of beam time (46 % of 6384 hours) were spent by user experiments (Fig. 2a). 1880 hours (29 %) were used for FEL studies, for work on the photon beam lines and photon diagnostics, and for preparing the user runs; approximately 10 % (664 hours) were used for accelerator studies and 14 % (885 hours) for maintenance. The availability of the machine during scheduled operation was 92 %. The total downtime due to component failures was 8 %. The increase of downtime compared to 6 % in 2008 is mainly due to a major site-wide power outage and failure of one RF station which is being replaced during the shutdown. During scheduled FEL user runs 80 % of the time was actually available for experiments, 10.5 % was required for tuning and changing the wavelength of the FEL, and 1 % for setting up the machine (Fig. 2b). Generally user experiments are scheduled such as to minimise the number of beam parameter changes in order to maximize the efficiency.

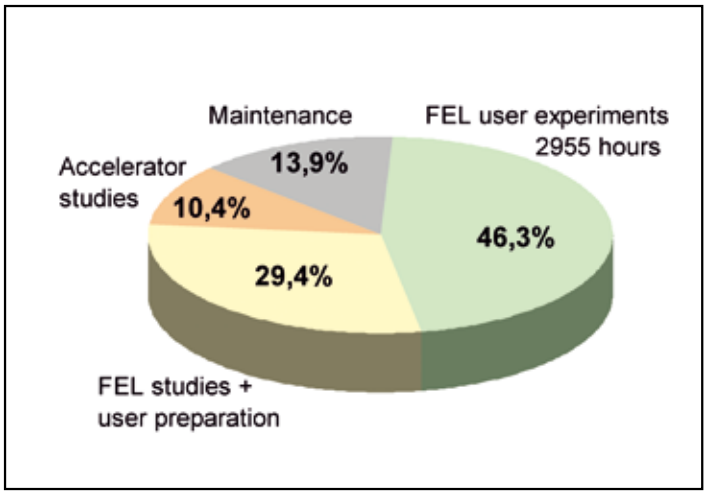

Figure 2a

Scheduled beam time distribution in 2009 before the start of the shutdown on 21st September.

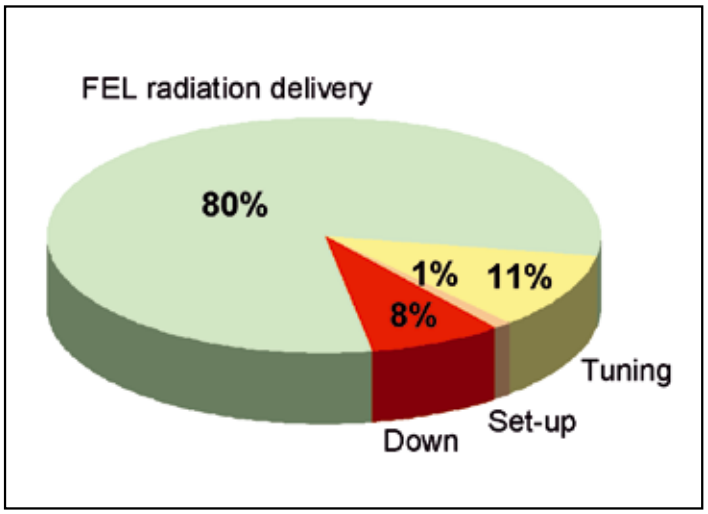

Figure 2b

Beam delivery during scheduled user operation in 2009.

The experimental program run at FLASH during 18 weeks of beam time in 2009 covered again a wide spectrum of applications, ranging from atomic and molecular physics to the study of ultrafast processes in solids. Selected results are presented in the highlight section of this report. The number of scientific publications resulting from experiments at FLASH has been steadily increasing; about 30 papers appeared in high-impact journals in 2009. Links to these papers may be found at http://hasylab.desy.de/facilities/flash/publications/selected_publications/index_eng.html.

A joint effort was made at the end of the operation period in September to demonstrate long-pulse, high beam-loading operation of the accelerator. Although driven by an international ILC collaboration, this work is highly relevant for FLASH and the European XFEL because it prepared the ground for providing long FEL pulse trains for user experiments. Stable machine operation for several hours was demonstrated with 800 bunches of 3 nC charge (Fig. 3). The next step will be to achieve lasing with long bunch trains and to provide routinely long FEL pulse trains for user experiments. The success of many science projects depends on a high average number of pulses. It is therefore important to pursue this development, in particular because FLASH and European XFEL are the only free-electron lasers worldwide that are able to deliver thousands of pulses per second because they make use of superconducting accelerators.

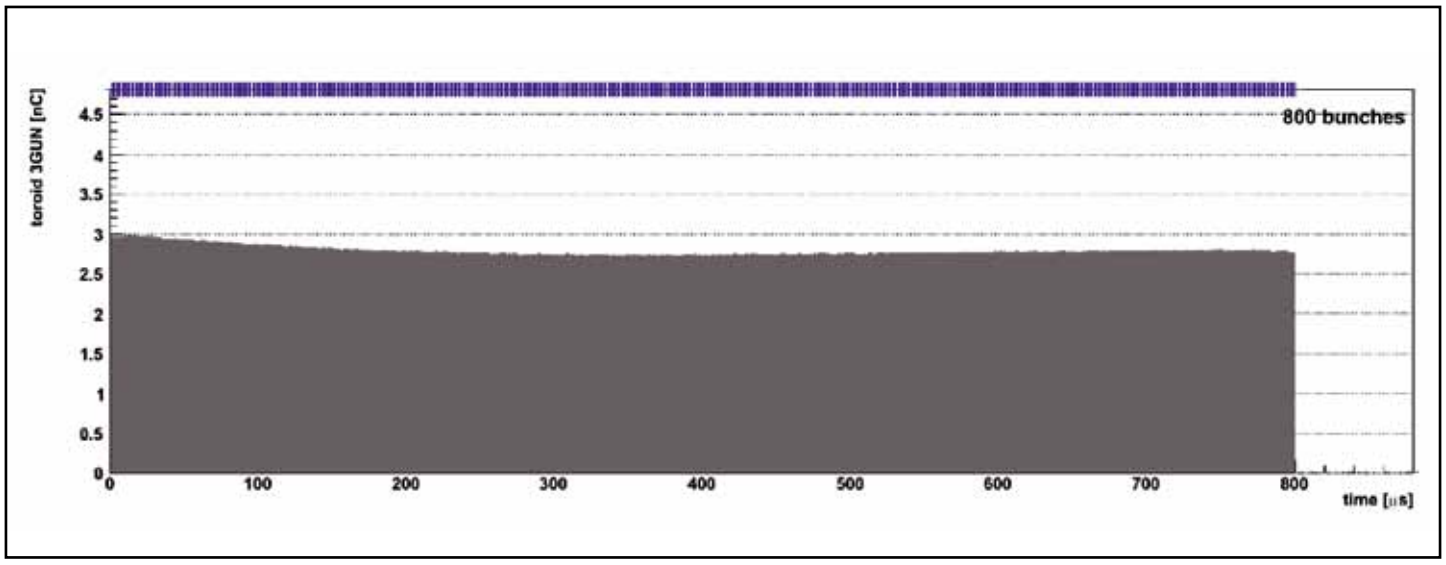

Figure 3

Linac operation with a train of 800 bunches of 3 nC charge at a rate of 1 MHz.

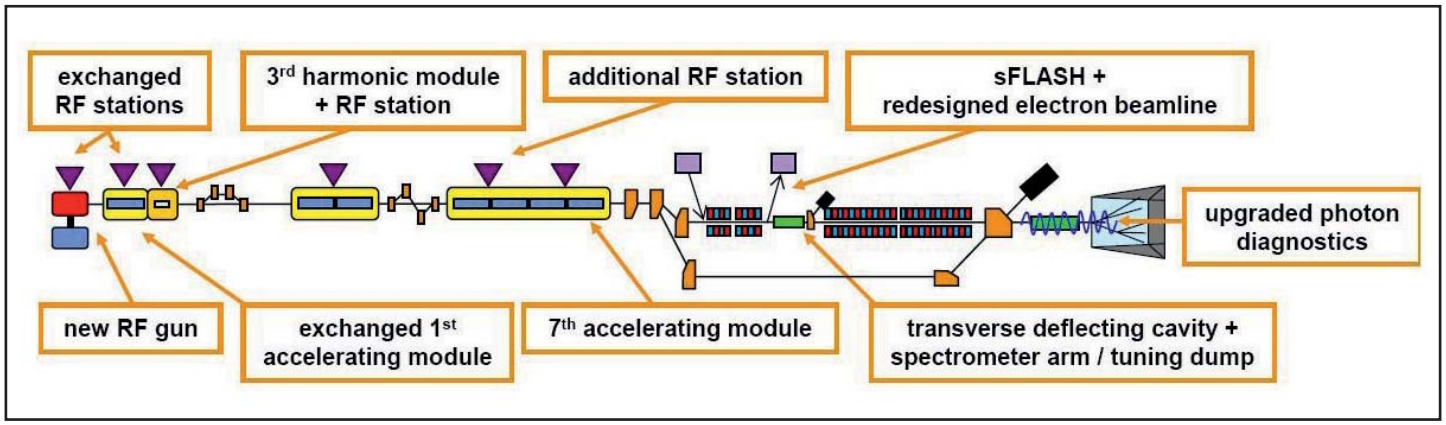

Figure 4

Overview of the upgrade activities during the shutdown.

The shutdown of five months is required for a major upgrade of the facility. An overview of the activities is shown in Fig. 4. The RF electron gun which has been in operation since about six years and exhibits aging effects and high dark current, will be exchanged by a new gun that was conditioned and operated at PITZ at DESY Zeuthen. This new gun will be equipped with two waveguide arms, two circulators and a directional coupler such that it can be operated at up to 60 MV/m gradient in the future resulting in lower electron beam emittance and better FEL performance.

The first accelerator module (ACC1) will be replaced to achieve higher gradients and better performance for long bunch trains. Attached to ACC1 is the new 3rd harmonic module (ACC39) containing four 3.9 GHz cavities (Fig. 5). This module has been developed in collaboration with Fermilab (FNAL, USA). It is required to compensate the curvature of the longitudinal electron phase space introduced by off-crest operation of ACC1 in order to compress the electron bunches more efficiently. Depending on the bunch charge, this unit will allow producing very short bunches in the 10 fs range, but also much longer bunches of several hundred fs as required for the seeding project (sFLASH).

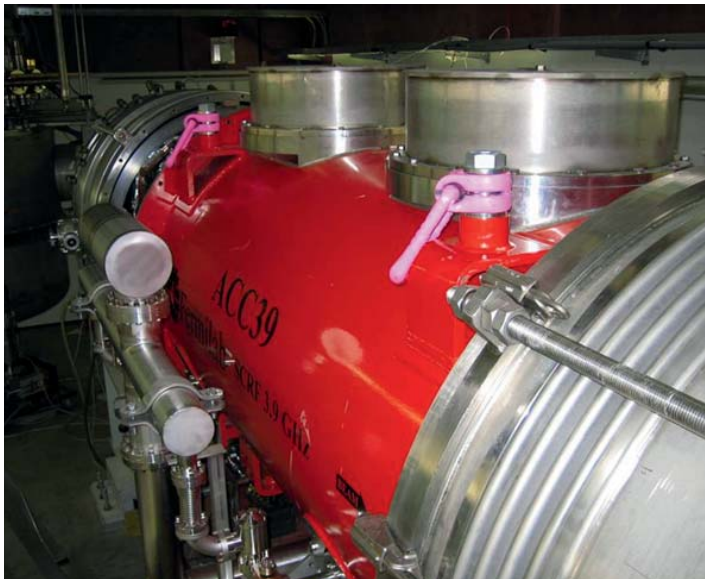

Figure 5

The 3rd harmonic module (ACC39).

A seventh accelerator module has been added to increase the electron beam energy to 1.2 GeV. This will allow reducing the minimum wavelength to below 5 nm, coming very close to the carbon K-edge at 4.2 nm. The third harmonic of the FEL with about 10^{10} photons per pulse will cover the L edges of the 3d elements down to ~1.5 nm wavelength, allowing the study of fast dynamics of magnetic systems. Fig. 6 shows the new module PXFEL1 in the ACC7 position during installation behind module 6 in the accelerator tunnel. As the name indicates, it is the first prototype module for the European XFEL for which the vessel and the so-called cold mass were produced in China. It was tested on the cryomodule test bench at DESY (CMTB) demonstrating a record average gradient of 30 MV/m. Another RF station has been added to optimise operation with seven modules. In addition, two old RF stations have been replaced after more than ten years of operation.

In parallel to the energy upgrade, a HHG seeded FEL section is added to the present SASE FEL including a station for high-resolution pump-probe experiments. The main objective of this project, called sFLASH, is to test and develop the technology for direct seeding with an external laser source for a future extension of the FLASH facility. The sFLASH installations affect a ~40 m long section in the tunnel, including four new undulator modules, new beamlines for the seed laser light and the seeded output radiation, the transversely deflecting LOLA cavity LOLA cavity that was previously installed in the ACC7 area, the ACC7 area and other components. The harmonic laser (HHG) source has already been set up and is currently under test in the laser hutch (building 28g) next to the accelerator tunnel. A spectrum of the laser harmonics is shown in Fig. 7. Seeding will be tested at 35 nm and 13 nm wavelength. The sFLASH project is a joint effort of University Hamburg and DESY with funding from BMBF.

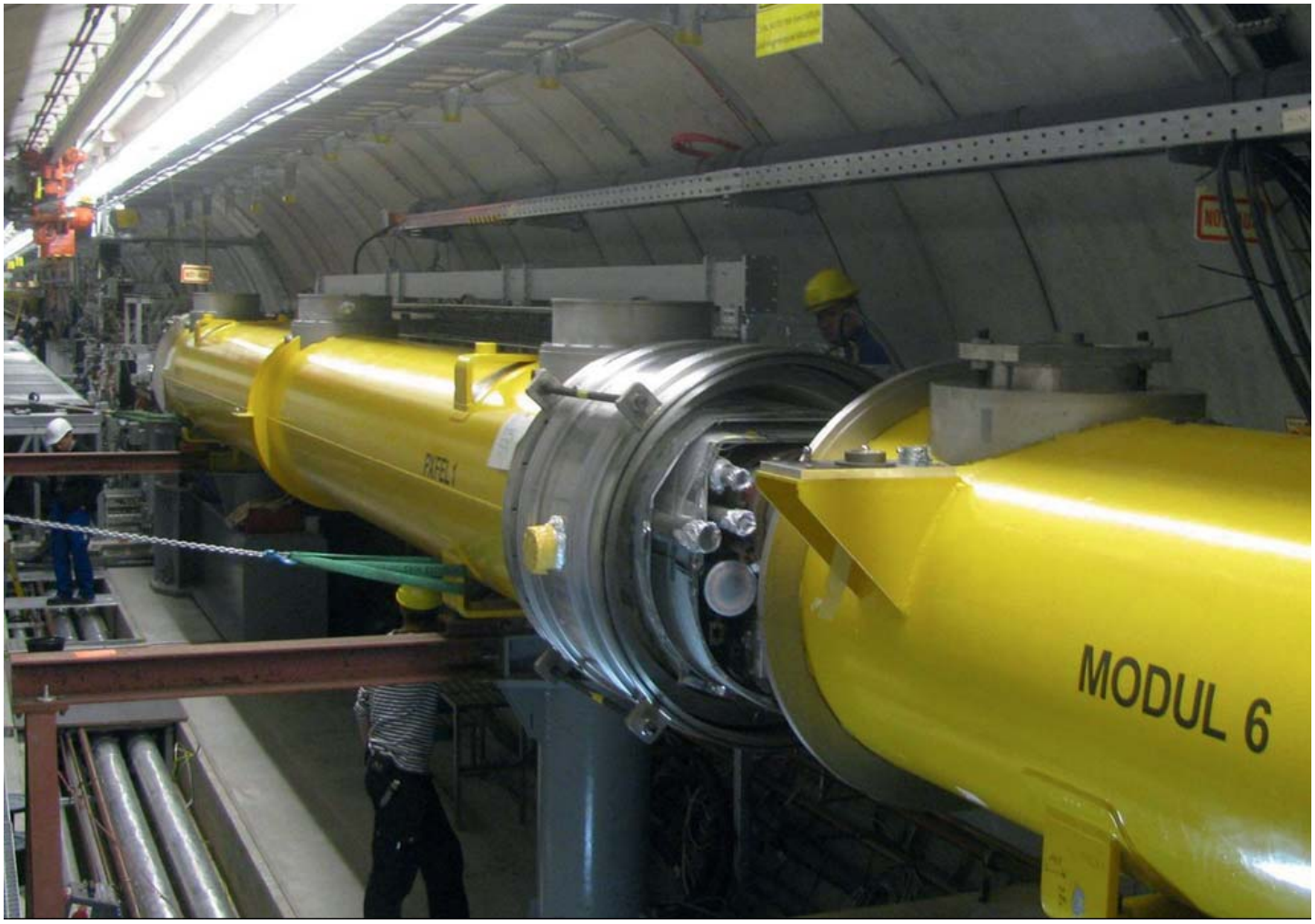

Figure 6

The 7th accelerator module (PXFEL1) during installation in the FLASH tunnel.

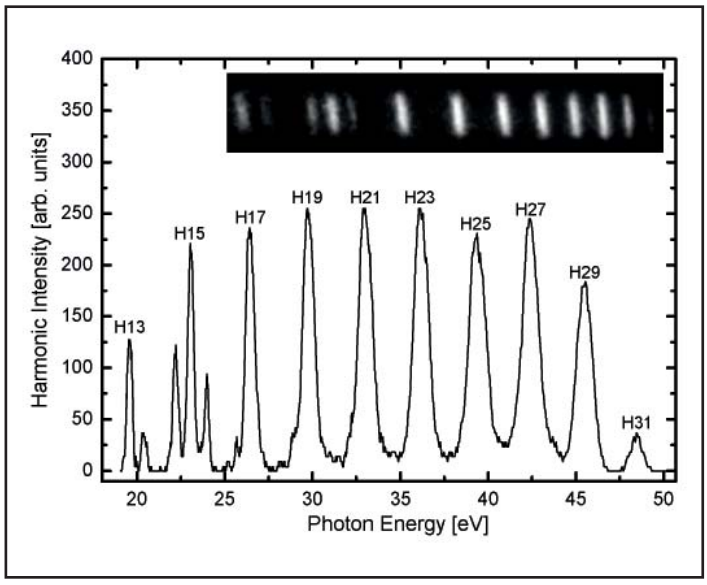

Figure 7

Spectrum of the harmonic source used for seeding.

In addition to these large installations the shutdown is used for several other changes and upgrades of the facility as well as maintenance of infrastructure. In order to increase the stability and reliability, the RF electron gun will now be driven by the new diode pumped photocathode laser, the old flash lamp pumped laser will remain as backup. Likewise, a second master oscillator will be installed as backup. After the shutdown the accelerator will operate at 10 Hz repetition rate rather than at 5 Hz as in the past. Also photon diagnostics and beam lines are upgraded. Important additions will be two new photon spectrometers, one based on a varied line spacing grating, the other one on ion and electron time-of-flight measurement. These devices will provide for the first time online wavelength information for the operators and users (for details see the section “New Technologies and Developments”).

Contact: Josef Feldhaus, josef.feldhaus@desy.de

PETRA III.

Brilliant light for first experiments

In the course of 2009 the most important milestones in the PETRA III project were achieved. Reconstruction work of the storage ring was completed and the first experiments received X-rays on their optics and on first samples. In detail the most important steps have been:

- In March the last components in the new octant were installed, the tunnel was closed.
- On March 24 the first positrons were injected into PETRA III.
- During the Easter weekend the machine crew managed to store the first stable beam in the ring.
- First X-ray light on the frond-end screens inside the tunnel was seen at the end of April.
- On July 17 the first monochromatic beam was observed at beamline P09.
- On September 21 the design value for the horizontal emittance of 1 nmrad could be measured.
- On October 12 the first users started their experiment at beamline P08.

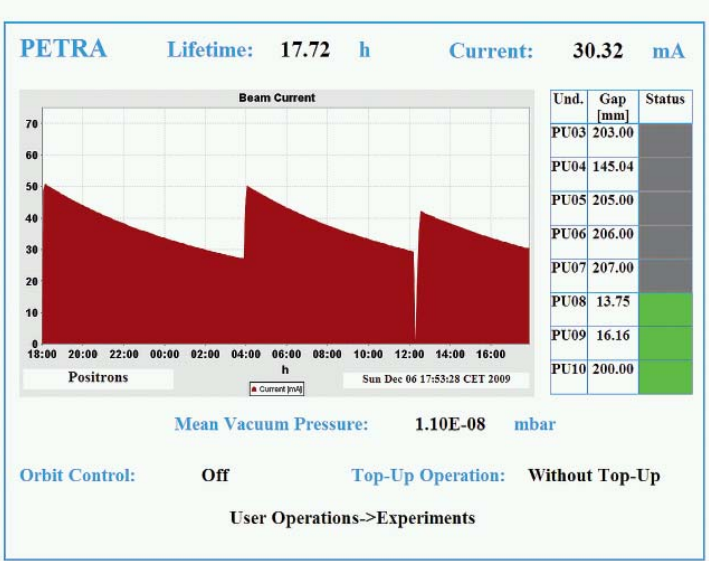

Figure 1

The PETRA III accelerator status display on Dec. 4, 2009.

Storage ring

The upgrade of the machine - more or less a complete rebuilding - was realised by the machine crew of DESY within only 21 months. It started in July 2007 when the first magnets were removed from the tunnel. The last machine component was installed in March 2009. During this time the upgrade team cleared out and newly equipped the complete PETRA tunnel. The coils of the 214 bending magnets, 140 sextupoles and 396 quadrupole magnets were replaced and characterised off-line. The complete 2.3-kilometre-long beam pipe was redesigned. In particular in the new octant very complex outlet chambers and absorbers had to be developed to cope with the high heat-load of the radiation from both insertion devices and bending magnets. More than 2000 new vacuum pumps were installed. In addition, the cooling water supply system and the magnet controls were replaced. Altogether more than 700 kilometres of power and signal cables were put in.

The interlock system was modernised and successfully approved by the legal authorities. In parallel the entire control system was renewed.

After the first injection on March 23 it took roughly three weeks until the beam was steered around the ring and a closed orbit could be reached. The most difficult passage for the PETRA III machine crew headed by Klaus Balewski was the 300 metres in the new experiment hall where the positron beam had to pass through the undulator vacuum chambers of only seven millimetres height.

Since this remarkable event many hours have been spent to bake out the vacuum chambers. The integrated current has now reached a value of 80 Ah. Some 100 Ah are required for standard user operation. This goal is within reach until the end of 2009. At the time of writing this report, a maximum positron current of 50 mA could be stored and fillings with a rather long lifetime could be realised (see Figure 1). Also on the agenda for the remaining part of 2009 is the activation of the orbit-feedback system, designed to stabilise the position of the positron beam within fractions of a micrometer.

Insertion devices

During 2009 eight undulators have been installed in the tunnel during several service weeks. There are now two canted pairs in sector 4 (PU5 and PU6) and sector 6 (PU8 and PU9), respectively. In sector 7 the 5-m long U29 undulator is delivering beam for P10. Two more 2-m U29 undulators were installed in sectors 2 and 5, the latter one being a temporary substitute for the 4-m in-vacuum undulator planned for this beamline. This device, optimised for hard X-rays in the range of 100 keV and beyond is planned to be installed by the end of 2010.

Finally, in sector 3 the 5-m APPLE II undulator built at HZB in Berlin has been installed in August (see Figure 2). It produces soft X-ray light with variable polarisation between 200 eV and 3 keV in the first harmonic. An even wider range is accessible for special polarisation states. By now four devices are opera-

Figure 2

The 5 m APPLE II undulator for P04 just before installation into the machine tunnel.

tional, three have already delivered beam to the experiments. In October a first spectrum of the fundamental of PU10, the 5-m long U29, was measured at the coherence beamline. The measured line-width of the undulator fundamental at 7.6 keV was 100 eV, in perfect agreement with the simulated value.

Beamlines and experiments

During the year the PETRA III hall was filled with more and more experimental hutches (see Figure 3). Except for the holiday season, on average every month one hutch was completed and equipped with media. This includes the entire cabling, supply of cooling water, liquid nitrogen, gases, Ethernet, air conditioning, safety and interlock system. By now, three sectors with 16 hutches are operational.

In the optics hutches six monochromators have been installed: Three cryogenically cooled PETRA standard monochromators (P08, P09, P10) and two water cooled systems for the High Energy Materials Science beamline P07.

The last one in the list is the newly developed “large-offset monochromator” (LOM1200, see Figure 4). Via two pairs of Si(311) and Si(511) crystals mounted in a huge vacuum tank it deflects the monochromatic beam 1250 mm upwards. After completing the mechanical and electrical installation, the LOM was pre-aligned using a built-in laser system that is guided through the vacuum vessel parallel to the X-ray beam with a horizontal offset of 40 mm. After approval of the safety systems, the LOM was commissioned in early October and since then delivers stable beam to the experimental hutch of P08 which was built on a solid concrete pedestal on top of the beampipe of P09. The stability of the LOM1200 will be measured and published as soon as the stability of the incident beam has reached its design value.

Figure 3

View into the experimental hall, looking over sectors 5 and 6 up to the north end.

Figure 4

The LOM 1200 installed in the optics hutch of P08.

A second large-offset monochromator (LOM500) is currently being assembled for the small-and wide-angle scattering beamline P03. Its properties are described in a dedicated article in the New-Technologies-and-Developments section of this report. It should become operational in March 2010.

Inside the experimental hutches several diffractometers have already been installed and commissioned. In P07 a heavy load (200 kg) general purpose diffractometer optimised for very hard X-rays is waiting for first beam.

In P08 two diffractometers have been set up. The first one is a high precision 8-circle diffractometer for high resolution diffraction. The second one is a liquid interface scattering apparatus (LISA) developed and installed by the University of Kiel in the frame of the German “Verbundforschung”.

In P09 another high precision 6+2-circle diffractometer with full polarisation analysis is ready for the first experiments. (see Figure 5). At this beamline the first monochromatic X-rays were observed in July (see Figure 6). First test samples have been measured successfully. In the last experimental hutch of P09 a hard X-ray photoelectron emission spectrometer has been installed together with Universities of Mainz and Würzburg (in the frame of a “Verbundforschungs”-project). In mid October they have taken beam and performed the first experiments, as reported in a special section following this article.

In all other sectors activities are ongoing to achieve user operation in the course of the year 2010. In the following the current status of all sectors will be described in brief.

In sector 1 (P01: Nuclear resonant and inelastic scattering) the construction of the experimental hutches has started. The optics hutch is finished and equipped with first installations. First beam is expected in spring 2010.
In sector 2 (P02: High resolution powder diffraction and extreme conditions beamline and P03: Small- and wide-angle scattering) the optics hutches are finished as well as the experimental hutches of P03. P03 expects first beam in March 2010, after installation of the LOM500 (see above). Due to its late start, P02 will not be ready before summer 2010.
In sector 3 (P04: Variable polarization soft X-rays) several main components have been delivered and are now being commissioned off-line. Due to problems with the production of high quality varied-line-spacing (VLS) gratings the start of this beamline is considerably delayed. First beam is expected in summer 2010.
In sector 4 (P05: Tomography and Imaging (operated by GKSS) and P06: Hard X-ray nano-probe) the work on the hutches is about to be finished. Currently the installation of media and interlock system is in full swing. Monochromators are already waiting to be installed, as well as many end-station components. First beam for this sector is expected in March 2010.
In sector 5 (P07: High Energy Materials Science, GKSS and DESY) most of the work has been finished. Only minor work remains to be completed. The interlock system has been approved by the authorities in mid October. First beam is expected after the completion of the radiation shielding in December 2009.
Sector 6 (P08: High resolution diffraction and P09: Resonant scattering and diffraction) is completed as well. Users are using commissioning beamtime since October 2009. The optics and main diffractometers and spectrometers are on-line. The first experiments are explained later in this paragraph.
In sector 7 (P10: Coherence beamline) the first experiments to characterise the beam have been performed in the optics hutch. In December the beam will be guided into the two experimental hutches where instruments are currently being installed.
In sector 8 (P11: Protein crystallography and Bio Imaging, DESY, HZI and MPG and P12: BioSAXS, EMBL and GKSS) the first experimental hutch is almost completed. Infrastructure and equipment will be installed in the first half of 2010 so that first beam for these experiments is expected for the second quarter of 2010.
In sector 9 EMBL will install two beamlines for Macromolecular Crystallography (P13 und P14). The call for tender for the experimental hutches has just terminated, so that installation of the beamlines may start in spring 2010.

Eight workshops were organised during this year dedicated to discuss the progress of the more advanced beamlines with the users and to sharpen the scientific case and the specifications for the remaining experiments. More details and summaries can be found in News-and-Events section of this report.
Besides the beamline workshops a series of events took place in and around PETRA III in 2009. It started with the celebration

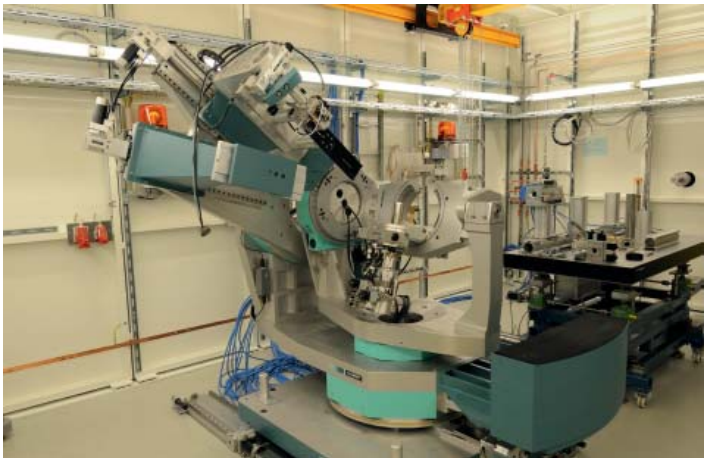

Figure 5
The high precision 8-circle diffractometer of P09.

of the completion of the machine in spring of this year and culminated in two major events in November that followed shortly after each other: On Nov. 7, during the DESY open day, PETRA III was nominated as “Ort der Ideen” by an initiative of the German federal president that highlights a particular interesting site every day of the year. Finally, PETRA III was officially inaugurated during a ceremony on November 16th that was attended by more than 700 guests from all over the world.

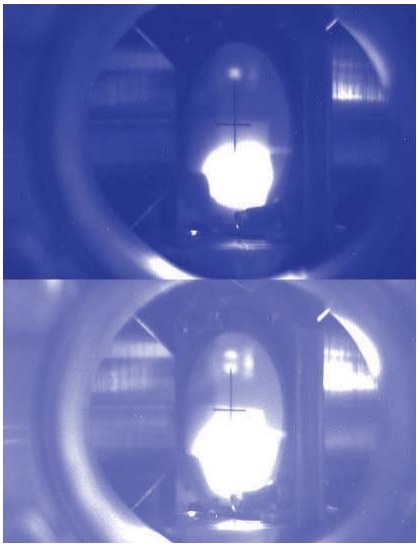

Figure 6
First monochromatic light in the PETRA III experimental hall. The small spot above the large spot originating from the white undulator radiation is the monochromatic beam at 12 keV. After detuning the monochromator the spot displays a vertical splitting, as expected.

The first PETRA III beamlines will be able to serve regular users in 2010. We are looking forward to welcome users for test experiments right after the winter shutdown (very likely at the beginning of March 2010). Regular user operation with shifts scheduled within the HASYLAB beamtime allocation scheme is expected for the second half of 2010 for the most advanced beamlines.
In the meantime users are invited to submit informal proposals to join the commissioning process. Please contact the beamline scientists for more details on the procedure and the status of the individual beamlines.

Contact: Hermann Franz, hermann.franz@desy.de
Ralf Röhlsberger, ralf.roehlsberger@desy.de
Klaus Balewski, klaus.balewski@desy.de

First experiments at PETRA III.

Experiments at the High Resolution Diffraction Beamline P08

In October 2009 beamline P08 at PETRA III has gone online for the first test experiments. P08 is designed for experiments which require very high resolving power in reciprocal space and/or in real space. In the experimental area a high precision 6-circle diffractometer (Kohzu) and the liquid diffractometer LISA (University of Kiel) are installed. The first beam time was dedicated for commissioning LISA, the second for commissioning the 6+2-circle diffractometer.

LISA: A new surface X-ray diffractometer for liquid-liquid interface studies

There are many important questions about the nature of nanoscale structures at liquid – liquid interfaces, including electrochemical interfaces, biomolecular systems and complex fluids. A team at Kiel University (B. Murphy et al.) has designed a dedicated Liquid Interface Scattering Apparatus (LISA) for the PETRA III high resolution diffraction beamline P08. Using a double crystal beam-tilter, LISA enables reflectivity and grazing incidence diffraction investigations at liquid – liquid interfaces without moving the sample. The beam position at the sample remains constant over the full range of incidence angles minimizing vibrations at the liquid – liquid interface during data collection. First successful measurements with LISA were carried out at 9.5 keV during a series of night shifts in the first half of November, indicating that the instrument performs according to expectations (Fig. 1).

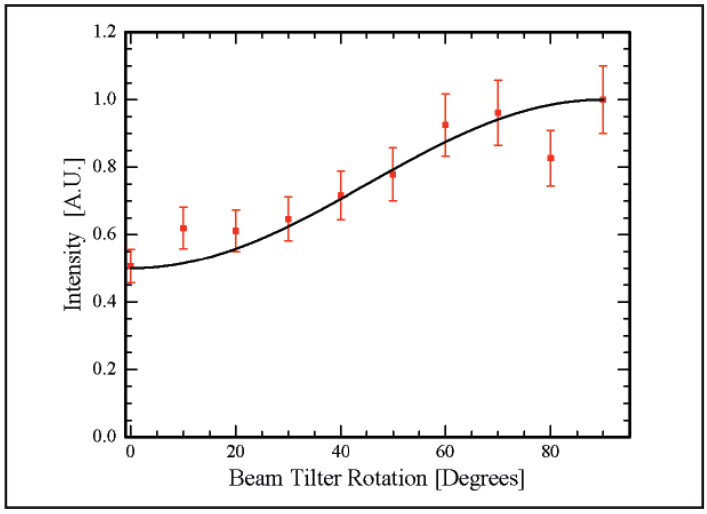

Figure 1

The measured intensity at the sample position over 90° is in excellent agreement with theoretical expectations (solid line), and shows that the polarisation at 9.5 keV is 50 %. The data was collected with a ring current of 0.8 mA.

High resolution diffraction on PbSe dislocation networks

The first user group at P08 (E. Wintersberger et al., University of Linz) used part of the commissioning time to investigate dislocation networks in PbSe/PbTe heterostructures. X-ray diffraction data of a sample with a periodic dislocation network were recorded at 9.5 keV with a maximum ring current of 10 mA using a Mythen strip detector. The sample investigated was a 6.1 nm PbSe layer grown on top of a 100 nm PbTe buffer layer which was deposited on a CdTe substrate. The periodic dislocation network resides at the interface between the PbSe and the PbTe layer. According to previously performed STM analysis of similar samples the period of the dislocation network should be approximately 10 nm. Reciprocal space maps were recorded for the (002) and (115) diffraction vectors (see Fig. 2) using a Mythen detector. In the (002) diffraction side oscillations from the periodic network are visible up to the 3rd order. From a rough first evaluation of the recorded data a period of 10.4 nm was obtained which supports the value found in STM work.

Contact: Oliver Seeck, oliver.seeck@desy.de
Carsten Deiter, carsten.deiter@desy.de

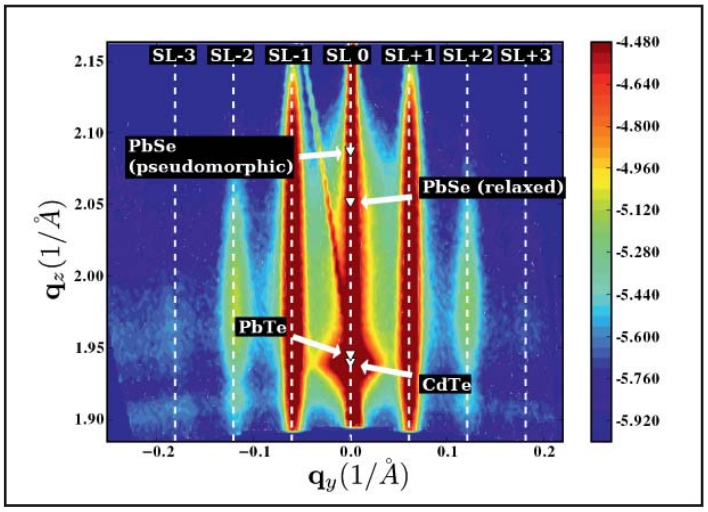

Figure 2

Reciprocal space map at the (002) reflection of a PbSe/PbTe/CdTe heterostructure.

Online polarisation analysis via photoelectron spectroscopy at P09

A diagnosis tool for several important beamline parameters has been set up for the XUV range of the P04 beamline. This angle resolving photoelectron spectrometer has been commissioned for the soft X-ray range but is also very promising for analysing the degree of polarisation in the hard X-ray regime of beamline P09 where it has been tested recently. The outstanding advantage of the method is that due to a very dilute gas target the beam is essentially unaffected so the users can benefit from an online parameter feedback within seconds during their data acquisition.

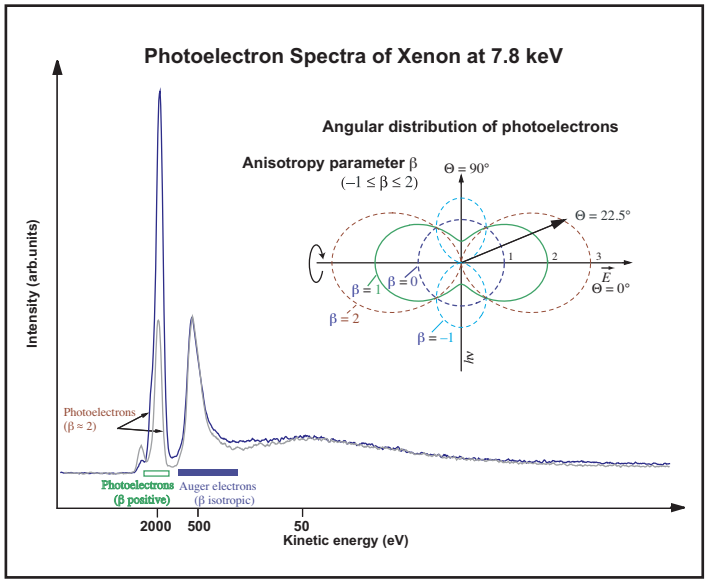

Figure 3

Photoelectron spectra of Xenon at a photon energy of 7.8 keV. The dark blue curve and the light grey curve show the 22.5° and 90° time-of-flight detector signals, respectively. Angles are measured relative to the horizontal direction. The ratio between the photoelectron peaks of both detectors points to a positive β of about 1. The outer areas of the photoelectron peak (accented) show a β of almost 2.

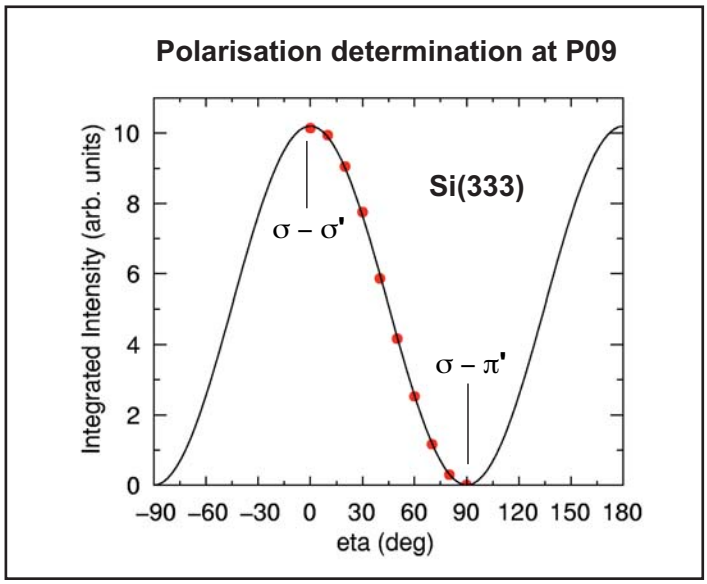

Figure 4

Polarisation dependence measured at 7.83 keV at the P09 beamline on the Si(333) reflection using a pyrolytic graphite crystal as polarisation analyser.

The gas target is injected in the chamber where it interacts with the incoming photons (7.8 keV). Direct photoionisation leads to polarisation dependent angular distributions of electrons with different kinetic energies. From the angular distribution the polarisation can implicitly be determined for any known anisotropy parameter β (Fig. 3). An independent determination of the polarisation at P09 was performed on the Si(333) Bragg reflection with a pyrolytic graphite (006) crystal as an analyser (Fig. 2). This method in combination with the angular distribution measurements forms the basis for creating a β–value data base. The data base will then be used to determine the total degree of polarisation.

The data shown in Fig. 3 are time of flight spectra of a detector located at a position of 22.5° (dark blue) and at the 90° position (light grey) with respect to the plane of polarisation. Normalised to the isotropic Auger electron signal they show a pronounced angular distribution in the photoelectron lines. It can clearly be seen that an anisotropy according to a positive β parameter is measured. These first polarisation measurements for X-ray photons of 7.8 keV show that also the hard X-ray regime is now accessible for this type of method.

Contact: Jens Viefhaus, jens.viefhaus@desy.de
Jörg Strempfer, joerg.strempfer@desy.de

Hard X-ray photoelectron spectroscopy at P09

Following intensive off-line tests for a few months, the instrument for hard X-ray photoelectron spectroscopy (HAXPES) in the last experimental hutch at P09 received PETRA III undulator beam at a ring current around 20-30 mA for first test experiments in late November 2009. The HAXPES activities at P09 are part of a collaboration between University Mainz, University Würzburg and DESY.

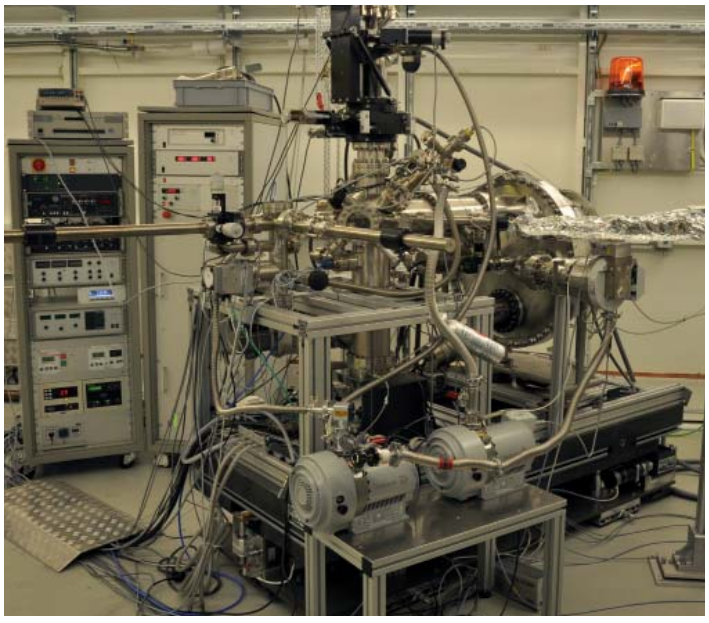

Figure 5

HAXPES instrument in experimental hutch 3 of PETRA III beamline P09

The UHV-chamber including the high-voltage electron spectrometer (Fig. 5) is located 95 m from the source. For the initial experiments, the direct monochromatic beam from the Si(311) high-heatload monochromator was used yielding a beam footprint of about 1.5 x 2.5 mm^2 at the sample position. Although only part of this rather large beam is accepted by the analyzer, the observed counting rates were already sufficient for core level studies on multi-layered materials where the increased probing depths obtained with HAXPES (around 10 nm) is most effectively used to study electronic properties at buried interfaces.

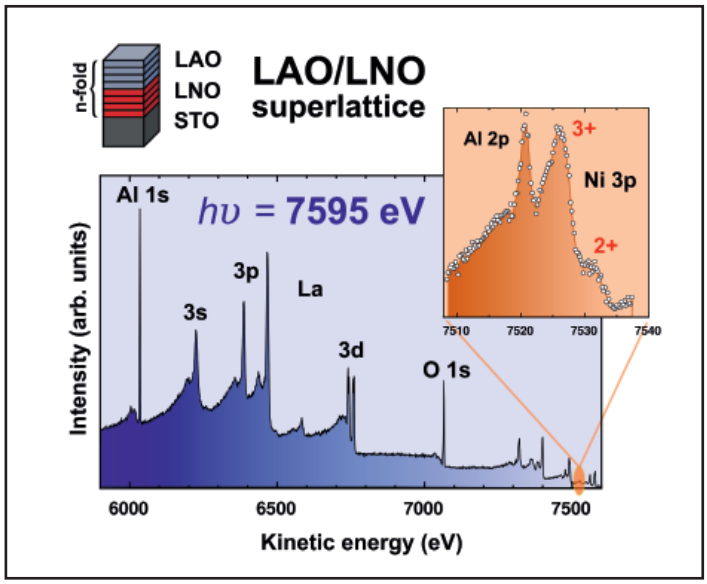

Figure 6

High energy electron spectra from $LaAlO_3$ / $LaNiO_3$ superlattices obtained with the HAXPES instrument at P09

Oxide heterostructures have lately aroused marked interest due to the unexpected new physics occurring at their interfaces. As a very recent example, theory has predicted that for a 1 unit-cell $LaAlO_3$ / 1 unit-cell $LaNiO_3$ (LAO/LNO) oxide heterostructure the substrate-imposed strain together with electron correlations induces a single-sheet cuprate-like Fermi surface within the LNO interface [1] with the prospect of high-temperature superconductivity. As a first step to characterize such an interface, HAXPES measurements at 7.6 keV photon energy on LAO/LNO superlattices with thicker layers [2] were performed to probe the chemical state of Ni near the buried interface. From the high energy electron spectra of the Ni 3p core level (Fig. 6) an interesting valency change from Ni^{3+} to Ni^{2+} can be inferred which might be due to electronic reconstruction.

Contact: Wolfgang Drube, wolfgang.drube@desy.de

References

1. P. Hansmann et al, Phys. Rev. Lett. 103, 016401 (2009)
2. Samples provided by H.-U. Habermeier, MPI-FKF Stuttgart, Germany

First commissioning activities at the Coherence Beamline P10

Sector 7 of PETRA III is home to the Coherence Beamline P10. During summer, the 5-m long U29 undulator and the double crystal monochromator (DCM) were installed at the beamline thus enabling P10 to become one of the first PETRA III beamlines to receive monochromatic X-rays. The first X-ray beam was successfully guided over the DCM and detected on a fluorescence screen on September 18.

To perform first X-ray beam commissioning activities we designed an optical table setup incorporating flight path and slits as well as an X-ray eye and ESRF type APD as detectors (Fig. 7). However, most of our activities were restricted to the optics hutch of P10 and to beam currents below 1 mA. While these are certainly not perfect conditions, they still allowed us to get a feeling of how to operate a beamline at PETRA III, to calibrate optical beamline components and to test the interaction of the various control and interlock systems.

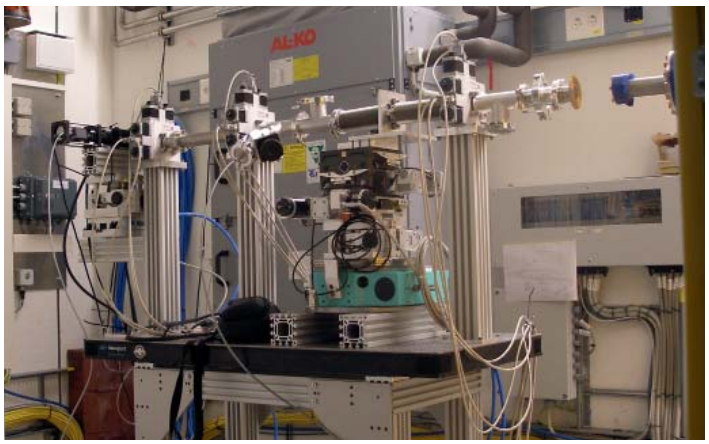

Figure 7

Beam commissioning setup in the optic hutch of P10

First, our work focused on the alignment and calibration of the monochromator. Second, the functionality and limits of the undulator were investigated. Only small corrections will be needed to reach the specified minimum gap settings.

In addition, our setup allowed us to follow the performance improvements of the PETRA III storage ring with the X-ray beam as probe. P10 is situated in a low beta section of the storage ring and we observed a much smaller beam size and the corresponding increase of the peak intensity after all damping wigglers were installed. We hope to see further improvements as more and more components like the beam position feedback system are getting online.

Finally, we passed a radiation safety survey which enables us to take monochromatic X-rays at ring currents of up to 50 mA in the optics hutch. This allows us to get more reliable monochromatic flux estimates and opens the opportunity to look at coherence properties of the photon beam.

Contact: Michael Sprung, michael.sprung@desy.de

European XFEL.

A year of foundations

The European X-ray Free-Electron Laser Facility, or European XFEL, will generate ultra-short X-ray flashes – 30 000 times per second and with a brilliance that is a billion times higher than that of the best conventional X-ray radiation sources available today. The facility will comprise a 1.7 km long superconducting electron accelerator delivering low emittance electron bunches at 17.5 GeV to three X-ray free-electron laser (FEL) undulators, which are up to 256 m long each. Two undulators for the hard X-ray regime and one for soft X-rays will operate in the self-amplified spontaneous emission (SASE) mode and produce FEL radiation that is guided through beam transport sections to several experiment stations. The six experiment stations of the initial configuration will enable a wide range of scientific applications and experimental techniques.

What will distinguish the European XFEL from other X-ray sources is the temporal resolution of its light pulses on a femtosecond scale, its highly coherent X-rays and high peak intensities, and the combination of these features. The superconducting linear accelerator will deliver up to 30 000 electron bunches per second, allowing great flexibility in beam distribution and the delivery of FEL pulse patterns. The average brightness of the European XFEL will be much greater compared to other X-ray FEL facilities and its flexible operating conditions will allow for quasi-parallel operation of several experiment stations and provide additional options for the stabilization of the electron and X-ray beam delivery.

European XFEL

Signing of the Convention

The European XFEL is an international project that governments of twelve nations are committed to fund: Denmark, France, Germany, Greece, Hungary, Italy, Poland, Russia, Slovakia, Spain, Sweden and Switzerland. China and the UK are also planning to participate.

The rules for this international collaboration are set out in an intergovernmental Convention and its bylaws. The Convention has been prepared in six language versions (English, French, German, Italian, Russian and Spanish), which were checked by translators at a conference held in Berlin on 21 to 23 September 2009. At the end of the conference, government representatives from each participating country initialled the Convention texts in the different languages, certifying that the versions are correct and in agreement with each other. The conference was organized jointly by the German Federal Ministry of Education and Research and the German Federal Foreign Office.

The "Convention concerning the Construction and Operation of a European X-ray Free-Electron Laser Facility" - as the official title of the convention reads - was signed in a festive event in the large banquet room of Hamburg's town hall on 30 November 2009. With their signatures, representatives from ten nations laid the foundations for the European XFEL under international law. For internal reasons, France and Spain had to postpone the signing to a later date.

Figure 1

The European XFEL will be located mainly in underground tunnels, which can be accessed on three different sites. The 3.4-kilometre-long facility will run from DESY in Hamburg (right) via Osdorfer Born (middle) to the town of Schenefeld in Schleswig-Holstein (left). The Schenefeld site will host the research campus on which international teams of scientists will carry out experiments with the X-ray flashes.

Foundation of the company

The legal body managing the European XFEL project was founded on 28 September 2009 and is listed in the commercial register of the Hamburg district court with number HRB 1111165. It is a company with limited liability under German law and the official name is "European X-ray Free-Electron Laser Facility GmbH", in short: "European XFEL GmbH". The shareholders of the company are research institutions, funding agencies and, in some cases, the countries themselves, usually represented through a research ministry. They are designated by the various governments. Until the Convention had been signed and in order to move ahead with the project, DESY founded the company alone in an initial step. A second batch of five shareholders joined at the occasion of the Convention signing while those countries that require further internal administrative steps following the signing of the Convention are expected to join the European XFEL GmbH early 2010.

Before the company is ready to conclude employment contracts, place orders and issue subcontracts for machine components, its staff and financial rules had to be confirmed by the shareholders' assembly – the European XFEL Council – in its session on 19 October 2009. In general, financial contributions of the partner countries to the company are expected after the accession of the corresponding shareholder. During the preparation phase of the project, a number of contracts, including those for the construction of the tunnels, have been concluded by DESY on behalf of the European XFEL. Now preparations are underway for the company to take over these contracts. A host agreement regulating the services some DESY groups provide to the European XFEL GmbH was prepared and comes into place now.

With the foundation of the European XFEL GmbH, two managing directors were appointed: Massimo Altarelli as the Chairman of the Management Board and Karl Witte as the Administrative Director. On 19 October 2009, the Council of the European XFEL GmbH confirmed the designation of three scientific directors, who are to complete the Management Board: Serguei Molodtsov (photon diagnostics, sample environment, soft X-ray scientific instruments, technical support), Andreas Schwarz (construction, undulators, detectors, data management) and Thomas Tschentscher (X-ray optics, optical lasers, hard X-ray scientific instruments). Through a very successful and ongoing recruitment campaign, 14 engineers and scientists from many different countries joined the project in 2009. The administrative staff had been also growing successfully.

Figure 2
The DESY campus, status June 2009. The civil construction site for the injector complex of the European XFEL is seen in the foreground.

In-kind contributions

The construction costs of the facility amount to just over 1 billion Euro (price levels of 2005). The host country, Germany (the federal government, Hamburg and Schleswig-Holstein), covers over half of these costs, while Russia contributes about one quarter and the other international partners between 1 and 3.5 percent each.

To a great extent, the European XFEL facility is also being realized through in-kind contributions by shareholders and partners. These contributions are of interest for the partner countries since they allow spending of funds for personnel and construction at home while at the same time participating in an international project. The interest of the European XFEL project in this far more complicated way of funding is the possibility to use experience and technical know-how of partner institutes that might not be accessible otherwise. Proposals for in-kind contributions are evaluated by an In-Kind Contribution Review Committee in terms of appropriateness, technical feasibility and associated cost. Following recommendation by this committee, a contract is prepared that defines the deliverables, milestones, timeline and value of the contribution. The contributing partner has to receive funding from their national funding agency to carry out the committed work. Upon successful delivery of the in-kind contribution, the agreed value is credited by the European XFEL GmbH as part of the respective country's contribution. The largest in-kind contribution to the project will be the linear accelerator and its infrastructure, coordinated by and with large contributions from DESY.

After many years during which DESY had been central in preparing the project, the European XFEL GmbH took over in 2009. Nevertheless, DESY will keep playing a special role that is defined in a collaboration agreement with the European XFEL company. DESY is the largest partner and will be the host laboratory of the project for the coming years. DESY's contributions in the accelerator area, which includes many of the project work packages which are led and performed by the accelerator division of DESY, are of essential importance to the European XFEL. DESY will lead and coordinate the European XFEL Accelerator Consortium that has been established to construct and commission the superconducting accelerator. This consortium also coordinates the integration of all in-kind contributions to the accelerator and the associated infrastructure by partner institutes from different countries. Specific contributions by DESY are also planned for the photon beam systems. The development and construction of two-dimensional detectors and gas detectors for single-shot X-ray intensity and beam position diagnostics are most notable at present; other contributions are expected to develop in the future.

Construction work

The civil construction for all underground buildings (shafts and tunnels) of the European XFEL officially started on 8 January 2009. Preceding work included the preparation of access roads and setting up the logistics for the construction site crews. Trees and surface vegetation on the three building sites (DESY-Bahrenfeld, Osdorfer Born and Schenefeld) were removed, buildings for the construction personnel were set up and fences for personnel safety were erected. Before major soil moving activities could commence, the entire area had to be checked for ammunition residues from World War II.

Work is now well underway to complete the shaft buildings on all three sites. The diaphragm walls stabilising the shafts have been constructed and the earth removal inside the shafts has reached groundwater level. Once the shafts are completed by pouring an underwater concrete plate, they will be prepared for the two tunnel boring machines that are currently under construction at the company Herrenknecht in Schwanau, Germany.

Figure 3
The large construction area south of the city of Schenefeld, viewed in southeastern direction towards DESY.

The start of the tunnel boring is scheduled for April 2010. In parallel to these activities, work has also started on the construction of the accelerator module test facility (AMTF) hall located on a former football field on the DESY site in close proximity to the HERA cryogenics hall. Starting in 2011, the hall will be used to test the technical properties of the more than 800 accelerating cavities produced by external companies and a total of 100 accelerator modules before they can be installed in the accelerator. On 21 July 2009, the German Federal Research Minister Professor Annette Schavan, Hamburg's Science Senator Dr. Herlind Gundelach and Schleswig-Holstein's Research Minister Dr. Jörn Biel met at DESY in Hamburg to lay the cornerstone for this test hall and sign an agreement for the participation in the European XFEL facility.

Public relation activities

The six-page flyer "Enlightening Science", which summarizes the essentials of the European XFEL at a glance, was published in August 2009. It is available in English and German from the European XFEL GmbH and at DESY-PR, and can be ordered by mail or downloaded from www.xfel.eu.
At the Schenefeld construction site, a public information point was established in October 2009. From a viewing platform, visitors can watch the construction work; a seminar room is available for presentations and posters are on display that inform about the project. The information point is among the many activities that aim at establishing a good relationship to the neighbours of the construction sites.

Workshops

The European XFEL is planned to be operated as a user facility, similar to facilities such as ESRF or PETRA III. To reach this goal, a close connection to the future user community is necessary. The project therefore aims at stimulating the exchange and discussion with the future users during regular users' meetings and workshops that focus on scientific and instrumental aspects of the planned experiment stations for the facility. The 3rd European XFEL Users' Meeting was held on 28-29 January 2009 and was attended by more than 250 people from 18 countries. Although the start of operations is still several years away, the long lead-times for development and procurement make it necessary to define the major requirements of the experiment stations early during construction of the facility. This task was continued during 2009 by organizing a further 4 workshops (as part of a series of six workshops) for the science and instrumentation of the European XFEL: the high energy density science workshop in Oxford (30 March-1 April), the spectroscopy and coherent scattering workshop in Villingen (2-4 June), the materials imaging and dynamics workshop in Grenoble (28-29 October) and the femtosecond X-ray experiments workshop in Budapest (9-11 December).
The results from these workshops will, together with the previously defined scope, provide important input to the development of a conceptual design for the FEL beam transport system, the photon diagnostics and the experiment stations. Experts from the user community shall be asked to participate in the review of the beamline and instruments design.

2009 was a year of important foundations for the European XFEL concerning both legal and construction aspects. Finally, the project is ready to start the construction of its accelerator and photon system components.

Contact: Massimo Altarelli, massimo.altarelli@xfel.eu
Karl Witte, karl.witte@xfel.eu

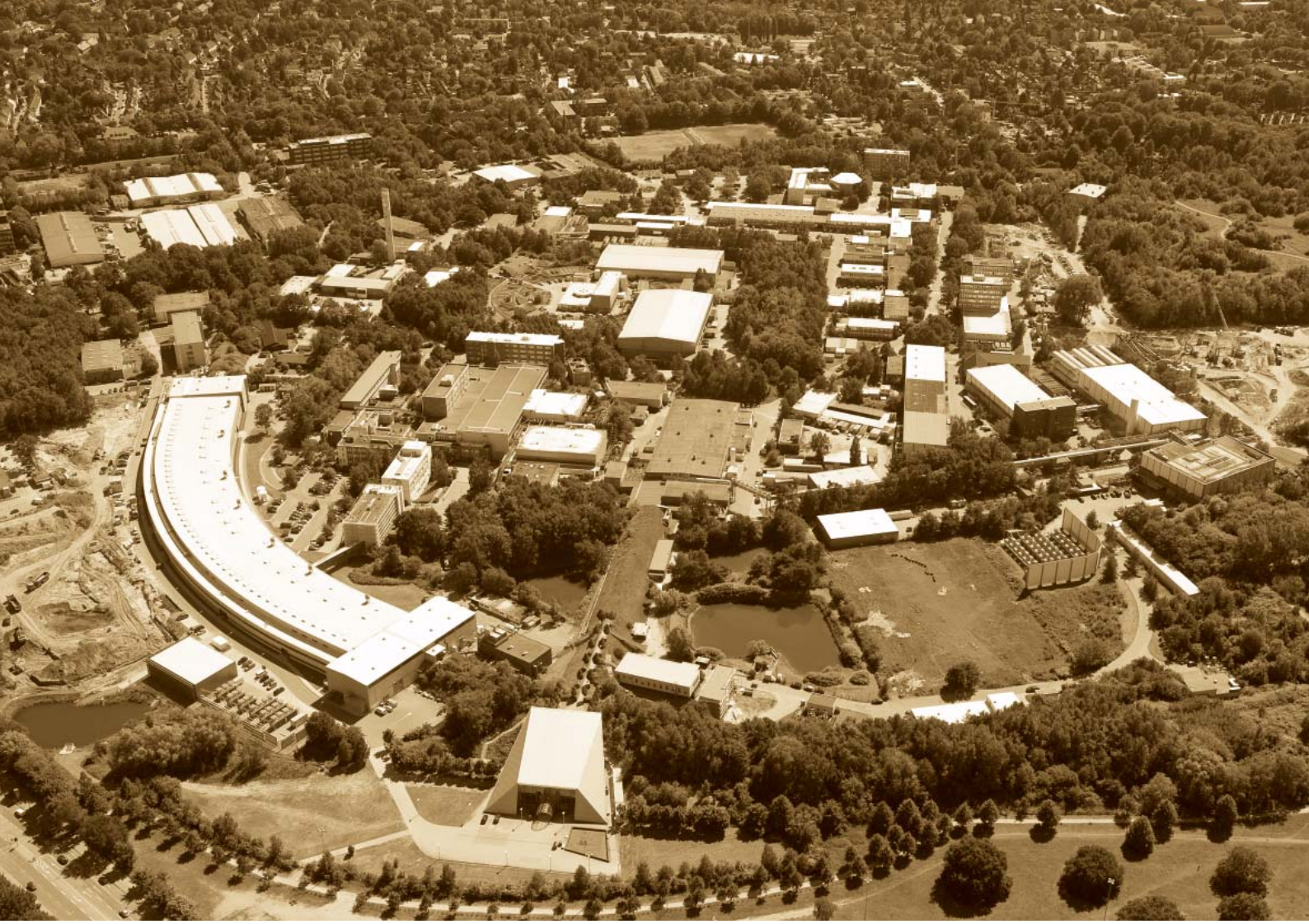

New Technologies and Developments.

Direct seeding at FLASH.

Photon diagnostics for sFLASH

Currently FLASH operates in the regime of self-amplified spontaneous emission (SASE) delivering gigawatt pulses with wavelengths between 6.5 nm and 40 nm in the femtosecond (fs) domain. Due to its start-up from noise, the radiation consists of a number of uncorrelated modes resulting in reduced longitudinal coherence and shot-to-shot fluctuations of the output pulse energy and arrival time. During the FLASH shutdown in 2009 a new acceleration module will be installed that allows to generate electron bunches with ten times larger pulse durations (~ 250 fs) compared to the short-pulse SASE configuration. The relaxed timing requirements of the new configuration give the option to externally seed FLASH with high-order harmonics generated in a gas target. This so-called sFLASH project has several benefits compared to the SASE operation. It makes it possible to achieve higher shot-to-shot stability with a pulse duration given by the weak nJ seed pulse of the order of 20 fs. The longitudinal coherence is expected to be greatly improved, i.e. the laser is phase-locked. The FEL output is naturally synchronized with the external seed laser, thus enabling precise pump-probe experiments [1].

A key tool of the sFLASH photon diagnostic end-station is an intensity monitor which is based on the detection of light scattered from a gold mesh at 45° with respect to the incoming FEL beam using micro-channel plate (MCP) detectors. The purpose of this device is to measure the gain curve of the seeded FEL, i.e. 6-7 orders of magnitude in photon flux from spontaneous emission to FEL saturation. Since the dynamic range of a single MCP is 3-4 orders of magnitude only, three MCPs are mounted at different geometries with respect to the incident photon beam. Two of the MCP detectors are placed on axis with the mesh in between to detect scattered light in forward and backward direction, respectively, while the direct FEL beam passes through a 9 mm hole in the centre. A third MCP is located at 90°. The different geometric acceptances and corresponding cross-sections increase the dynamic range of detection in order to meet the requirements.

The MCP-based detector has been cross-calibrated with the gas monitor detector (GMD) at BL1 of FLASH. The GMD measures the pulse energy of FLASH on a shot-to-shot basis [2]. The amplification curve of sFLASH was simulated attenuating the SASE beam from the µJ range down to the pJ range using the gas attenuator, metallic filters and by detuning SASE to have only spontaneous emission from the SASE undulator [3]. This situation is similar to the starting point of the commissioning phase of sFLASH. The MCP output signals were recorded for different detector settings and attenuation of the FEL. The obtained data has been calibrated to the simultaneously measured GMD output. The resulting calibration curve covers 6-7 orders of magnitude in photon flux as shown in Fig. 1.

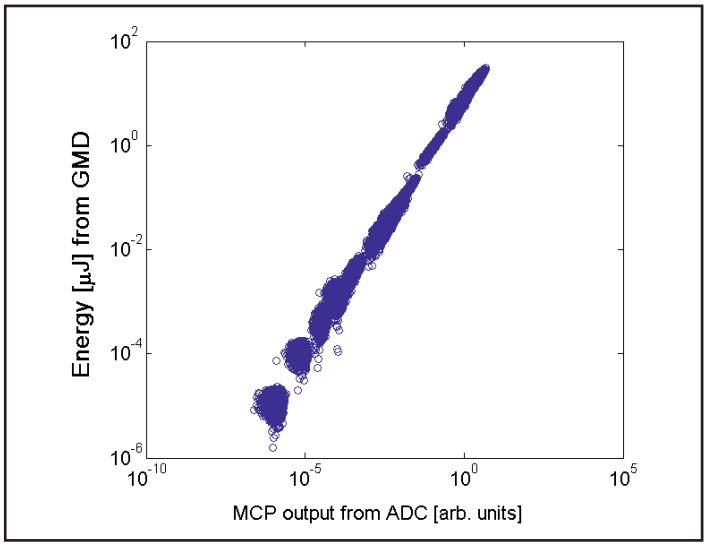

Figure 1

Pulse energy derived from the gas monitor detector (GMD) plotted versus the MCP output for different detector settings. The plot shows that the sFLASH intensity monitor covers 6-7 orders of magnitude in photon flux.

In addition the sFLASH photon diagnostic setup is equipped with apertures to reduce stray light from the undulator, fluorescence screens to image the seeded FEL and a grazing incidence XUV-spectrometer to measure single-shot spectra at high resolution of $\lambda/\Delta\lambda \sim 1000$. The spectrometer will allow matching the undulator gap with the HHG-seed wavelength, a prerequisite for the successful seeding experiment.

Collaboration: DESY, University of Hamburg, Helmholtz-Zentrum Berlin, PSI
Contact: Francesca Curbis (Uni Hamburg), francesca.curbis@desy.de,
Tim Laarmann (DESY-HASYLAB), tim.laarmann@desy.de

References

1. A. Azima et al., "Experimental Layout of 30 nm High Harmonic Laser Seeding at FLASH", Proceedings of 11th European Particle Accelerator Conference (EPAC'08) in Genoa, Italy, June 23–27, 2008.
2. K. Tiedtke et al., "Gas detectors for X-ray lasers", J. Appl. Phys. 103, 094511 (2008).
3. K. Tiedtke et al., "The soft X-ray free-electron laser FLASH at DESY: beamlines, diagnostics and end-stations", New J. Phys. 11, 023029 (2009).

A high average-power laser amplifier for FEL seeding.

High repetition rate few-cycle pulse amplification

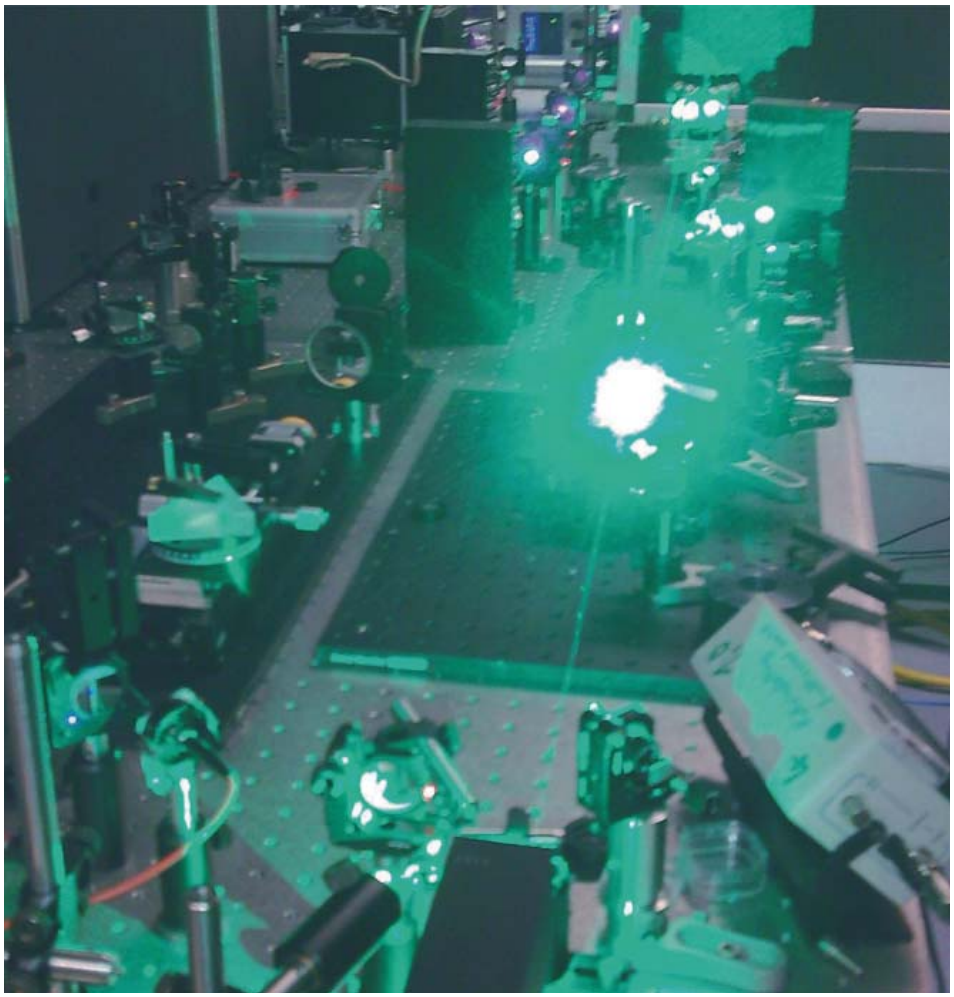

Figure 1
First stage of the ultrashort-pulse optical parametric chirped pulse amplifier (OPCPA).

A planned extension of the FLASH facility (FLASH II), which was outstandingly evaluated, will be based on laser-driven high-harmonic seeding. To fulfil this task, ultra-short laser pulses (< 10 fs) with high single pulse energy (> 1 mJ) at the repetition rate of the electron bunches (1 MHz in a burst mode with a duty cycle of ~1%), are required. A laser amplifier with such pulse parameters at a reduced burst repetition rate of 100 kHz is currently under development. Parts of the optical parametric chirped pulse amplifier (OPCPA)-pump were tested in December 2008 yielding 4 mJ of single pulse energy. The optical pump amplifier seeding scheme, a stretcher and adaptive compressor which supports the bandwidth for pulses of such short duration were recently successfully tested in combination with a single OPCPA stage (see Fig.1). The next step is to amplify the pump pulses further to 20 mJ and beyond, which is required for pumping the last OPCPA stage.

Contact: Franz Tavella, franz.tavella@desy.de

Authors:
F. Tavella, A. Willner, S. Düsterer, T. Tschentscher, H. Schlarb, J. Rossbach

Online photoionization spectrometer (OPS).

Measuring photons while you use them!

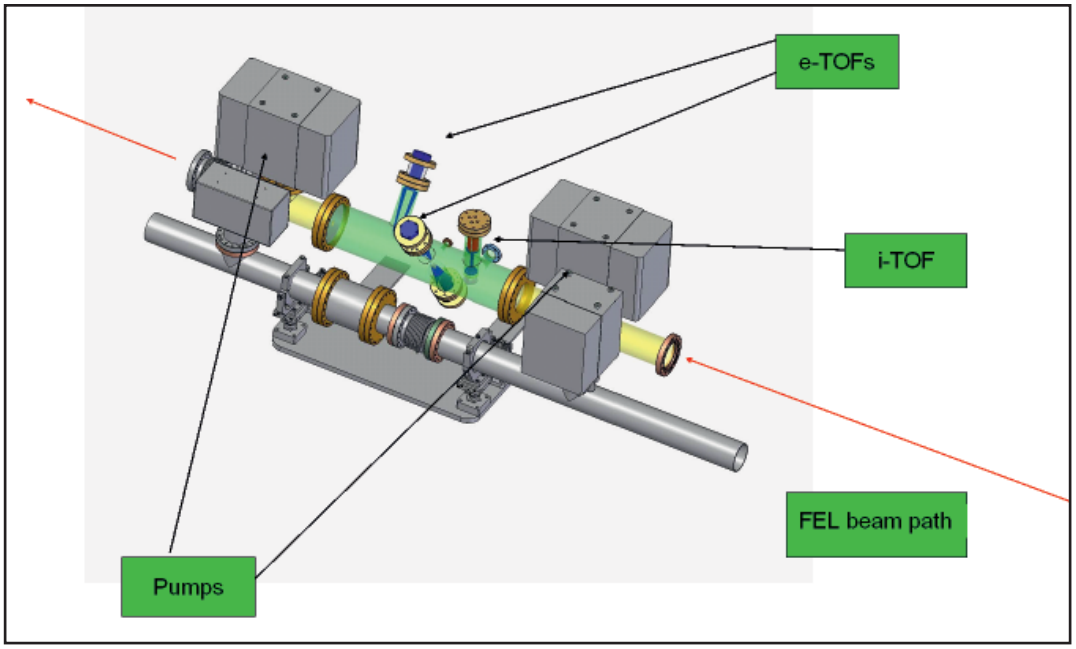

Figure 1
The future OPS chamber to be installed in the tunnel.

The need for a method to measure the photon wavelength and photon bunch properties of a Self-Amplifying Spontaneous Emission (SASE) free-electron laser (FEL) while not degrading the photon beam is obvious. The users need to know what the properties of the light they are using are, and the operators need to know if the photons they are delivering are the ones their models predicted, all while also taking experimental data. Therefore, the photon diagnostic group at the free-electron laser in Hamburg (FLASH) has developed the Online Photoionization Spectrometer (OPS), a powerful new tool that uses noble gases and ion and electron time-of-flight (TOF) spectroscopy to meet the needs of the users and operators. The electron time of flight spectrometers measure the kinetic energy of electrons kicked out by photons from the shells of noble gases with known electron binding energies, allowing calculating the wavelength of the incoming photons and seeing if there are any higher order modes or shifts in the beam. The ion TOFs look at the ratio between doubly and singly charged photoions of the gas and evaluate the photon wavelength by comparing them to the ratios taken from literature. Both of these methods allow the vast majority of the photons to go through to the experiment, as the gas density used for these measurements is low, from about 10^{-7} to 10^{-6} mbar. The transmission of the gas should be higher than 99 % at these pressures.

Since the project's proposal and start in 2008, the concept for the OPS has been tested at the DORIS III BW3 beamline [1]. The chamber, newly designed to fit into the FLASH tunnel, will be installed in late 2009 and early 2010, during the FLASH shutdown and upgrade period, and be tested and functional by mid 2010. Further improvements have been designed into the chamber thanks to the results of other tests. One of the major developments is that the chamber will be built out of mu-metal, a steel alloy designed to be non-permeable to magnetic fields. This kind of chamber will greatly reduce the effect these fields have on the sensitivity of our electron TOFs, giving the users and operators more reliable and precise results about the photon bunch properties of the FEL. The ion TOF has been made more robust and larger for a better fit in the tunnel and for higher precision. Figure 1 shows the layout of the OPS chamber in the tunnel.

Contact: Pavle Juranic, pavle.juranic@desy.de
Kai Tiedtke, kai.tiedtke@desy.de

Reference:

P. Juranic et al., "Using I-TOF spectrometry to measure photon energies at FELs", J. Instrumentation, 4, P09011 (2009).

Comparative measurements of FLASH beamline foci.

Different methods in competition!

A compact and self-supporting Hartmann-type wavefront sensor has been used at FLASH for characterizing the FEL beam quality and fine-adjustment of beamline optics. The system is compact enough for operation behind user experiments. It utilizes a rectangular array of pinholes which divides the beam into sub-rays, illuminating a phosphor coated CCD chip. Single-pulse wavefronts are reconstructed from the centroid deviations relative to a reference spot pattern. All relevant beam parameters such as beam waist and size, Rayleigh length, divergence and M^2 are evaluated from the second spatial and angular moments deduced from wavefront and beam profile.

At the FLASH beamline BL2, the measured focal spot sizes and positions have been directly compared to standard beam characterization techniques based on caustic measurements along the beam waist of the BL2 focus. The caustic was determined either using a phosphor screen and camera or by imprinting the FEL focus onto PMMA samples.

In a first evaluation of the measured results, the waist position of the BL2 focus as determined by the Hartmann sensor differs by a few percent from the direct caustic techniques. The focus diameter appears to be somewhat overestimated by the Hartmann sensor while the PMMA imprints appear to underestimate the focus. As opposed to the caustic measurements, the Hartmann sensor provides wavefronts and intensity profiles of single shots. Improved alignment of the ellipsoidal mirror at BL2 resulted in a reduction of the wavefront rms roughness by more than a factor of three from 9.2 nm to 2.6 nm.

Collaboration: DESY, Laser-Laboratorium Göttingen (LLG)
Contact: Elke Plönjes (DESY-HASYLAB), elke.ploenjes@desy.de
Kai Tiedtke (DESY-HASYLAB), kai.tiedtke@desy.de
Klaus Mann (LLG), klaus.mann@llg-ev.de
Bernhard Flöter (LLG), bernhard.floeter@llg-ev.de

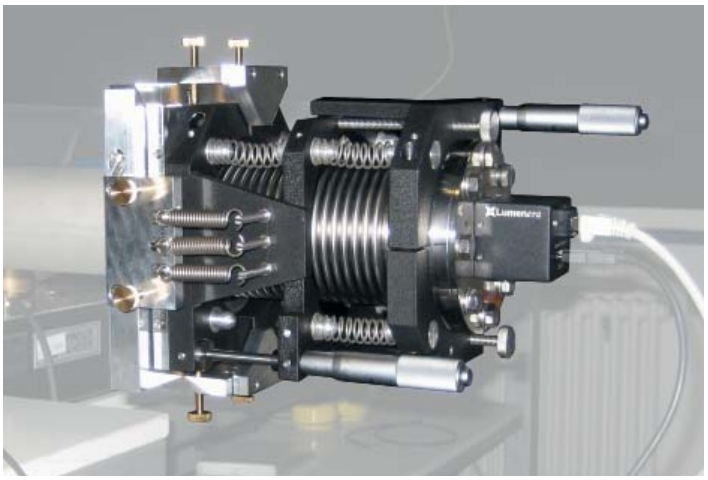

Figure 1
XUV Hartmann sensor of LLG.

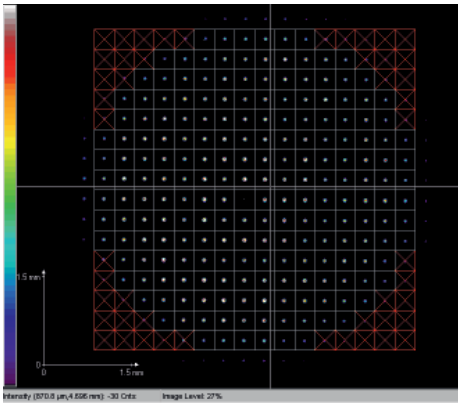

Figure 2
Spot pattern recorded at FLASH BL2.

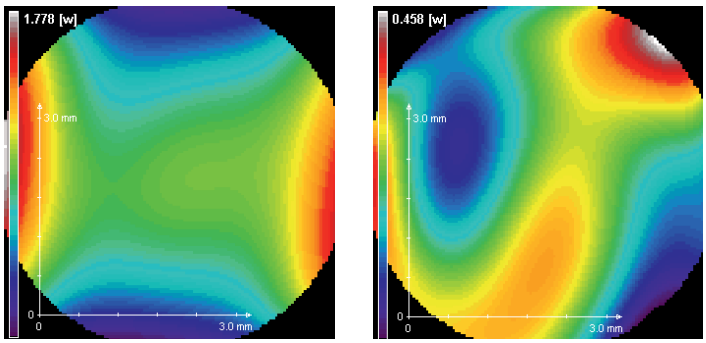

Figure 3
Wavefront aberrations corresponding to the spot pattern before (left) and after mirror alignment (right). The peak-to-valley aberration of the wavefront in terms of λ (26 nm) is indicated.

The compound refractive lens changer for PETRA III.

Versatile on-axis optics for broad energy range synchrotron beamlines

Compound Refractive Lenses (CRL) are excellent on-axis focusing optics. At third generation sources, they are used for micro- and nanofocusing of X-ray beams [1,2]. Their focal length f depends on the radius of curvature R of the lenses and the product of the real part of the refractive index δ and the number of lenses N, f ~ R/(Nδ). Thus, CRLs are strongly chromatic optics with their focal length depending on the energy E of the incident X-ray beam, as δ ~ 1/E². This means to change the focal length and to adapt f to a specific energy E, either R or N has to be changed. However, typical third generation synchrotron beamlines, such as the Micro- and Nanofocusing X-ray scattering beamline MiNaXS (P03) of PETRA III [3], deliver a broad monochromatic energy band, e.g. 8 ≤ E ≤ 23 keV in the case of MiNaXS. The beamline is sketched in Figure 1. Here, two sets of Beryllium CRL are used to focus the X-ray beam delivered by an undulator down to a beam size of 40x20 µm² or 17x10 µm². This allows for adapting the divergence of the focused beam and enabling tuning the resolution of the beamline [4]. However, to achieve this flexibility, the focus position must be kept constant at the sample position for the whole energy range and for all micro-focus beam sizes to ensure stability and reduced alignment times. This in turn leads to a setup, where the number of lenses (with their radius of curvature being constant R=197 µm in the case of MiNaXS) and their position relative to the sample need to be adapted, as the total distance source (undulator) to sample is constant. Therefore, versatile on-axis optics for synchrotron beamlines with broad energy ranges have been developed.

In order to adjust the lenses parallel to the beam, four degrees of freedom, i.e. two rotation- and two translation axes, are necessary. To do so, a parallel kinematics robot (Hexapod) is installed. The Hexapod combines all these movements. It is mounted on a linear stage, ensuring a desired travel range of ±500 mm along the beam around the nominal lens set position. The Hexapod offers the possibility to choose a user defined rotation point. This simplifies the adjustment of the lens system extremely. Figure 2 shows the vacuum setup of the lens system with the installed lens changer. All components are installed in vacuum and mounted on a granite girder to minimize vibrations of the sensitive setup. Additionally the vacuum chamber is decoupled from the CRL-setup with membrane bellows.

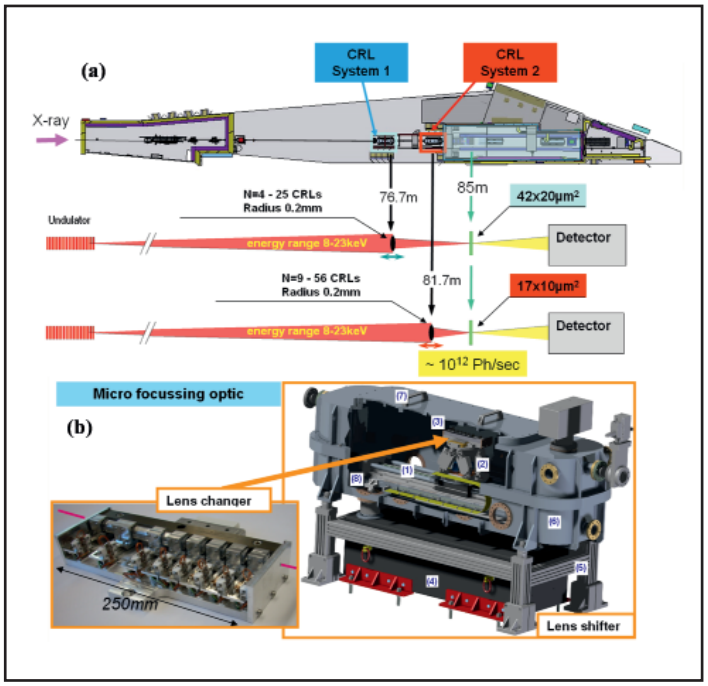

Figure 1

(a) Beamline Layout of the MiNaXS Beamline and the focusing conditions with the two lens systems. Sample position is in a distance of 85 m seen from source. The focal spot for both configurations is on the sample.

(b) Illustration of the lens shifter and changer setup at the Micro and Nanofocus X-ray scattering beamline MiNaXS (P03) at PETRA III. On the left is a photo of the lens changer which is installed in the vacuum chamber. The right illustration shows the lens shifter vacuum setup: (1) 1000 mm translation stage, (2) M-824 Hexapod, (3) CRL-system with up to 63 movable lenses, (4) granite girder, (5) support frame, (6) vacuum chamber, (7) maintenance flange, (8) column of kinematic mount system.

Table 1 summarizes the specifications for the linear stage (left) and the Hexapod (right).

Travel range ± 500 mm	Travel range 45 mm linear, 25° rotation
Load capacity 500 N	Load Capacity 100 N
Stepper motor driven	Servomotor driven
Repeat accuracy <±10 µm	Repeat accuracy ±0.5 µm
Vacuum suitable <1x10^{-6} mbar	Vacuum suitable <1x10^{-6} mbar

The inset in Figure 1b shows the lens changer with 6 stacks of lenses and 2 movable pinhole slits. Up to 63 CRL can be installed in this changer. In order to cover the full energy range of the beamline any number of lenses between 1 and 63 is needed. To achieve this, the lenses are arranged in stacks in binary configuration (1, 2, 4, 8, 16, and 32). Each stack can be individually moved in and out of the X-ray beam by piezo-motors with an accuracy of <5 µm.

The dimension of the changer is only ca. 250x150x50 mm^3. This small dimension enables us to install the complete system on the long translation stage to keep the focal spot for the whole energy range (of roughly 20 keV) at nearly the same size and at the same position.

To summarize, we designed and tested an on-axis CRL device which is now installed at MiNaXS. Moreover, the on-axis CRL device offers the possibility to mount lenses with different radii of curvature. This allows for adapting both N and R for the desired focal length. The on-axis CRL device will also be installed at other experimental stations, such as the imaging beamline P06 of PETRA III.

Contact: Ralph Döhrmann, ralph.doehrmann@desy.de

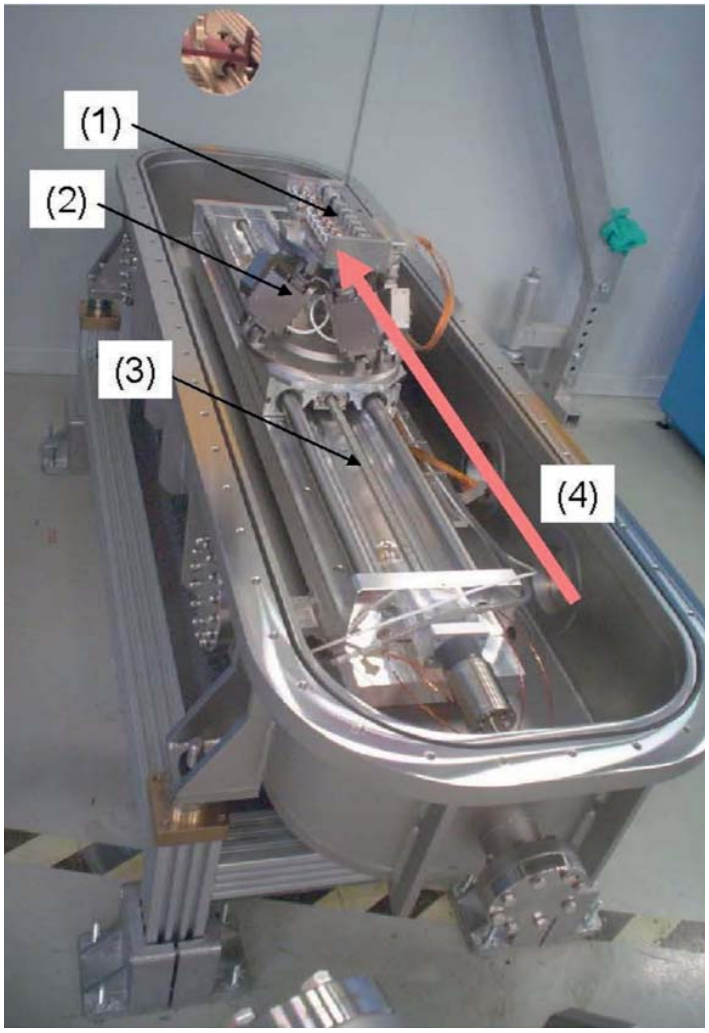

Figure 2

Photo of a lens shifter setup in the vacuum vessel in its final position at the MiNaXS Beamline. Distance of this system to the source is 81.7 m. (1) lens changer, (2) 6-axis kinematic mount, (3) linear translation, (4) X-ray beam.

Authors

R. Döhrmann, S. Botta, G. Falkenberg, T. Schubert, S.V. Roth

References

1 S. V. Roth, M. Kuhlmann, H. Walter, A. Snigirev, I. Snigireva, B. Lengeler, C. Schroer, M. Burghammer, C. Riekel and P. Müller-Buschbaum: "Colloidal silver nanoparticle gradient layer prepared by drying between two walls of different wettability", J. Phys.: Condens. Matter 21, 264012 (2009).

2. B. Lengeler, C. G. Schroer, M. Kuhlmann, B. Benner, T. F. Günzler, O. Kurapova, F. Zontone, A. Snigirev and I. Snigireva: "Refractive X-ray lenses", J. Phys. D: Appl. Phys. 38, A218 (2005).

3. S.V. Roth, R. Döhrmann, R. Gehrke, H. Schulte-Schrepping, U. Hahn, H. Franz, R. Röhlsberger, M. Lohmann, H. Graafsma, E. Weckert: "Status and development of the µSAXS/WAXS-Beamline for PETRA III", HASYLAB Annual Report 2007, pp.175 (2007).

4. S.V. Roth, R. Döhrmann, M. Dommach, M. Kuhlmann, I. Kröger, R. Gehrke, H. Walter, C. Schroer, B. Lengeler, P. Müller-Buschbaum, "Small-angle options of the upgraded ultrasmall-angle X-ray scattering beamline BW4 at HASYLAB", Rev. Sci. Instrum. 77, 085106 (2006).

Thermal-gradient monochromator for high energy X-rays.

More flux on the sample

For high energy X-rays (E > 60 keV) the rocking curve of a perfect silicon crystal used as Laue monochromator is Lorentzian shaped with a width of less than 1 arcsec and a reflectivity of 50 % or less. Most of the experiments at the high energy X-ray station BW5 at DORIS III need flux but only a moderate angular resolution of about 20-40 arcsec, i.e. 0.5-1 % energy bandwidth out of the white beam. If a crystal with bent lattice planes in the direction of the beam is used as monochromator, the scattering width of the rocking curve, which is proportional to the bandwidth, is given by the bending radius (Fig.1) and the reflectivity is up to 100 %.

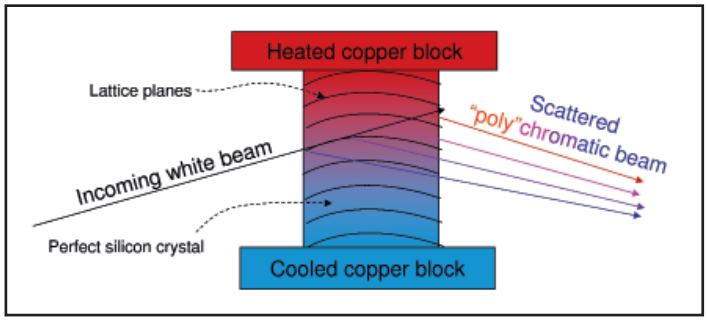

Figure 1

Schematic drawing of the monochromator. The lattice planes of the silicon crystal are bent in order to relax the crystal. For the incoming white beam the Bragg angle is continually changing while travelling through the crystal. The scattered beam has now an energy dispersion across its angular profile.

Therefore, a flux gain of up to a factor of 100 is achievable. An easy and very controlled way to bend the lattice planes of a crystal is to heat one side of the crystal and to cool the other side (Figs. 1,2). The resulting mismatch of lattice constants over the crystal width will bend the lattice planes to relax the crystal. The reflectivity increases, because the extinction of the scattered beam decreases with bending. But if the bending is large, the scattering is less efficient, so that the reflectivity decreases again (Fig. 3) [1-4]. Opposite to a perfect crystal, the choice of the reflection has less impact on the flux, since the scattered intensity is only proportional to $\cot(\theta_B)$, where θ_B is the Bragg angle. Therefore, a higher order reflection can be used for stronger suppression of higher harmonics. Si(111) and Si(311) crystals in the size of 0.5 cm x 1 cm x 1cm are available as monochromator crystals. Experiments have shown that the behaviour of the monochromator is perfectly predictable according to the theory.

Contact: Uta Rütt, uta.ruett@desy.de

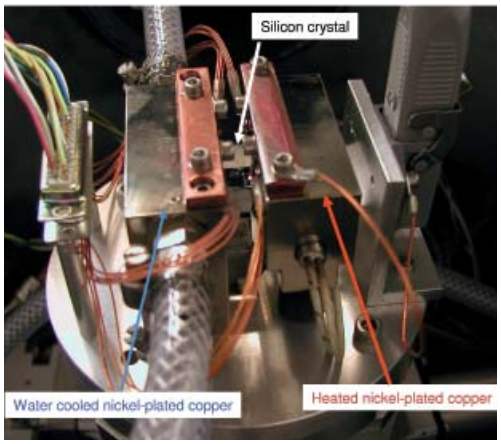

Figure 2

Setup of the monochromator that allows one to generate a temperature gradient across the crystal.

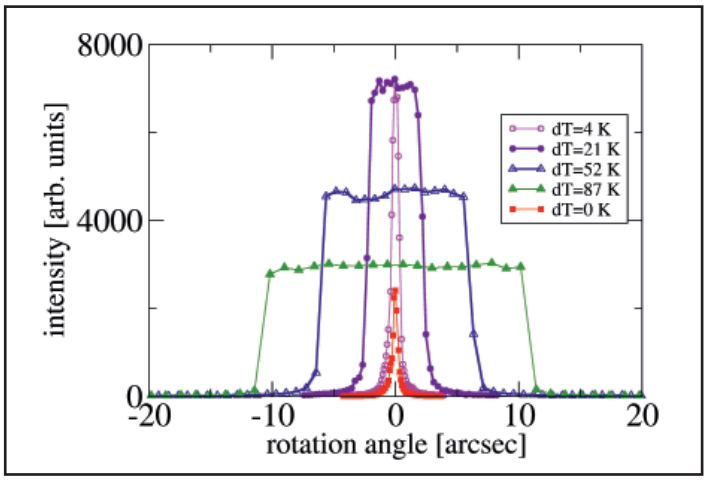

Figure 3

Rocking curves of the Si(311) reflection for different temperature gradients across the crystal.

References

1. S. Keitel, C. Malgrange, T. Niemöller and J.R. Schneider. "Diffraction of 100 to 200 keV X-rays from an Si1-xGex gradient crystal: comparison with results from dynamical theory." Acta Cryst. (1999). A55, 855-863.
2. R. Smither, K. Abu Saleem, M. Beno, C. Kurtz, A. Khounsary and N. Abrosimov, "Diffraction efficiency and diffraction bandwidth of thermal-gradient and composition-gradient crystals", Rev. Sci. Instr. 76, 123107 (2005).
3. R. K. Smither, K.A. Saleem, D.E. Roa, M.A. Beno, P. von Ballmoos and G. K. Skinner, "High diffraction efficiency, broadband, diffraction crystals for use in crystal diffraction lenses" Exp. Astron. 20, 201 (2005).
4. F. Balibar, F.N. Chukhovskii and C. Malgrange, "Dynamical X-ray propagation – A theoretical approach to the creation of new wavefields", Acta Cryst. A39, 387 (1983).

Silicon drift diode detectors for X-ray spectroscopy.

New compact energy dispersive X-ray detectors

DESY's Silicon Drift Diode (SDD) detector module development project ended in the year 2009 with the delivery of 4 complete detector modules including a data acquisition system and power supply unit (Fig. 1). The complete systems are now available for user experiments at DESY beamlines. The project had the aim to design and build a detector system for methods like fluorescence yield X-ray absorption fine structure (fl-XAFS) spectroscopy.

Energy-dispersive semiconductor detectors find widespread applications, e.g., in the registration of fl-XAFS spectra. Fluorescence detection of XAFS spectra is an indirect way to measure the changes of the absorption coefficient (μd) as a function of the energy of the incoming monochromatic X-ray beam. It is indispensable for the registration of XAFS spectra from diluted samples and from samples which are too thick for standard transmission experiments. Today most often high purity Ge and Si(Li) pn-diode detectors are used for this task.

SDDs are known to be fast energy dispersive detectors which can yield very good energy resolution near to the Fano limit in set-ups optimised for this purpose. According to the demands of fl-XAFS spectroscopy applications the new detector systems are optimised to give reasonably good energy resolution (200 - 400 eV FWHM of Mn Kα) at high count rates of up to several 100 kHz per cell [1]. The readout integrated circuit (ROIC) for our detector module was designed by DESY/FEC group [2].

Figure 1
SDD detector module and combined data acquisition and power supply unit.

Different from HPGe or Si(Li) detectors the SDD modules achieve good spectral resolution without cryogenic cooling. This was a prerequisite for the construction of compact detector modules usable in sample environments with space restrictions. The present modules have a length and wrench size of 21.2 cm and 1.6 cm, respectively. Contrary to detectors containing cryogenic liquids the new modules can be used in any geometry for instance looking on the sample from the top.

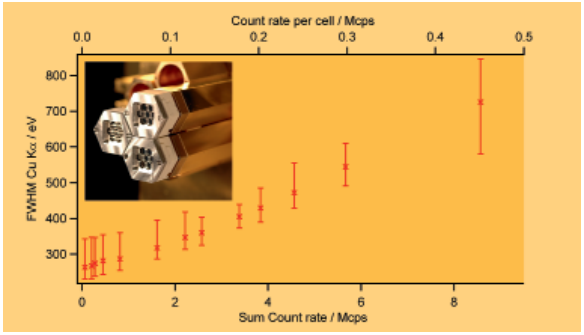

Figure 2
Spectral resolution of the best 3 (sum count rates of 19 cells) modules, measured as FWHM of the Cu Kα emission line.

Each cell of the monolithic 7 cell SDD chip with integrated JFET has an active area of 7 mm². The substrate has a thickness of 450 μm. The chips were manufactured by PN-sensors, Munich, Germany. The SDD detector system is consisting of the actual detector module and a compact PXI based data acquisition and power supply unit. The sensor head of the SDD module is made of AlN ceramics parts to avoid artefacts in the fluorescence spectra due to X-ray fluorescence from detector components. The choice of these materials and the substrate thickness of 450 μm determine the main working range to be 2-17 keV. The ROIC is mounted directly behind the SDD only separated by a layered (Al/Ti/Ta) radiation protection shield and connected via short bond wires.

Important for a good peak/background ratio is a Zr mask which covers the cell's borders. This averts charge splitting events caused by the absorption of photons in the border region between neighbouring cells. For low count-rates (10 kcps), the average Cu-Kα line width was found to be (271 ± 46) eV at a chip temperature of 10° C. The best performance achieved was (223 ± 7) eV at 10° C and (294 ± 10) eV at 24° C. At high integrated count rates, the linewidth measured at room temperature increased to 400 eV @ 0.2 Mcps and 550 eV @ 0.3 Mcps per cell, respectively (Fig 2). The linearity of the energy scale is better than 1 % over most of the working range [3]. The short dead time, compared to the HPGe and Si(Li) detector systems, allows the registration of fl-EXAFS spectra at high count rates without significant detector dead time induced damping of the EXAFS oscillations [4].

Contact: Edmund Welter, edmund.welter@desy.de

References

1. K. Hansen, C. Reckleben, I. Diehl, H. Klär, "A compact 7-cell Si-drift detector module for high-count rate X-ray spectroscopy", NIM A 589, 250–258 (2008).
2. I. Diehl, K. Hansen, C. Reckleben, "A Mixed-Signal Readout Chip for a 7-Cell Si-Drift Detector in 0.35um BiCMOS Technology", Proc. of ESSCIRC, 296-299 (2007).
3. Hansen, K., C. Reckleben, I. Diehl, H. Klär, E. Welter "Fast X-ray Spectroscopy using Si-drift Detectors", IEEE Trans. Nucl. Sci. 56, 1666-1670 (2009)
4. E. Welter, K. Hansen, C. Reckleben and I. Diehl „A fast energy-dispersive multi-element detector for X-ray absorption spectroscopy" J. Synchr. Rad. 16, 293-298 (2009)

Large offset monochromator for the MiNaXS beamline at PETRA III

Separating the beams

The canted undulator photon beamlines P02 and P03 (sector 2) at PETRA III are separated by 5 mrad in the horizontal plane. To provide enough space for the experiments the beam paths are separated in the vertical plane. The Large Offset Monochromator (LOM500) at beamline P03 displaces the beam downwards by 0.49 m. The monochromatic beam passes through the experimental station of P02. The system is designed for an energy range of 8-25 keV and a beam position stability of 1µm at the experimental station. Due to the high power density at the first crystal, a liquid nitrogen cooling system for both crystals is mandatory.

This Large Offset Monochromator will be equipped with a silicon crystal (Si 111) pair and a multilayer pair. The first of the two multilayers is placed in a separate vacuum chamber, 6 m in front of the main vessel. The first of the two silicon crystals is placed in the smaller, round chamber of the main vessel. The long

Figure 1
The LOM-500 system installed in the P03 optics hutch.

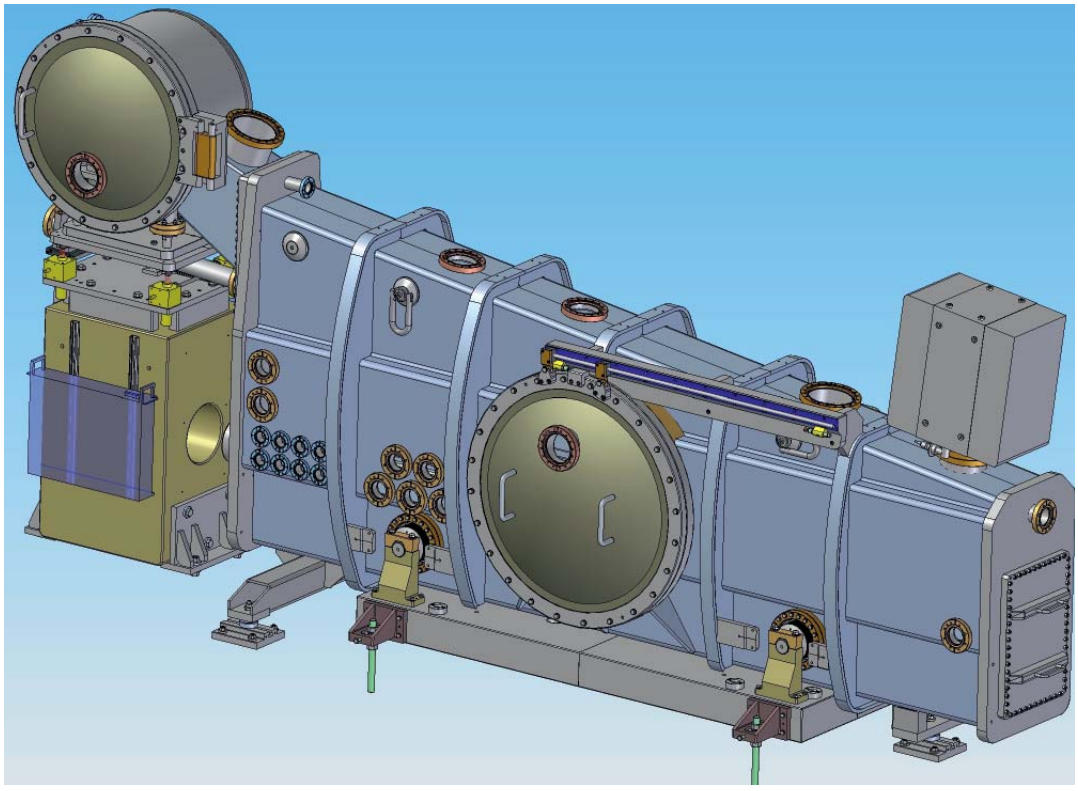

Figure 2
3D model of the Large Offset Monochromator (LOM500) at beamline P03. The white photon beam enters the LOM500 from the left at a beam height of 1.40 m and the monochromatic beam exits the system at a beam height of 0.91 m above the experimental floor.

Figure 3
The Large Offset Monochromator vessel at the manufacturers site.

chamber on the right side contains a precision linear rail to maintain the fixed exit photon beam condition. It has a travel range of approximately 2.5 m with a height error smaller than +/- 20 µm and angular deviations smaller than +/- 55 µrad (pitch and yaw). All degrees of freedom of the crystal systems in the main vessel are controlled by stepper motors. The positions of all translations and goniometers are controlled by high resolution optical encoders. A multi-axis piezo driven table is placed below the second crystal and multilayer system to compensate deviations in height and angle while moving the system along the rail. The assembling of the system started in early November 2009.

Contact: Jan Horbach (DESY-FS Beamline Technology), jan.horbach@desy.de

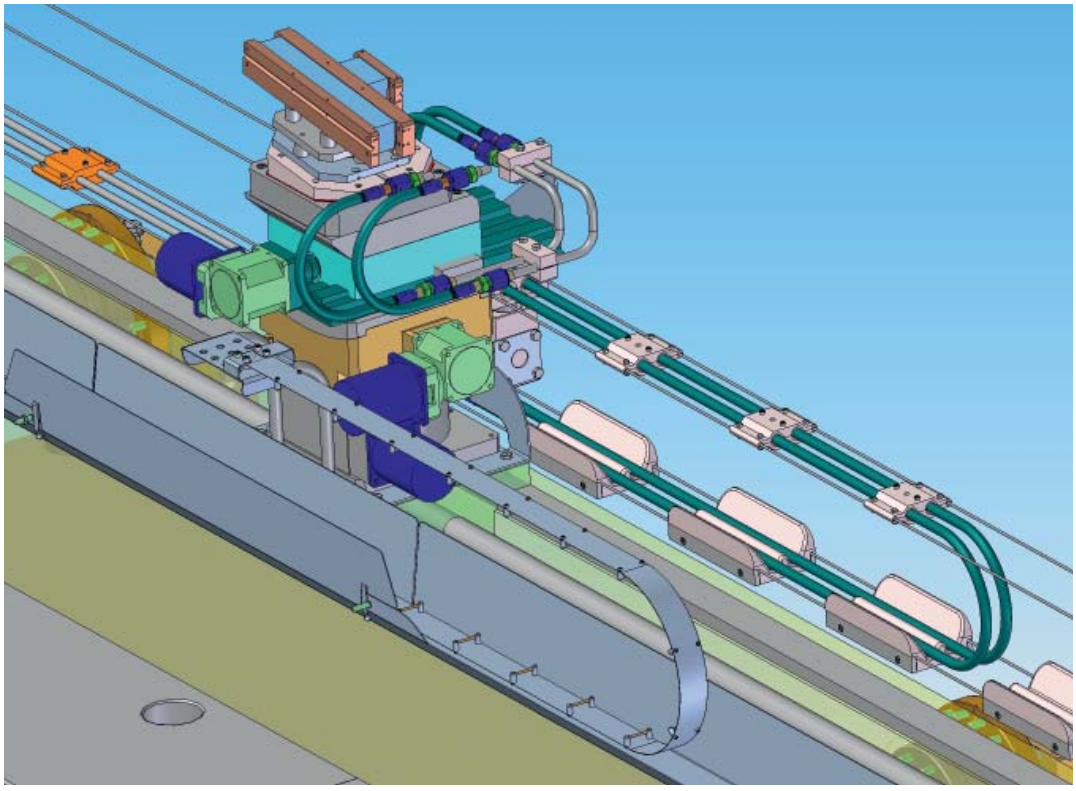

Figure 4
Crystal optics (Si 111 crystal and multilayer) mounted on the translation stage. The cable guide (flexible metal sheet) for electric cabling is located on the left side of the axis, the wire rope guide for the flexible liquid nitrogen pipes on the right side.

Fast bunch train shutter for FLASH.

Selected light

A new rotating fast bunch train shutter to select single photon bunch trains of the free-electron laser FLASH has been developed. FLASH is based on superconducting linear accelerator technology and provides electron bunch trains with a repetition rate between 5 and 10 Hz, the FEL process generates photon bunch trains with the same time structure. This repetition rate allows the use of mechanical shutters to select single bunch trains for experiments. The shutter currently installed at FLASH is based on the wire scanner design [1] moving a carbon blade in and out of the beam path. The continuous operation of this shutter wears out the vacuum bellow inside the system.

Therefore, a different design has been adopted which does not depend on a direct mechanical coupling of the shutter blade. The shutter consists of a slotted glassy carbon disk with a thickness of 1 mm. The disk contains 6 equidistant slits, each providing a beam aperture of 20 mm. The disk rotation in vacuum is generated by a special magnetic rotary feed through combined with a DC-motor outside of the vacuum system. The feed through couples the rotation of the motor to the disk inside the vacuum without using bellows, mechanical- or fluidic-couplings.

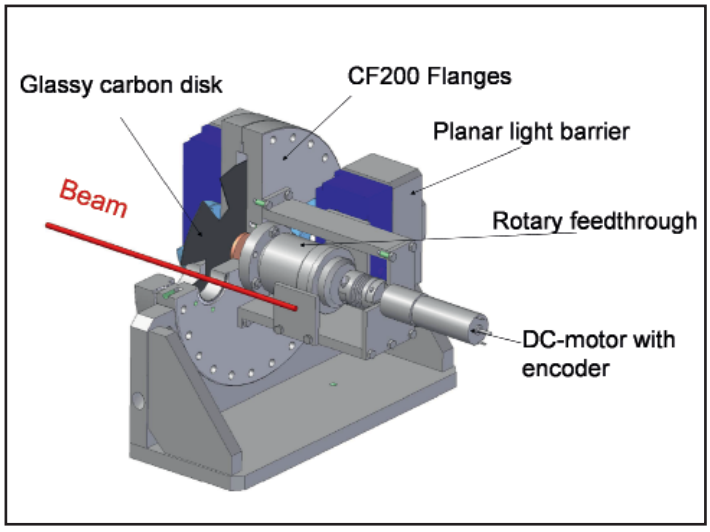

Figure 1

Design of the bunch train shutter. The vessel is made out of CF200 flanges. The slotted disk is driven by a DC servo motor outside of the vacuum. A magnetic rotary feed through couples the rotation of the motor into the vacuum vessel. A planar light barrier is used to reference and monitor the position of the disk.

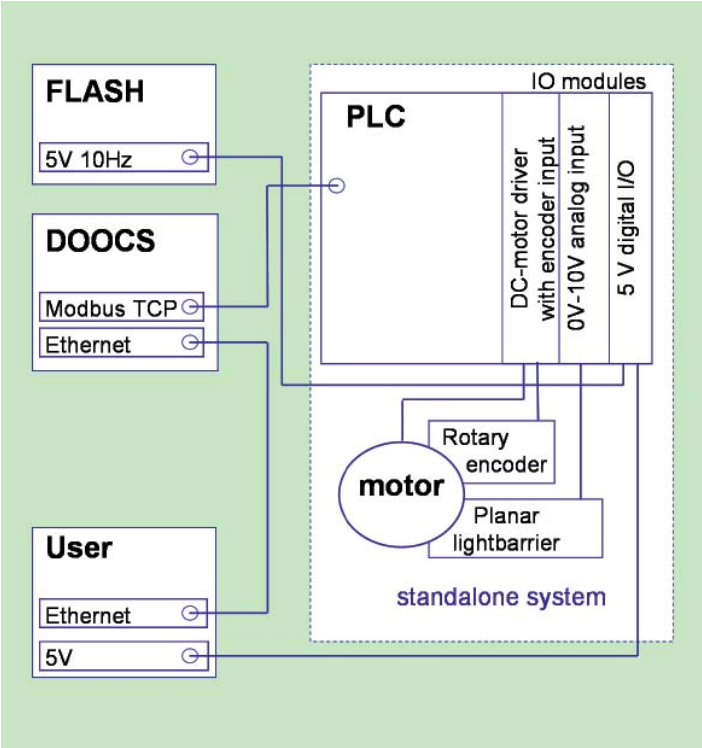

Figure 2

Control system chart of the shutter system showing the interaction between the FLASH timing, the standalone shutter system PLC, DOOCS and the user control interface.

The shutter can be opened and closed by digital signals. The user commands are routed by the FLASH-control system DOOCS via Ethernet to the PLC. The status of the shutter is transferred from the PLC via Modbus-TCP to the control system. A control panel is available in LabVIEW VI (Windows) and in JDDD javaWS (platform independent). The operation modes of the shutter are: “disabled” (open shutter), “single bunch train”, “reduced bunch train frequency” and “closed shutter”.

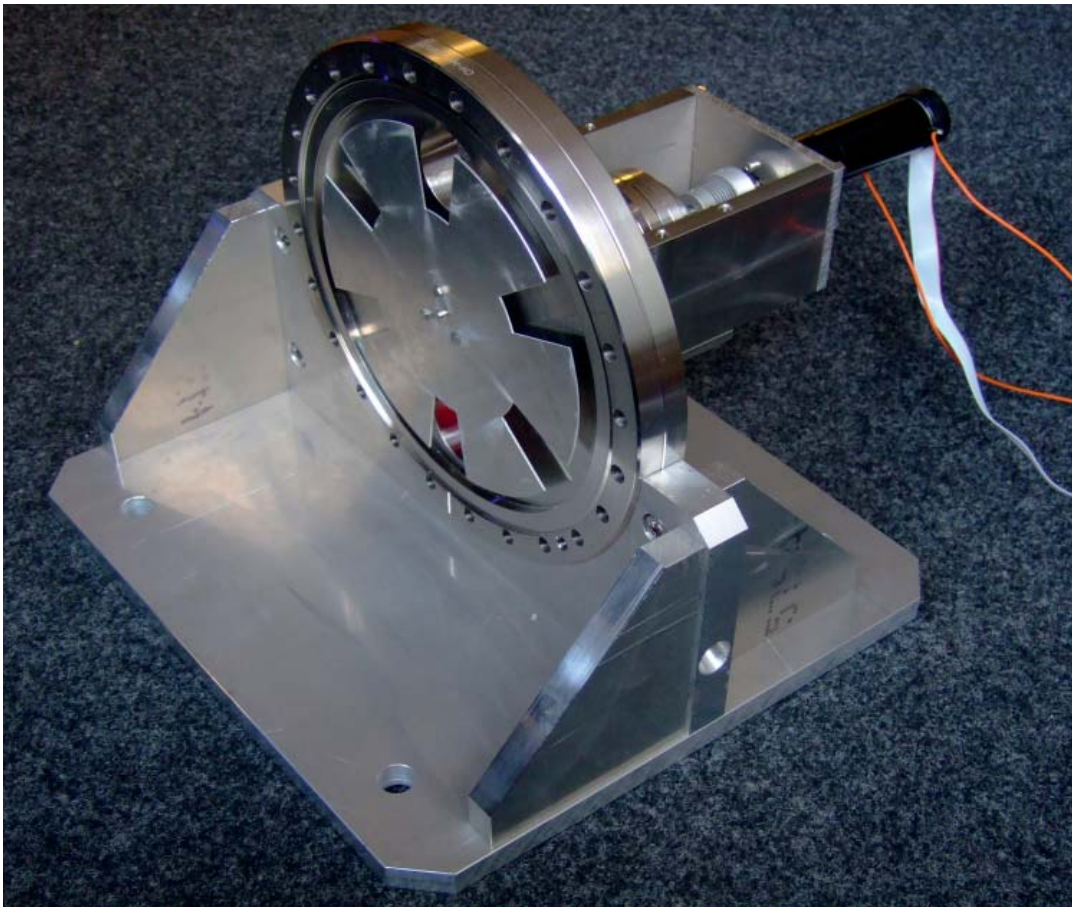

Figure 3

Partially opened prototype of the new shutter fitted with an aluminium disc.

On power up the controller is referencing its position. The shutter is driven until the planar light barrier detects the maximum aperture size. This defines the open position of the shutter. The movements in the states “single bunch train” and “reduced bunch train frequency” are always executed synchronously to the signals of FLASH control system and therefore to the bunch trains. This synchronized movement allows triggering an operation of the shutter on external user signals independent from the FLASH timing. After a “step” signal, the next following FLASH control pulse is waited for. When the PLC detects a rising edge on the pulse-signal, the motor rotates the disk by 3^0 > within 100ms. This rotation changes the state of the shutter from the closed to the open state or vice-versa. This procedure is automatically executed twice, restoring the initial state of the shutter. In the “reduced pulse frequency” mode the shutter provides bunch trains with a constant frequency. The ratio of the reduced frequency and the FLASH frequency can be an integer number only. Typically a reduced bunch train frequency of 1-2 Hz is used to adapt to the readout speed of cameras and detectors.

Contact:
Horst Schulte-Schrepping (DESY-FS Beamline Technology),
horst.schulte-schrepping@desy.de

References

1. **“A mechanical shutter to select single bunch trains at the FLASH facility at DESY”, M. Bräuer, U.Hahn, and S.Toleikis; TUPPH064 Proceedings FEL 2006 – BESSY, Berlin, Germany, FEL 06 Proceedings (2006), 470-473**

New beam position monitors.

Diamonds and RF electronics: a perfect match

DESY and ESRF are collaborating to develop diamond Photon Beam Position Monitors (PBPMs), and with the support of Instrumentation Technologies we are investigating the performance of signal readout of these devices based on RF signal processing techniques. This has already demonstrated position sensitivity better than 50nm. The first systems are for small monochromatic focused beams, close to the sample. Since space around the sample is limited and valued the devices have to be thin. They should absorb only a small fraction of the incident flux, while still giving enough signal in order to be able to measure small beam movements. Single Crystal Diamonds (SCDs) are the best candidates to fulfil these requirements. They are near perfect, very homogeneous, fast, low-Z, and both thermally and mechanically very robust, making them ideal for an X-ray BPM.

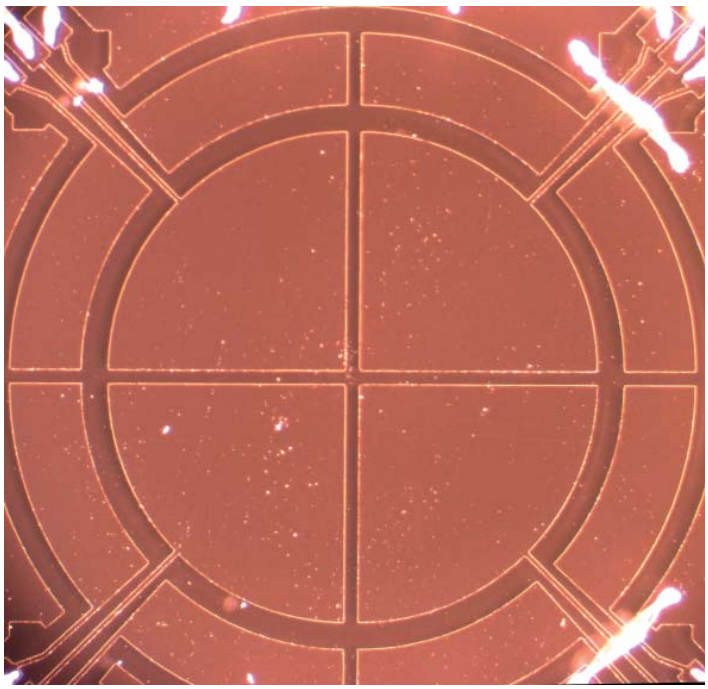

Figure 1

Microscope image of the 4-quadrant scCVD diamond detector.

The e-h pair creation energy is ~12 eV and the low Z gives enough transparency for photons above 5 keV making diamond suitable for the range between 5-30 keV. The sensor thickness is in practice limited by mechanical properties and the fabrication process to some microns up to approximately half a millimetre. The homogeneous and pure, electronic grade scCVD material provides long charge life times, so that biasing with an electric field of 1 V/micron provides fast and nearly 100 % charge collection efficiency. The simplest quadrant motif has a cross like separation gap and a common backplane (see Figure 1). It requires relatively simple crosstalk insensitive sensing electronics, but has the drawback of sharp and not well-defined corners in the centre (spatial linearity). In the case of very small beams, the gaps between electrodes define the sensitivity and region of linearity. Its dimension is limited by the mask precision and should not exceed the sensor thickness.

Charge collected on the electrodes can be measured directly by the electrometers or in the case of pulsed sources by measuring the RF energy of the pulses. The proportion of energy between the four electrodes represents the position in the transverse plane and is the same for DC and for higher harmonics up to the RF accelerator frequency, which is the most suitable because it covers RF signal extraction at all possible synchrotron fill patterns.

A diamond sensor can be described as a current generator with a parallel capacitor and circuits with inductance and RF transformers provide best sensor to cable impedance matching. With an appropriate input band-pass filter and a first stage preamplifier the optimal combination of noise figure and nonlinear distortion can be achieved. All these requirements fit into the processing scheme of a Libera Brilliance readout system

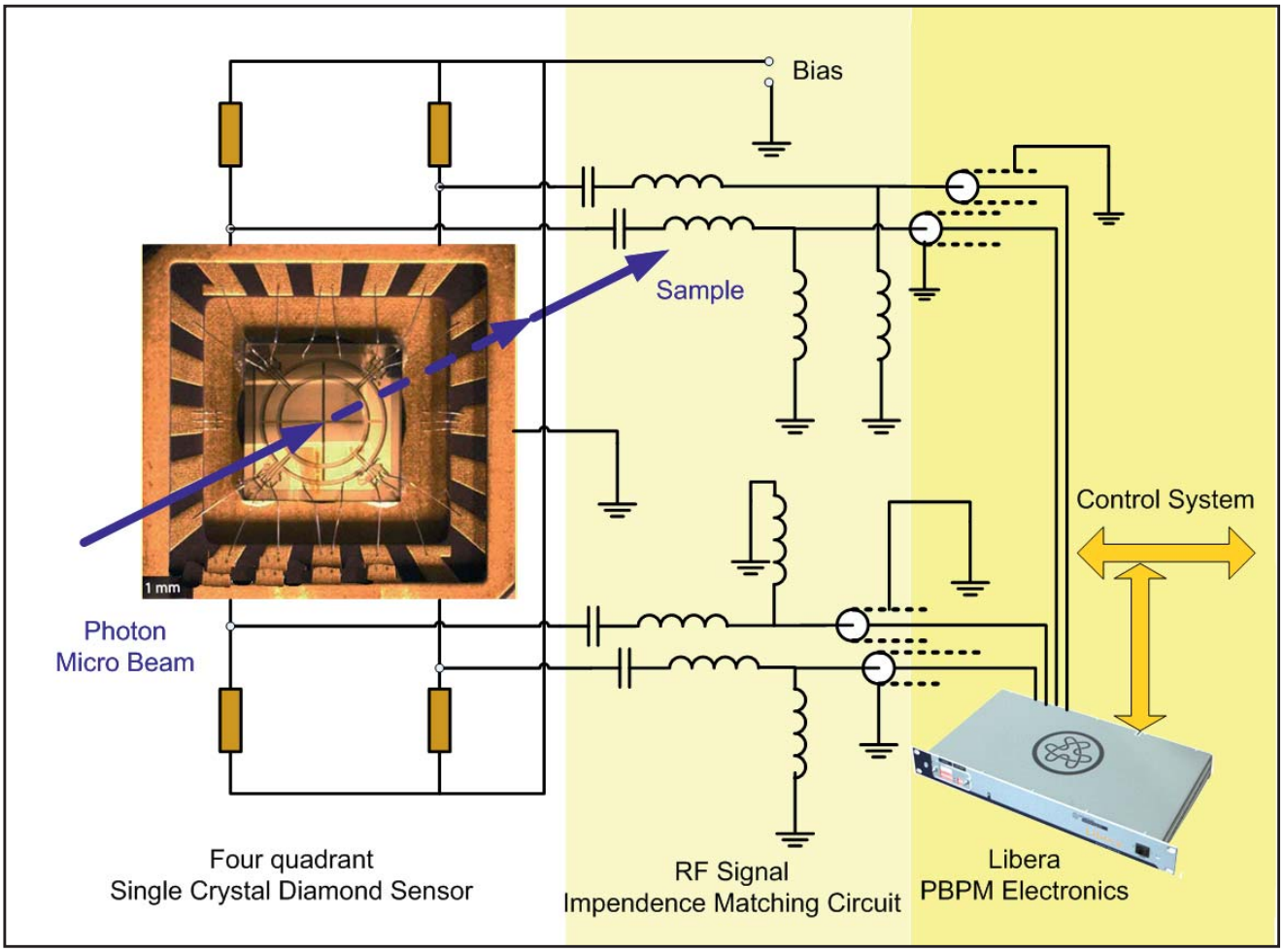

Figure 2

Readout of the quadrant detector using RF techniques

(Figure 2), so that only a minor modification of the RF front-end was necessary. This system has the important advantage of using an arbitrary bandwidth with corresponding spatial resolution. The setup was placed on the DORIS III F4 beam line, using a filtered white beam with a peak energy at 25 keV. A motorized slit was used to create a 25 µm x 25 µm beam and a 0.5 mm thick silicon diode for flux measurements. The Diamond sensor was 4 mm x 4 mm x 0.3 mm, had a 0.1 mm gap between the quadrant electrodes and was mounted on an X-Y table for alignment and scanning.

An ultimate resolution (rms) of 10 nm was observed by scanning as well as with long term (several seconds) single point monitoring. In the last case the response to a mechanical shock introduced three meters away from the hutch was observed and is given in Figure 3. The data (processed to 130 kHz data rate) results in 300/130/40/20 nm rms noise at 50/10/1/0.2 kHz bandwidth.

These results show the excellent performance of the DESY/ESRF/Instrumentation Technologies developed system consisting of 4-quadrant single crystal diamonds read out by a modified Libera Brilliance readout system. Currently a series of sensors and readout electronics are prepared for installation on the PETRA III and ESRF beamlines.

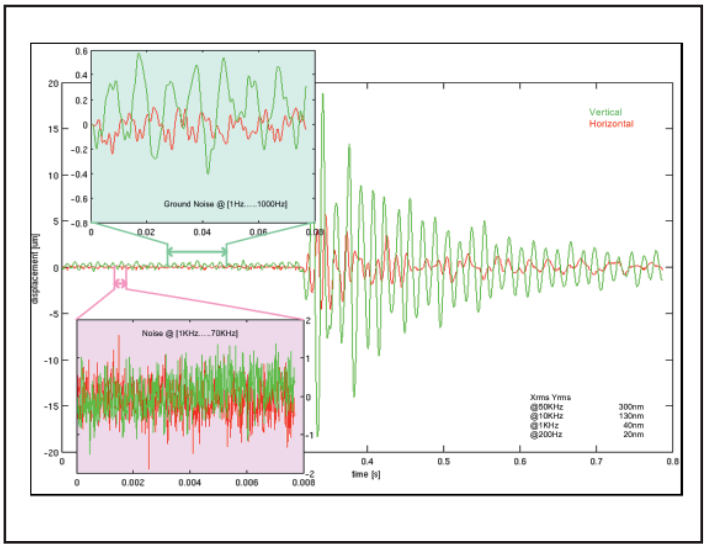

Figure 3

Response to a mechanical shock.

Contact: Heinz Graafsma, heinz.graafsma@desy.de

Authors:
J. Morse (ESRF), B. Solar (Instrumentation Technologies), H. Graafsma (DESY)

HORUS.

A bridge between application and detector scientists

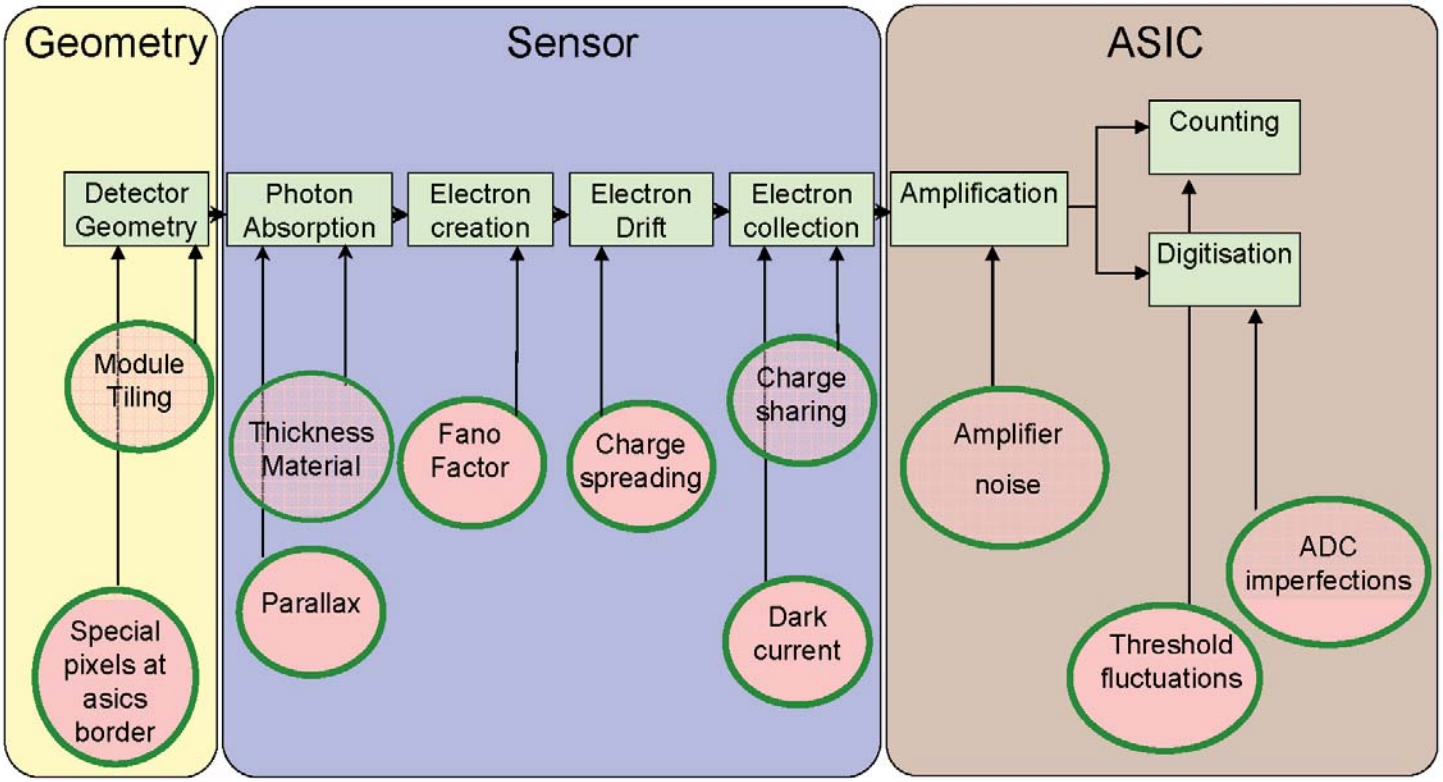

Figure 1

HORUS structure.

HORUS (HPAD Output Response fUnction Simulator) is a program simulating all the physical and electronic processes impacting the detective quantum efficiency of a detector. It was written in IDL (the Interactive Data Language). The program follows step by step the various physical and electrical processes involved in the signal detection process (Figure 1: HORUS structure). It is developed as part of the European XFEL AGIPD detector development program, and thus reflects the implementation of this particular detector, but HORUS can easily be adapted to any other Hybrid Pixel detector, or, with greater changes to the program, to any other type of detector.

The program can be used both to study the overall detector performance as function of various technological choices, and to simulate the degradation of any input image in order to optimize the detector development process, and to study the detector impact on the scientific application.

An example is displayed in Figure 2, where the response probability distribution function is shown for a pulse of 10 photons incident on an AGIPD detector pixel.

The presence of several peaks indicates that some of the pixels which nominally received 10 photons, actually detected less photons. The right most peak corresponds to exactly 10 photons

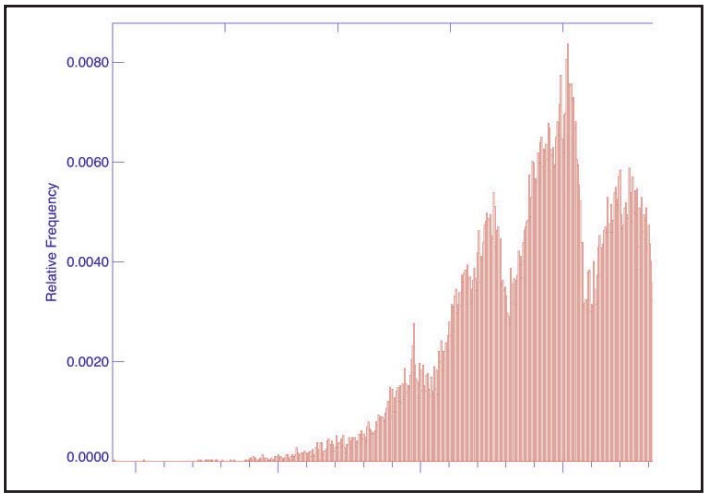

Figure 2

Simulated detector response to a pulse of 10 photons incident on an AGIBD detector pixel.

recorded by the pixel. The last but one peak corresponds to only 9 photons being detected, etc. This is expected since the process of absorption of each of the photons is independent of the absorption of the other photons, so each photon has a probability of 90 % of being absorbed and detected, and this trial is repeated 10 times. Then the width (and partial overlap of the peaks) is a trace of the detector internal noise, and of the charge sharing effect occurring between the pixels in the sensor. This sort of analysis is extremely useful to optimize the development process and evaluate how each technological choice impacts the overall detection process.

Figure 3 illustrates how one can simulate the modification of a diffraction pattern (left) after it has been recorded by the detector (right). The detector dead areas are clearly visible, but also more subtle modifications (such as the actual number of recorded photon, signal spreading, etc.) are fully simulated, enabling a careful evaluation of the detector impact on the experiment, and a possible integration of the specific detector behaviour in the data treatment process.

Contact: Heinz Graafsma, heinz.graafsma@desy.de

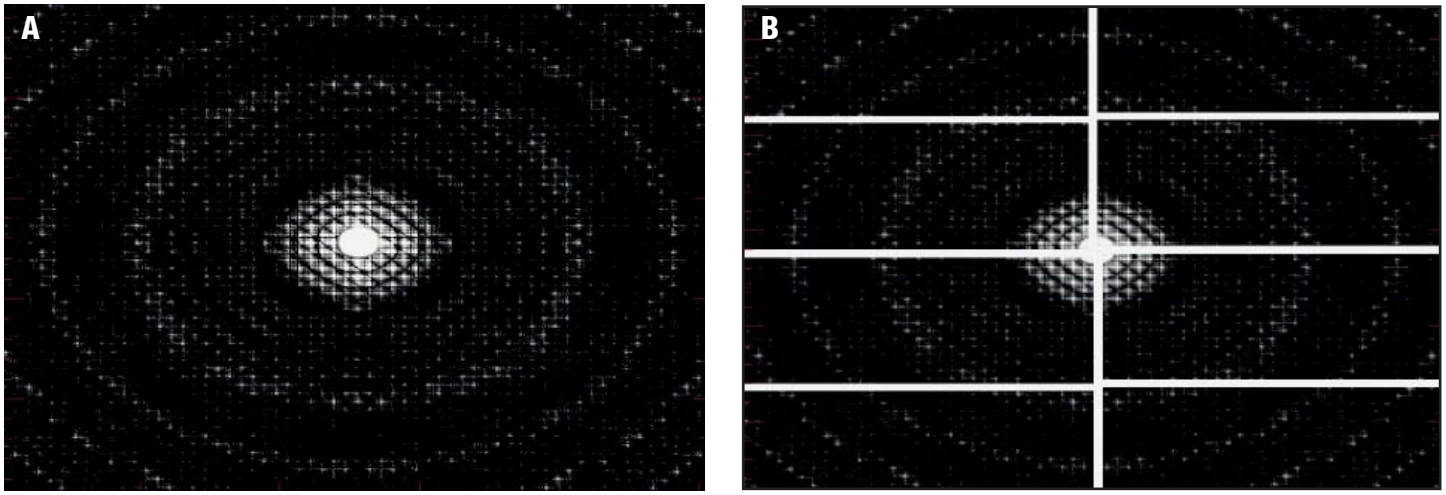

Figure 3

Diffraction pattern of a coherent diffraction imaging (CDI) experiment. A at the entrance of the detector, and B recorded by the detector as simulated by HORUS.

HORUS is available by contacting its authors.

Author

Guillaume Potdevin, guillaume.potdevin@desy.de

References

1. **"Performance simulation of a detector for 4th generation photon sources: The AGIPD", G. Potdevin, U. Trunk, H. Graafsma for the AGIPD Consortium.**
2. **"Nuclear Instruments and Methods in Physics Research Section A", Proceedings of the 10th IWORID workshop.**
3. **"HORUS, an HPAD X-ray detector simulation program", G. Potdevin, U. Trunk, H. Graafsma for the AGIPD Consortium., JINST 4 P09010 doi: 10.1088/1748-0221/4/09/P09010 (2009).**

Computing at PETRA III.

Collaborate to create software efficiently

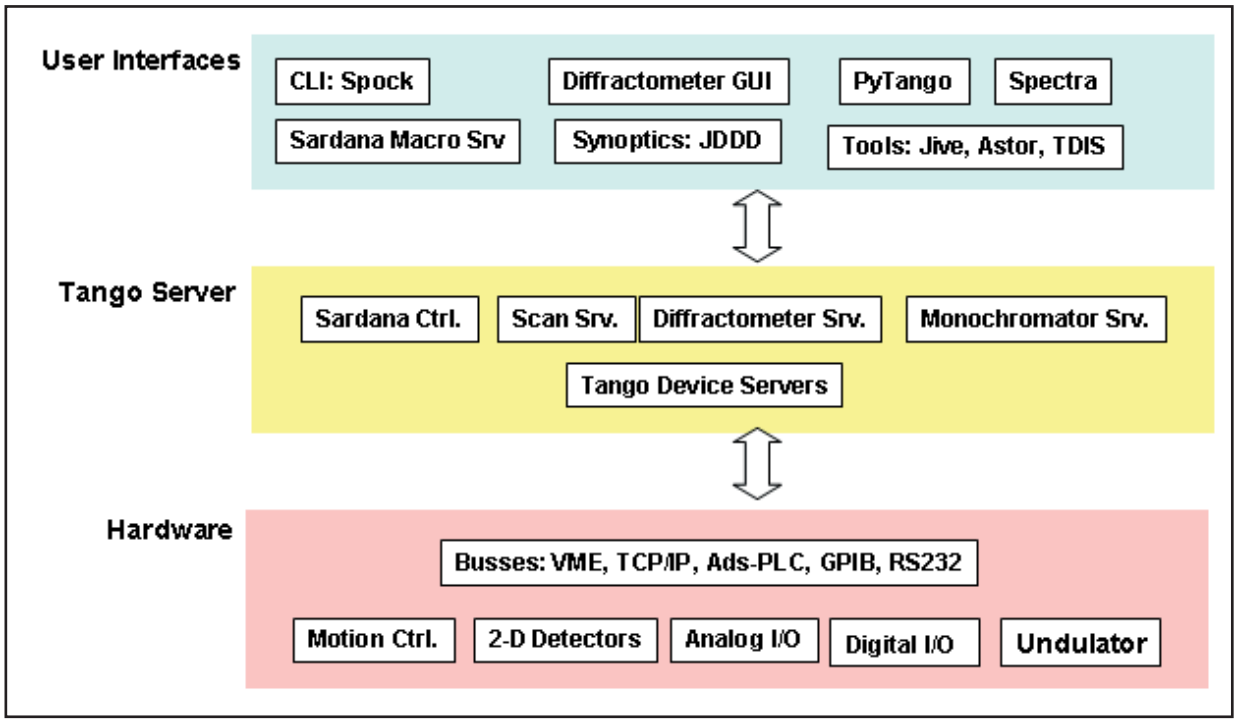

Figure 1
The PETRA III Online Computing Model

Online Computing

During the past months of experiment commissioning at PETRA III the important components of the online control system went into operation. It has already been pointed out in the preceding annual report that the experiments use Tango as the communication layer between the hardware and the user interfaces. A big effort went into the production of device servers. Up to now about 25 different classes have been implemented and tested. These are servers for stepping motors, PLC based motion controllers and servers for our standard VME boards. Device servers are directly coupled to the hardware via VME, TCP/IP, ADS, GPIB, or RS232. A second layer of Tango servers exists that exports compound devices like diffractometers and monochromators to the clients. The diffractometer server, created at SOLEIL, is of special importance. It implements crystal orientation methods and maps coordinates from direct to reciprocal space for different diffractometer types. Among them is the Eulerian-6C which is used at P08 and P09.

The clients used so far are Spectra as the general purpose program, the diffractometer GUI of SOLEIL, the Tango tools Jive and Astor of the ESRF, JDDD of DESY-MCS and Python scripts. The latter use the PyTango interface which was created at SOLEIL and the ESRF. The Sardana suite of ALBA consisting of the command line interface Spock, the macro server and the controller interface is currently being prepared to become operational as soon as possible.

It was a strategic decision to join the Tango collaboration (ESRF, SOLEIL, ALBA, ELETTRA, DESY) not only because of the Tango protocol itself, but also to participate in developments of user interfaces and other high level applications. The objectives are to benefit from the work of our colleagues in the partner institutes, to avoid parallel developments and to define standards for user interfaces and data formats. This approach reduces the programming effort and has the second advantage that users will appreciate to work with similar computing environments in the different Tango institutes. The list of software components that have been imported from our partners, for some of them DESY made substantial contributions, clearly demonstrates that the collaborative work is very successful.

Data storage and data processing

The PETRA III experiments use DESY-central facilities for data storage. Currently two file servers with a total capacity of 180 TB have been installed. Each of the servers has 4 x 10 GE network interfaces that are managed by two processors, see Figure 2. This layout is sufficiently redundant to cope with hardware failures. Another safety measure is the 'snapshot' feature. It uses 20 % of the available disk space for a system that allows users to retrieve files that have accidentally been deleted. The disk space is organized in volumes. Each volume is assigned to a specific beamline and can be accessed from Linux and Windows. Tapes can be used for long term data storage. It is expected that some users of high data rate experiments need the DESY data storage because of limited IT resources at their home institutes. Therefore an interface for remote data access has to be created. Data will be processed on blade centres. So far, the computer centre prepared a system consisting of 16 blades. Each blade has 8 CPU cores and 24 GB of RAM. Two of the blades will be allocated for data management. Other blades can be assigned to high data rate experiments for exclusive usage. The remaining blades will be collected in a load balanced pool for general applications. The layout of the file and compute servers has been designed to make both systems scalable. Additional hardware will be installed, if necessary.

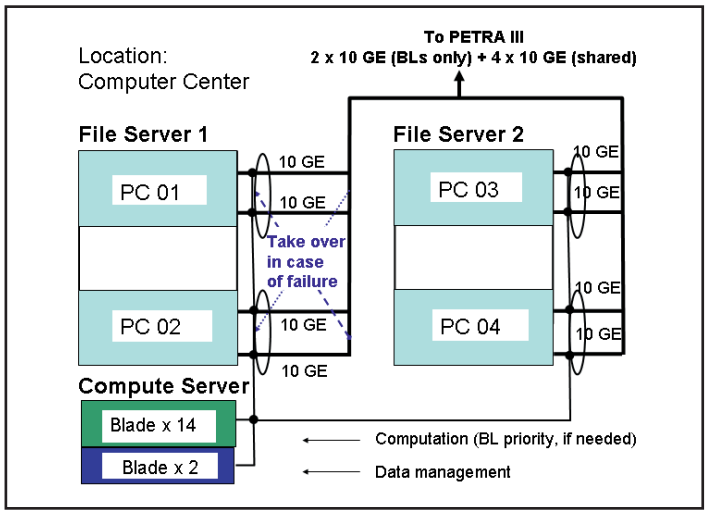

Figure 2

File and compute server for PETRA III

Scientific Software Support

In order to enhance the scientific outcome of the PETRA III beam times it is planned to provide our users with software tools for online and offline purposes. Online tools typically perform the following tasks: the alignment of the instrument, the quality assurance of the sample, the optimization of exposure times by monitoring the statistics and the control of parameters of in situ measurements. These tools help to improve the data quality by generating fast feedback information for an immediate adjustment of the ongoing measurement. Offline tools in general are more CPU time consuming. They will run on the central compute servers to do first reconstruction steps, automated feature extraction on large data sets and statistical analyses like classification (see Figure 3) or principal component analysis. A fraction of the offline tools can be designed as general purpose applications which are useful for different kinds of measurements. Others are limited to a specific technique. For these cases, software developments can be optimized, if institutes which pursue similar scientific projects join forces and start to collaborate. There are national and international initiatives that foster this objective. Several online and offline applications have already been developed for the DORIS experiments where they have been successfully utilized. They are ready to be used at PETRA III.

Contact: Thorsten Kracht, thorsten.kracht@desy.de

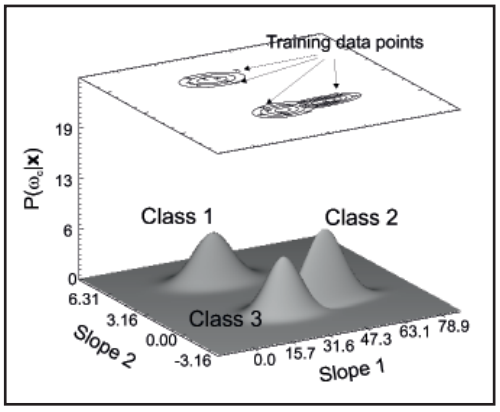

Figure 3

Supervised classification: Conditional probability density function.

Authors:
Teresa Núñez Pardo de Vera, André Rothkirch, Thorsten Kracht

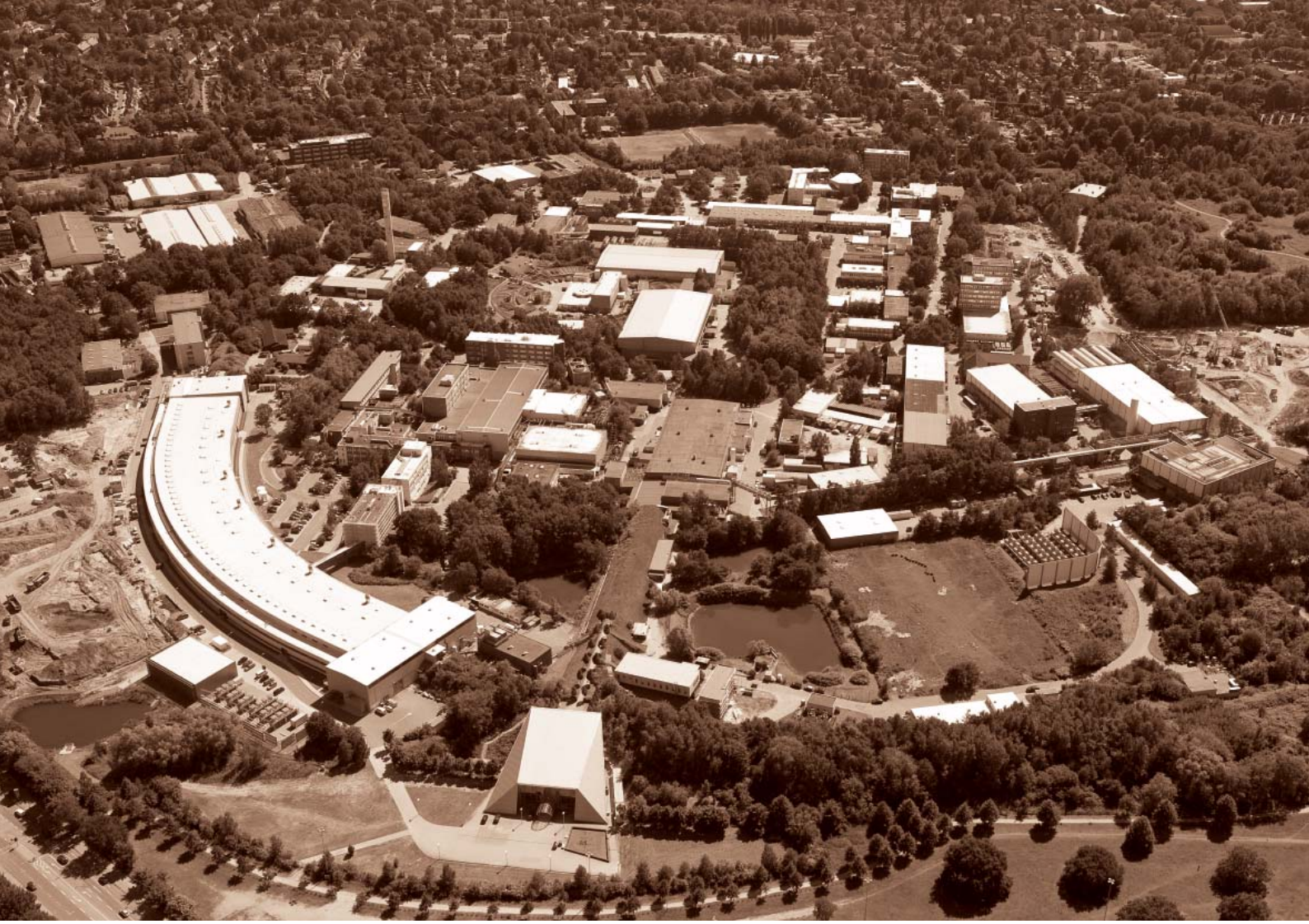

Facts and Numbers.

Lightsource characteristics.

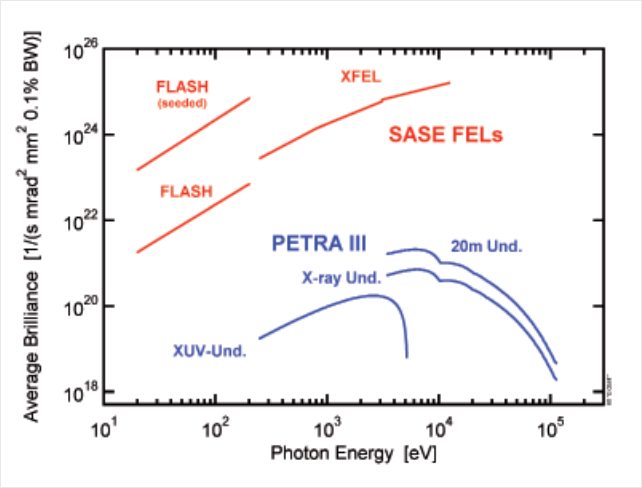

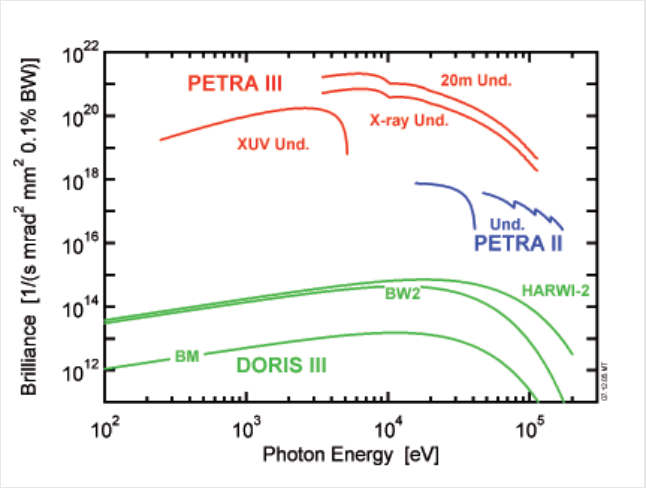

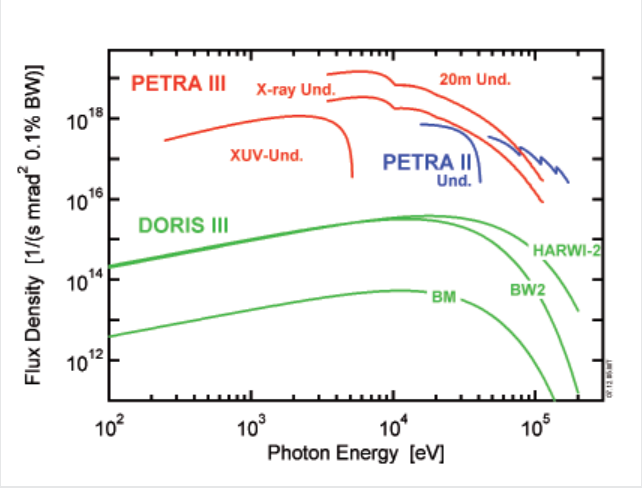

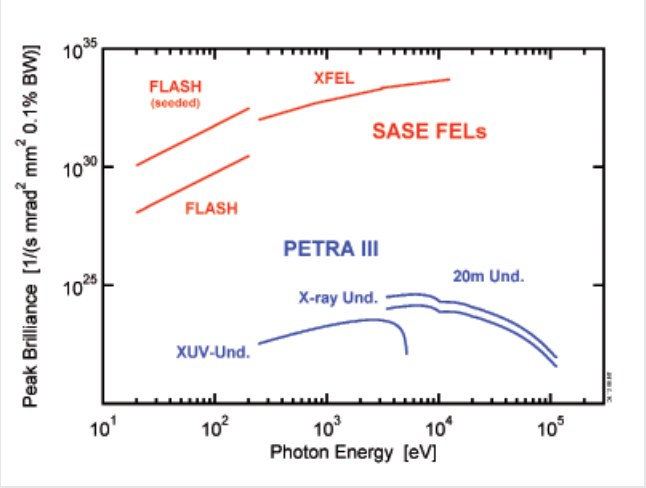

Storage ring sources

Free-electron laser sources
(in comparison with PETRA III)

DORIS III.

Beamlines and parameters

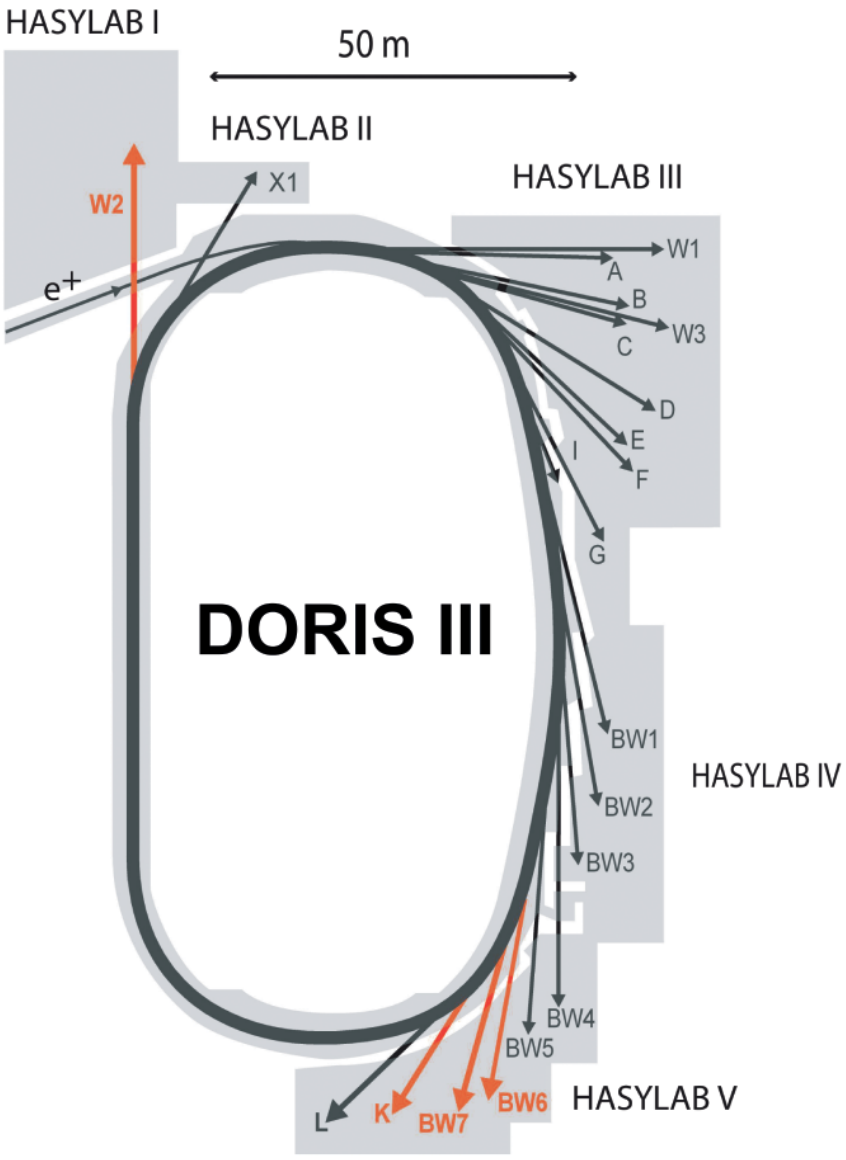

Machine parameters DORIS III (Present values)

Positron energy	4.45 GeV
Circumference of the storage ring	289.2 m
Number of buckets	482
Number of bunches	1 (for tests), 2, and 5
Bunch separation (minimum)	964 ns (for tests), 480 ns, and 192 ns
Positron beam current	140 mA (5 bunches)
Horizontal positron beam emittance	410 nmrad (rms)
Coupling factor	3%
Vertical positron beam emittance	12 nmrad (rms)
Positron beam energy spread	0.11% (rms)
Curvature radius of bending magnets	12.18 m
Magnetic field of bending magnets	1.218 T
Critical photon energy from bending magnets	16.0 keV

DORIS III beamtime statistics 2009

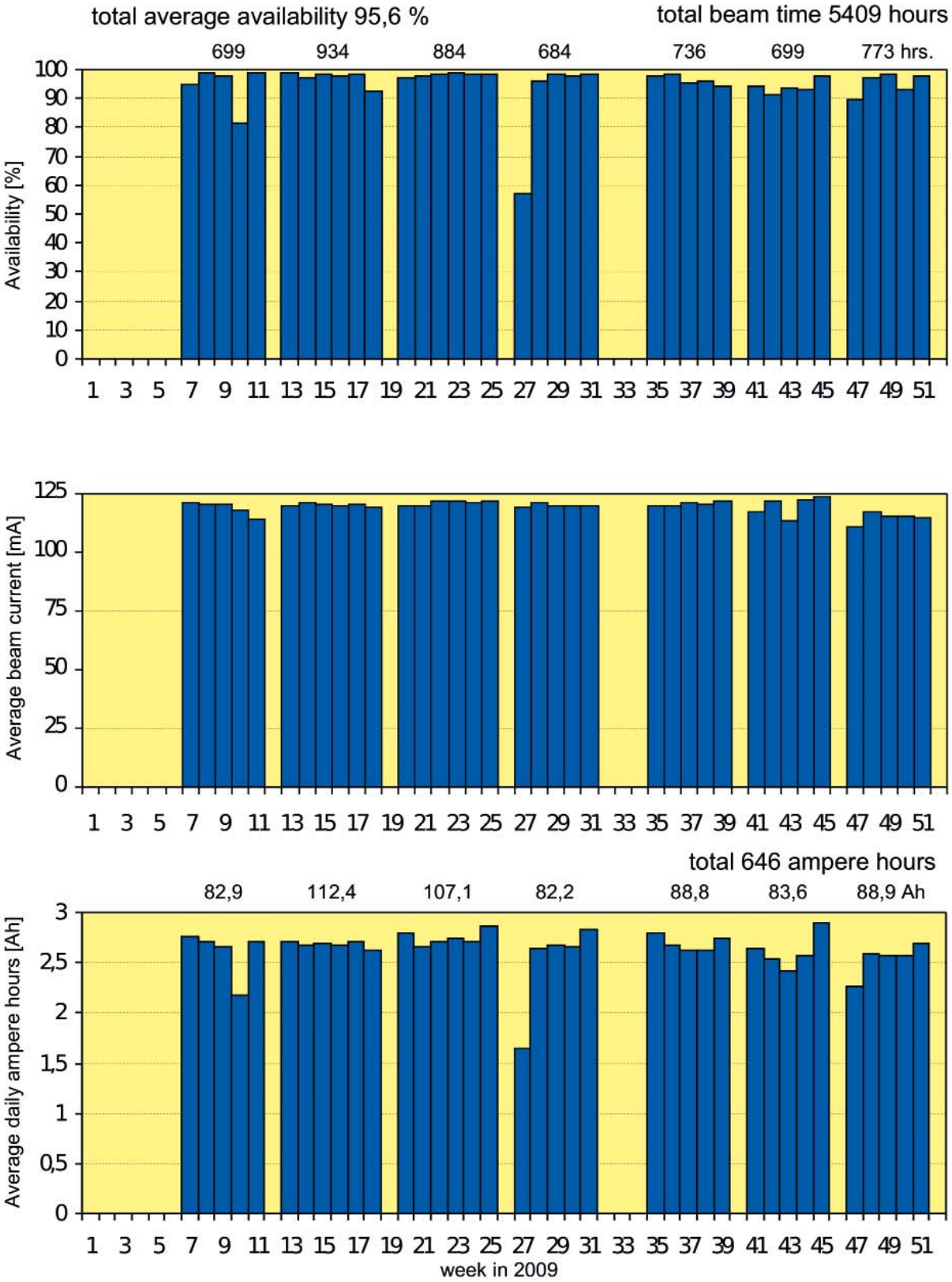

Availability = Useable beam time for HASYLAB in % of scheduled beam time
Criterion: Beam current ≥ 40 mA; run duration ≥ 1 hour

Year	2007	2008	**2009**
Total integrated ampere hours	627	214	**646**

DORIS III beamlines and instruments

A1 X-ray absorption spectroscopy		
Bending magnet (Ec = 16 keV)		
Instrument for in-situ XAFS including fast energy scanning	2.4 – 8 keV	DESY
A2 Small-angle X-ray scattering		
Bending magnet (Ec = 16 keV)		
Multi setup instrument for (simultaneous) small and wide angle scattering from soft matter samples	8 keV	DESY
B1 Anomalous small-angle X-ray scattering		
Bending magnet (Ec = 16 keV)		
Instrument for anomalous scattering (ASAXS)	5 – 35 keV	DESY
B2 X-ray powder diffraction		
Bending magnet (Ec = 16 keV)		
Heavy duty diffractometer including special setups for in-situ studies (refurbished, operational again spring 2009)	5 – 44 keV	DESY
BW1 X-ray diffraction / scattering		
4m X-ray undulator		
Horizontal diffractometer for liquid surface scattering	9.5 keV	DESY
UHV instrument for surface diffraction / standing waves including MBE sample preparation	2.4 – 12 keV	DESY U Bremen
Multi purpose heavy load 8-circle diffractometer	5 – 18 keV	DESY
Rheometer	9.9 keV	DESY
BW2 X-ray spectroscopy / diffraction / tomography		
4m X-ray wiggler (Ec = 15.4 keV)		
UHV instrument for hard X-ray photoelectron spectroscopy	2.4 – 10 keV	DESY
X-ray micro-tomography setup	6 – 24 keV	GKSS
Heavy load vertical diffractometer with CCD detector arm for grazing incidence diffraction	5 – 11 keV	DESY
BW3 Soft X-ray spectroscopy		
4m XUV (double) undulator		
High-resolution SX-700 plane grating monochromator, beam port for user supplied instruments	50 – 1500 eV	DESY
BW4 Ultra small-angle X-ray scattering		
2.7m X-ray wiggler (Ec = 15.4 keV)		
Flexible instrument for (ultra) small angle (grazing incidence) scattering experiments	6 – 14 keV	DESY
BW5 High-energy X-ray diffraction		
4m X-ray wiggler (Ec = 26 keV)		
Triple axis diffractometer in horizontal Laue scattering geometry including high magnetic field (10T) sample environment	60 – 250 keV	DESY
BW6 Macromolecular crystallography		
4m X-ray wiggler (Ec = 15.4 keV)		
End-station for protein crystallography, optimized for MAD or SAD	4 – 20 keV	MPG

BW7A Macromolecular crystallography		
4m X-ray wiggler (Ec = 15.4 keV)		
Crystallographic end-station with CCD detector, double multilayer optics, optimized for high-flux fast data collection	12.8 keV	EMBL
BW7B Macromolecular crystallography		
4m X-ray wiggler (Ec = 15.4 keV)		
Crystallographic end-station with CCD detector, new high-precision Phi spindle, EMBL Hamburg robotic sample changer (MARVIN)	14.7 keV	EMBL
C X-ray absorption spectroscopy / diffraction		
Bending magnet (Ec = 16 keV)		
Setup for high-energy XAFS in-situ studies including fast energy scanning	5 – 44 keV	DESY
Vertical diffractometer for grazing incidence X-ray diffraction	5 – 44 keV	DESY
D1 (X33) Small-angle X-ray scattering		
Bending magnet (Ec = 16 keV)		
Instrument optimized for automated solution scattering studies of biological macromolecules	8 keV	EMBL
D3 Chemical crystallography		
Bending magnet (Ec = 16 keV)		
4-circle diffractometer	8 – 50 keV	DESY
D4 Grazing incidence X-ray scattering		
Bending magnet (Ec = 16 keV)		
2-circle diffractometer, horizontal scattering plane	5 – 20 keV	DESY
E1 (Flipper2) Soft X-ray spectroscopy		
Bending magnet (Ec = 16 keV)		
UHV instrument for soft X-ray photoelectron spectroscopy	10 – 150 eV	U Hamburg
E2 X-ray reflectometry / grazing incidence diffraction		
Bending magnet (Ec = 16 keV)		
6-circle diffractometer for reflectometry & high-resolution diffraction	4 – 35 keV	DESY / RWTH Aachen
F1 Chemical crystallography		
Bending magnet (Ec = 16 keV)		
Kappa-diffractometer for low/high-temperature / high-pressure single-crystal diffraction	5 – 41 keV white beam	U Hamburg
F2 X-ray diffraction / VUV spectroscopy		
Bending magnet (Ec = 16 keV)		
Hutch1 MAX80 Multi-Anvil-X-ray apparatus for high pressure X-ray diffraction	5 – 80 keV white beam	GFZ
Hutch2 UHV instrument for angle-resolved UV photoelectron spectroscopy	5 – 41 eV	U Hamburg
F3 Energy dispersive scattering		
Bending magnet (Ec = 16 keV)		
Horizontal diffractometer with heavy load sample stage	white beam	DESY U Kiel

F4 X-ray test beam			
	Bending magnet (Ec = 16 keV)		
	Used for detector characterization		DESY
G3 Diffraction X-ray imaging			
	Bending magnet (Ec = 16 keV)		
	4-circle diffractometer for position resolved diffraction	5.4 – 26 keV	DESY
I (Superlumi) UV luminescence spectroscopy			
	Bending magnet (Ec = 16 keV)		
	Superlumi setup for luminescence analysis	3 – 40 eV	DESY
K1.1 (X11) Macromolecular crystallography			
	Bending magnet (Ec = 16 keV)		
	Crystallographic end-station with large surface area flat panel detector, cryoshutter, single horizontal axis of rotation	15.3 keV	EMBL
K1.2 (X12) Macromolecular crystallography			
	Bending magnet (Ec = 16 keV)		
	Crystallographic end-station with CCD and fluorescence detector, single axis of rotation, opt. for MAD and SAD	6 – 18 keV	EMBL
K1.3 (X13) Macromolecular crystallography			
	Bending magnet (Ec = 16 keV)		
	Crystallographic end-station with CCD detector, cryoshutter, micro-spectrophotometer, single horizontal axis of rotation, optimised for automated expert data collection	15.3 keV	EMBL
L X-ray micro probe			
	Bending magnet (Ec = 16 keV)		
	X-ray microprobe combining fluorescence analysis, absorption spectroscopy and diffraction	5 – 80 keV white beam	DESY
W1 X-ray spectoscopy / diffraction			
	2m X-ray wiggler (Ec = 8 keV)		
	High-resolution fluorescence in vacuo spectrometer	4 – 11.5 keV	DESY
	Heavy load diffractometer for grazing incidence diffraction in vertical or horizontal scattering geometry	4 – 11.5 keV	DESY
W2 (HARWI II) High-energy X-ray engineering materials science			
	4m X-ray wiggler (Ec = 26 keV)		
	Hutch1 Materials Science Diffractometer (heavy load up to 600 kg) Micro-tomography setup (attenuation and phase contrast) Diffraction-tomography "DITO" instrument	60 – 250 keV 20 – 250 keV 20 – 150 keV	GKSS GKSS TU Dresden TU Berlin
	Hutch2 MAX200x Multi-Anvil X-ray apparatus for high pressure and temperature conditions	white beam	GFZ
W3 VUV spectroscopy			
	Bending magnet (Ec = 16 keV)		
	Angle-resolved photoelectron spectrometer with high energy resolution	8 – 32 eV	U Kiel
X1 X-ray absorption spectroscopy			
	Bending magnet (Ec = 16 keV)		
	Setup for high-energy fast-scanning XAFS for in-situ studies including chemistry lab	7 – 100 keV	DESY

FLASH.

Beamlines and parameters

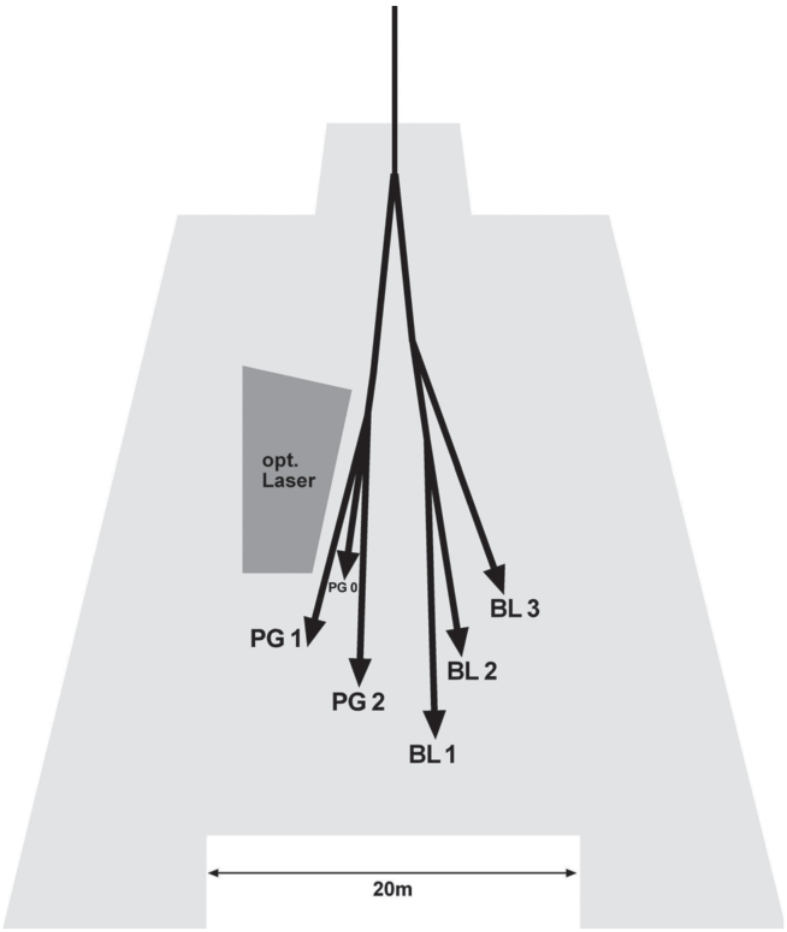

Machine parameters FLASH (as achieved in 2008)

Electron energy (max.)	1.0 GeV
Length of the facility	315 m
Normalized emittance	2 mm mrad (rms)
Emittance	1 nm rad (rms)
Bunch charge	1 nC
Peak current	2 kA
Bunches per second (typ. and max.)	150 and 4000
Lasing parameters	
Photon energy (max.)	180 eV (fundamental)
Wavelength (min.)	6.9 nm (fundamental)
Pulse duration (FWHM)	10 - 50 fs
Peak power	1 - 5 GW
Bunch energy (average)	10 -100 µJ
Photons per bunch	10^{12} - 10^{13}
Average brilliance	10^{17}-10^{19} photons/sec/mm^2/mrad^2/0.1%
Peak brilliance	10^{29} - 10^{30} photons/sec/mm^2/mrad^2/0.1%
Spectral bandwidth	1 % (FWHM)

FLASH beamlines and user instruments

(including instrumentation provided by university groups and funded by the BMBF „Verbundforschung“)

BL1		
	Focused FEL beam, 100µm spot size	DESY
	Instrumentation for the preparation and electron and ion spectroscopy of mass-selected clusters	U Rostock
	Magnetic X-ray diffraction imaging and holography	DESY HZB (BESSY)
	Pump-probe setup for the study of transient response of melting/ablating solids	U Duisburg-Essen
	Setup for resonant soft X-ray scattering	CFEL U Oxford
	Experimental system for the spectroscopic study of molecular desorption from surfaces of solids	U Münster
	Single-shot cross-correlator	U Hamburg
BL2		
	Focused FEL beam, 20µm spot size	DESY
	Instrumentation for two-colour pump probe experiments of atoms and molecules	DESY DCU Dublin LIXAM/CNRS Paris
	Reaction microscope for the study of multiple ionization processes of atoms and molecules	MPI-K Heidelberg
	Velocity map imaging spectrometer (electrons and ions) for atoms and molecules in strong fields	AMOLF Amsterdam
	Setup for angle-resolved photoelectron spectroscopy (ARPES) of atoms and molecules	FHI Berlin
	Station for spectroscopy of rare gas clusters and nanoparticles	TU Berlin
	Single-shot single-particle (time-resolved) diffraction imaging of nanostructures and biological samples	CFEL LLNL Livermore U Uppsala
	Setup for Thomson scattering spectroscopy to probe plasma dynamics in a liquid hydrogen jet	DESY LLNL Livermore U Oxford U Rostock
	Instrumentation for measuring damage thresholds and optical properties of solid samples	ASCR Prague DESY IFPAS Warsaw LLNL Livermore
	Setup for electron and ion spectroscopy to study multi-photon processes in gases	DESY PTB Berlin U Hamburg

BL3		
	Unfocused FEL beam	DESY
	Magneto-optical trap & reaction microscope to study ultra-cold plasmas	MPI-K Heidelberg
	Setup with multilayer optics for sub-micron focusing to create and study plasmas and warm dense matter	U Belfast CFEL DESY U Oxford
	System for angle-resolved photoelectron spectroscopy (ARPES) and ion spectroscopy of metal vapors	DESY U Hamburg
	Microfocus setup for spectrometry of multi-photon processes in rare gases at extreme power densities	DESY PTB Berlin
	XUV beam splitter with variable delay for photon diagnostics and time-resolved experiments	DESY HZB (BESSY) U Münster
	Split multilayer-mirror & reaction microscope for time-resolved spectroscopy of small molecules	MPI-K Heidelberg
	Microfocus setup for time-resolved imaging of rare gas clusters	TU Berlin
	Experimental station for pump-probe experiments combining µJ-level, few-cycle THz and XUV FEL pulses	DESY U Hamburg
PG1		
	Plane grating monochromator, microfocus (5µm spot size)	DESY, U Hamburg
	High-resolution two-stage spectrometer for inelastic (Raman) scattering (permanent installation)	DESY U Hamburg
PG2		
	Plane grating monochromator (50µm focus)	DESY, U Hamburg
	Setup for resonant inelastic X-ray scattering (RIXS) and photoelectron spectroscopy of solids	U Hamburg
	Electron beam ion trap (EBIT) for high-resolution spectroscopy of highly charged ions	MPI-K Heidelberg
	Ion source and trap for spectroscopic studies of the photo-fragmentation of molecular ions and radicals (permanent installation)	U Aarhus MPI-K Heidelberg
	System for angle-resolved photoelectron spectroscopy (ARPES) of solids and surfaces	U Kiel
	Setup for the study of fs-dynamics of magnetic materials	U Hamburg HZB (BESSY)
	XUV beamsplitter with variable delay for time resolved experiments	U Hamburg
	Soft X-ray diffraction imaging system for magnetic materials and nanostructures	DESY U Hamburg U Heidelberg HZB (BESSY) FH Koblenz

Note: instruments are non-permanent installations unless noted otherwise

PETRA III.

Beamlines and parameters

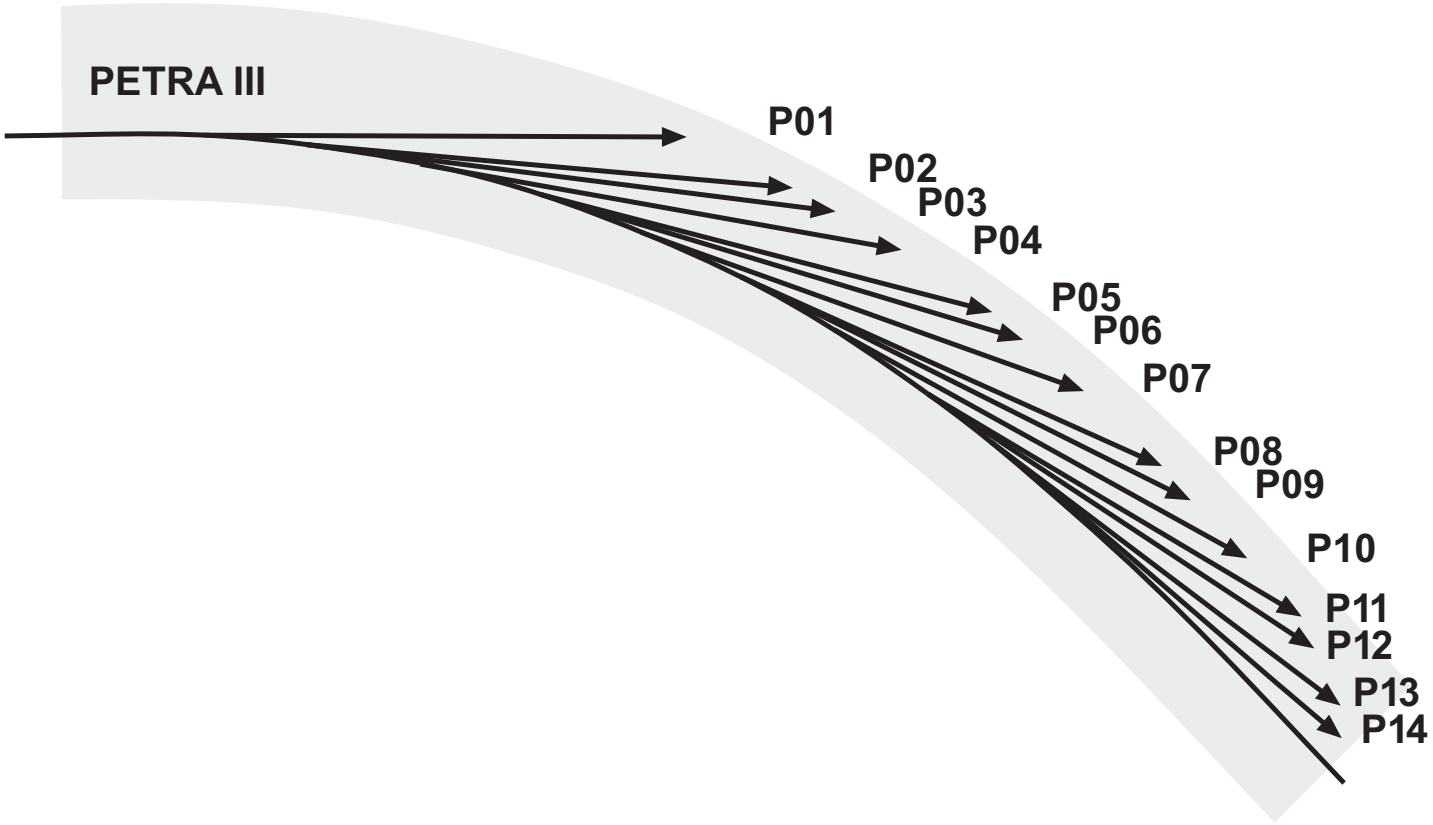

Machine parameters PETRA III (Design values)

Positron energy	6.0 GeV
Circumference of the storage ring	2304 m
Number of buckets	3840
Number of bunches	960 and 40
Bunch separation	8 ns and 192 ns
Positron beam current	100 mA (top-up mode possible)
Horizontal positron beam emittance	1 nmrad (rms)
Coupling factor	1%
Vertical positron beam emittance	0.01 nmrad (rms)
Positron beam energy spread	0.1% (rms)
Curvature radius of bending magnets	22.92 m (new part of the ring)
Magnetic field of bending magnets	0.873 T (new part of the ring)
Critical photon energy from bending magnets	20.9 keV (new part of the ring)

PETRA III beamlines and instruments under construction

(including instrumentation provided by university groups and funded by the BMBF „Verbundforschung“)

P01 Inelastic and Nuclear Resonant Scattering		
10 m undulator (U32), high-ß		
Hutch1 Nuclear resonant scattering setup Nuclear lighthouse effect spectrometer	6 – 40 keV	DESY
Hutch2 Spectrometer for inelastic scattering with nanobeam	6 – 40 keV	DESY
Hutch3 Nuclear resonant scattering with special sample environments: Extreme conditions and UHV	6 – 40 keV	DESY
P02 Hard X-Ray Diffraction		
2 m undulator (U23), high-ß		
Hutch1 Powder diffraction side station High-resolution powder diffractometer	60 keV	DESY TU Dresden
Hutch2 Station for diffraction experiments under extreme conditions (high p, high T) Laser heating for the extreme conditions station	8 – 100 keV	DESY U Frankfurt
P03 Micro- and Nanobeam Wide and Small Angle X-ray Scattering (MINAXS)		
2 m undulator (U29), high-ß		
Hutch1 General Purpose µSAXS/WAXS station Setup for in-situ deposition experiments, AFM µGISAXS option with ellipsometer	8 – 23 keV	DESY TU München
Hutch2 Setup for nanobeam Scanning-Experiments (SAXS/WAXS, GISAXS) Nanofocus endstation including in-situ deformation experiments	8 – 23 keV	DESY U Kiel
P04 Variable Polarization Soft X-rays		
5 m APPLE undulator (UE65), high-ß		DESY
UHV-diffractometer for elastic and inelastic resonant XUV scattering	0.2 - 3.0 keV	U Köln
Ultra-high resolution XUV photoelectron spectrometer for in-situ real-time investigation of dynamic processes in nano structures	0.2 - 3.0 keV	U Kiel U Würzburg
PIPE: instrument for flexible two-beam experiments to investigate mass selected ions (atoms to nano particles) with photons	0.2 - 3.0 keV	U Giessen U Hamburg FU Berlin U Frankfurt
Soft X-ray absorption spectrometer with variable polarization at 30 mK	0.2 - 3.0 keV	U Hamburg U München
Nano focus apparatus for spatial and time resolving spectroscopy	0.2 - 3.0 keV	U Hamburg FH Koblenz
P05 Imaging beamline		
2 m undulator (U29), low-ß		
Hutch1 Micro tomography setup for absorption, phase enhanced and phase contrast tomography	5 – 50 keV	GKSS
Hutch2 Nano tomography instrument combining hard X-ray microscopy and tomography	5 – 50 keV	GKSS
P06 Hard X-ray Micro/Nano-Probe		
2 m undulator (U32), low-ß		
Hutch1 Instrument for imaging at (sub-)micrometer spatial resolution applying X-ray fluorescence, X-ray absorption and X-ray diffraction techniques	2.4 - 100 keV	DESY
Hutch2 Instrument for imaging by coherent X-ray diffraction and X-ray fluorescence with nanoscopic resolution	5 – 50 keV	DESY TU Dresden

P07 High Energy Materials Science (HEMS)		
4 m in-vacuum undulator (U19), high-ß		
Hutch1 Test facility	53 / 87 keV (fixed)	GKSS
Hutch2 Multi purpose diffractometer for bulk and interfaces	50 – 250 keV	DESY
Hutch3 Heavy-load (1t) diffractometer	50 – 250 keV	GKSS
Hutch4 3D-XRD strain and stress mapper Instrument for microtomography Software for high-resolution strain analysis	50 – 250 keV	GKSS GKSS TU Berlin
P08 High-resolution diffraction		
2 m undulator (U29), high-ß		
Hutch1 High-resolution diffractometer X-ray diffractometer for liquid interfaces studies Extension for external sample environments and coherent scattering	5.4 – 30 keV	DESY U Kiel U Dortmund
P09 Resonant scattering / diffraction		
2 m undulator (U32), high-ß		
Hutch1 High precision diffractometer for resonant scattering and diffraction	2.4 – 50 keV	DESY
Hutch2 Heavy load diffractometer for resonant scattering and diffraction, high magnetic fields	2.4 – 50 keV	DESY
Hutch3 High-resolution hard X-ray photoelectron spectroscopy instrument	2.4 – 15 keV	DESY U Mainz U Würzburg
P10 Coherence applications		
5 m undulator (U29), low-ß		
Hutch1 Instrument for X-ray photon correlation spectroscopy and coherent diffraction imaging in SAXS geometry, rheology setup	4 – 25 keV	DESY
Hutch2 Instrument for X-ray photon correlation spectroscopy and coherent diffraction imaging at large angles X-ray waveguide setup Apparatus for lensless microscopy of biological cells Setup for XPCS with reference beams	4 – 25 keV	DESY U Göttingen U Dortmund
P11 Biological imaging / diffraction		
2 m undulator (U32), high-ß		
Single-axis diffractometer for macromolecular crystallography Setup for imaging of biological systems	6 – 33 keV 3 – 12 keV	HZI/ DESY MPG
P12 Biological small-angle X-ray scattering		
2 m undulator (U29), high-ß		
Instrument for biological SAXS on protein solutions and time resolved experiments, biomembrane related and soft matter research, tunable sample-detector distance	4 – 20 keV	EMBL GKSS
P13 Macro molecular crystallography I		
2 m undulator (U29), high-ß		
Instrument for highly collimated beams and variable focus size, in crystallo spectroscopies	4 – 17 keV	EMBL
P14 Macro molecular crystallography II		
2 m undulator (U29), high-ß		
Protein micro-crystallography instrument	7 – 35 keV	EMBL

Committees 2009.

Photon Science Committee PSC	
Colin Norris (Chair)	Diamond, CCLRC, UK
Simone Techert (Vice Chair)	Max-Planck-Institut Göttingen, D
Don Bilderback	Cornell University, USA
Peter Fratzl	Max-Planck-Institut Potsdam, D
Michael Fröba	Universität Hamburg, D
Janos Hajdu	University of Uppsala, S
Roland Horisberger	PSI Villigen, CH
Koen Janssens	University of Antwerp, B
Vladimir V. Kvardakov	Kurchatov Institute Moscow, RUS
Franz Pfeiffer	TU München, D
Harald Reichert	ESRF Grenoble, F
Jean-Pierre Samama	Synchrotron Soleil, F
Peter Siddons	NSLS Brookhaven, USA
Joachim Ullrich	Max-Planck-Institut Heidelberg, D
Edgar Weckert	DESY Hamburg, D
Philip J. Withers	University of Manchester, UK
Jörg Zegenhagen	ESRF Grenoble, F
Wilfried Wurth	Universität Hamburg, D (until May 2009)
Wiebke Laasch (PSC Secretary)	DESY Hamburg, D

Project Review Panel PRP1: VUV- and Soft X-Ray - Spectroscopy	
Wolfgang Drube (PRP Secretary)	DESY Hamburg, D
Marco Kirm	University of Tartu, EE
Thomas Möller	TU Berlin, D
Project Review Panel PRP2: X-Ray - Hard Condensed Matter - Spectroscopy	
Wolfgang Drube (PRP Secretary)	DESY Hamburg, D
Johannes Hendrik Bitter	Utrecht University, NL
Wolfgang Grünert	Universität Bochum, D
Thorsten Ressler	TU Berlin, D
Laszlo Vince	Ghent University, B
Project Review Panel PRP3: X-Ray - Hard Condensed Matter / Diffraction and Imaging	
Hermann Franz (PRP Secretary)	DESY Hamburg, D
Hans Boysen	Universität München, D
Bo Brummerstedt Iversen	Aarhus University, DK
Christan Kumpf	FZ Jülich, D
Bert Müller	University Basel, CH
Andreas Schreyer	GKSS Geesthacht, D
Project Review Panel PRP4: Soft X-Ray - FEL Experiments (FLASH)	
Josef Feldhaus (PRP Secretary)	DESY Hamburg, D
Massimo Altarelli	DESY/XFEL Hamburg, D
Robert Donovan	University of Edinburgh, UK
Roger W. Falcone	Lawrence Berkely Lab., USA
Maya Kiskinova	Sincrotrone Trieste, I
Jon Marangos	Imperial College London, UK
Gerard Meijer	Fritz-Haber-Institut Berlin, D
Jan Michael Rost	Max-Planck-Institut Dresden, D
Christian Schroer	TU Dresden, D
Bernd Sonntag	Universität Hamburg, D
Urs Staub	PSI Villigen, CH
Svante Svensson	Uppsala University, S
Edgar Weckert	DESY Hamburg, D
Gwyn P. Williams	Jefferson Lab., USA
Project Review Panel PRP5: X-Ray - Soft Condensed Matter / Scattering	
Rainer Gehrke (PRP Secretary)	DESY Hamburg, D
Tiberio Ezquerra	CSIC Madrid, E
Jochen S. Gutmann	Universität Mainz, D
Beate Klösgen	Univ. of Southern Denmark, DK
Oskar Paris	Max-Planck-Institut Potsdam, D


DESY.

Photographs and Graphics:
Lars Berg, Münster
Michael Bogumil, Hamburg
CFEL
DESY
EMBL
Falcon Crest (aerial photographic enterprise), Hamburg
GFZ
GKSS
Rüdiger Nehmzow, Düsseldorf
Max-Planck Unit for Structural Molecular Biology
Dominik Reipka, Hamburg
Reimo Schaaf, Schönwalde
University of Hamburg
Ed. Züblin AG

Figures of the Research Highlights were reproduced by permission from authors or journals.

Acknowledgement

We would like to thank all authors and everyone who helped in the creation of this annual report.

Imprint

Publishing and Contact:
Hamburger Synchrotronstrahlungslabor HASYLAB
at Deutsches Elektronen-Synchrotron DESY
A Research Centre of the Helmholtz Association
Notkestr. 85
D-22607 HAMBURG, Germany

Phone: +49 40 8998-2304
Fax: +49 40 8998-4475

E-mail: hasylab@desy.de
www.desy.de. and hasylab.desy.de

ISBN 978-3-935702-39-3

Realization:
Ralf Röhlsberger, Martin von Zimmermann

Editing:
Wolfgang Caliebe, Wolfgang Drube, Rainer Gehrke,
Heinz Graafsma, Christian Gutt, Joerg Harms,
Wiebke Laasch, Wolfgang Morgenroth, Alke Meents,
Ralf Röhlsberger, Martin von Zimmermann

Layout: Britta Liebaug, Heike Becker

Printing: Heigener Europrint GmbH, Hamburg

Copy deadline: 31 December 2009

Editorial Note:
The authors of the individual scientific contributions published in this report are fully responsible for the contents.

HELMHOLTZ
ASSOCIATION

Deutsches Elektronen-Synchrotron
A Research Centre of the Helmholtz Association

The Helmholtz Association contributes to solving major challenges facing society, science and industry with top scientific achievements in six research areas: Energy, Earth and Environment, Health, Key Technologies, Structure of Matter, Transport and Space. With 28000 employees in 16 research centres and an annual budget of approximately 2.8 billion euros, the Helmholtz Association is Germany's largest scientific organisation. Its work follows in the tradition of the great natural scientist Hermann von Helmholtz (1821-1894).

www.helmholtz.de